AD_____

GRANT NUMBER DAMD17-97-1-7168

TITLE: A Kinesin-Related Protein Required for the Mitotic Spindle Assembly

PRINCIPAL INVESTIGATOR: Claire E. Walczak, Ph.D.

CONTRACTING ORGANIZATION: University of California, San Francisco
San Francisco, California 94143-0962

REPORT DATE: May 1999

TYPE OF REPORT: Final

PREPARED FOR: U.S. Army Medical Research and Materiel Command
Fort Detrick, Maryland 21702-5012

REPORT DOCUMENTATION PAGE

Form Approved
OMB No. 0704-0188

1. AGENCY USE ONLY *(Leave blank)*	2. REPORT DATE	3. REPORT TYPE AND DATES COVERED
	May 1999	Final (1 May 97 - 30 Apr 99)

4. TITLE AND SUBTITLE

A Kinesin-Related Protein Required for the Mitotic Spindle Assembly

5. FUNDING NUMBERS

DAMD17-97-1-7168

6. AUTHOR(S)

Walczak, Claire E., Ph.D.

7. PERFORMING ORGANIZATION NAME(S) AND ADDRESS(ES)

University of California, San Francisco
San Francisco, California 94143-0962

8. PERFORMING ORGANIZATION REPORT NUMBER

9. SPONSORING / MONITORING AGENCY NAME(S) AND ADDRESS(ES)

U.S. Army Medical Research and Materiel Command
Fort Detrick, Maryland 21702-5012

10. SPONSORING / MONITORING AGENCY REPORT NUMBER

11. SUPPLEMENTARY NOTES

12a. DISTRIBUTION / AVAILABILITY STATEMENT

Approved for public release; distribution unlimited

12b. DISTRIBUTION CODE

13. ABSTRACT *(Maximum 200 words)*

Mitosis is the process by which cells faithfully segregate their genetic material. This process is carried out by the mitotic spindle, which consists of a dynamic array of microtubules responsible for distributing replicated chromatids to each daughter cell. This proposal focuses on XKCM1, a kinesin-related protein required for mitotic spindle assembly *in vitro*. Our previous results indicated that XKCM1 acts by controlling the polymerization dynamics of microtubules which are necessary for spindle assembly. We have carried out a detailed mechanistic biochemistry study which showed that XKCM1 acts by binding to microtubules, causing a conformational change of the microtubule that results in microtubule depolymerization. This was a very novel and unexpected finding and has strong implications in understanding the biochemical mechansims of this class of protein as well as understanding the role of microtubule dynamics in cellular fuction. We have shown that inhibition of a specific pool of XKCM1, that which is bound to kinetochores, causes a misalignment of chromosomes on the spindle. This data provides the first molecular handle on a protein that can couple microtubule dynamics to chromosome movement. The analysis of its function in live cells will be an important area of future research.

14. SUBJECT TERMS			15. NUMBER OF PAGES
Breast Cancer			113
			16. PRICE CODE
17. SECURITY CLASSIFICATION OF REPORT	18. SECURITY CLASSIFICATION OF THIS PAGE	19. SECURITY CLASSIFICATION OF ABSTRACT	20. LIMITATION OF ABSTRACT
Unclassified	Unclassified	Unclassified	Unlimited

FOREWORD

Opinions, interpretations, conclusions and recommendations are those of the author and are not necessarily endorsed by the U.S. Army.

____ Where copyrighted material is quoted, permission has been obtained to use such material.

____ Where material from documents designated for limited distribution is quoted, permission has been obtained to use the material.

____ Citations of commercial organizations and trade names in this report do not constitute an official Department of Army endorsement or approval of the products or services of these organizations.

CEW ____ In conducting research using animals, the investigator(s) adhered to the "Guide for the Care and Use of Laboratory Animals," prepared by the Committee on Care and use of Laboratory Animals of the Institute of Laboratory Resources, national Research Council (NIH Publication No. 86-23, Revised 1985).

____ For the protection of human subjects, the investigator(s) adhered to policies of applicable Federal Law 45 CFR 46.

CEW ____ In conducting research utilizing recombinant DNA technology, the investigator(s) adhered to current guidelines promulgated by the National Institutes of Health.

CEW In the conduct of research utilizing recombinant DNA, the investigator(s) adhered to the NIH Guidelines for Research Involving Recombinant DNA Molecules.

____ In the conduct of research involving hazardous organisms, the investigator(s) adhered to the CDC-NIH Guide for Biosafety in Microbiological and Biomedical Laboratories.

Claire E Walczak 5/31/99

PI - Signature Date

TABLE OF CONTENTS:

XKCM1: A KINESIN-RELATED PROTEIN REQUIRED FOR MITOTIC SPINDLE ASSEMBLY

INTRODUCTION:

The faithful segregation of genetic material to daughter cells which occurs during mitosis is essential for the survival of an organism. This process is carried out by the mitotic spindle, which consists of a dynamic array of microtubules responsible for distributing replicated sister chromatids to each daughter cell. During mitosis, mechanical force is essential to separate spindle poles, to bring chromosomes to the equatorial plate at metaphase, to maintain the intact spindle, and to drive the separation of sister chromatids at anaphase. Many of these processes are likely to involve the use of microtubule-based motor proteins which couple the energy of ATP hydrolysis to force production and translocation along the microtubule (reviewed [1-3]). Kinesin is the originally identified member of a family of proteins, called kinesin-related proteins (KRPs), which have high sequence similarity to the motor domain of kinesin. Several KRPs are implicated in the assembly and function of mitotic and meiotic spindles (reviewed in [1, 2]).

To explore further the mechanisms of mitotic spindle assembly and motor protein function, I isolated KRPs from *Xenopus* that might be important in this process. One of the identified KRPs, which I named XKCM1 (for *Xenopus* Kinesin Central Motor 1) is essential for mitotic spindle assembly *in vitro*, localizes to centromeres, and regulates the polymerization dynamics of microtubules [4, 5]. This proposal focuses on the further study of the *in vivo* function of XKCM1, its biochemical activity, and the beginnings of an analysis of its structure.

BODY:

XKCM1 is Required for Spindle Assembly.

XKCM1 (*Xenopus* Kinesin Central Motor 1) is an 85 kDa protein with an N-terminal globular domain, a central kinesin-like motor domain and a short C-terminal alpha-helical tail. It is a simple dimer with no associated subunits [4, 5] XKCM1 is a member of the Kin I (Kinesin internal) family of KRPs that have their catalytic domain in the central part of the molecule [6]. Antibodies to XKCM1 stain mitotic kinetochores and spindle poles in tissue culture cells and on spindles assembled in *Xenopus* egg extracts. To probe the function of XKCM1, we took advantage of the ability to form spindles in *Xenopus* egg extracts. In the absence of XKCM1 function, large microtubule asters are formed that have both longer and more numerous microtubules. This long microtubule defect can be rescued by the addition of purified XKCM1 protein suggesting that these results are due specifically to loss of XKCM1 and not to loss of some other protein. The extremely long microtubules seen in the XKCM1-depleted structures suggested that some aspect of microtubule dynamics was altered in the absence of XKCM1 function. To test this possibility, we measured the parameters of dynamic instability in extracts that lacked XKCM1 activity. We found that the microtubules behaved normally in the absence of XKCM1 function except that they transited from growth to shrinkage less frequently (catastrophe frequency) suggesting that XKCM1 itself may be promoting microtubule depolymerization. This was a novel and unexpected finding for a kinesin-related protein.

Purified XKCM1 Protein Destabilizes Microtubules

Based on the above studies, it was possible that XKCM1 itself acted at the end of a microtubule to trigger depolymerization [7]. Alternatively, it was possible that XKCM1 acted as a conventional motor protein that walked along a microtubule and translocated a cargo protein or molecule that was responsible for triggering microtubule catastrophes. To distinguish between these models, we tested the effect of purified XKCM1 protein on the dynamics of pure microtubules. Purified recombinant XKCM1 completely inhibited microtubule assembly off axonemes; a similar activity was observed with native XKCM1 purified by immunoaffinity (Figure 1 a).

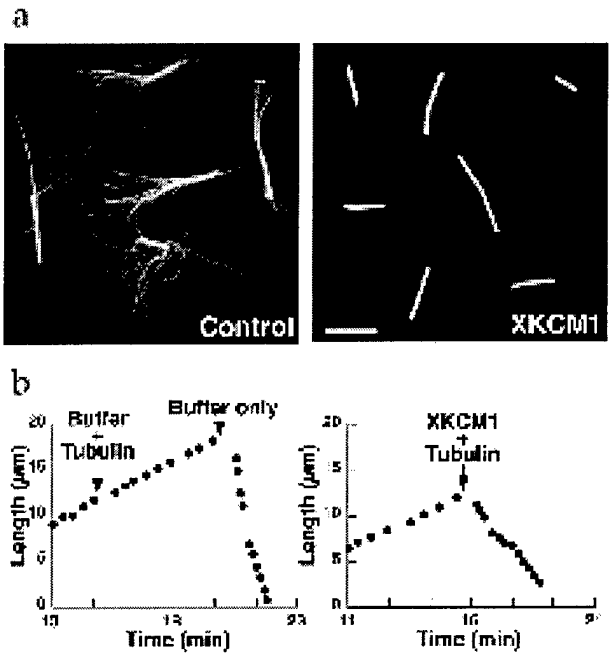

Figure 1. *Pure XKCM1 induces catastrophes of dynamic microtubules. a) Microtubules were assembled off axonemes in the presence of a control buffer or XKCM1 protein. b) Length vs. time plots of a microtubule treated with control buffer plus tubulin followed by buffer alone (left graph) or with XKCM1 plus tubulin (right graph). The rapid change in slope from positive to negative indicates that a catastrophe has occurred.*

These results strongly favor the idea that XKCM1 itself is responsible for triggering microtubule depolymerization. To determine what parameter of dynamic instability was being affected, we used real-time video microscopy to analyze the fate of prepolymerized microtubules after exposure to pure XKCM1 [8]. Microtubules were polymerized off axonemes, then the solution was replaced with a mixture of tubulin and control buffer or tubulin and XKCM1 (Figure 1b). In the control, all microtubules remained in the polymerization phase. In contrast, when XKCM1 was added, nearly all the microtubule ends had transited to the depolymerization phase indicating that a catastrophe had occurred. These results demonstrate that pure XKCM1 directly inhibits microtubule polymerization and acts as a catastrophe factor that can destabilize polymerizing microtubule ends.

XKCM1 is not a Conventional Motor Protein

Our original model implied that XKCM1 uses ATP-dependent motility to target to the plus ends of microtubules where it induces microtubule depolymerization. One can make several testable predictions from this model. In attempts to observe microtubule motor activity, we performed standard motility assays that have been used to demonstrate motility of other kinesins [9]. When XKCM1 was adsorbed to a coverslip and taxol microtubules were added, the microtubules bound to the surface and

exhibited depolymerization of microtubules from both the plus ends and the minus ends at equivalent rates. Motility of the bound microtubules was never observed.

XKIF2, another Kin I Kinesin, Also Destabilizes Microtubules

The ability of XKCM1 to induce microtubule depolymerization was an unexpected activity for a KRP. To determine whether the observed depolymerization activity was unique to XKCM1, or whether it was conserved in other Kin I family members, we tested whether *Xenopus* KIF2 (XKIF2), another Kin I kinesin, could also depolymerize microtubules. XKIF2 is approximately 87% identical to mouse KIF2; its catalytic domain shares 75% identity with the catalytic domain of XKCM1 and only about 25% identity in regions outside the catalytic domain. Based on this homology, we would predict that XKIF2 is a conventional motor protein like mKIF2 [10] and not a microtubule destabilizing protein like XKCM1. When assayed for its effects on either dynamic microtubules or on stabilized microtubules, XKIF2 caused microtubule destabilization in a manner identical to that observed for XKCM1. These results strongly imply that Kin I kinesins are not conventional motor proteins but instead act as microtubule destabilizing enzymes.

A series of mechanistic studies were performed to determine how Kin I family members destabilize microtubules [5]. Based on these mechanistic studies, we propose a new model for XKCM1 (and other Kin I family members) activity (Figure 2). In this model, Kin I kinesins target to microtubule ends during polymerization and disrupt end structure. This step is depicted to occur in the absence of ATP hydrolysis. A catastrophe occurs which induces microtubule depolymerization and release of the Kin I-tubulin dimer complex. ATP hydrolysis dissociates Kin I from tubulin dimer and allows it to act again on another microtubule end. This mechanism is clearly distinct from that of kinesin and other KRPs which bind to the entire length of a microtubule and use the energy of ATP hydrolysis to walk along the microtubule [11, 12].

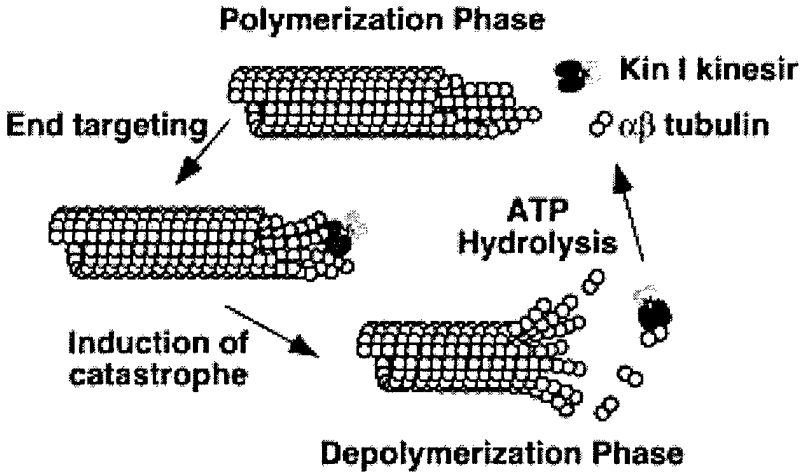

Figure 2. Model for XKCM1 inducing catastrophes. XKCM1 is postulated to act as a microtubule depolymerizing enzyme.

The Catalytic Domain of XKCM1 Binds to Microtubules

We hypothesized that like other KRPs, XKCM1 had distinct domains that might be important for different functions such as microtubule binding, cargo binding or dimerization [6]. To address this hypothesis, we generated glutathione-S-transferase (GST) fusion proteins to the N-terminal globular domain (GST-NT), the centrally located catalytic domain (GST-CD), and the C-terminal alpha-helical

tail (GST-CT). These were expressed in bacteria, purified, and analyzed biochemically. Hydrodynamic analysis using sucrose gradients and gel filtration chromatography [13] showed that both GST-NT and GST-CD were simple dimers in solution, presumably mediated by the GST which is dimeric [14]. In contrast, GST-CT appeared multimeric suggesting that the C-terminus of XKCM1 participates in dimerization of the protein.

The GST-NT, GST-CD, and GST-CT were also tested for their ability to bind to microtubules as assayed by sedimentation. Only GST-CD bound to microtubules suggesting that its kinesin-like domain still functions to bind microtubules. However, GST-CD did not induce microtubule depolymerization suggesting that other domains of the protein might contribute to this activity or that the protein expressed in bacteria is not fully functional. GST-CD was also not enriched at the ends of GMPCPP microtubules as is the full length XKCM1. This suggests that GST-CD may not be sufficient to induce a conformational change in the microtubule, which is a prerequisite for accumulation of XKCM1 at microtubule ends. However, if microtubule protofilament peels were induced by first adding full length XKCM1 protein, the GST-CD protein did enrich at the ends of these microtubules in the protofilament peels. These results suggest that the catalytic domain (GST-CD) has the ability to bind to sites exposed on the inner surface of the microtubule and may be sufficient to bind to tubulin dimers. A detailed analysis of which regions of XKCM1 are important for its microtubule destabilization is currently underway.

The N-terminus of XKCM1 is Targeted to Kinetochores and Disrupts Chromosome Alignment

The GST fusion proteins were also tested for their ability to affect spindle assembly in extracts. The fusion proteins were added to extracts prior to spindle assembly, spindles were assembled, sedimented onto coverslips, fixed and stained with antibodies. Anti-GST antibodies were used to follow the fate of the exogenously added fusion protein while antibodies to other domains of XKCM1 were used to follow the fate of the endogenous XKCM1 protein. Neither GST-CD nor GST-CT bound to the spindle when added to extracts, and spindle formation was normal. When the GST-NT protein was added to extracts, it bound to kinetochores during spindle assembly suggesting that the N-terminal domain of XKCM1 is sufficient for kinetochore localization (Figure 3).

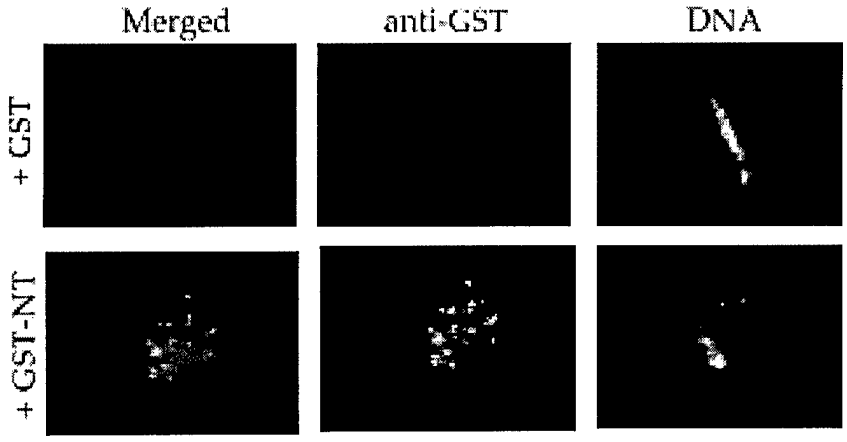

Figure 3. *The N-terminus of XKCM1 is sufficient to target to kinetochores. The top panels show spindles from extracts incubated with control GST protein. The bottom panels show spindles from extracts incubated with GST-NT protein.*

Addition of GST-NT to extracts displaced the endogenous XKCM1 from the kinetochore but did not displace CENP-E, another kinetochore KRP, showing the specificity of the reagent. The displacement of endogenous XKCM1 from kinetochores by GST-NT caused a misalignment of chromosomes on the metaphase plate (Figure 3). These results suggest that XKCM1 is important in chromosome positioning within the spindle. Because spindle formation proceeded normally in the presence of GST-NT, this suggests that the endogenous soluble pool of XKCM1 is not inhibited, and only the kinetochore-bound portion of XKCM1 is affected.

XKCM1 Dissociates from Kinetochores During Anaphase

We wondered whether XKCM1 function at kinetochores was also required to segregate chromosomes during anaphase as was observed for the MCAK protein in tissue culture cells [15]. Spindles were assembled in the presence of GST-NT and then induced to enter anaphase by the addition of calcium [16]. After 20', spindles were fixed and analyzed for their morphology and the location of their chromosomes. Chromosomes appeared to be distributed randomly on the spindle as if the chromosomes were not segregated properly. One possible interpretation of these results is that XKCM1 is required during anaphase to depolymerize microtubules from the kinetochore and thus move chromosomes. Alternatively it is possible that chromosomes segregate normally but because they started out misaligned, their final distribution on the spindle is random. To begin to distinguish between these two possibilities, we examined the localization of endogenous XKCM1 during anaphase on spindles assembled in extracts. To our surprise, XKCM1 staining was greatly diminished at kinetochores during anaphase in extracts. This is in contrast to the localization in tissue culture cell spindles where XKCM1 or its mammalian homologue, MCAK, remain associated with kinetochores throughout anaphase [4, 17]. One attractive explanation for these results is that they may reflect the different mechanisms of anaphase A chromosome movement between somatic cells and spindles assembled in extracts. During anaphase A in somatic cells, chromosomes move poleward with microtubule depolymerization occuring near the kinetochore [4, 17-24] - XKCM1 provides an attractive candidate for mediating this activity. Consistent with this idea, the mammalian MCAK protein has been recently implicated in anaphase chromosome segregation in cells [15]. In *Xenopus* extract assembled spindles, chromosomes move poleward with microtubule depolymerization occuring near the poles [25]. In this case, XKCM1 activity would no longer be needed at kinetochores. How does the extract or a cell distinguish between these mechanisms, how is that distinction communicated to the XKCM1 protein, and what can these results tell us about how chromosomes are segregated? These are questions that are currently being investigated in the lab.

How does XKCM1 Function in cells?

Based on our results of XKCM1 function in extracts, we propose several models of how XKCM1 functions in cells. First it is possible that XKCM1 is important in regulating the dynamics of microtubules in cells, specifically during the transition from interphase to mitosis. Second, XKCM1 may be important in controlling the dynamics of spindle microtubules in mitosis and thus be important in building a spindle. Third, kinetochore-bound XKCM1 may be important in regulating the local polymerization dynamics of kinetochore microtubules and thus be important in moving chromosomes during prometaphase or during anaphase. To begin to address these models, antibodies to XKCM1 were

injected into frog tissue culture cells during interphase. The cells were allowed to grow for 12 to 24 hrs, and then they were fixed and stained with anti-tubulin antibodies to visualize the microtubule cytoskeleton. Under these conditions, there was no change in the number of microtubules or in the morphology of the microtubule array. An alternative approach to this problem is to overexpress XKCM1 in cells by injection of purified protein or by overexpression of a transfected version of the protein. We generated a fusion protein between GFP (green fluorescent protein) and full length XKCM1. Preliminary studies showed that transient overexpression of XKCM1 in cells caused a marked decrease in the microtubule network of transfected cells supporting the idea that XKCM1 is a global regulator of microtubule dynamics in cells. Current experiments are aimed at quantitative correlations between XKCM1 levels in cells and the extent of the microtubule network.

To ask if XKCM1 is required for spindle assembly or for chromosome movement, anti-XKCM1 antibodies were microinjected into mitotic PtK2 cells, and the fate of the cells was followed by time-lapse video microscopy. Approximately 30% of the injected cells were arrested or delayed in mitosis, but no clear arrest point was detected nor were there any obvious defects in the motility of the chromosomes. These preliminary results suggest that under certain conditions, our antibodies are capable of inhibiting XKCM1 function when injected into cells and thus will be useful reagents for probing XKCM1 function. The observation that we can achieve some delay or block in mitosis suggests that XKCM1 is important in spindle assembly or chromosome movement in cells and future experiments will address this problem.

REFERENCES

1. Vernos, I. and E. Karsenti, *Motors involved in spindle assembly and chromosome segregation.* Curr. Opin. Cell Biol., 1996. **8**: p. 4-9.

2. Sawin, K.E. and S.A. Endow, *Meiosis, mitosis and microtubule motors.* Bioessays, 1993. **15**: p. 399-407.

3. Bloom, G. and S. Endow, *Motor proteins 1: kinesins.* Protein Profile, 1995. **2**: p. 1109-1171.

4. Walczak, C.E., T.J. Mitchison, and A. Desai, *XKCM1: A Xenopus kinesin-related protein that regulates microtubule dynamics during mitotic spindle assembly.* Cell, 1996. **84**: p. 37-47.

5. Desai, A., *et al.*, *Kin I kinesins are microtubule-destabilizing enzymes.* Cell, 1999. **96**: p. 69-78.

6. Vale, R.D. and R.J. Fletterick, *The design plan of kinesin motors.* Annu. Rev. Cell and Dev. Biol., 1997. **13**: p. 745-777.

7. Waters, J.C. and E.D. Salmon, *Cytoskeleton: a catastrophic kinesin.* Curr. Biol., 1996. **6**(4): p. 361-3.

8. Walker, R.A., *et al.*, *Dynamic instability of individual microtubules analysed by video light microscopy: rate constants and transition frequencies.* J. Cell Biol., 1988. **107**: p. 1437-1448.

9. Scholey, J.M., *Motility assays for motor proteins.* Methods in Cell Biology, ed. L. Wilson and P. Matsudaira. Vol. 39. 1993, San Diego: Academic Press, Inc. 304.

10. Noda, Y., *et al.*, *KIF2 is a new microtubule-based anterograde motor that transports membranous organelles distinct from those carried by kinesin heavy chain or KIF3A/B.* J. Cell Biol., 1995. **129**: p. 157-167.

11. Howard, J., *Molecular motors: structural adaptations to cellular functions.* Nature, 1997. **389**(6651): p. 561-567.

12. Howard, J., *The movement of kinesin along microtubules.* Annu. Rev. Physiol., 1996. **58**: p. 703-729.

13. Siegel, L.W. and K.J. Monty, *Determination of molecular weights and frictional ratios of proteins in impure systems by use of gel filtration and density gradient centrifugation. Application to crude preparations of sulfite and hydroxylamine reductases.* Biochim. Biophys. Acta, 1966. **112**: p. 346-362.

14. Warholm, M., *et al.*, *Glutathione transferase from human liver.* Methods Enzymol., 1985. **113**: p. 499-505.

15. Maney, T., *et al.*, *Mitotic centromere-associated kinesin is important for anaphase chromosome segregation.* J. Cell Biol., 1998. **142**: p. 787-801.

16. Shamu, C.E. and A.W. Murray, *Sister chromatid separation in frog egg extracts requires DNA topoisomerase II activity during anaphase.* J. Cell Biol., 1992. **117**(5): p. 921-934.

17. Wordeman, L. and T.J. Mitchison, *Identification and partial characterization of mitotic centromere-associated kinesin, a kinesin-related protein that associates with centromeres during mitosis.* J. Cell Biol., 1995. **128**(1-2): p. 95-104.

18. Mitchison, T.J., *et al.*, *Sites of microtubule assembly and disassembly in the mitotic spindle.* Cell, 1986. **45**: p. 515-527.

19. Mitchison, T.J. and E.D. Salmon, *Poleward kinetochore fiber movement occurs during both metaphase and anaphase-A in newt lung cell mitosis.* J. Cell Biol., 1992. **119**: p. 569-582.

20. Wadsworth, P. and E.D. Salmon, *Analysis of the treadmilling model during metaphase of mitosis using fluorescence redistribution after photobleaching.* J Cell Biol, 1986. **102**: p. 1032-1038.

21. Gorbsky, G.J., P.J. Sammak, and G.G. Borisy, *Chromosomes move poleward in anaphase along stationary microtubules that coordinately disassemble from their kinetochore ends.* J. Cell Biol., 1987. **104**: p. 9-18.

22. Gorbsky, G.J., P.J. Sammak, and G.G. Borisy, *Microtubule dynamics and chromosome motion visualized in living anaphase cells.* J. Cell Biol., 1988. **106**: p. 1185-1192.

23. Zhai, Y., P.J. Kronebusch, and G.G. Borisy, *Kinetochore microtubule dynamics and the metaphase-anaphase transition.* J. Cell Biol., 1995. **131**: p. 721-734.

24. Waters, J.C., *et al.*, *The kinetochore microtubule minus-end disassembly associated with poleward flux prodcues a force that can do work.* Mol. Biol. Cell, 1996. **7**: p. 1547-1558.

25. Desai, A., *et al.*, *Anaphase A chromosome movement and poleward spindle microtubule flux occur at similar rates in Xenopus extract spindles.* J. Cell Biol., 1998. **141**: p. 703-713.

APPENDIX

1) Key research accomplishments:

- The identification and characterization of the XKCM1 protein
- The discovery that XKCM1 is not a conventional motor protein but rather a microtubule destabilizing enzyme
- The finding that XKCM1 function at kinetochores is required for chromosome alignment in frog egg extract spindles

2) Reportable Outcomes:

a) Manuscripts: abstracts, presentations:

Desai, A. and Walczak, C.E. (submitted). Assays for Microtubule Destabilizing Kinesins. Methods in Mol. Biol. (invited chapter for special issue on Kinesin protocols).

Heald, R. and Walczak, C.E. (1999). Microtubule-based motor function in mitosis. Curr. Opin. Struc. Biol. 9: 268-274 (Review).

Desai, A., Verma, S., Mitchison, T.J., and Walczak, C.E. (1999) Kin I Kinesins are Microtubule Destabilizing Enzymes. Cell 96: 69-78.

Desai, A., Murray, A., Mitchison, T.J., and Walczak, C.E. (1999). The Use of Xenopus Egg Extracts to Study Mitotic Spindle Assembly and Function in Vitro. Methods in Cell Biol. 61: 385-412

Sharp, D.J., McDonald, K.L., Brown, H.M., Matthies, H.J., Walczak, C.E., Vale, R.D., Mitchison, T.J., and Scholey, J.M. (1999). Visualization of the Bipolar Kinesin, KLP61F, on Microtubule Bundles within Spindles of Drosophila Early Embryos. J. Cell Biol. 144: 125-138.

Shirasu, M., Yonetani, A., and Walczak, C.E. (1999). Microtubule Dynamics in Xenopus Egg Extracts Microsc. Res. Tech. 44: 435-445. (Review)

Walczak, C.E., Vernos, I., Mitchison, T.J., Karsenti, E., and Heald, R. (1998). A Model for the Proposed Roles of Different Microtubule Based Motor Proteins in Establishing Spindle Bipolarity. Curr. Biol. 8: 903-913.

Field, C.M., Oegema, K. Zheng, Y., Mitchison, T.J., and Walczak, C.E. (1998). Purification of Cytoskeleton Proteins using Peptide Antibodies. Methods Enz. 298: 525-541.

Abstracts:

Microtubule Destabilization by XKCM1 and XKIF2- Two Internal Motor Domain Subfamily Kinesins (A. Desai, T.J. Mitchison, and C.E. Walczak). Mol. Biol. Cell (1997) 8: 3a.

Dissecting the Function of Kinetochore-Bound XKCM1 in Chromosome Movement in vitro and in vivo (C.E. Walczak, A. Desai, and T.J. Mitchison). Mol. Biol. Cell (1997) 8: 125a.

Presentations:

Microtubule Destabilization by XKCM1 and XKIF2- Two Internal Motor Domain Subfamily Kinesins (A. Desai, T.J. Mitchison, and C.E. Walczak). Presented at the ASCB Annual Meeting by A. Desai.

Dissecting the Function of Kinetochore-Bound XKCM1 in Chromosome Movement in vitro and in vivo (C.E. Walczak, A. Desai, and T.J. Mitchison). Presented at the ASCB Annual Meeting by C.E. Walczak.

b) Patents and licenses: None.
c) Degrees obtained: None
d) Cell lines, tissue ore serum repositories: None
e) Informatics: None
f) Funding applied for:
An RO1 Grant from the National Institutes of Health. Based on the percentile score, that grant will be funded as of 8/1/99.
g) Employment or research opportunities:
This grant supported my research during the last 1.5 years of my post-doctoral training. During that time, I was also searching for an independent position as an assistant professor. I applied for approximately 65 jobs, received 19 interviews and 7 job offers. I am currently an Assistant Professor of Biochemistry and Molecular Biology in the Medical Sciences Program at Indiana University in Bloomington, IN.

3) One copy of each of the above manuscripts and abstracts is attached:

Assays for Microtubule Destabilizing Kinesins

Arshad Desai* and Claire E. Walczak#

*Program in Cell Biology, EMBL Heidelberg, Germany 69117 and #Medical Sciences Program, Indiana University, Bloomington, IN 47405

Arshad Desai
Program in Cell Biology
European Molecular Biology Laboratory
Meyerhofstrasse 1
D-69117 Heidelberg, Germany
Ph: +49 6221 387 337
Fax: +49 6221 387 512
e-mail: Arshad.Desai@EMBL-Heidelberg.de

Address all correspondence to:
Claire E. Walczak
Medical Sciences Program
Indiana University
Jordan Hall 104
1001 East 3rd St.
Bloomington, IN 47405
Ph: (812) 855-5919
Fax: (812) 855-4436

e-mail: cwalczak@indiana.edu

1. INTRODUCTION

The kinesin superfamily is a large family of microtubule (MT)-stimulated ATPases that couple the energy of ATP hydrolysis to force production (reviewed in 1, 2). Conventional kinesin was identified as a motor protein that could translocate along MT polymers. Since the molecular cloning of kinesin (3), well over one hundred additional proteins have been identified that share high sequence homology with the catalytic domain of kinesin. Many of these kinesin-related proteins (KRPs) have also been shown to be MT-based motor proteins using *in vitro* motility assays (reviewed in 2).

Although kinesin and many KRPs share high sequence homology in their catalytic domain, recent evidence suggests that some kinesin superfamily members may not act as conventional motor proteins but may be microtubule destabilizing enzymes (4-6). The first hints at this function came from studies on the yeast Kar3 protein. Analysis of the *in vitro* motility of a bacterially expressed fragment of Kar3 revealed that it slowly depolymerizes MTs from the minus ends as it translocates along MTs toward the minus end (5). The most striking example of the ability of some KRPs to destabilize MTs came from studies of the Kin I KRPs XKCM1 and XKIF2 (4). Both XKCM1 and XKIF2 were shown to directly destabilize MTs in an ATP-dependent manner. Their ability to destabilize MTs does not involve classical motor activity. Furthermore, this MT-destabilization activity can be distinguished mechanistically from that of conventional kinesin and other kinesin family motors.

Here we describe the biochemical assays used to analyze the effect of MT destabilizing kinesins on various MT substrates. These assays will be useful to discern the mechanism of other KRPs that have been proposed to act as MT destabilizing enzymes based on genetic studies (6-9). In addition, these assays will be useful to analyze the mechanism of other MT dynamics regulators.

2. MATERIALS

1. Pure enzyme preparation: We use recombinant XKCM1 or XKIF2 purified from insect Sf-9 cells using conventional chromatographic techniques (4). The final preparation was eluted from a MonoS cation exchange column in BRB80 (section 2, #4) + 1 mM DTT + 10 μM MgATP + 1 μg/ml leupeptin, pepstatin A, chymotrypsin + ~ 300 mM KCl. Fractions were supplemented with 10% sucrose (w/v), aliquoted, frozen in liquid nitrogen, and stored at –80 °C. (see Note 1).
2. Recycled tubulin: We use phosphocellulose-purified bovine brain tubulin that has been cycled at least one additional time after purification using standard procedures (10) (http://skye.med.harvard.edu/newprotocols/toc.html). All tubulin is stored in aliquots at –80 °C in IB (50 mM K-glutamate, 0.5 mM $MgCl_2$). Tubulin concentration is determined using $\varepsilon_{tubulin,280\ nm} = 115{,}000\ M^{-1}cm^{-1}$.

3. Fluorescent tubulin: Tubulin polymer is labeled with fluorescent dyes using standard procedures (10) (http://skye.med.harvard.edu/newprotocols/toc.html).

4. BRB80 Buffer: (80 mM Pipes, 1 mM $MgCl_2$, 1 mM EGTA, pH 6.8 with KOH). This buffer is also made as a 5X stock for many of the experiments. Sterile filter and store at 4 °C (see Note 2).

5. MgATP: Sigma A-2383. The disodium salt of ATP is made up as a 0.5 M stock in water to which an equimolar amount of $MgCl_2$ is added so the final concentration of the solution is 0.5 M $MgCl_2$ and 0.5 M ATP. Solution is sterile-filtered and stored in aliquots at –20 °C.

6. MgAMPPNP: Sigma A-2647. The dilithium salt of AMPPNP is made up as a 0.1 M stock in water to which an equimolar amount of $MgCl_2$ is added so the final concentration of the solution is 0.1 M $MgCl_2$ and 0.1M AMPPNP. Solution is sterile-filtered and stored in aliquots at –20 °C.

7. MgGTP: Sigma G-8877. The disodium salt of GTP is made up as a 0.1 M stock in water. Solution is sterile-filtered and stored in aliquots at –20 °C.

8. MgGDP: Sigma G-7127 The disodium salt of GDP is made up as a 0.1 M stock in. Solution is sterile-filtered and stored in aliquots at –20 °C.

9. GMPCPP: Unfortunately, there is no commercial source of GMPCPP and it must be synthesized in house (11). All stocks are at 0.1 M GMPCPP in water. They are stored in aliquots at –20 °C.

10. Axonemes: axonemes are prepared according to standard procedures as described previously (12). They are stored at –20 °C in 50% v/v glycerol, 5 mM Pipes, 0.5 mM EDTA, 1 mM 2-mercaptoethanol, pH 7.0 with KOH.

11. BRB80 + 1% glutaraldehyde: This is 1X BRB-80 containing 1% final concentration of glutaraldehyde. Make fresh before use.

12. BRB80 + 30% glycerol: Make by adding glycerol to 1X BRB80 buffer. This solution can be stored at 4 °C.

13. Spindown tubes: These are 15 ml corex tubes that have been modified to hold a coverslip at the bottom of the tube so that samples can be readily centrifuged onto coverslips. They have been described previously (13).

14. Flow-chambers: These are microscope slides that have been modified to create a flow cell and are used routinely in studies of microtubule dynamics and motility assays. They have been described previously (14).

15. Oxygen Scavenging Mix (OSM): (200 μg/ml glucose oxidase, 35 μg/ml catalase, 4.5 mg/ml glucose, 0.5% 2-mercaptoethanol). This is made fresh daily from concentrated stocks of each of the components.

16. Taxol: Paclitaxel- Sigma T7402.

3. METHODS

3.1 Preparation of Microtubule Substrates

The effects of kinesins on MT dynamics can be assayed by using three different types of MT substrates. The first type of substrate is a dynamic MT. For this experiment, we use MTs that have been polymerized off axoneme seeds in the presence of GTP. These samples can be analyzed by either fixed time point assays (section 3.2.1) or in real time (section 3.2.2). The other two types of substrates are MTs stabilized with the non-hydrolyzable GTP analog GMP-CPP or with the MT stabilizing drug taxol (section 3.3).

3.1.1 Preparation of Dynamic MTs Nucleated from Axonemes

1. Make 225 µl of 20 µM tubulin mix on ice such that at 15 µM the BRB80 concentration is 1X and the GTP concentration is 0.5 mM. For a recycled tubulin stock of 150 µM concentration, the reaction mix would be as follows: 60 µl 5X BRB80; 30 µl 150 µM recycled tubulin; 1.5 µl 100 mM GTP; water to 225 µl.
2. Incubate tubulin mix at 0 °C for 5', spin 90,000 rpm 5' at 2 °C in a TLA100 rotor. Transfer supernatant to a cold tube on ice.

3.1.2 Preparation of GMPCPP MTs

GMPCPP is the best current GTP analog for tubulin polymerization. GMPCPP is a potent nucleator of microtubules. Therefore, at tubulin concentrations of 1 mg/ml or higher, very

numerous and short microtubules are formed in the presence of GMPCPP. If longer GMPCPP microtubules are desired, nucleation can be limited by diluting the tubulin to ~2-3 μM (0.2 - 0.3 mg/ml). We generally make a 1-3 mg/ml CPP tubulin mix and store it at –80 °C in small aliquots. Directly polymerizing this mix results in short GMPCPP seeds. Diluting the mix while thawing it results in formation of longer GMPCPP microtubules.

1. On ice mix unlabeled tubulin and labeled tubulin (1-3 mg/ml final) at an appropriate ratio in 1X BRB80 with 1 mM DTT and 0.5-1 mM GMPCPP. Incubate at 0 °C for 5'-10'.
2. Clarify mix in TLA100 rotor at 90K for 5' at 2 °C.
3. For the visual assay (section 3.3.1), freeze supernatant in 5-10 μl aliquots in liquid nitrogen and store at –80 °C.
4. To form long GMPCPP microtubules, thaw a CPP mix tube by adding in enough warm BRB80 + 1 mM DTT such that the final tubulin concentration is 2-3 μM (pipet in 37 °C BRB80 + 1 mM DTT, mix by gently pipeting up and down until the frozen seed mix pellet is thawed, then place in 37 °C water bath). Incubate at 37 °C for 30' or longer. Free GMPCPP can be removed as described in 3.1.3 or the CPP microtubules can be used directly for assays.

5. For the sedimentation assay (section 3.3.2), polymerize the supernatant at 37 °C for 30'. Pellet the polymerized MTs in a TLA100 rotor (90K 5' at 25-30 °C), discard supernatant and resuspend pellet in 0.8 – 1X the starting volume of BRB80 + 1 mM DTT.
6. MT concentration, i.e., concentration of tubulin dimer in MT polymer, in the resuspended pellet is determined from the A_{280} of an aliquot of the sedimented and resuspended MTs diluted in BRB80 + 5 mM $CaCl_2$ and incubated at 0 °C for 10' to induce depolymerization (using $\varepsilon_{tubulin,280\ nm} = 115{,}000\ M^{-1}cm^{-1}$). The appropriate resuspension buffer diluted in parallel is used as a blank. (see Note 3)

3.1.3 Preparation of Taxol-stabilized MTs

1. On ice mix unlabeled tubulin and labeled tubulin (visual assay, section 3.3.1) or unlabeled tubulin alone (sedimentation assay, section 3.3.2) at an appropriate ratio in 1X BRB80 with 1 mM DTT and 1 mM GTP. Incubate at 0 °C for 5'.
2. Clarify mix in TLA100 rotor at 90K for 5' at 2 °C. Incubate supernatant at 37 °C for 1'-2'.
3. Add taxol stepwise to equimolar as follows (for 1 mg/ml tubulin) (see Note 4):
4. Pipet in the taxol and immediately flick the tube to mix it in.
5. Add 1/100 vol 10 μM taxol; Incubate at 37 °C for 5'-10'
6. Add 1/100 vol 100 μM taxol; Incubate at 37 °C for 5'-10'
7. Add 1/100 vol 1000 μM taxol; Incubate at 37 °C for 15'

8. Pellet microtubules over a warm 40% glycerol in BRB80 cushion. Spin at 75K for 15' in a TLA100, 100.2 or 100.3 rotor, aspirate and wash sample/cushion interface, rinse pellet and resuspend in warm BRB80 + 1 mM DTT + 10-20 μM taxol (taxol should be at least equimolar and preferably in excess to the tubulin).

3.2 Assays on Dynamic MTs

The effects of kinesins on MT dynamics are first assessed on dynamic MTs nucleated off *Tetrahymena* axonemes (12). *Tetrahymena* axonemes are ciliary fragments that serve as nuclei for MT polymerization. The effect of kinesins on MTs polymerized off axonemes can be assessed using both fixed (section 3.2.1) and real-time (section 3.2.2) assays as described below.

3.2.1 Fixed Time-point Assay

The effect of a purified kinesin or partially pure fraction on MT assembly is assayed on 15 μM tubulin polymerized off *Tetrahymena* axonemes at 37 °C in the presence of ATP. In addition to concentration of the kinesins tested, the time of incubation, the adenine nucleotide, the final salt concentration, as well as the tubulin concentration can be varied. The kinesin can also be added after allowing MT assembly for some duration although we prefer to do this experiment live using VE-DIC (section 3.2.2). Note that tubulin requires GTP for polymerization and GTP can be used as a substrate by some kinesins (15) so any interpretation of

non-hydrolyzable adenine nucleotide analogs added into the reaction must take into account this possibility.

The following protocol is for 6 reactions – a convenient number to pellet in one HB-6 rotor.

1. Prepare assay mixes on ice:
   a. 30 µl tubulin mix (section 3.1.1)
   b. 2 µl 30 mM MgATP
   c. purified kinesin or fraction and KCl such that final volume is 40 µl and final concentration of KCl is 50 – 75 mM (all reactions to be compared must have similar, i.e. ± 5 mM, KCl concentration)
2. Mix and add axonemes (<1 µl for typical axoneme preparations), mix again and transfer 10 µl to a new tube on ice. (see Note 5).
3. Transfer the 10 µl reactions to 37°C. Stagger tubes by 30s.
4. After 7' at 37°C, add 100 µl BRB80 + 1% glutaraldehyde (at RT), mix gently with a cutoff P200 tip and incubate at RT for 3'. Dilute with 900 µl RT BRB80, mix by gentle inversion and load 100 µl onto a 5 ml BRB80 + 30% glycerol cushion in a spindown tube.
5. Sediment at 16 °C for 20' at 10,000 rpm in an HB-6 rotor.
6. Aspirate partially, rinse sample-cushion interface 2 times with BRB80, aspirate completely and postfix in –20 °C methanol for 5'

7. Rehydrate 2 times with TBSTx and perform anti-tubulin immunofluorescence as described (12). An example of typical results is shown in Figure 1A.

3.2.2 Real-time Assay

To assess the effect of a kinesin on prepolymerized MTs we utilize flow cells and real-time VE-DIC analysis. Briefly, we use double stick-tape flow cells made from clean coverslips (http://skye.med.harvard.edu/newprotocols/toc.html) (14) and axonemes as nucleating structures for MTs.

1. Axonemes are adsorbed to flow cell surfaces for 3', the surface blocked with 5 mg/ml BSA for 5' after which the chamber is rinsed with 3-4 chamber volumes of BRB80.
2. 2-3 chamber volumes of tubulin mix (section 3.1.1) is introduced (the mix is prepared in BRB80 buffer containing GTP and ATP).
3. After ~10' when significant MT assembly is evident from both ends of axonemes we flow in a mix of the kinesin diluted into the initial tubulin mix and record the effect on the prepolymerized MTs. Storage buffer diluted similarly is used as a control (see Note 6)

3.3. Assays on Stabilized MT Substrates

To characterize how a kinesin destabilizes MTs, we analyze its effect on MTs stabilized by the drug taxol or by polymerization with GMPCPP, a GTP analog that is essentially

nonhydrolyzable by tubulin over the time course of most experiments (11, 16). Because taxol and GMPCPP eliminate the intrinsic GTP hydrolysis-driven destabilization mechanism of tubulin, depolymerization of stabilized MTs requires input of free energy and multiple rounds of action. Thus, these substrates are very useful to analyze if the action of a destabilizer is catalytic and if so to analyze the details of the reaction mechanism. In this section we describe a quick qualitative visual assay to test if a kinesin depolymerizes such MTs (section 3.3.1) as well as a more rigorous sedimentation assay (section 3.3.2). In addition we describe a microscopy assay to look at the depolymerization reaction in real-time (section 3.3.3).

3.3.1. Qualitative Visual Fluorescence Assay

Fluorescent stabilized MTs are polymerized from a mixture of unlabeled and labeled tubulin (generally with tetramethylrhodamine;) as described in section 3.1.2 or section 3.1.3 above depending on whether they are stabilized with GMPCPP or taxol. We generally use a ratio of 1 part labeled tubulin to 7 parts unlabeled tubulin.

In this assay, the adenine nucleotide, the type and amount of kinesin as well as the final salt concentration can be varied. To rigorously assess the effects of these manipulations, the sedimentation assay described in 3.3.2 should be performed on the variations (see Note 7).

1. At RT mix the following:

   1 µl 15 mM MgATP or 50 mM MgAMPPNP

1 µl 5X BRB80

1-3 µl purified kinesin or fraction to be tested; for a new protein the final KCl concentration should be varied between 0 and 100 mM.

2. Add 5 µl of ~2-3 µM GMPCPP MTs or ~2 µM taxol-stabilized MTs (in BRB80 + 10-20 µM taxol; the final taxol concentration should be 2-3X the final tubulin concentration).
3. After 5', 10' etc. at RT, squash 1.5 µl under an 18x18 mm coverslip and view by epifluorescence microscopy. A typical example is shown in Figure 1B.

3.3.2 Sedimentation Assay

Taxol and GMPCPP MTs are polymerized from unlabeled tubulin as described (sections 3.1.2 and 3.1.2). Polymerized MTs are sedimented and resuspended to ~10-15 µM in BRB80 + 1 mM DTT (for GMPCPP MTs) and BRB80 + 20 µM taxol + 1 mM DTT (for taxol-stabilized MTs). The stabilized MT stock concentrations are then adjusted to 2X the final desired MT concentration using the appropriate resuspension buffer (see Note 8).

1. For a 100 µl reaction prepare a 50 µl mix at RT comprised of 1X BRB80, 1 mM DTT, MgATP (2-4 mM) or MgAMPPNP (10 mM), the kinesin to be tested and KCl such that the final KCl concentration in 100 µl will be 50 – 75 mM. To this mix add 50 µl of 4 µM stabilized MTs (final 2 µM tubulin in MT polymer). Incubate at RT for 15' – 30'.

2. Sediment 80 µl in a TLA100 rotor at 100,000 rpm for 5' at 23 °C. The residual 20 µl can be frozen in liquid nitrogen and used to estimate total recovery if desired.
3. Remove supernatant as thoroughly as possible and save; resuspend pellet in 80 µl BRB80 + 5 mM $CaCl_2$ + same KCl concentration as reaction and incubate on ice for 10'.
4. Analyze 20 - 25 µl of the supernatant and the resuspended pellet on a 10% SDS-PAGE gel followed by Coomassie staining. The amount of tubulin in the supernatant and pellet can be quantified by densitometry of a scanned Coomassie-stained gel. In addition, western blotting of ~5 µl supernatant and pellet can be used to assess where the kinesin used in the assay fractionates.

3.3.3 Real-time Assay

We used real-time analysis of XKCM1-induced depolymerizing GMPCPP MTs to show that the depolymerization action of this kinesin acted on ends and not via a severing mechanism and also to determine the polarity of action – an important criterion to distinguish between motility-based targeting to ends versus direct targeting to ends. The assay we used allowed us to film depolymerization of GMPCPP MTs and then unambiguously assign polarity to the substrate MTs.

1. Coat double-stick tape flow cell surfaces with the MT glue for 3' (see Note 9).

2. Block the flow cell surfaces with 5 mg/ml BSA in BRB80. This preparation binds MTs to the coverslip surface without significantly releasing, moving or depolymerizing them in the presence of ATP in the time scale of this assay.

3. Introduce segmented GMPCPP MTs into the flow cell for 2' – adjust the time and concentration of the segmented MTs to result in a "good" density on the surface (see Note 10).

4. Rinse extensively with BRB80 + 1 mM DTT + 1.5 mM MgATP + 1X OSM.

5. Introduce the kinesins to be tested into the flow cell (in our case 20 nM XKCM1, preincubated for 10' on ice with 30-fold molar excess of either anti-XKCM1 antibody or an irrelevant rabbit IgG) adjusted to BRB80 + 1 mM DTT + 1.5 mM MgATP + 1 mg/ml BSA + 1X OSM.

6. Monitor the reaction using timelapse fluorescence microscopy with a 60X, 1.4 NA Nikon objective and a video/cooled CCD camera. We routinely collect one image every 10 –20 s with each exposure being 0.5 – 1 s.

7. After 10'-15', introduce ~200 nM K560 into the flow cell and record the motility of the observed MTs to retroactively and unambiguously assign their polarity.

3.4 Immunofluorescence Assay

To determine if the kinesin of interest targeted specifically to the ends of the microtubules or if it bound all along the walls of the microtubules, it is necessary to carry out immunofluorescence analysis of the kinesin localization during the depolymerization reaction. For immunofluorescence analysis of kinesins on GMPCPP MTs it is necessary to have a glutaraldehyde resistant primary antibody to the kinesin. We have had good success obtaining glutaraldehyde-resistant antibodies by pretreating antigens prior to injection with glutaraldehyde.

1. Mix ~50 nM XKCM1 with 1-2 μM GMPCPP MTs in 1.5 mM MgATP or 5 mM MgAMPPNP in BRB80+ 1mM DTT.
2. After 3' (ATP) or 15' (AMPPNP) at RT, fix 3 μl with 30 μl of RT BRB80 + 1% glutaraldehyde and incubate at RT for 3'.
3. Dilute with 800 μl of RT BRB80 and sediment 50 μl onto a coverslip (gently mix by inversion just before withdrawing the 50 μl).
4. For the sedimentation put 5 ml BRB80 in a spindown tube and underlay (using a very cutoff 1ml pipet tip) with 2 ml of BRB80 + 10% glycerol. Pipet the 50 μl fixed diluted reaction on top of the BRB80 and sediment 1-1.5 hrs at 12-13K in a HB-6 rotor at 20 °C. If the MTs are too dense or too sparse, adjust the amount sedimented in subsequent expts.
5. After sedimentation, postfix in –20 °C methanol for 5', rehydrate and process for indirect immunofluorescence using glutaraldehyde-resistant anti-XKCM1 and anti-tubulin antibodies.

The results of such an experiment performed with XKCM1 in the presence of 5 mM MgAMPPNP is shown in Figure 1C (see Note 11).

3.5 Tubulin Dimer Binding Assays

In our analysis of Kin I kinesins we found that ATP hydrolysis is not required for MT end targeting nor for induction of a conformational change at the MT end. Therefore, we hypothesized that it is used to recycle XKCM1/XKIF2 by dissociating them from tubulin dimer. With dynamic MT substrates, disruption of end structure would presumably induce a catastrophe, releasing a small number of XKCM1/XKIF2-tubulin dimer complexes and a much larger number of free tubulin dimers as the unstable GDP-tubulin core of the MT depolymerizes. The XKCM1/XKIF2-tubulin dimer complex would need to dissociate to allow the XKCM1/XKIF2 to act again at a new MT end. This hypothesis predicts that an XKCM1/XKIF2-tubulin dimer complex should persist in the presence of AMPPNP but not ATP. To test this, we developed a gel filtration chromatography assay to analyze the interaction of Kin I kinesins versus K560 with tubulin dimer in the presence of ATP or AMPPNP. The assay is designed for small scale analysis using a Pharmacia SMART system thus requiring only small amounts of protein and nucleotide analogs (see Note 12).

6. SMART system should be set at 20 °C. Prepare ATP Column Buffer or AMPPNP Column Buffer consisting of: 1XBRB80 +75 mM KCl + 200 μM MgATP or 200 μM MgAMPPNP + 20 μM GDP + 1 mM DTT

7. Make 80 ml buffer without nucleotides or DTT, degas, then add nucleotides plus DTT and wash 1 pump into the buffer. To do this, pour ~40 ml buffer into a 50 ml conical, transfer the pump frit to the buffer (use a plastic transfer pipet to suck off water adhered to the sides of the frit) and while the pump is washing pour in the other 40 ml of buffer. With some practice one can use ~60 ml for 3 runs needed per experimental condition. NOTE: the buffer volumes described are for 10 ml pumps; some systems are equipped with 20 ml pumps which will require twice the buffer volume). The buffer volume is minimized primarily because of the expense of AMPPPNP.

8. Rinse system and 20 μl loop well with the Column Buffer. Install the Superose 6 column and equilibrate at 20 μl/min for 2 hours followed by 40 μl/min for 1 hour (20 column volumes).

9. Mix either 10 μM Tubulin + 2 μM kinesin to be tested or 10 μM tubulin alone or 2 μM kinesin alone in a buffer of the following final composition: BRB80 + 75 mM KCl + 1 mM DTT + 50 μM GDP + 3 mM MgATP/3 mM MgAMPPNP. Mix all buffer and nucleotide components before adding the proteins. Incubate at RT for 15', then spin filter using a 0.45 μm Ultrafree MC filter at 7000 rpm in an eppendorf microfuge for 2' at RT. Fractionate the

filtrate on the Superose 6 at 40 µl/min collecting 50 µl fractions. The total program is 2.9 ml after start of injection: collect fractions between 0.5 and 2.2 ml after start of injection.

10. Add 17 µl 4X Sample Buffer to each 50 µl fraction and analyze 30-35 µl on a 10% SDS-PAGE gel followed by Coomassie-staining. An example of a typical run is shown in Figure 1D.

4. NOTES

1. It is important to measure the salt concentration of the eluted fractions from each of the different preparations and to make up a control buffer that corresponds exactly to this buffer composition for all of the assays described.
2. When working with microtubules, especially with microtubules stabilized with GMPCPP, it is essential to make all buffers as potassium salts. It has been shown that the combination of glycerol and sodium ions can induce hydrolysis of GMPCPP and thus decrease the stability of these microtubule preparations (17).
3. GMPCPP MTs are cold-labile so they should not be stored on ice.
4. If taxol is added all at once it will cause tubulin precipitation! If polymerizing 2 mg/ml tubulin, use 2 µM, 20 µM and 200 µM steps
5. The axoneme concentration must be optimized for each prep such that 1 µl of the reaction (the volume pelleted onto the coverslip) results in a "good" density when viewed using a 60X

objective. "Good" density is when the axonemes are not too sparse but are also not so dense as to prevent easy photography and length measurements of the nucleated MTs.

6. A major problem with the analysis of kinesins using such an assay is the tendency of the kinesins to adsorb to flow cell surfaces and as a consequence to rigor bind MTs to surfaces as well as to remove the kinesin from solution. This problem disallows use of such an assay to quantitatively assess the effects of kinesins on the individual parameters of microtubule dynamics. Nevertheless, this assay was extremely important in our analysis since it provided direct evidence that XKCM1 is a catastrophe-inducing kinesin.

7. Using this type of quick assay we can detect depolymerization activity in lysates of insect cells infected by baculoviruses coding for Kin I kinesins but not control virus-infected cells. In addition, we can monitor depolymerization activity during purification.

8. In our assays the final concentration of MTs used was low (2 μM) because the released end product from the depolymerization induced by Kin I kinesins is competent to repolymerize To minimize complications in interpretation arising from potential repolymerization we performed the analysis at low MT concentrations. Analysis of varying MT concentration could possibly be performed using nocodazole to trap released tubulin dimer and prevent repolymerization. However, potential interference from nocodazole at MT ends might complicate interpretation of such an analysis.

9. MT glue : a preparation used to coat a flow cell such that it will bind MTs but not release, move or depolymerize them in the presence of ATP. We used a very dilute SP-Sepharose fraction from a insect cell lysate expressing low levels of XKIF2 that satisfied these three criteria. Alternatives include NEM-treated Xenopus extract (14, 18) or a mutant kinesin (19) although different adherence methods may significantly affect the observed rates of depolymerization.

10. Segmented GMPCPP MTs that have dimly labeled plus and minus end segments polymerized off brightly labeled GMPCPP MT seeds were prepared by diluting bright GMPCPP seeds (1:2 rhodamine labeled : unlabeled tubulin) into 1.5 μM dim GMPCPP tubulin mix (1:11 rhodamine labeled : unlabeled tubulin) and incubating at 37°C for 1-2 hours. All GMPCPP mixes contained 500 μM GMPCPP

11. In addition to this method, morphological analysis of GMPCPP MTs incubated with XKCM1 can also be performed using negative stain electron microscopy. In this case reaction mixes are pipeted onto a glow-discharged carbon and formvar-coated copper grid, negative stained using uranyl acetate and viewed in an electron microscope (see (4) for further details).

12. For each two-protein (i.e. Kin I kinesin-tubulin or K560-tubulin) combination there are 3 runs in ATP Column Buffer and 3 runs in AMPPNP Column Buffer (each protein alone plus the two-protein mixture). The reaction mixes should be prepared from frozen stocks, incubated and immediately injected onto the column after filtration. After the 3 runs in one

nucleotide state are done, equilibrate the column in the other nucleotide state as described in step 1. and then do the other 3 reactions.

ACKNOWLEDGEMENTS

C.E.W. was supported by the USAMRMC Breast Cancer Research Program and A.D. by a Howard Hughes Medical Institute predoctoral fellowship. The authors wish to thank Tim Mitchison in whose lab these assays were initially developed.

5. REFERENCES

1. Hirokawa, N., Noda, Y., and Okada, Y. (1998) Kinesin and dynein superfamily proteins in organelle transport and cell division. *Curr. Opin. Cell Biol.* **10**, 60-73.

2. Vale, R.D. and Fletterick, R.J. (1997) The design plan of kinesin motors. *Annu. Rev. Cell and Dev. Biol.* **13**, 745-777.

3. Yang, J.T., Laymon, R.A., and Goldstein, L.S.B. (1989) A three-domain structure of kinesin heavy chain revealed by DNA sequence and microtubule binding analyses. *Cell* **56**, 879-889.

4. Desai, A., Verma, S., Mitchison, T.J., and Walczak, C.E. (1999) Kin I kinesins are microtubule-destabilizing enzymes. *Cell* **96**, 69-78.

5. Endow, S.A., Kang, S.J., Satterwhite, L.L., Rose, M.D., Skeen, V.P., and Salmon, E.D. (1994) Yeast Kar3 is a minus-end microtubule motor protein that destabilizes microtubules preferentially at the minus ends. *Embo J* **13**, 2708-2713.

6. Saunders, W., Hornack, D., Lengyel, V., and Deng, C. (1997) The *Saccharomyces cerevisiae* kinesin-related motor Kar3p acts at preanaphase spindle poles to limit the number and length of cytoplasmic microtubules. *J. Cell Biol.* **137**, 417-431.

7. Cottingham, F.R. and Hoyt, M.A. (1997) Mitotic spindle positioning in Saccharomyces cerevisiae is accomplished by antagonistically acting microtubule motor proteins. *J. Cell Biol.* **138**, 1041-1053.

8. DeZwaan, T.M., Ellingson, E., Pellman, D., and Roof, D.M. (1997) Kinesin-related KIP3 of Saccharomyces cerevisiae is required for a distinct step in nuclear migration. *J. Cell Biol.* **138**, 1023-1040.

9. Huyett, A., Kahana, J., Silver, P., Zeng, X., and Saunders, W.S. (1998) The Kar3p and Kip2p motors function antagonistically at the spindle poles to influence cytoplasmic microtubule numbers. *J. Cell Sci.* **111**, 295-301.

10. Hyman, A., Drechsel, D., Kellogg, D., Salser, S., Sawin, K., Steffen, P., Wordeman, L., and Mitchison, T. (1991) Preparation of modified tubulins. *Meth. Enzymol.* **196**, 478-485.

11. Hyman, A.A., Salser, S., Drechsel, D.N., Unwin, N., and Mitchison, T.J. (1992) Role of GTP hydrolysis in microtubule dynamics: information from a slowly hydrolyzable analogue, GMPCPP. *Mol. Biol. Cell* **3**, 1155-1167.

12. Mitchison, T.J. and Kirschner, M.W. (1984) Dynamic instability of microtubule growth. *Nature* **312**, 237-242.

13. Evans, L., Mitchison, T., and Kirschner, M. (1985) Influence of the centrosome on the structure of nucleated microtubules. *J. Cell Biol.* **100**, 1185-1191.

14. Vale, R.D. (1991) Severing of stable microtubules by a mitotically activated protein in Xenopus egg extracts. *Cell* **64**, 827-839.

15. Shimizu, T., Toyoshima, Y.Y., and Vale, R.D. (1993) *Use of ATP analogs in motor assays*, in "Motility Assays for Motor Proteins" (J.M. Scholey, Editor 167-176. Academic Press, Inc., San Diego.

16. Caplow, M., Ruhlen, R.L., and Shanks, J. (1994) The free energy for hydrolysis of a microtubule-bound nucleotide triphosphate is near zero: all of the free energy for hydrolysis is stored in the microtubule lattice. *J. Cell Biol.* **127**, 779-788.

17. Caplow, M. and Shanks, J. (1996) Evidence that a single monolayer tubulin-GTP cap is both necessary and sufficeint to stabilize microtubules. *Mol. Biol. Cell* **7**, 663-675.

18. McNally, F.J. and Vale, R.D. (1993) Identification of katanin, an ATPase that severs and disassembles stable microtubules. *Cell* **75**, 419-429.

19. Hartman, J.J., Mahr, J., McNally, K., Okawa, K., Shimizu, T., Vale, R.D., and McNally, F. (1998) Katanin, a microtubule-severing protein, is a novel AAA ATPase that targets to the centrosome using a WD40-containing subunit. *Cell* **93**, 277-287.

FIGURE LEGEND:

Figure 1. Examples of results from various assays used to detect microtubule destabilization activity. (A). Results from fixed time-point assay on dynamic microtubules showing microtubules incubated with a control buffer (left-hand panel) or XKCM1 (right-hand panel). (B) Results from a qualitative visual fluorescence assay on stabilized microtubule substrates showing GMPCPP microtubules incubated with a control buffer (left-hand panel) or XKCM1 (right-hand panel). The small inset shows the results of the same samples run on a sedimentation analysis. (C) Results from the immunofluorescence analysis showing the localization of tubulin (left-hand panel) and XKCM1 (right-hand panel) during microtubule depolymerization. (D) Results from the tubulin dimer binding assays showing the nucleotide-dependency of XKIF2 binding to tubulin as analyzed by gel filtration chromatography. Reproduced from Desai et. al (1999) Cell 96: 69-78 with permission from the publisher.

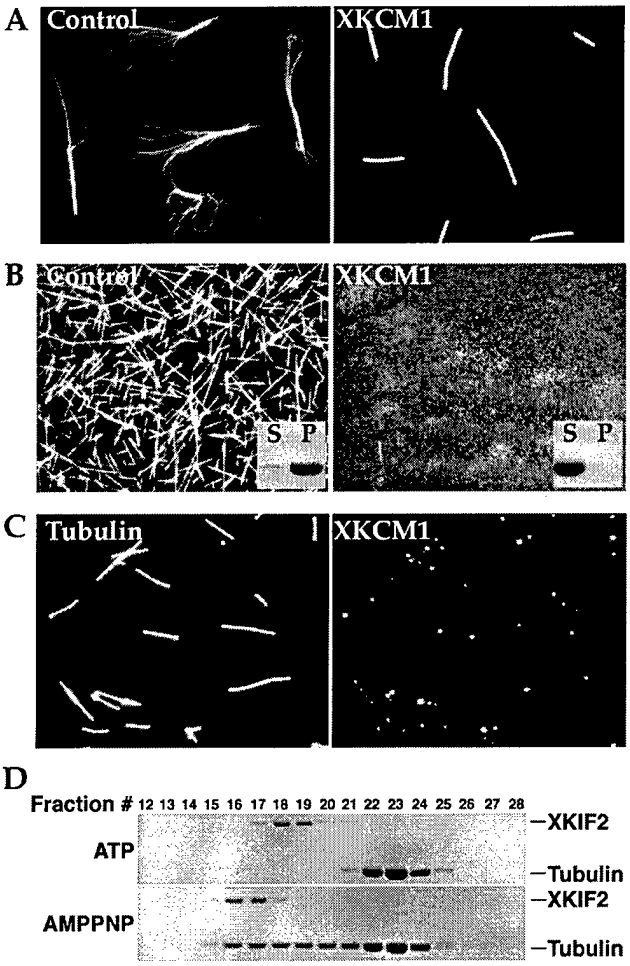
A
Control
XKCM1
B
Control
XKCM1
S P
S P
C
Tubulin
XKCM1
D
Fraction # 12 13 14 15 16 17 18 19 20 21 22 23 24 25 26 27 28
ATP
AMPPNP
—XKIF2
—Tubulin
—XKIF2
—Tubulin

Microtubule-based motor function in mitosis

Rebecca Heald* and Claire E Walczak†

Microtubule-based motors are essential both for the proper assembly of the mitotic spindle and for chromosome segregation. Mitotic motors in the yeast *Saccharomyces cerevisiae* exhibit either overlapping or opposing activities in order to achieve proper spindle function, whereas the analysis of motors using vertebrate cytoplasmic extracts has revealed less functional redundancy. In several systems, biochemical, genetic and two-hybrid approaches have been used both to identify associated nonmotor proteins and to address the molecular mechanisms behind kinetochore movements during chromosome alignment and segregation.

Addresses
*Department of Molecular and Cell Biology, 311 LSA, University of California, Berkeley, CA 94720-3200, USA;
e-mail: heald@socrates.berkeley.edu
†Indiana University, Medical Sciences Program, Jordan Hall 306, Bloomington, IN 47405, USA; e-mail: cwalczak@indiana.edu
Correspondence: Claire E Walczak

Current Opinion in Structural Biology 1999, **9**:268–274

http://biomednet.com/elecref/0959440X00900268

 ISSN 0959-440X

Abbreviations

BUB1	budding uninhibited by benzimidazole
CENP-E	centromere protein E
CLIP-170	cytoplasmic linker protein 170
KRP	kinesin-related protein
MCAK	mitotic centromere-associated kinesin
NuMA	nuclear/mitotic apparatus protein

Introduction

Mitosis is the process by which a cell faithfully and accurately distributes its genetic material to two daughter cells. This process is carried out on the mitotic spindle, the macromolecular apparatus that functions to physically segregate the duplicated chromosomes into two complete sets. The spindle is composed of microtubules and associated proteins that, together, create the forces that are necessary both to assemble and orient the spindle apparatus and to drive chromosome segregation during anaphase. Microtubule-based motor proteins, which couple the energy of ATP hydrolysis to movement and force production, are central to these processes.

The past year has seen significant advances in our understanding of the molecular mechanisms by which motor proteins function during mitosis. The integration of individual motor activities in spindle formation and function has been elucidated both *in vivo*, through yeast genetics, and *in vitro*, with the use of vertebrate cytoplasmic extracts. Information is also emerging regarding the physical interactions among motor and nonmotor proteins in the spindle. In addition, chromosome alignment and segregation is an area of intense research that is beginning to yield a molecular foundation for understanding the functions of motor proteins at the kinetochore. The analysis of different motor functions during mitosis has benefited immensely from technical advances in real-time imaging of living cells.

In this review, we discuss papers published since 1997 that address the role of microtubule-based motors in mitosis. Although actively investigated in a broad range of organisms, we focus primarily on motor function in the yeast *S. cerevisiae* and in vertebrate cells and cytoplasmic extracts. We have attempted to highlight papers providing insight into the function of the spindle as a whole, but these represent only a fraction of the exciting work characterized by this field.

Motors in spindle assembly

Several recent studies have examined how multiple motor proteins function in concert in a single system. The most thorough analysis has been carried out in the yeast *S. cerevisiae*, as complete genome sequencing has revealed all of the motor proteins in this organism.

Budding yeast spindle assembly and chromosome segregation

S. cerevisiae division occurs through an unconventional mechanism, in which the daughter cell buds off from the mother cell. This requires the proper positioning of the spindle in the mother-bud neck. Recent studies have demonstrated a role for two different kinesin-related proteins (KRPs) in this process, Kip2p and Kip3p, as well as a role for cytoplasmic dynein, encoded by the *DYN1* gene [1,2,3••,4•,5••,6]. None of these genes is essential and major defects are apparent only when more than one of them is deleted. Careful cytological and genetic analyses, however, have revealed that the functions of these proteins are overlapping, but not identical [4•,5••,7]. Spindle positioning at the mother-bud neck appears to be accomplished primarily by Kip3p, whereas dynein function appears to be important to ensure the insertion of the spindle into the bud during anaphase [5••]. Kip2p is thought to contribute to nuclear positioning by exerting a force towards the mother cell that antagonizes the force exerted by Kip3p and dynein [4•].

Like spindle positioning, spindle assembly and function is also achieved through the activities of multiple motors. The major players in spindle assembly and chromosome segregation are the KRPs Cin8p and Kip1p. Both Cin8p and Kip1p are important for spindle pole separation and anaphase spindle elongation, but the effects due to the loss of Cin8p are more severe than those due to the loss of Kip1p [8–10]. The actions of Cin8p and Kip1p are opposed by the activity of the KRP Kar3p, which provides an inward force that is relieved at the onset of anaphase [11•,12]. Dynein also contributes to anaphase chromosome segregation, perhaps by pulling the spindle through the mother-bud neck

34. Tuma PL, Stachniak MC, Collins CA: **Activation of dynamin GTPase by acidic phospholipids and endogenous rat brain vesicles.** *J Biol Chem* 1993, **268**:17240-17246.

35. Kjeldgaard M, Nyborg J, Clark BFC: **The GTP binding motif: variations on a theme.** *FASEB J* 1996, **10**:1347-1368.

36. Nogales E, Downing KH, Amos LA, Lowe J: **Tubulin and FtsZ form a distinct family of GTPases.** *Nat Struct Biol* 1998, **5**:451-458.

37. • Muhlberg AB, Warnock DE, Schmid SL: **Domain structure and intramolecular regulation of dynamin GTPase.** *EMBO J* 1997, **16**:6676-6683.
This paper defines the GTPase effector domain (GED), located in the C-terminal half of dynamin between the proline-rich and pleckstrin homology (PH) domains, and shows that the GED is necessary for efficient GTPase activity. This paper also shows that the PH domain is not required for self-assembly and may act as a negative regulator of the GTPase activity.

38. Ferguson KM, Lemmon MA, Schlessinger J, Sigler PB: **Crystal structure at 2.2 Å resolution of the pleckstrin homology domain from human dynamin.** *Cell* 1994, **79**:199-209.

39. Timm D, Salim K, Gout I, Guruprasad L, Waterfield M, Blundell T: **Crystal structure of the pleckstrin homology domain from dynamin.** *Nat Struct Biol* 1994, **1**:782-788.

40. Zheng J, Cahill SM, Lemmon MA, Fushman D, Schlessinger J, Cowburn D: **Identification of the binding site for acidic phospholipids on the PH domain of dynamin: implications for stimulation of GTPase activity.** *J Mol Biol* 1996, **255**:14-21.

41. Salim K, Bottomley MJ, Querfurth E, Zvelebil MJ, Gout I, Scaife R, Margolis RL, Gigg R, Smith CI, Driscoll PC *et al.*: **Distinct specificity in the recognition of phosphoinositides by the pleckstrin homology domains of dynamin and Bruton's tyrosine kinase.** *EMBO J* 1996, **15**:6241-6250.

42. Schmid SL, Sever S, Muhlberg AB, Damke H: **Novel mechanisms coordinating dynamin GTPase activity and regulating endocytosis.** *Mol Biol Cell* 1998, **9**:128.

43. Okamoto PM, Herskovits JS, Vallee RB: **Role of the basic, proline-rich region of dynamin in Src homology 3 domain binding and endocytosis.** *J Biol Chem* 1997, **272**:11629-11635.

44. Grabs D, Slepnev VI, Songyang Z, David C, Lynch M, Cantley LC, De Camilli P: **The SH3 domain of amphiphysin binds the proline-rich domain of dynamin at a single site that defines a new SH3 binding consensus sequence.** *J Biol Chem* 1997, **272**:13419-13425.

45. Gout I, Dhand R, Hiles ID, Fry MJ, Panayotou G, Das P, Truong O, Totty NF, Hsuan J, Booker GW *et al.*: **The GTPase dynamin binds to and is activated by a subset of SH3 domains.** *Cell* 1993, **75**:25-36.

46. Miki H, Miura K, Matuoka K, Nakata T, Hirokawa N, Orita S, Kaibuchi K, Takai Y, Takenawa T: **Association of Ash/Grb-2 with dynamin through the Src homology 3 domain.** *J Biol Chem* 1994, **269**:5489-5492.

47. Carr JF, Hinshaw JE: **Dynamin assembles into spirals under physiological salt conditions upon the addition of GDP and gamma-phosphate analogues.** *J Biol Chem* 1997, **272**:28030-28035.

48. Hinshaw JE, Schmid SL: **Dynamin self-assembles into rings suggesting a mechanism for coated vesicle budding.** *Nature* 1995, **374**:190-192.

49. Scaife R, Venien-Bryan C, Margolis RL: **Dual function C-terminal domain of dynamin-1: modulation of self-assembly by interaction of the assembly site with SH3 domains.** *Biochemistry* 1998, **37**:17673-17679.

50. Takei K, McPherson PS, Schmid SL, De Camilli P: **Tubular membrane invaginations coated by dynamin rings are induced by GTP-γ S in nerve terminals.** *Nature* 1995, **374**:186-190.

51. Takei K, Mundigl O, Daniell L, De Camilli P: **The synaptic vesicle cycle: a single vesicle budding step involving clathrin and dynamin.** *J Cell Biol* 1996, **133**:1237-1250.

52. • Takei K, Haucke V, Slepnev V, Farsad K, Salazar M, Chen H, De Camilli P: **Generation of coated intermediates of clathrin-mediated endocytosis on protein-free liposomes.** *Cell* 1998, **94**:131-141.
In this study, dynamin-decorated tubules were shown to form when liposomes were incubated either with cytosol, GTPγS and ATP, or with purified dynamin in the absence or presence of GTP or GTPγS. This work establishes that transmembrane or anchor proteins are not necessary for the assembly of the clathrin coat and dynamin spirals onto the lipid bilayer.

53. Lin HC, Barylko B, Achiriloaie M, Albanesi JP: **Phosphatidylinositol (4,5)-bisphosphate-dependent activation of dynamins I and II lacking the proline/arginine-rich domains.** *J Biol Chem* 1997, **272**:25999-26004.

54. Klein DE, Lee A, Frank DW, Marks MS, Lemmon MA: **The pleckstrin homology domains of dynamin isoforms require oligomerization for high affinity phosphoinositide binding.** *J Biol Chem* 1998, **273**:27725-27733.

55. Baba T, Damke H, Hinshaw JE, Ikeda K, Schmid SL, Warnock DE: **Role of dynamin in clathrin-coated vesicle formation.** *Cold Spring Harb Symp Quant Biol* 1995, **60**:235-242.

56. Shpetner HS, Herskovits JS, Vallee RB: **A binding site for SH3 domains targets dynamin to coated pits.** *J Biol Chem* 1996, **271**:13-16.

57. David C, McPherson PS, Mundigl O, De Camilli P: **A role of amphiphysin in synaptic vesicle endocytosis suggested by its binding to dynamin in nerve terminals.** *Proc Natl Acad Sci USA* 1996, **93**:331-335.

58. Wang LH, Sudhof TC, Anderson RG: **The appendage domain of alpha-adaptin is a high affinity binding site for dynamin.** *J Biol Chem* 1995, **270**:10079-10083.

59. Gonzalez-Gaitan M, Jackle H: **Role of *Drosophila* alpha-adaptin in presynaptic vesicle recycling.** *Cell* 1997, **88**:767-776.

60. Artalejo CR, Lemmon MA, Schlessinger J, Palfrey HC: **Specific role for the PH domain of dynamin-1 in the regulation of rapid endocytosis in adrenal chromaffin cells.** *EMBO J* 1997, **16**:1565-1574.

61. Jost M, Simpson F, Kavran JM, Lemmon MA, Schmid SL: **Phosphatidylinositol-4,5-bisphosphate is required for endocytic coated vesicle formation.** *Curr Biol* 1998, **8**:1399-1402.

62. Nakayama M, Yazaki K, Kusano A, Nagata K, Hanai N, Ishihama A: **Structure of mouse Mx1 protein.** *J Biol Chem* 1993, **20**:15033-15038.

63. Shin HW, Shinotsuka C, Torii S, Murakami K, Nakayama K: **Identification and subcellular localization of a novel mammalian dynamin-related protein homologous to yeast Vps1p and Dnm1p.** *J Biochem (Tokyo)* 1997, **122**:525-530.

64. Ma X, Ehrhardt DW, Margolin W: **Co-localization of cell division proteins FtsZ and FtsA to cytoskeleton structures in living *Escherichia coli* cells by using green fluorescent protein.** *Proc Natl Acad Sci USA* 1996, **993**:12998-13003.

Figure 1

Motors involved in mitosis in the yeast *S. cerevisiae*. As the cell enters mitosis, Kip3p is important in positioning of the nucleus at the site of the mother-bud neck. Kip2p, Kar3p and dynein also contribute to spindle positioning. As the cell enters anaphase, Cin8p is important for the fast phase of anaphase spindle elongation, while Kip1p is important for the slow phase of spindle elongation. Dynein is proposed to contribute to chromosome segregation through its action on cytoplasmic microtubules. At the end of mitosis, Kip3p is important for the breakdown of the spindle microtubules.

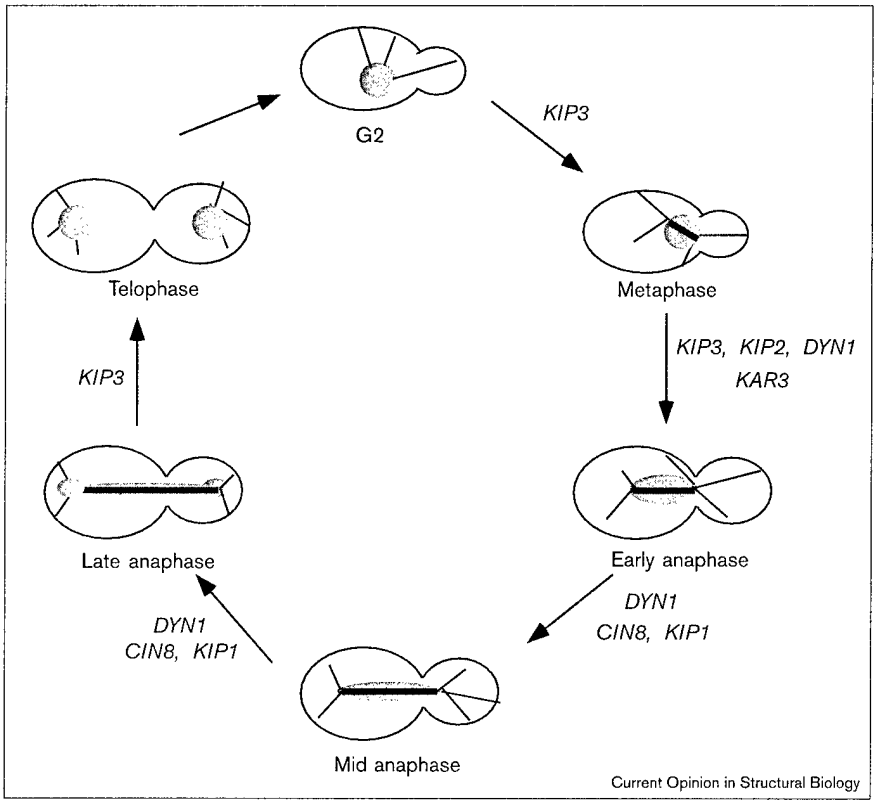

[3••,5••,13]. At the end of anaphase, Kip3p is thought to promote the breakdown of the spindle, as *kip3* mutants have longer spindles that persist relative to the wild type [14••].

The analysis of motors in yeast and other organisms is benefiting tremendously from the use of time-lapse video microscopy combined with the fluorescent tagging of proteins. This approach has allowed researchers to analyze the dynamics of spindles, microtubules, chromosomes and centromeres in wild type and mutant living cells [3••,6,14••,15••,16,17]. In *S. cerevisiae*, such elegant genetic and morphological analyses have allowed the assignment of specific motors to given functions, as outlined in Figure 1.

Do motors regulate microtubule dynamics?

One interesting finding that has emerged from recent yeast studies is that the deletion of many of the motor proteins affects microtubule stability. The deletion of *KAR3*, *DYN1* or *KIP3* causes an increase in the number and length of cytoplasmic microtubules, whereas the deletion of *KIP2* causes a reduction in the number and length of cytoplasmic microtubules [3••,4•,5••,7,12]. Of these motors, only Kar3p has been analyzed *in vitro* in motility assays and has been shown to destabilize microtubule minus ends [18] and only *dyn1Δ* cells have been examined carefully for effects on microtubule dynamics *in vivo* [3••]. It will be important to determine whether these motors regulate microtubule stability directly or indirectly through altering microtubule attachments to cellular structures, such as the cortex or other microtubules.

Establishing spindle bipolarity

An alternative approach to the *in vivo* analyses of spindle function in yeast and other organisms has been to reconstitute aspects of spindle assembly in cell-free systems [19–21]. This approach allows biochemical examination of protein function through immunodepletion and antibody blocking experiments. During the past year, the roles of several motor proteins have been better defined using these *in vitro* approaches in *Xenopus* egg extracts [22•,23,24,25••] and in HeLa cell extracts [26•,27]. These experiments have generated a model for the proposed roles of several different motors in determining bipolar spindle structure, as outlined in Figure 2. The *Xenopus* chromokinesin Xklp1 appears to mediate chromatin–microtubule attachments, independent of kinetochores, and contributes to spindle pole extension. Eg5, a highly conserved tetrameric motor, is crucial for establishing spindle bipolarity by providing a microtubule bundling and antiparallel sorting activity. The motors cytoplasmic dynein and XCTK2 are both important in spindle pole formation, with dynein playing the dominant role. In contrast to experiments in yeast, the disruption of individual motors in vertebrate cell extracts often has dramatic effects, which has made motor functions easier to dissect in these systems. This surprising observation may be explained by the fact that extract systems are more easily perturbed or

Figure 2

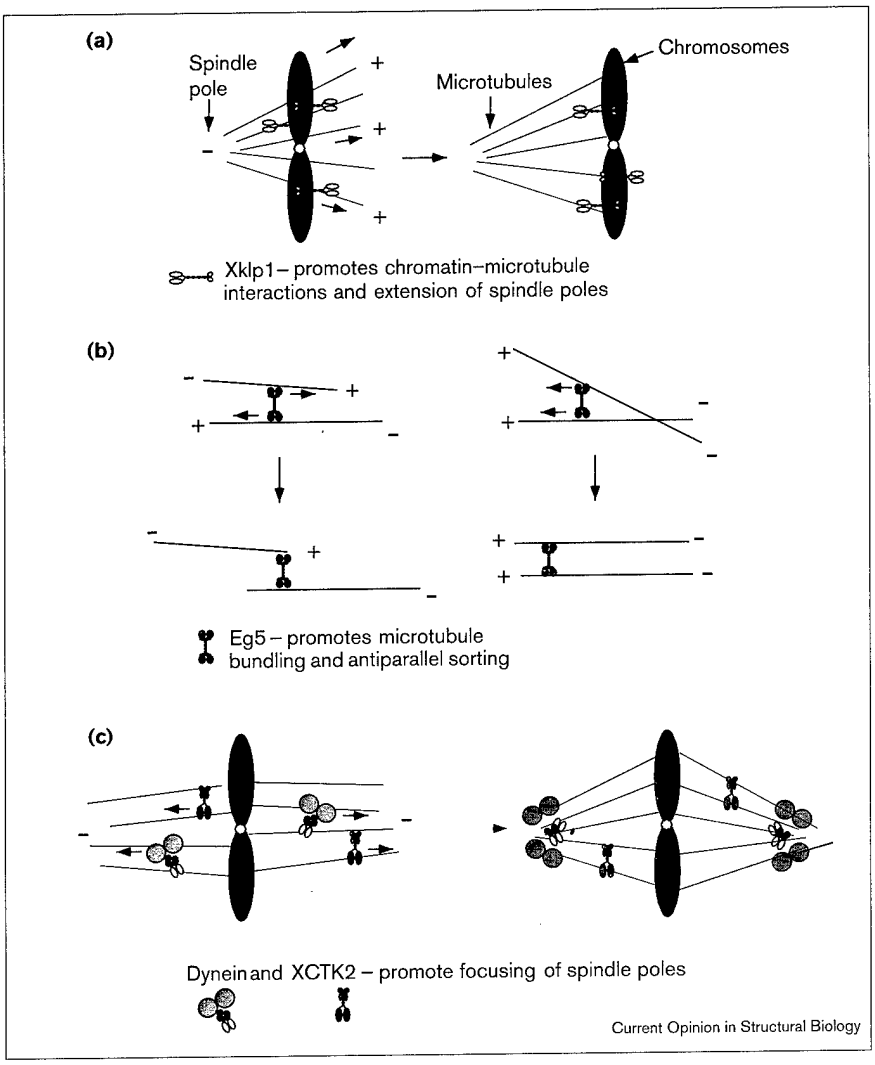

Proposed roles of different motors in generating a bipolar spindle in vertebrate cells. **(a)** Chromosomally localized Xklp1 connects microtubules to chromosome arms and provides a force for extending spindle poles. **(b)** As it is a plus-end-directed tetramer, Eg5 could contribute to spindle bipolarity by bundling microtubules to form a bipolar axis and by sorting microtubules into an antiparallel array. **(c)** Both minus-end-directed motors, cytoplasmic dynein and XCTK2 are involved in the organization and focusing of microtubule minus ends into spindle poles.

that only a subset of vertebrate spindle motors have been identified or that this discrepancy may reflect a true difference in the level of motor redundancy between budding yeast and vertebrate cells.

Motor-associated proteins

Two major questions with respect to motor protein function in the spindle are how are the motor interactions with the spindle regulated and what nonmotor proteins are involved in motor targeting. These questions have been difficult to address because most motor interactions appear to be labile. Several groups have made significant progress in this area through the use of biochemical and two-hybrid screening analyses.

Interactions in the spindle

Cytoplasmic dynein localization and its spindle pole focusing activity appear to depend on its interaction with both the dynein-activating complex dynactin and the nuclear/mitotic apparatus protein (NuMA), as similar defects in pole formation result from their disruption [22•,23,26•,28]. In support of these interactions, a complex containing dynein, dynactin and NuMA was isolated from *Xenopus* egg extracts [29]; however, dynein interactions have proved to be less tractable in other systems [27]. Dynactin may serve as a linker protein between different motors in the spindle. Recent studies have shown that the $p150^{glued}$ subunit of dynactin interacts with the phosphorylated version of the human Eg5 C-terminal tail domain in a two-hybrid assay [30]. Previous work indicated that the phosphorylation of Eg5 family tail domains is essential for the localization of the motor to the spindle [31–33]. The universality of this mechanism is questioned, however, by a recent study showing that the phosphorylation of the tail of the *Schizosaccharomyces pombe* homolog of Eg5, Cut7, is not required for spindle localization [34]. Therefore, how Eg5 associates with the spindle and the role of dynactin in this process remains to be fully elucidated.

Figure 3

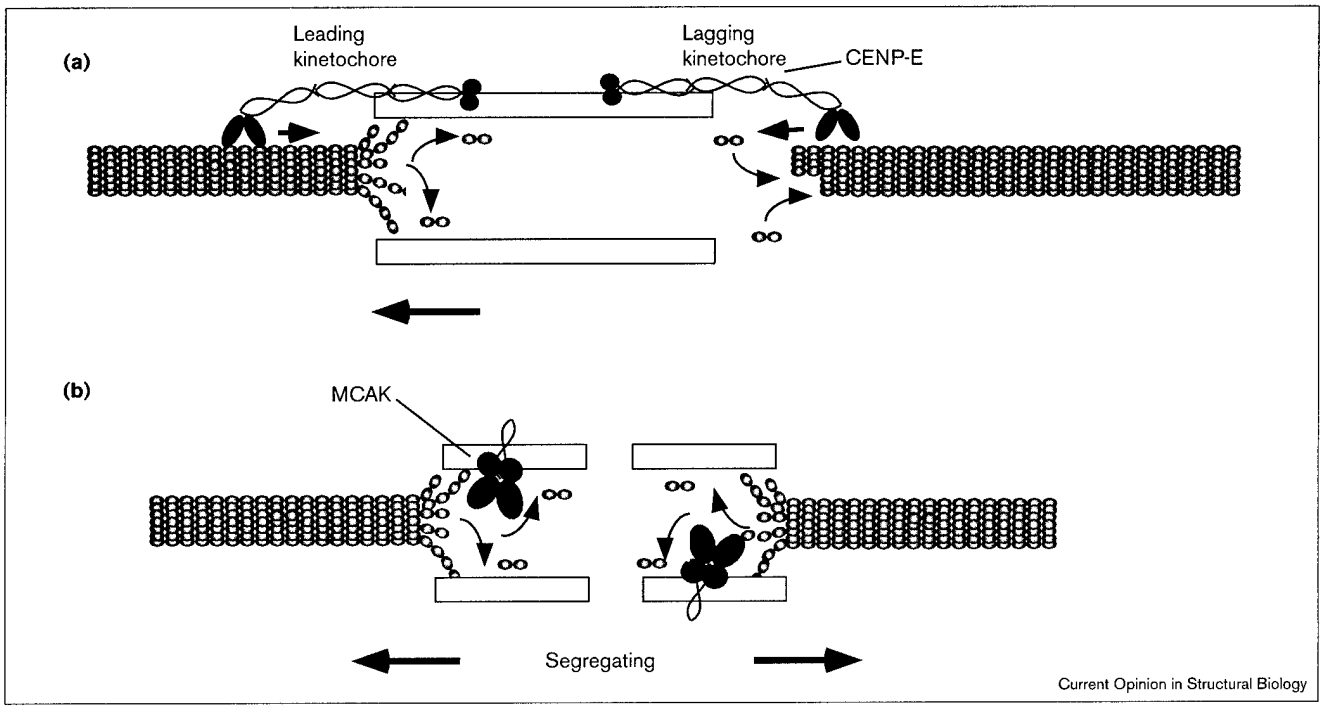

Proposed motor protein function at the kinetochore. **(a)** CENP-E, a plus-end-directed kinesin, is thought to act at the leading kinetochore (direction of movement indicated by the arrow) by maintaining attachment to the microtubule. At the lagging kinetochore, CENP-E acts to stabilize kinetochore–microtubule interactions. **(b)** MCAK function at kinetochores contributes to anaphase chromosome segregation. MCAK, which is proposed to act as a microtubule-destabilizing enzyme, may function by inducing microtubule depolymerization at kinetochores during anaphase.

Recent experiments on the C-terminal spindle-targeting domain of the *Xenopus* motor Xklp2, which is involved in centrosome separation, have revealed that two factors in mitotic extracts are required for the proper localization of Xklp2. A novel microtubule-associated protein (TPX2) mediates the binding of the Xklp2 tail to microtubules, whereas the dynein–dynactin complex is required for the accumulation of Xklp2 at microtubule minus ends [35]. Therefore, motor targeting appears to be a complex process depending on interactions between both motor and nonmotor proteins.

Interactions at the kinetochore

The dynein–dynactin complex also appears to play an important role in targeting proteins to the kinetochore, including the microtubule/vesicle-binding protein CLIP-170 (cytoplasmic linker protein 170). The overexpression of the dynactin subunit p50 (dynamitin) causes a decrease in CLIP-170 staining at kinetochores in mammalian tissue culture cells [36•]. Like dynein–dynactin, the association of CLIP-170 with the kinetochore appears to be required for prometaphase chromosome alignment [36•]. The current model is that dynactin is required for the targeting of dynein and other proteins to kinetochores, but what proteins recruit dynactin? The key to this may be ZW10, a *Drosophila melanogaster* kinetochore protein required for chromosome segregation [37,38••,39•]. Mutations in the *ZW10* gene abolish the localization of dynein at kinetochores. This link may be mediated by dynactin, as p50/dynamitin interacts with ZW10 in a yeast two-hybrid assay [39•]. Thus, ZW10 may be one of the initial components recruited to the kinetochore, onto which motor complexes assemble.

Two-hybrid analysis may prove to be an effective way of determining and confirming the associations of proteins on the spindle and at the kinetochore. A two-hybrid screen using the kinetochore-targeting domain of centromere protein E (CENP-E) was used to isolate interacting proteins from a cDNA library [40•]. This screen identified CENP-E itself, as well as CENP-F, another known kinetochore protein, indicating the validity of the approach. In addition, a BUB1-related kinase, hBUBR1, was identified. BUB1 (budding uninhibited by benzimidazole) kinases have been shown to be conserved between yeast and mammals, and are required for regulating mitotic checkpoints at the kinetochore [41•]. Therefore, the connection between CENP-E and BUB1 links kinetochore motor proteins that are important for moving chromosomes with the checkpoint machinery, which determines chromosome misattachment and signals the cell to delay mitosis until all the chromosomes are attached and aligned.

Motors in chromosome movement

Both motors and microtubule dynamics appear to regulate kinetochore movements and chromosome positioning, making it a challenge to study their relative roles. Several recent studies have begun to elucidate the molecular mechanisms by which two kinetochore-associated kinesins may function [42••–44••] (Figure 3). Using a variety of techniques, CENP-E was shown to be important for chromosome alignment. One study used a combination of microinjection and transfection experiments to show the importance of CENP-E function in aligning chromosomes *in vivo* [43••]. Under these conditions, CENP-E-depleted kinetochores were not capable of establishing stable bipolar connections on the spindle, which inhibited their ability to align on the metaphase plate. A complementary study in *Xenopus* egg extracts showed that CENP-E functions as a plus-end-directed microtubule motor that is essential for chromosome alignment during metaphase [42••]. The requirement for CENP-E in chromosome positioning is consistent with earlier studies indicating a role for this motor in coupling chromosome movement with microtubule depolymerization [45]. The mitotic centromere-associated kinesin (MCAK), another kinetochore KRP, was shown to be important in chromosome segregation [44••]. Using antisense-induced depletion of MCAK from kinetochores or transfection of dominant-negative constructs, a lagging chromosome phenotype was observed during anaphase, indicating a defect in chromosome segregation. MCAK is the mammalian homolog of the *Xenopus* XKCM1 protein, which was shown to be a microtubule-destabilizing enzyme [46,47••]. It is not yet clear whether the role of MCAK/XKCM1 at the kinetochore involves microtubule destabilization.

Conclusions

The role of motor proteins in mitosis is becoming more evident, but the mechanisms of spindle assembly and chromosome movement are not yet fully understood. Elegant genetic and microscopy studies in budding yeast have begun to define the roles of motor proteins in this system. Future biochemical experiments will determine the motility properties of each motor and will clarify their effects on microtubule dynamics. In addition, an important issue is to measure the dynamics of individual microtubules within the yeast spindle. This has proven to be difficult, because the yeast spindle consists of a bundle of microtubules that is difficult to resolve. The great advances in high-resolution microscopy and the innovative scientists behind these advances will soon transcend these barriers.

Motor targeting appears to be a complex process involving interactions among both motor and nonmotor proteins. Cytoplasmic dynein, which plays a role in both spindle pole assembly and kinetochore function, appears to interact with dynactin at multiple sites in the cell, and the dynein–dynactin complex interacts specifically with NuMA and the Xklp2 tail at spindle poles, and with ZW10 at kinetochores. The identification of other motor-associated proteins through genetic, biochemical and two-hybrid analyses will help to address the complex process of motor targeting and will expand our knowledge of how the spindle functions as a macromolecular assembly.

Studies of two different motor proteins at the kinetochore are finally allowing us to address the complex movements required for chromosome alignment in metaphase and chromosome segregation in anaphase. Inhibitors generated against both CENP-E and MCAK/XKCM1 will be valuable tools for probing the movements of chromosomes on the spindle using high-resolution video microscopy in living cells. In addition, electron microscopy studies will allow us to probe the ultrastructural basis of chromosome movement by comparing normal and defective spindles and kinetochores.

The achievements during the past several years in this field have been outstanding and they will continue to be so as more reagents and techniques become available to us. This rapid progress is exciting as we continue to advance our understanding of this remarkable area of cell biology.

Acknowledgement

We thank Jan Paluh at the University of California, Berkeley for critical reading of the manuscript.

References and recommended reading

Papers of particular interest, published within the annual period of review, have been highlighted as:

- • of special interest
- •• of outstanding interest

1. Eshel D, Urrestarazu LA, Vissers S, Jauniaux J-C, van Vliet-Reedijk JC, Planta RJ, Gibbon IR: **Cytoplasmic dynein is required for normal nuclear segregation in yeast.** *Proc Natl Acad Sci USA* 1993, **90**:11172-11176.

2. Li Y, Yeh E, Hays T, Bloom K: **Disruption of mitotic spindle orientation in a yeast dynein mutant.** *Proc Natl Acad Sci USA* 1993, **90**:10096-10100.

3. •• Carminati JL, Stearns T: **Microtubules orient the mitotic spindle in yeast through dynein-dependent interactions with the cell cortex.** *J Cell Biol* 1997, **138**:629-641.
The authors used green fluorescent protein–tubulin to visualize and measure microtubule dynamics in living yeast cells and found that cytoplasmic microtubules exhibit dynamic instability. Dynein mutant cells were demonstrated to have altered dynamics and defects in cortical interactions.

4. • Cottingham FR, Hoyt MA: **Mitotic spindle positioning in *Saccharomyces cerevisiae* is accomplished by antagonistically acting microtubule motor proteins.** *J Cell Biol* 1997, **138**:1041-1053.
A detailed genetic analysis was used to determine which motor proteins are important for spindle positioning. The authors found that both Kip3p and dynein play a role that is antagonized by Kip2p.

5. •• DeZwaan TM, Ellingson E, Pellman D, Roof DM: **Kinesin-related *KIP3* of *Saccharomyces cerevisiae* is required for a distinct step in nuclear migration.** *J Cell Biol* 1997, **138**:1023-1040.
This paper presents a detailed analysis of *kip3* mutants, showing the requirement for this protein in spindle positioning. The authors used time-lapse microscopy of living yeast cells undergoing mitosis to achieve a careful and thorough characterization of the mutant phenotype.

6. Yeh E, Skibbens RV, Cheng JW, Salmon ED, Bloom K: **Spindle dynamics and cell cycle regulation of dynein in the budding yeast, *Saccharomyces cerevisiae*.** *J Cell Biol* 1995, **130**:687-700.

7. Miller RK, Heller KK, Frisen L, Wallack DL, Loayza D, Gammie AE, Rose MD: **The kinesin-related proteins, Kip2p and Kip3p, function differently in nuclear migration in yeast.** *Mol Biol Cell* 1998, **9**:2051-2068.

8. Hoyt MA, He L, Loo KK, Saunders WS: **Two *Saccharomyces cerevisiae* kinesin-related gene products required for mitotic spindle assembly.** *J Cell Biol* 1992, **118**:109-120.

9. Roof DM, Meluh PB, Rose MD: **Kinesin-related proteins required for assembly of the mitotic spindle.** *J Cell Biol* 1992, **118**:95-108.

10. Geiser JR, Schott EJ, Kingsbury TJ, Cole NB, Totis LJ, Bhattacharyya G, He L, Hoyt MA: ***Saccharomyces cerevisiae* genes required in the absence of the CIN8-encoded spindle motor act in functionally diverse mitotic pathways.** *Mol Biol Cell* 1997, **8**:1035-1050.

11. • Saunders W, Hornack D, Lengyel V, Deng C: **The *Saccharomyces cerevisiae* kinesin-related motor Kar3p acts at preanaphase spindle poles to limit the number and length of cytoplasmic microtubules.** *J Cell Biol* 1997, **137**:417-431.
The authors found that Kar3p acts to control both the number and the length of cytoplasmic microtubules in the preanaphase spindle. They also found that Kar3p is localized to spindle poles during metaphase, but its staining is lost by late anaphase.

12. Saunders W, Lengyel V, Hoyt MA: **Mitotic spindle function in *Saccharomyces cerevisiae* requires a balance between different types of kinesin-related motors.** *Mol Biol Cell* 1997, **8**:1025-1033.

13. Saunders WS, Koshland D, Eshel D, Gibbons IR, Hoyt MA: ***Saccharomyces cerevisiae* kinesin- and dynein-related proteins required for anaphase chromosome segregation.** *J Cell Biol* 1995, **128**:617-624.

14. •• Straight AF, Sedat JW, Murray AW: **Time-lapse microscopy reveals unique roles for kinesins during anaphase in budding yeast.** *J Cell Biol* 1998, **143**:687-694.
Using green fluorescent protein-labeled centromeres and microtubules, the authors followed mitosis in living wild-type yeast cells and mutants of *cin8*, *kip1* and *kip3*. The precise contributions of each of these motors to spindle function was determined. Cin8p is important during the initial rapid phase of anaphase B, while Kip1p contributes to the slow phase of spindle elongation. Kip3p appears to be important for the proper timing of spindle disassembly.

15. •• Straight AF, Marshall WF, Sedat JW, Murray AW: **Mitosis in living budding yeast: anaphase A but no metaphase plate.** *Science* 1997, **277**:574-578.
This was the first live analysis of mitosis in yeast in which both microtubules and chromosomes were followed because they were labeled with green fluorescent protein. The authors demonstrated that yeast chromosomes do not align in a metaphase plate configuration that is typical of mammalian cells, but do exhibit both anaphase A and anaphase B type chromosome movements.

16. Ding DQ, Chikashige Y, Haraguchi T, Hiraoka Y: **Oscillatory nuclear movement in fission yeast meiotic prophase is driven by astral microtubules, as revealed by continuous observation of chromosomes and microtubules in living cells.** *J Cell Sci* 1998, **111**:701-712.

17. Endow SA, Komma DJ: **Centrosome and spindle function of the *Drosophila* Ncd microtubule motor visualized in live embryos using Ncd-GFP fusion proteins.** *J Cell Sci* 1996, **109**:2429-2442.

18. Endow SA, Kang SJ, Satterwhite LL, Rose MD, Skeen VP, Salmon ED: **Yeast Kar3 is a minus-end microtubule motor protein that destabilizes microtubules preferentially at the minus ends.** *EMBO J* 1994, **13**:2708-2713.

19. Compton DA: **Production of M-phase and I-phase extracts from mammalian cells.** *Methods Enzymol* 1998, **298**:331-339.

20. Desai A, Murray A, Mitchison TJ, Walczak CE: **The use of *Xenopus* egg extracts to study mitotic spindle assembly and function *in vitro*.** *Methods Cell Biol* 1999, **61**:385-412.

21. Heald R, Tournebize R, Vernos I, Murray A, Hyman A, Karsenti E: ***In vitro* assays for mitotic spindle assembly and function.** In *Cell Biology: A Laboratory Handbook*. Edited by Celis J. New York: Cold Spring Harbor Press; 1998, **2**:326-335.

22. • Heald R, Tournebize R, Habermann A, Karsenti E, Hyman A: **Spindle assembly in *Xenopus* egg extracts: respective roles of centrosomes and microtubule self-organization.** *J Cell Biol* 1997, **138**:615-628.
The authors used extracts from *Xenopus* eggs to examine spindle assembly in the presence and absence of centrosomes. They found that dynein is required for spindle pole formation in both cases, but that centrosomes serve as the dominant sites for pole formation.

23. Merdes A, Cleveland DW: **Pathways of spindle pole formation: different mechanisms; conserved components.** *J Cell Biol* 1997, **138**:953-956.

24. Walczak CE, Verma S, Mitchison TJ: **XCTK2: a kinesin-related protein that promotes mitotic spindle assembly in *Xenopus laevis* egg extracts.** *J Cell Biol* 1997, **136**:859-870.

25. •• Walczak CE, Vernos I, Mitchison TJ, Karsenti E, Heald R: **A model for the proposed roles of different microtubule-based motor proteins in establishing spindle bipolarity.** *Curr Biol* 1998, **8**:903-913.
These investigators examined the role of motor proteins in spindle assembly using *Xenopus* egg extracts and DNA-coated beads. As the spindles assemble in the absence of centrosomes, their formation is highly dependent on the action of microtubule-based motors. Models are proposed that show how multiple motors function in generating the bipolar microtubule array.

26. • Gaglio T, Dionne MA, Compton DA: **Mitotic spindle poles are organized by structural and motor proteins in addition to centrosomes.** *J Cell Biol* 1997, **138**:1055-1066.
The authors examined the role of dynein in spindle pole formation both in somatic cells and in mitotic asters assembled in HeLa cell extracts. They found that dynein and dynactin are required to focus microtubule minus ends.

27. Gaglio T, Saredi A, Bingham J, Hasbani J, Gill SR, Schroer TA, Compton DA: **Opposing motor activities are required for the organization of the mammalian mitotic spindle pole.** *J Cell Biol* 1996, **135**:399-414.

28. Echeverri CJ, Paschal BM, Vaughan KT, Vallee RB: **Molecular characterization of the 50-kD subunit of dynactin reveals function for the complex in chromosome alignment and spindle organization during mitosis.** *J Cell Biol* 1996, **132**:617-633.

29. Merdes A, Ramyar K, Vechio JD, Cleveland DW: **A complex of NuMA and cytoplasmic dynein is essential for mitotic spindle assembly.** *Cell* 1996, **87**:447-458.

30. Blangy A, Arnaud L, Nigg EA: **Phosphorylation by p34cdc2 protein kinase regulates binding of the kinesin-related motor HsEg5 to the dynactin subunit p150.** *J Biol Chem* 1997, **272**:19418-19424.

31. Blangy A, Lane HA, d'Hérin P, Harper M, Kress M, Nigg EA: **Phosphorylation by p34cdc2 regulates spindle association of human Eg5, a kinesin-related motor essential for bipolar spindle formation *in vivo*.** *Cell* 1995, **83**:1159-1169.

32. Sawin KE, Mitchison TJ: **Mutations in the kinesin-like protein Eg5 disrupting localization to the mitotic spindle.** *Proc Natl Acad Sci USA* 1995, **92**:4289-4293.

33. Walczak CE, Mitchison TJ: **Kinesin-related proteins at mitotic spindle poles: function and regulation.** *Cell* 1996, **85**:943-946.

34. Drummond DR, Hagan IM: **Mutations in the bimC box of Cut7 indicate divergence of regulation within the bimC family of kinesin related proteins.** *J Cell Sci* 1998, **111**:853-865.

35. Wittmann T, Boleti H, Antony C, Karsenti E, Vernos I: **Localization of the kinesin-like protein Xklp2 to spindle poles requires a leucine zipper, a microtubule-associated protein, and dynein.** *J Cell Biol* 1998, **143**:673-685.

36. • Dujardin D, Wacker UI, Moreau A, Schroer TA, Rickard JE, De Mey JR: **Evidence for a role of CLIP-170 in the establishment of metaphase chromosome alignment.** *J Cell Biol* 1998, **141**:849-862.
The authors examined the localization and function of CLIP-170 at kinetochores. They found that dynein–dynactin is required for CLIP-170 targeting, which is mediated by the C-terminal domain of CLIP-170. The overexpression of this domain inhibited the association of the endogenous protein with kinetochores and caused a delay in the prometaphase alignment of chromosomes.

37. Williams BC, Karr TL, Montgomery JM, Goldberg ML: **The *Drosophila* l(1)zw10 gene product, required for accurate mitotic chromosome segregation is redistributed at anaphase onset.** *J Cell Biol* 1992, **118**:759-773.

38. •• Starr DA, Williams BC, Li Z, Etemad-Moghadam B, Dawe RK, Goldberg ML: **Conservation of the centromere/kinetochore protein ZW10.** *J Cell Biol* 1997, **138**:1289-1301.
Mutations in the *D. melanogaster* ZW10 kinetochore protein cause defects in chromosome segregation. In this paper, the conservation of a ZW10 sequence in widely divergent organisms, including *Caenorhabditis elegans, Arabidopsis thaliana,* and humans, is demonstrated. The localization of ZW10 in mammalian tissue culture cells is similar to that observed in *Drosophila* embryos and RNA inhibition in *C. elegans* produces defects that are similar to that of the *Drosophila* mutant, suggesting conservation of function as well.

39. • Starr DA, Williams BC, Hays TS, Goldberg ML: **ZW10 helps recruit dynactin and dynein to the kinetochore.** *J Cell Biol* 1998, **142**:763-774.
The authors present an analysis of kinetochores in *Drosophila zw10* mutants. The failure to recruit dynein and dynactin suggests that ZW10 plays a role in targeting the motor complex to kinetochores.

40. • Chan GK, Schaar BT, Yen TJ: **Characterization of the kinetochore binding domain of CENP-E reveals interactions with the kinetochore proteins CENP-F and hBUBR1.** *J Cell Biol* 1998, **143**:49-63.
The kinetochore-binding domain of CENP-E was identified and used in a yeast two-hybrid screen to identify putative CENP-E interacting proteins.

Both CENP-E and another known kinetochore protein, CENP-F, were isolated in this screen, indicating its likely specificity. In addition, hBUBR1, a human BUB1-related kinase, was also identified, indicating a link between CENP-E and checkpoint control proteins.

41. Taylor SS, McKeon F: **Kinetochore localization of murine Bub1 is**
• **required for normal mitotic timing and checkpoint response to spindle damage.** *Cell* 1997, **89**:727-735.

This paper describes the identification of a murine homolog of the yeast *BUB1* gene, which has been implicated in mitotic checkpoint control. Murine Bub1p localizes to kinetochores and appears to be required for checkpoint function, as well as for normal mitotic timing.

42. Wood KW, Sakowicz R, Goldstein LS, Cleveland DW: **CENP-E is a**
•• **plus end-directed kinetochore motor required for metaphase chromosome alignment.** *Cell* 1997, **91**:357-366.

This paper demonstrated the requirement for CENP-E function in chromosome alignment using the *Xenopus* egg extract system. The authors also showed that the bacterially expressed CENP-E motor domain acts as a plus-end-directed microtubule motor *in vitro*.

43. Schaar BT, Chan GK, Maddox P, Salmon ED, Yen TJ: **CENP-E**
•• **function at kinetochores is essential for chromosome alignment.** *J Cell Biol* 1997, **139**:1373-1382.

Through a combination of antibody microinjection and transfection of dominant-negative constructs, these authors showed that CENP-E is required for chromosome alignment on the metaphase plate. Some of the chromosomes failed to even establish bipolar microtubule connections, suggesting a role for CENP-E in this process as well.

44. Maney T, Hunter AW, Wagenbach M, Wordeman L: **Mitotic**
•• **centromere-associated kinesin is important for anaphase chromosome segregation.** *J Cell Biol* 1998, **142**:787-801.

The authors used a combination of antisense treatment of cells and the transfection of dominant-negative constructs to show the importance of MCAK in anaphase chromosome segregation.

45. Lombillo VA, Nislow C, Yen TJ, Gelfand VI, McIntosh JR: **Antibodies to the kinesin motor domain and CENP-E inhibit microtubule depolymerization-dependent motion of chromosomes *in vitro*.** *J Cell Biol* 1995, **128**:107-115.

46. Walczak CE, Mitchison TJ, Desai A: **XKCM1: a *Xenopus* kinesin-related protein that regulates microtubule dynamics during mitotic spindle assembly.** *Cell* 1996, **84**:37-47.

47. Desai A, Verma S, Mitchison TJ, Walczak CE: **Microtubule**
•• **destabilization by a subfamily of kinesins.** *Cell* 1999, **96**:69-78.

The authors used a series of *in vitro* assays to demonstrate that two members of the Kin I subfamily of kinesins act exclusively as microtubule-destabilizing enzymes. The mechanism of microtubule destabilization is distinct from the mechanism of motility established for other kinesins.

Cell, Vol. 96, 69–78, January 8, 1999, Copyright ©1999 by Cell Press

Kin I Kinesins Are Microtubule-Destabilizing Enzymes

Arshad Desai,*§ Suzie Verma,† Timothy J. Mitchison,‡ and Claire E. Walczak†‖
*Department of Biochemistry and Biophysics
†Department of Cellular and Molecular Pharmacology
University of California
San Francisco, California 94143
‡Department of Cell Biology
Harvard Medical School
Boston, Massachusetts 02115

Summary

Using in vitro assays with purified proteins, we show that XKCM1 and XKIF2, two distinct members of the internal catalytic domain (Kin I) kinesin subfamily, catalytically destabilize microtubules using a novel mechanism. Both XKCM1 and XKIF2 influence microtubule stability by targeting directly to microtubule ends where they induce a destabilizing conformational change. ATP hydrolysis recycles XKCM1/XKIF2 for multiple rounds of action by dissociating a XKCM1/XKIF2–tubulin dimer complex released upon microtubule depolymerization. These results establish Kin I kinesins as microtubule-destabilizing enzymes, distinguish them mechanistically from kinesin superfamily members that use ATP hydrolysis to translocate along microtubules, and have important implications for the regulation of microtubule dynamics and for the intracellular functions and evolution of the kinesin superfamily.

Introduction

Microtubules (MTs) are noncovalent polar polymers of αβ-tubulin heterodimers found in all eukaryotic cells that play an essential role in cell division, cytoplasmic organization, generation and maintenance of cell polarity, and many types of cell movements. MTs are inherently dynamic polymers that transduce energy derived from nucleotide hydrolysis into polymer dynamics. In addition, the surface of the MT polymer serves as a track on which motor proteins transport cargoes throughout the cell. These two distinct facets of the MT polymer are central to the many biological functions of the MT cytoskeleton.

MTs are 25 nm diameter, 12–15 protofilament polymers that utilize polymerization-induced GTP hydrolysis on β-tubulin to generate dynamic instability—a behavior where polymerizing and depolymerizing MTs coexist in the same population, infrequently interconverting between these two states (Mitchison and Kirschner, 1984; Erickson and O'Brien, 1992; Desai and Mitchison, 1997). Polymerizing MT ends are thought to maintain a stabilizing "cap" of GTP/GDP.P_i-tubulin, the loss of which results in exposure of an unstable GDP-tubulin core and rapid depolymerization. Thus, tubulin has a built-in lattice destabilization mechanism driven by GTP hydrolysis on β-tubulin. Kinetically, hydrolysis and phosphate release result in a GDP-tubulin lattice that has a >1000-fold higher subunit off rate from an MT end than GTP-tubulin (Walker et al., 1988). Structurally, GDP-tubulin protofilaments are thought to prefer a conformation with increased outward curvature relative to GTP-tubulin protofilaments (Melki et al., 1989; Mandelkow et al., 1991; Müller-Reichert et al., 1998). In the lattice of a polymerizing MT, GDP-tubulin protofilaments are constrained to being straight, presumably by lattice interactions, but during depolymerization they can relax into the preferred curved conformation. The free energy released during this relaxation is thought to drive the rapid depolymerization phase of dynamic instability. Consistent with these ideas, tubulin polymerized with GMPCPP, a slowly hydrolyzable GTP analog, forms stable MTs that do not undergo dynamic instability (Hyman et al., 1992; Caplow et al., 1994). Taxol, a drug isolated from the bark of the yew tree that binds tubulin, also stabilizes MTs by suppressing dynamic instability (Horwitz, 1994).

MT polymerization dynamics are fundamentally important to the intracellular functions of the MT cytoskeleton, as best illustrated by analysis of chromosome movement (Inoué and Salmon, 1995). In vivo, the intrinsic dynamic instability of tubulin is extensively regulated (Cassimeris, 1993; McNally, 1996; Desai and Mitchison, 1997). MTs in vivo turn over much more rapidly than MTs assembled from pure tubulin in vitro, in large part because of an increase in the frequency of transitions from the polymerization phase to the depolymerization phase, called the frequency of catastrophe (Belmont et al., 1990; Verde et al., 1992). This finding is consistent with modeling studies showing that regulation of catastrophe frequency is an extremely efficient way to rapidly modulate MT dynamics (Verde et al., 1992). The observed high frequency of catastrophe has been suspected to result from the action of cellular proteins that destabilize the stabilizing caps at polymerizing MT ends.

In addition to being dynamic polymers, MTs also serve as tracks for motor proteins. Conventional kinesin, the founding member of the kinesin superfamily, was identified on the basis of its ability to use energy derived from ATP hydrolysis to translocate along the MT lattice (Vale et al., 1985). In the last decade, ~100 eukaryotic proteins have been identified that contain a domain homologous to the ~300 amino acid catalytic ATPase domain of conventional kinesin (Vale and Fletterick, 1997; Hirokawa et al., 1998). Based solely on sequence alignments of their catalytic domains, the majority of kinesins have been classified into eight subfamilies with a minority being "orphans" (Vale and Fletterick, 1997). These subfamily categorizations are supported to varying extents by location of the catalytic domain within the polypeptide chain of the protein, by analysis of the quaternary

§To whom correspondence should be addressed at the following present address: European Molecular Biology Laboratory, Meyerhofstrasse 1, D-69117 Heidelberg, Germany (e-mail: arshad.desai@embl-heidelberg.de).
‖Present address: Indiana University, Medical Sciences, Bloomington, Indiana 47405.

structures of the native proteins, and by the similarity of the biological processes in which members of a subfamily derived from different organisms are implicated. Approximately 20% of identified kinesins have been reported to have motor activity in in vitro motility assays. Among the kinesins characterized in vitro is at least one member of each of the eight subfamilies, strongly supporting the assertion that kinesins are mechanochemical ATPases that translocate along the MT lattice.

Previously, we described a kinesin, XKCM1, that is involved in regulating MT dynamics in frog egg extracts (Walczak et al., 1996). Depletion of XKCM1 resulted in a dramatic increase in MT polymerization, suggesting that XKCM1 promotes MT destabilization in egg cytoplasm. Analysis of MT dynamics showed that depletion of XKCM1 did not influence the rates at which MTs polymerized or depolymerized in extracts but did result in a 4-fold reduction in the catastrophe frequency. These results indicate that XKCM1 acts, either directly or indirectly, to destabilize the ends of polymerizing MTs in frog egg extracts. The dramatic effect of XKCM1 depletion indicated that XKCM1 is an important regulator of MT polymerization in egg cytoplasm, prompting us to investigate how XKCM1, a kinesin, has such a striking effect on MT dynamics.

XKCM1 is one of eight kinesins in the internal catalytic domain subfamily (Kin I subfamily for Kinesin Internal; Vale and Fletterick, 1997). This subfamily also includes MCAK, a hamster kinesin implicated in cell division (Wordeman and Mitchison, 1995; Maney et al., 1998), and mouse KIF2 (mKIF2), implicated in nervous system function (Noda et al., 1995; Morfini et al., 1997). Kin I kinesins were expected to be motor proteins on the basis of their sequence homology to kinesins. Consistent with this expectation, fast plus end–directed motility was reported for mKIF2 (Noda et al., 1995), suggesting that motility was likely to be central to the mechanism of MT destabilization by XKCM1. Therefore, at the conclusion of our previous study, we proposed that XKCM1 used plus end motility to target itself to MT ends where it either directly destabilized the MT end or indirectly aided destabilization by delivering a catastrophe-inducing factor (Walczak et al., 1996).

In this paper we show that pure XKCM1 and XKIF2 (*Xenopus* KIF2; 87% overall identity to mKIF2) directly destabilize MTs in a catalytic, ATP-dependent manner. More significantly, we find no involvement of motor activity in MT destabilization. Instead, we find that both XKCM1 and XKIF2 target directly to MT ends where they trigger a destabilizing conformational change. Catalytic domain ATP hydrolysis, used to power motility in kinesins that translocate along the MT lattice, is instead used to dissociate a complex of XKCM1/XKIF2 with tubulin dimer released upon MT depolymerization. The distinction of the molecular mechanism for MT destabilization from that of motility, and the similar in vitro behavior of XKCM1 and XKIF2, two functionally distinct Kin I kinesins, lead us to conclude that Kin I kinesins are MT-destabilizing enzymes and not motor proteins. These results represent not only a characterization of the mechanism of a MT-destabilizing enzyme but also reveal the existence of a novel molecular mechanism inherent to the kinesin superfamily that is distinct from the mechanism of motility.

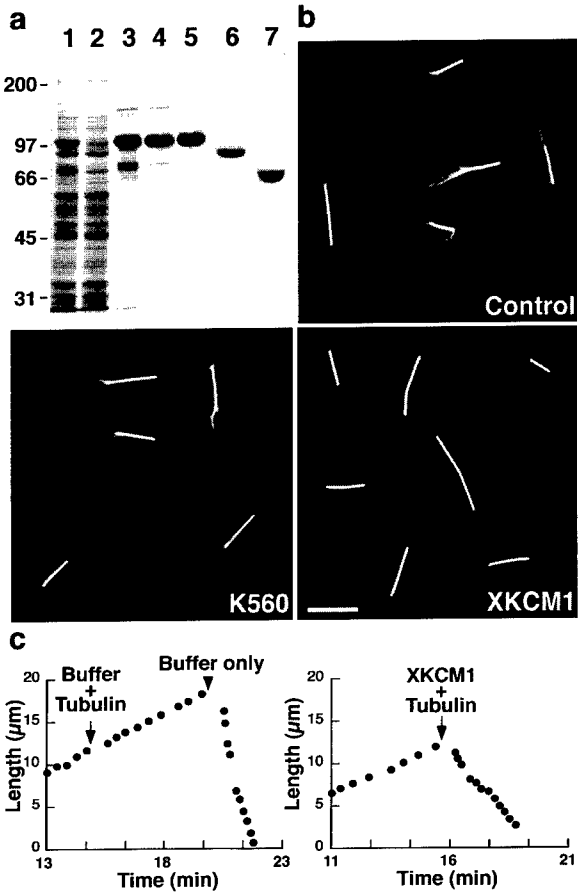

Figure 1. Purified XKCM1 Inhibits MT Assembly and Induces Catastrophes

(a) Baculovirus expression and purification of XKCM1 and XKIF2. Clarified Sf-9 cell lysate (1), SP Sepharose flowthrough (2), SP Sepharose elution (3), Superose 6 elution (4), and Mono S elution (5) from an XKIF2 prep. Lane 6 shows XKCM1 prepared similarly. Lane 7 shows K560 purified from bacteria.

(b) XKCM1 inhibits MT polymerization off axonemes. Bovine brain tubulin (15 μM) was polymerized off axonemes in the presence of a control buffer, 80 nM K560, or 80 nM XKCM1 in BRB80 + 70 mM KCl + 0.5 mM GTP + 1.5 mM MgATP. After 7 min at 37°C, the reactions were fixed, pelleted onto coverslips, and processed for tubulin immunofluorescence. Bar, 10 μm.

(c) XKCM1 induces catastrophes. Life history traces of MT plus ends polymerizing off axonemes with 7 μM frog egg tubulin in assembly buffer (BRB80 + 1 mM GTP + 1.5 mM MgATP). Time 0 is when the tubulin was introduced into the flow cell. At times indicated by the arrows, the solution in the flow cell was exchanged by a mixture of 7 μM frog egg tubulin and either a control buffer (left panel) or 80 nM XKCM1 (right panel) in assembly buffer. The control buffer trace also shows rapid depolymerization following isothermal dilution with BRB80 buffer alone (arrowhead).

Results

XKCM1 Inhibits Microtubule Assembly and Induces Catastrophes

Our previous study established that XKCM1, a Kin I kinesin, promoted MT destabilization in frog egg extracts (Walczak et al., 1996). To determine whether purified Kin I kinesins could directly destabilize MTs, we expressed full-length, untagged XKCM1 and XKIF2 in

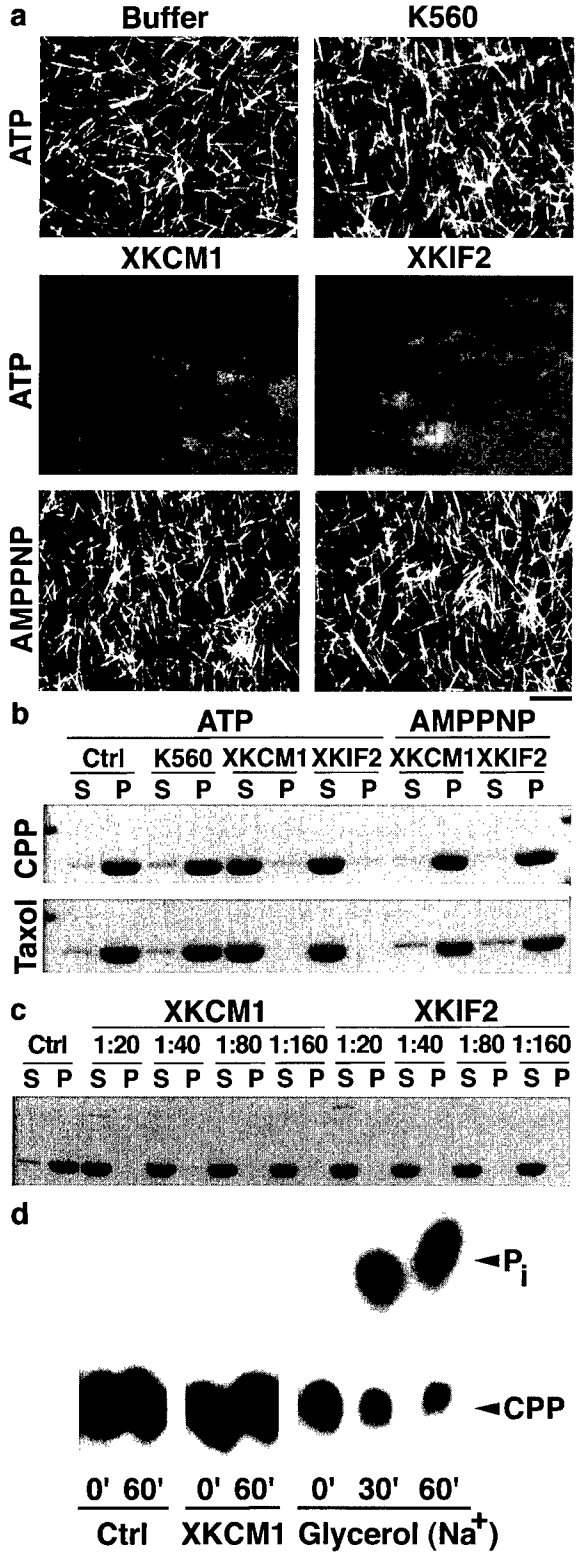

Figure 2. XKCM1 and XKIF2 Depolymerize Stabilized MT Substrates

(a) Visual assay of depolymerization of GMPCPP MTs. GMPCPP MTs (1.5 μM) were mixed with K560/XKCM1/XKIF2 (10 nM) or a control buffer in ATP or AMPPNP, as indicated. Panels show microscope fields after 15 min of incubation at RT. Similar results were obtained with taxol-stabilized MTs. Bar, 10 μm.

baculovirus and purified them by conventional chromatography (Figure 1a). As a control we used K560, a plus end–directed motor protein that is the 560 aa N-terminal fragment of human conventional kinesin (Woehlke et al., 1997). We tested the effect of XKCM1 and K560 on MT polymerization nucleated off axonemes. Pure XKCM1, in the presence of ATP and at concentrations highly substoichiometric to tubulin, completely inhibited MT assembly off axonemes, whereas K560 had no effect (Figure 1b). A similar activity was exhibited by native XKCM1 purified by immunoaffinity from frog egg extracts (data not shown).

To determine what parameter of MT dynamic instability was being affected, we used video microscopy to analyze the fate of prepolymerized MTs after exposure to XKCM1. Purified frog egg tubulin was used for this assay because it is the physiological substrate of XKCM1, it assembles robustly at room temperature, and it has an extremely low intrinsic frequency of catastrophe ($<0.00011\ s^{-1}$ for plus ends and $<0.0003\ s^{-1}$ for minus ends at 7 μM). MTs were polymerized off axonemes adhered to the surface of a flow cell. The solution in the flow cell was then replaced with a mixture of tubulin and control buffer or tubulin and XKCM1. Without XKCM1, all MT ends observed remained in the polymerization phase (n = 25 plus ends; 18 minus ends; Figure 1c). In contrast, in the presence of XKCM1, nearly all MT ends had transited to the depolymerization phase (n = 35/36 plus ends; 11/13 minus ends; Figure 1c), indicating that the MTs had undergone a catastrophe. The introduced XKCM1 rapidly adsorbed to the flow cell surfaces, resulting in binding of the MTs to the coverslip surface and significant reduction in their depolymerization rate relative to MTs depolymerized by dilution in buffer without tubulin (Figure 1c). This adsorption prevented us from determining whether XKCM1 influenced the rate of depolymerization of dynamic MTs in solution. These results demonstrate that pure XKCM1 directly inhibits MT polymerization and is a potent catastrophe factor that can destabilize polymerizing MT ends.

XKCM1/XKIF2 Catalytically Depolymerize Stabilized Microtubules

To characterize how XKCM1 destabilizes MTs, we analyzed its effect on MTs stabilized by the drug taxol or

(b) Sedimentation analysis of GMPCPP (CPP) and taxol MT depolymerization. Reactions, identical to those in (a), were sedimented after 30 min at RT, and supernatants (S) and pellets (P) were analyzed by SDS-PAGE.

(c) XKCM1/XKIF2 act catalytically. Taxol MTs (1.5 μM) were incubated for 30 min at RT with the indicated substoichiometric molar amounts of XKCM1/XKIF2 and analyzed as in (b). Depolymerization is complete even at 1:160 molar ratio of XKCM1/XKIF2:tubulin (control reactions indicated that 85%–90% of the tubulin in the reaction is polymer; thus, at 1:160 XKCM1/XKIF2:total tubulin molar ratio, the relevant molar ratio of XKCM1/XKIF2:tubulin polymer is ~1:140). XKCM1/XKIF2 are visible in the supernatant at the two highest concentrations used (1:20 and 1:40).

(d) Analysis of GMPCPP hydrolysis during GMPCPP MT depolymerization. GMPCPP MTs (1.5 μM) containing [γ-^{32}P]GMPCPP were mixed with a control buffer (Ctrl) or 40 nM XKCM1 (XKCM1) in BRB80 + 1.5 mM MgATP or adjusted to 60% glycerol in Na-BRB80 [Glycerol (Na+)]. At the indicated time, the reaction was stopped and hydrolysis assayed by thin layer chromatography.

by polymerization with GMPCPP, a GTP analog that is essentially nonhydrolyzable by tubulin over the time course of most experiments (Hyman et al., 1992; Caplow et al., 1994). Because taxol and GMPCPP eliminate the intrinsic GTP hydrolysis-driven destabilization mechanism of tubulin, depolymerization of stabilized MTs requires input of free energy and multiple rounds of action at an MT end. We used fluorescent stabilized MTs to qualitatively assay the effect of XKCM1/XKIF2/K560 on their stability. In the presence of ATP, substoichiometric amounts of XKCM1 depolymerized both GMPCPP- and taxol-stabilized MTs; purified XKIF2 had an identical activity, whereas K560 had no depolymerizing activity (Figure 2a). The activity of both XKCM1 and XKIF2 required ATP and was inhibited by the nonhydrolyzable ATP analog, AMPPNP (Figure 2a). Addition of an anti-XKCM1 antibody inhibited the activity of XKCM1 but not of XKIF2 (data not shown), suggesting that the observed depolymerization activity is not due to a cofractionating contaminant.

We used sedimentation and SDS-PAGE analysis to analyze the extent of stabilized MT depolymerization in our reactions. This analysis confirmed the conclusions derived from the qualitative visual assays (Figure 2b). To demonstrate that XKCM1/XKIF2 catalytically depolymerize stabilized MTs in the presence of ATP, we titrated XKCM1/XKIF2 while keeping the concentration of the substrate MTs constant. This analysis demonstrated that each XKCM1/XKIF2 dimer can release at least 140 tubulin dimers (Figure 2c), suggesting a catalytic mechanism. Gel filtration analysis indicated that the end product of GMPCPP MT destabilization by XKCM1/XKIF2 is 6S tubulin dimer; in addition, 85% ± 5% (n = 2 experiments) of the tubulin released into the supernatant was capable of repolymerizing into MTs (data not shown).

If GMPCPP MTs are treated with glycerol in the presence of sodium ions, the normal β-γ phosphate bond of GMPCPP bound to β-tubulin is hydrolyzed, and the MT lattice is destabilized (Caplow et al., 1994). To test whether XKCM1/XKIF2 destabilize GMPCPP MTs by a similar mechanism, we analyzed XKCM1-induced depolymerization of fluorescent GMPCPP-stabilized MTs containing [γ-^{32}P] GMPCPP. Depolymerization was monitored using fluorescence microscopy, and GMPCPP hydrolysis was monitored using thin layer chromatography. Treatment with glycerol in the presence of sodium ions was used as a positive control (Figure 2d). This assay showed that XKCM1 depolymerizes GMPCPP MTs without inducing hydrolysis of the β-tubulin-bound GMPCPP (Figure 2d). This result demonstrates that catalytic depolymerization of stabilized MTs by XKCM1/XKIF2 occurs independently of the intrinsic lattice destabilization mechanism of tubulin and suggests that XKCM1/XKIF2 do not induce catastrophes by stimulating GTP hydrolysis at polymerizing MT ends. In addition, this result implicates ATP hydrolysis by these kinesins as the free energy source in the catalytic depolymerization of stabilized MTs.

XKCM1/XKIF2 Depolymerize Stabilized Microtubules Equivalently from Both Ends and Do Not Exhibit Motor Activity

A previous report that mKIF2 is a fast plus end–directed MT motor (Noda et al., 1995) suggested that XKCM1/XKIF2 use ATP-dependent motility to target to MT plus ends, where they induce end destabilization (Walczak et al., 1996; Waters and Salmon, 1996). A prediction of this hypothesis is that depolymerization would occur preferentially from the plus end of the MT. To test this hypothesis, we monitored XKCM1-induced depolymerization of GMPCPP MTs in real time using an assay that unambiguously assigns polarity to the substrate MTs. GMPCPP MTs with dimly labeled plus and minus end segments polymerized off brightly labeled GMPCPP MT seeds (Figure 3a) were adhered to the surface of a flow cell, exposed to either XKCM1 inactivated by preincubation with an anti-XKCM1 antibody (control) or XKCM1 preincubated with an irrelevant antibody (XKCM1), and monitored by time lapse fluorescence microscopy. After ~10 min, the plus end–directed K560 motor was introduced into the flow cell, and the resulting motility of the MTs was recorded to retroactively and unambiguously assign their polarity. Using this assay, we found that XKCM1 depolymerized GMPCPP MTs from both ends at nearly equivalent rates (Figures 3a, 3b, and 3c). A similar result was obtained using taxol-stabilized MTs as substrates (data not shown). These results suggest that XKCM1 does not use directed motility to reach an MT end. They also demonstrate that stabilized MTs are depolymerized endwise and not by an internal severing mechanism as described for katanin, an MT-severing ATPase (McNally and Vale, 1993; Hartman et al., 1998).

In attempts to observe MT motor activity, we performed standard motility assays that have been used

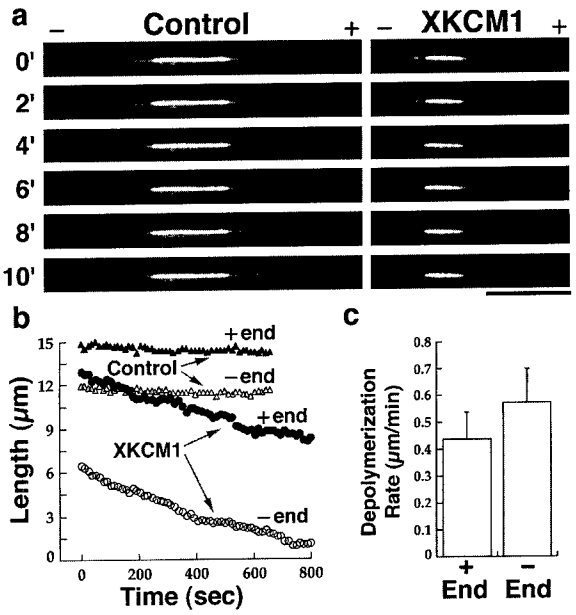

Figure 3. Real Time Analysis of GMPCPP MT Depolymerization

(a) Panels show fate of segmented GMPCPP MTs in a control versus XKCM1 reaction. Plus and minus signs indicate MT polarity. Both reactions contained 20 nM XKCM1; the control was preincubated with an anti-XKCM1 antibody (30-fold molar excess), while the XKCM1 reaction was preincubated with an equivalent amount of an irrelevant rabbit IgG.

(b) Length versus time traces of plus and minus end segments of the MTs shown in (a).

(c) Summary of analysis of 14 MTs showing the depolymerization rate at both MT ends is nearly equivalent.

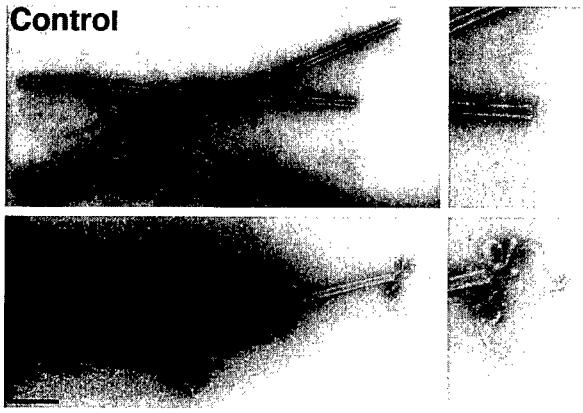

Figure 4. Ultrastructural Analysis of GMPCPP MTs Being Depolymerized by XKCM1

Protofilament peeling is evident at GMPCPP MT ends undergoing XKCM1-induced depolymerization. Reactions containing 1.5 μM GMPCPP MTs and 40 nM XKCM1 in BRB80 + 1 mM DTT + 1.5 mM MgATP were analyzed by negative stain electron microscopy after incubation at RT for 3 min. Right panels show a higher magnification view. Similar structures were observed in reactions containing XKIF2. Bar, 200 nm for left panels.

to demonstrate motility of other kinesins (Cohn et al., 1993). When XKCM1/XKIF2 were adsorbed to a coverslip surface and taxol MTs added, the MTs bound to the surface and exhibited slow bipolar depolymerization. However, motility of the bound MTs was never observed (data not shown). In parallel assays, K560 exhibited robust motility without any MT depolymerization. Preliminary ATPase analysis of XKCM1 and XKIF2 showed that both proteins have very weak MT-stimulated ATPase, inconsistent with their being fast plus end–directed motors (data not shown). Cumulatively, these results suggest that XKCM1/XKIF2 directly target to MT ends, prompting us to investigate how this targeting occurs and what happens at ends to cause destabilization.

XKCM1/XKIF2 Induce a Destabilizing Conformational Change at Microtubule Ends

One attractive possibility for the mechanism of end destabilization is that XKCM1/XKIF2 physically disrupt end structure. Consistent with this idea, negative stain electron microscopy of GMPCPP MTs during depolymerization induced by either XKCM1 or XKIF2 revealed the presence of peeling protofilaments at their ends (Figure 4). Such peeled protofilaments were found on most of the residual GMPCPP MTs in the process of being depolymerized by XKCM1/XKIF2, whereas the ends of control buffer-treated GMPCPP MTs were blunt (Figure 4; $n > 200$ MTs). Where clearly visible, we observed protofilament peels at both MT ends, consistent with our finding that XKCM1 depolymerizes GMPCPP MTs from both ends (also see Figure 5d). These protofilament peels are reminiscent of the structure of rapidly depolymerizing dynamic MT ends, where relaxation of the exposed GDP-tubulin subunits to their preferred "curved" state can generate protofilament bulbs (Mandelkow et al., 1991; Tran et al., 1997). Because XKCM1/XKIF2 do not induce GMPCPP hydrolysis (Figure 2d), these kinesins must have the ability to change tubulin protofilament structure, independent of the nucleotide state of the tubulin. Extension of these results to dynamic MTs suggests that these kinesins induce catastrophes by physically disrupting end structure and not by stimulating GTP hydrolysis on tubulin subunits at polymerizing MT ends.

XKCM1/XKIF2 Target to and Induce a Destabilizing Conformational Change at Microtubule Ends in AMPPNP

To analyze the role of catalytic domain ATP hydrolysis in MT destabilization by XKCM1/XKIF2, we attempted to determine which of the following three steps of the destabilization reaction cycle could occur in the presence of AMPPNP: (1) targeting to MT ends; (2) induction of the destabilizing conformational change; and (3) recycling for multiple depolymerization cycles.

To test whether XKCM1 targeted to MT ends in AMPPNP, GMPCPP MTs were incubated in the presence of AMPPNP and XKCM1, fixed and sedimented onto coverslips, and stained with an anti-XKCM1 antibody to visualize the XKCM1 protein. Under these conditions, XKCM1 targeted to and accumulated at both ends of GMPCPP MTs (Figures 5a, 5b, and 5c; similar results were obtained with XKIF2). XKCM1 was present at both ends of 87% of the MTs, one end of 8%, and neither end of 4% ($n = 303$ MTs). The observed end localization represents an intermediate in the destabilization reaction cycle because it was also observed in GMPCPP MTs undergoing depolymerization in the presence of ATP (data not shown; in this case XKCM1 was present at both ends of 73% of the MTs, at one end of 11%, and neither end of 16%; $n = 153$ MTs). Green fluorescent protein (GFP)-K560 (Pierce et al., 1997) used in a similar assay did not show end targeting and accumulation but localized all along the MTs (data not shown). The unique ability of XKCM1/XKIF2 to target to both MT ends in the presence of AMPPNP strongly argues against a role for ATP-dependent motility in end targeting and distinguishes them further from motile kinesins.

To test whether ATP hydrolysis by Kin I kinesins was necessary to induce the conformational change seen at GMPCPP MT ends, we analyzed GMPCPP MTs by negative stain electron microscopy in the presence of AMPPNP and XKCM1/XKIF2. Under these conditions there is no significant depolymerization of the GMPCPP MTs (Figures 2a and 2b). Protofilament peeling was clearly evident in the presence of AMPPNP and XKCM1/XKIF2, resulting in large protofilament bulbs at both MT ends (Figure 5d). These results suggest that the lattice-destabilizing conformational change is derived from the binding energy of XKCM1/XKIF2 at MT ends and not from ATP hydrolysis.

Unlike GMPCPP MTs, taxol MTs do not exhibit end accumulation of XKCM1/XKIF2 or protofilament peels even though they undergo bipolar depolymerization (data not shown). We suspect this reflects differences in the interactions of tubulin dimers within the lattices of the two different stabilized MT substrates (Mickey and Howard, 1995). The strong immunofluorescence

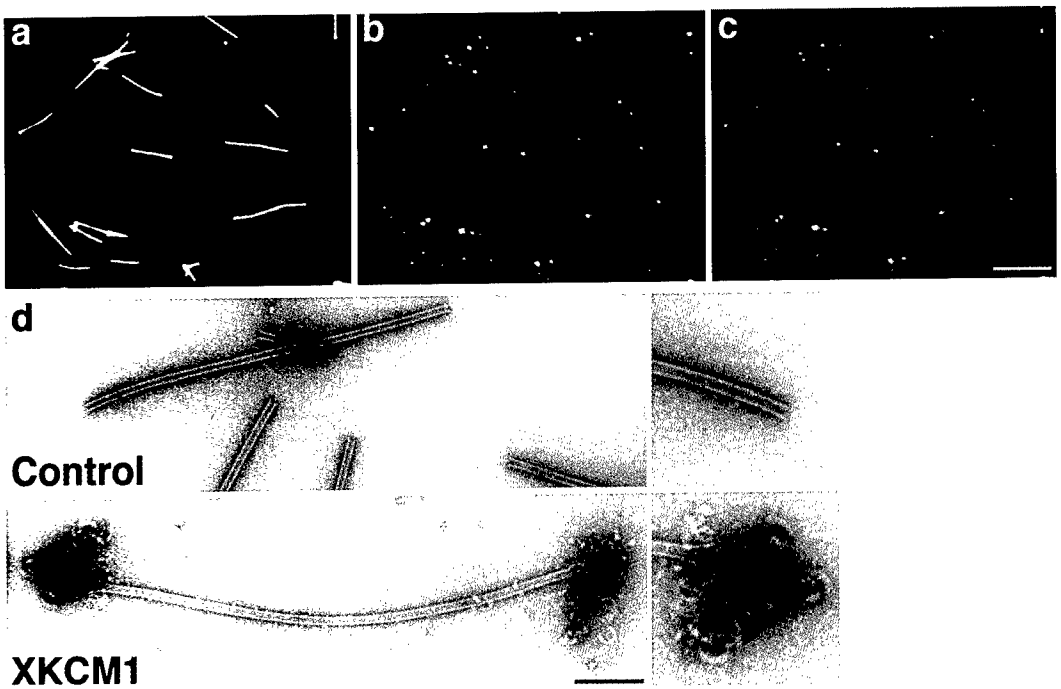

Figure 5. Targeting and Accumulation of XKCM1 at GMPCPP MT Ends in 5 mM MgAMPPNP

Panels show (a) GMPCPP MTs, (b) anti-XKCM1 immunofluorescence, and (c) a color overlay of a microscope field demonstrating that targeting and accumulation to both MT ends can occur in AMPPNP. Bar, 10 μm. (d) Negative stain analysis under similar conditions revealed the presence of protofilament bulbs at both MT ends in reactions containing XKCM1. Right panels show a higher magnification view. Similar results are obtained with XKIF2 in both assays and in reactions performed in the presence of apyrase and AMPPNP. Bar, 200 nm for left panels.

signal at GMPCPP MT ends presumably reflects accumulation of XKCM1/XKIF2 along protofilament peels generated as a consequence of strong longitudinal tubulin dimer interactions. In taxol-stabilized MTs, weaker longitudinal interactions would inhibit formation of the peels and instead result in release of XKCM1/XKIF2-bound tubulin dimers from the ends. This hypothesis is supported by sedimentation analysis in AMPPNP that indicates a greater soluble fraction of tubulin dimer and XKCM1/XKIF2 in reactions containing taxol MTs versus GMPCPP MTs (data not shown).

XKIF2 Forms a Nucleotide-Sensitive Complex with Tubulin Dimer

Because ATP hydrolysis is not required for MT end targeting or for induction of a conformational change at the MT end, we hypothesized that it is used to recycle XKCM1/XKIF2 by dissociating them from tubulin dimer. With dynamic MT substrates, disruption of end structure would presumably induce a catastrophe, releasing a small number of XKCM1/XKIF2–tubulin dimer complexes and a much larger number of free tubulin dimers as the unstable GDP-tubulin core of the MT depolymerizes. The XKCM1/XKIF2–tubulin dimer complex would need to dissociate to allow the XKCM1/XKIF2 to act again at a new MT end. This hypothesis predicts that an XKCM1/XKIF2–tubulin dimer complex should persist in the presence of AMPPNP but not ATP. To test this, we used gel filtration chromatography to analyze the interaction of either XKIF2 or K560 with tubulin dimer in the presence of ATP or AMPPNP (Figure 6). Consistent with our hypothesis, XKIF2 formed a complex with tubulin dimer in AMPPNP but not in ATP. K560 used at identical concentrations did not interact with tubulin dimer in either AMPPNP or ATP, further distinguishing XKCM1/XKIF2 from motile kinesins. This result is also consistent with XKCM1/XKIF2 having an affinity for MT ends that may have binding sites similar to those present in tubulin dimers/oligomers but buried by subunit interactions in the MT lattice.

Discussion

Kin I Kinesins Are Microtubule-Destabilizing Enzymes

Seven of the ten Kin I subfamily kinesins identified to date fall into two categories based on alignment of catalytic domain sequences (The Kinesin Home Page; http://www.blocks.fhcrc.org/~kinesin/). The first category is exemplified by MCAK/XKCM1, kinesins implicated in cell division (Wordeman and Mitchison, 1995; Walczak et al., 1996; Maney et al., 1998). The second category is exemplified by mKIF2, a kinesin implicated in neuronal function (Noda et al., 1995; Morfini et al., 1997). XKCM1 and X/mKIF2 share a high degree of homology in their catalytic domains (75% identity) but are divergent in their N- and C-terminal domains (20%–25% identity in each domain). Despite differences in primary sequence and biological function, our results show that both XKCM1 and XKIF2 destabilize MTs in vitro, leading us to conclude that members of both major categories of

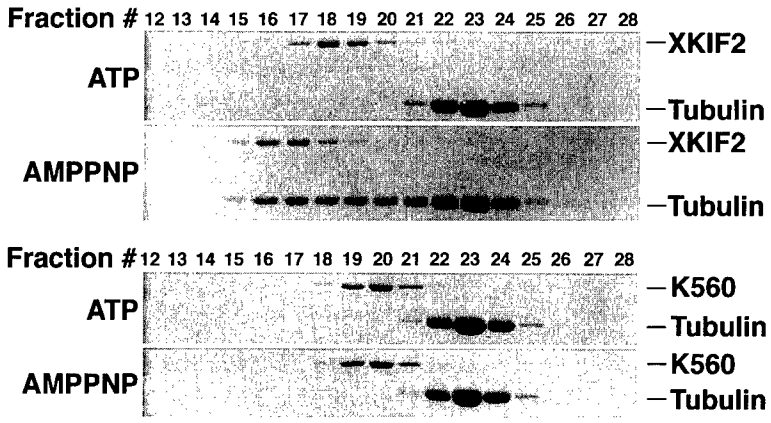

Figure 6. XKIF2 Forms a Nucleotide-Sensitive Complex with Tubulin Dimer

Mixtures of 2 μM XKIF2 or K560 and 10 μM tubulin dimer in buffer containing either ATP or AMPPNP were analyzed by gel filtration on a column equilibrated in buffer containing the same adenine nucleotide as the reaction. The elution volume of each protein of the two-protein mixture in ATP is identical to the elution volume of each protein analyzed individually in ATP. The observed shift for XKIF2 in the presence of tubulin dimer and AMPPNP represents a change in Stokes radius of 9 Å (from 69 Å to 78 Å).

Kin I kinesins are MT-destabilizing enzymes. The three more divergent members of the Kin I subfamily are DSK1, a diatom kinesin implicated in spindle elongation (Wein et al., 1996), and two kinesins identified by genomics, *C. elegans* 11d9 and *Leishmania* MCAK. It will be interesting to test whether these more divergent Kin I kinesins are also MT-destabilizing enzymes.

A Model for the Mechanism of Microtubule Destabilization by Kin I Kinesins

We propose a preliminary molecular mechanism for MT destabilization by Kin I kinesins (Figure 7). The key features of this mechanism are direct targeting of Kin I kinesins to MT ends, physical disruption of MT end structure, and utilization of catalytic domain ATP hydrolysis to dissociate a released complex of Kin I kinesins with tubulin dimer. Below we describe how our results support the key features of this model.

The targeting of Kin I kinesins directly to MT ends is supported by the equivalent depolymerization of GMPCPP MTs from both ends in the presence of ATP and by targeting and accumulation of XKCM1/XKIF2 at both ends of GMPCPP MTs in the presence of AMPPNP. These results suggest that Kin I kinesins have a special affinity for MT end structures, and they argue against models that invoke motility as a mechanism for targeting them to MT ends. The end structures recognized by Kin I kinesins are probably exposed protofilament edges at polymerizing MT ends (Chretien et al., 1995; Desai and Mitchison, 1997). This idea is supported by our finding that Kin I kinesins can interact with tubulin dimer, which may share sites with exposed protofilament edges that are buried within the lattice of the MT.

Our model proposes that binding of Kin I kinesins to MT ends induces a destabilizing conformational change that results in a catastrophe. Physical disruption of end structure is supported by negative stain analysis of GMPCPP MTs undergoing XKCM1 catalyzed depolymerization. Biochemical analysis showed that this disruption occurs without GMPCPP hydrolysis. These results highlight the remarkable ability of Kin I kinesins to destabilize tubulin conformation without triggering nucleotide hydrolysis on β-tubulin. Because XKCM1/XKIF2 induce a destabilizing conformational change at MT ends in the presence of AMPPNP, the lattice-destabilizing conformational change must be derived from the binding energy of these kinesins at MT ends and not from ATP hydrolysis.

In the presence of AMPPNP, XKCM1/XKIF2 do not significantly depolymerize GMPCPP MTs despite targeting to their ends and inducing a destabilizing conformational change. Thus, we propose that the role of ATP hydrolysis by Kin I kinesins is to make their action catalytic by dissociating a released complex with tubulin dimer. Consistent with this idea, gel filtration analysis provided evidence for a complex of XKIF2 with tubulin

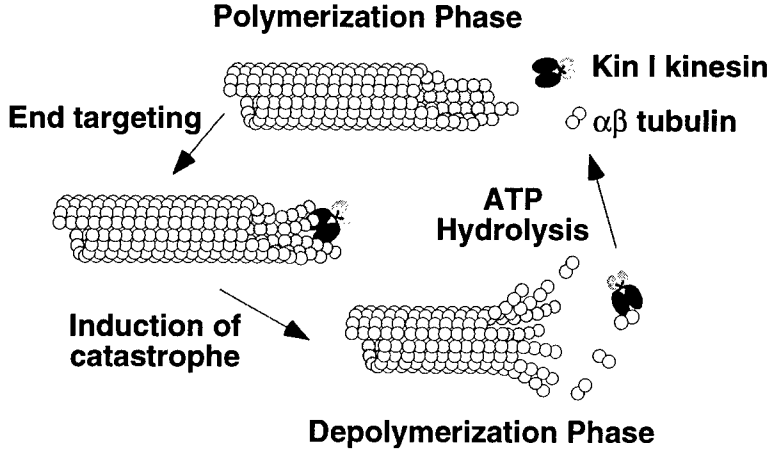

Figure 7. A Model for the Induction of MT Catastrophes by Kin I Kinesins

For simplicity, only one end of an MT is shown. Kin I kinesins target to MT ends during polymerization and disrupt end structure. A catastrophe occurs that induces MT depolymerization and release of a Kin I–tubulin dimer complex. ATP hydrolysis–dependent dissociation of a Kin I–tubulin dimer complex allows for repeated action. For simplicity, a 1:1 Kin I kinesin:tubulin dimer complex is depicted, and the tubulin GTPase cycle, nucleotide exchange on tubulin dimers and Kin I kinesins, and reverse reactions are not shown.

dimer in AMPPNP but not in ATP; such a complex was not observed with the motile K560 kinesin.

Relationship of Microtubule Destabilization by Kin I Kinesins to Potential Motor Activity

The key features of Kin I kinesins—unique affinity for MT ends, physical disruption of end structure, and use of catalytic domain ATPase activity to dissociate a complex with tubulin dimer—are also the features that strongly distinguish them from motile kinesins. Motile kinesins, such as K560 used in our assays, target to the outside surface along the length of the MT lattice, do not induce a destabilizing conformational change in the MT lattice, and use catalytic domain ATPase activity to power motility along the MT lattice. Our results also conclusively disprove the hypothesis that plus end motility targets XKCM1 to MT plus ends, where either XKCM1 itself or its cargo induces MT destabilization (Walczak et al., 1996; Waters and Salmon, 1996). In addition, the assays described here suggest that XKIF2 is not a plus end–directed MT motor. In contrast, fast plus end–directed motility was reported for mKIF2 (Noda et al., 1995). Because XKIF2 and mKIF2 are very similar in primary sequence (96% identity in the catalytic domain; 87% overall identity), we think it unlikely that the difference between our analysis of XKIF2 and the previously reported plus end motility of mKIF2 is species based. Resolving this discrepancy will require a reexamination of the reported motile activity of mKIF2.

Functional and Evolutionary Implications of Kin I Kinesins Being Microtubule-Destabilizing Enzymes

The robust MT-destabilizing activity of Kin I kinesins in vitro leads us to suspect that these kinesins are major regulators of MT dynamics inside cells. Consistent with this expectation, our previous characterization of XKCM1 in *Xenopus* extracts demonstrated it to be a major negative regulator of MT dynamics in egg cytoplasm (Walczak et al., 1996). A small fraction of XKCM1/MCAK also localizes to the centromere/kinetochore region where it presumably plays a role in chromosome movement. Deciphering this role will be aided by considering that XKCM1/MCAK may act exclusively as an MT-destabilizing enzyme and not as a motor protein (Maney et al., 1998). Similarly, analysis of the role of KIF2 in neuronal development will be aided by knowledge of its in vitro activity, and previous studies interpreting its function primarily as a motor protein may need to be reevaluated (Morfini et al., 1997).

Our findings also provide strong support for the hypothesis that regulation of MT dynamics is a fundamental intracellular activity of kinesins. Interestingly, KAR3 and KIP3, two of the six kinesins in the genome of the budding yeast *Saccharomyces cerevisiae*, have been genetically implicated in MT depolymerization (Cottingham and Hoyt, 1997; DeZwaan et al., 1997; Saunders et al., 1997; Huyett et al., 1998), and a bacterially expressed fragment of KAR3 that exhibits minus end motility also slowly depolymerizes MT minus ends in vitro (Endow et al., 1994). Neither of these two kinesins belongs to the Kin I subfamily, indicating that MT destabilization may be an activity selected for in other kinesins. The Kin I subfamily may represent an eventual specialization for exclusively performing the function of MT destabilization.

The ability of members of the kinesin superfamily to move toward either end of an MT (Vale and Fletterick, 1997; Hirokawa et al., 1998), to couple to the dynamic behaviour of MTs (Lombillo et al., 1995), and, as described here, to actively promote MT destabilization by a mechanism distinct from motility highlights the remarkable flexibility inherent in the design of kinesins. A chimera analysis of the relationship between the mechanisms of motility and destabilization, similar to that employed for opposite polarity kinesins (Case et al., 1997; Henningsen and Schliwa, 1997), will be important for exploring this remarkably flexible design. We speculate that coupling to or regulation of polymer dynamics may be evolutionary precedents to motor activity. Dynamic polymers most likely preceded the motor proteins that utilized these polymers as substrates, and coupling to or regulation of the dynamics of the polymers may be the function initially selected for that later evolved into motility.

Future Directions

Future insight into the reaction mechanism proposed here will come from many avenues, including determination of whether Kin I dimerization is required for the destabilization activity, identification of the minimal domain capable of carrying out the destabilization reaction, characterization of the ATPase activity of the catalytic domain, and further analysis of the Kin I–tubulin dimer complex. Elucidation of the detailed coupling of the ATPase cycle to MT destabilization, determination of the strength of coupling of binding to an MT end to the induction of catastrophe, and analysis of the relationship between mechanisms of motility and destabilization are more distant future challenges. The assays developed here will also allow a systematic dissection of other Kin I kinesins, as well as kinesins not belonging to this subfamily but implicated in MT destabilization, such as KIP3 and KAR3 from budding yeast. The potency of Kin I kinesins as MT destabilizers in vitro suggests their activity will be regulated in vivo either directly and/or by regulation of the susceptibility of the MT substrate to their action. Thus, in vitro analysis of the effect of Kin I kinesins on complex substrates, such as MTs coated with single or different MT associated proteins (MAPs) will also be important. Perhaps the most interesting future endeavor will be analysis of the biological functions of Kin I kinesins in light of their remarkable in vitro activity.

Experimental Procedures

Expression and Purification of Recombinant Proteins

Baculovirus expression was performed as described (Walczak et al., 1997) using either a full-length XKCM1 clone inserted into the BamHI to KpnI site of pVL1393N or a full-length XKIF2 clone inserted into the NotI to KpnI site of pVL1392N. Sf-9 cells (250 ml) expressing either XKCM1 or XKIF2 were pelleted, frozen in liquid nitrogen, and stored at −80°C. Frozen cell pellets were resuspended by vigorous pipeting in 25 ml of ice-cold lysis buffer (BRB80 + 125 mM KCl + 2 mM EGTA + 1 mM DTT + 0.5 mM MgATP + 1 mM PMSF +

10 μg/ml leupeptin/pepstatin/chymostatin [LPC]; BRB80: 80 mM PIPES, 1 mM $MgCl_2$, 1 mM EGTA [pH 6.8] with KOH). The lysate was cleared by centrifugation, loaded onto a HiTrap SP Sepharose column (Pharmacia), and eluted with an increasing KCl gradient. The peak of XKCM1/XKIF2 from the HiTrap SP column (assayed by SDS-PAGE) was loaded onto a Superose 6 gel filtration column (Pharmacia) equilibrated in BRB80 + 75 mM KCl + 1 mM DTT + 10 μM MgATP + 1 μg/ml LPC. The peak of full-length XKCM1/XKIF2 was loaded onto a 1 ml Mono S column (Pharmacia) equilibrated in BRB80 + 75 mM KCl + 1 mM DTT + 10 μM MgATP + 1 μg/ml LPC and eluted with an increasing KCl gradient. K560 (Woehlke et al., 1997) was purified from bacteria by nickel affinity followed by Superose 6 gel filtration in BRB80 + 200 mM KCl + 1 mM DTT + 10 μM MgATP + 1 μg/ml LPC. The final XKCM1/XKIF2/K560 fractions were supplemented with solid sucrose to 10% (w/v), aliquoted, frozen in liquid nitrogen, and stored at −80°C. Control buffers of ionic strength and composition identical to the purified protein fractions were used in control reactions, unless indicated otherwise. Protein concentration was determined colorimetrically using BSA as a standard (Bradford, 1976). All three proteins (XKCM1, XKIF2, and K560) are dimers as judged by sucrose density gradient and gel filtration analysis, and all reported concentrations are of the molar concentration of dimer in the reaction. For unknown reasons, X/mKIF2 migrate anomalously large on denaturing SDS-PAGE gels (apparent MW ~20 kDa larger than MW calculated from primary sequence).

General Microtubule Methods and Assays for Dynamic Microtubules

Purification of bovine brain/frog egg tubulin, labeling of bovine tubulin with fluorescent dyes, and polymerization of taxol/GMPCPP MTs from bovine tubulin was performed using standard procedures (Hyman et al., 1991). Preparation of [γ-^{32}P] GMPCPP and analysis of its hydrolysis were performed as described (Hyman et al., 1992). Fixed and real time assays on dynamic MTs nucleated off axonemes were performed as described (Mitchison and Kirschner, 1984; Walker et al., 1988) except that in the latter frog egg tubulin and double-stick tape flow cells were used, and the flow cell surface was blocked with 5 mg/ml BSA in BRB80 after adsorption of axonemes. For GMPCPP and taxol MT reactions, MT concentration (i.e., concentration of tubulin dimer in MT polymer) was determined from the A_{280} of an aliquot of sedimented and resuspended MTs diluted in BRB80 + 5 mM $CaCl_2$ and incubated at 0°C for 10 min to induce depolymerization (using ϵ-tubulin, 280 nm = 115,000 $M^{-1}cm^{-1}$).

Visual and Sedimentation Analysis of Stabilized Microtubule Depolymerization

For qualitative visual analysis of depolymerization of stabilized MTs, 40 nM XKCM1/XKIF2/K560 was mixed with 1.5 μM fluorescent GMPCPP/taxol MTs (1:9 rhodamine-labeled:unlabeled tubulin; ~1:40 molar ratio of XKCM1/XKIF2/K560:tubulin) in BRB80 + 70 mM KCl + 1 mM DTT + 1.5 mM MgATP/5 mM MgAMPPNP (+ 15 μM taxol for taxol MT reactions) and incubated at RT. At various intervals 1 μl of the reaction mix was squashed under an 18 × 18 mm coverslip and viewed by fluorescence microscopy using a 60X, 1.4 NA Olympus objective mounted on a Nikon Optiphot-2 microscope. Sedimentation analysis of depolymerization of stabilized MTs was performed using SDS-PAGE of supernatants and pellets generated by centrifuging 80 μl reactions at 100,000 rpm for 5 min in a TLA100 rotor at 23°C. The pellet was resuspended in 80 μl BRB80 + 70 mM KCl + 5 mM $CaCl_2$ on ice for 10 min with vigorous pipeting. Equivalent amounts (20–25 μl) of the supernatant and pellet were analyzed by 10% SDS-PAGE followed by Coomassie staining.

Real Time Analysis of GMPCPP Microtubule Depolymerization

Segmented GMPCPP MTs were prepared by diluting bright GMPCPP seeds (1:2 rhodamine-labeled:unlabeled tubulin) into 1.5 μM dim GMPCPP-tubulin mix (1:11 rhodamine-labeled:unlabeled tubulin) and incubating at 37°C for 1–2 hr. Double-stick tape flow cell surfaces were coated with a very dilute partially pure fraction of XKIF2 and blocked with 5 mg/ml BSA in BRB80. This preparation binds MTs to the coverslip surface without significantly releasing, moving, or depolymerizing them in the presence of ATP. Segmented GMPCPP MTs were allowed to bind to the flow cell surface and rinsed extensively with BRB80 + 1 mM DTT + 1.5 mM MgATP + 1X Oxygen Scavenging Mix (1X OSM: 200 μg/ml glucose oxidase, 35 μg/ml catalase, 4.5 mg/ml glucose, 0.5% 2-mercaptoethanol). XKCM1 (20 nM), preincubated for 10 min on ice with 30-fold molar excess of either anti-N-terminal XKCM1 antibody (Walczak et al., 1996) or an irrelevant rabbit IgG, was adjusted to BRB80 + 1 mM DTT + 1.5 mM MgATP + 1 mg/ml BSA + 1X OSM and introduced into the flow cell. The reaction was monitored using time lapse fluorescence microscopy with a 60X, 1.4 NA Nikon objective and a Princeton Instruments cooled CCD camera. After 10–15 min, ~200 nM K560 was introduced into the flow cell and the motility of the observed MTs recorded to retroactively and unambiguously determine their polarity.

Immunofluorescence Analysis and Negative Stain Electron Microscopy

Reactions of GMPCPP MTs and XKCM1/XKIF2 identical to those described above were fixed using 10 vol of 1% glutaraldehyde in BRB80, sedimented onto coverslips as described (Evans et al., 1985), postfixed in methanol, rehydrated, blocked with BSA, and processed for immunofluorescence using an affinity-purified anti-C-terminal XKCM1 antibody raised against the carboxy-terminal 138 amino acids of XKCM1. An affinity-purified anti-N-terminal XKIF2 antibody was used to detect XKIF2. To obtain antibodies that would recognize their antigens after fixation with glutaraldehyde, the immunogens were briefly fixed with glutaraldehyde prior to injection into rabbits. AMPPNP reactions were fixed after incubation at RT for 15 min; ATP reactions were fixed at the midpoint of depolymerization gauged by qualitative visual analysis. Negative stain electron microscopy was performed by adsorbing 1–2 μl of a reaction mix to a glow-discharged, formvar-coated, carbon-coated 200-mesh copper EM grid for ~10 s and applying 20 μl of 0.5% aqueous uranyl actetate while simultaneously absorbing it using a Whatman #1 filter paper strip. The grid was thoroughly dried prior to viewing with a Philips EM400 electron microscope.

Analysis of Tubulin Dimer Binding

XKIF2/K560 (2 μM) and tubulin dimer (10 μM) were incubated in BRB80 + 75 mM KCl + 1 mM DTT + 50 μM GDP + 3 mM MgATP/3 mM MgAMPPNP for 15 min at RT and 20 μl was analyzed by gel filtration using a Superose 6 column on a Pharmacia Smart system. The column was equilibrated in BRB80 + 75 mM KCl + 20 μM GDP + 200 μM MgATP/MgAMPPNP. Column fractions were analyzed by 10% SDS-PAGE followed by Coomassie staining. The column was calibrated using the following standards (Stokes radii are indicated in brackets): chymotrypsinogen (20.9 Å), ovalbumin (30.5 Å), aldolase (48.1 Å), catalase (52.2 Å), ferritin (61.0 Å), and thyroglobulin (85.0 Å). Stokes radii were estimated from a Porath correlation generated using the elution volumes of the standards (Siegel and Monty, 1966).

Acknowledgments

A. D. dedicates this work to Christine Mirzayan. We thank Peg Coughlin and Mei Lie Wong for assistance with electron microscopy, D. Pierce for GFP-kinesin, J. Hartman for advice on ATPase assays, and Matt Welch, Karen Oegema, Aaron Straight, Tarun Kapoor, Bruce Schnapp, and Ted Salmon for comments on the manuscript. C. E. W. was supported by the USAMRMC Breast Cancer Research Program, T. J. M. by grants from the National Institutes of Health and the Human Frontier Science Project, and A. D. by a Howard Hughes Medical Institute predoctoral fellowship.

Received October 14, 1998; November 17, 1998.

References

Belmont, L.D., Hyman, A.A., Sawin, K.E., and Mitchison, T.J. (1990). Real-time visualization of cell cycle-dependent changes in microtubule dynamics in cytoplasmic extracts. Cell *62*, 579–589.

Bradford, M.M. (1976). A rapid and sensitive method for the quantitation of microgram quantities of protein utilizing the principle of protein-dye binding. Anal. Biochem. *72*, 248–254.

Caplow, M., Ruhlen, R.L., and Shanks, J. (1994). The free energy for hydrolysis of a microtubule-bound nucleotide triphosphate is near zero: all of the free energy for hydrolysis is stored in the microtubule lattice. J. Cell Biol. *127*, 779–788.

Case, R.B., Pierce, D.W., Hom-Booher, N., Hart, C.L., and Vale, R.D. (1997). The directional preference of kinesin motors is specified by an element outside of the motor catalytic domain. Cell *90*, 959–966.

Cassimeris, L. (1993). Regulation of microtubule dynamic instability. Cell Motil. Cytoskel. *26*, 275–281.

Chretien, D., Fuller, S.D., and Karsenti, E. (1995). Structure of growing microtubule ends: two-dimensional sheets close into tubes at variable rates. J. Cell Biol. *129*, 1311–1328.

Cohn, S.A., Saxton, W.M., Lye, R.J., and Scholey, J.M. (1993). Analyzing microtubule motors in real time. Methods Cell Biol. *39*, 75–88.

Cottingham, F.R., and Hoyt, M.A. (1997). Mitotic spindle positioning in Saccharomyces cerevisiae is accomplished by antagonistically acting microtubule motor proteins. J. Cell Biol. *138*, 1041–1053.

Desai, A., and Mitchison, T.J. (1997). Microtubule polymerization dynamics. Annu. Rev. Cell Dev. Biol. *13*, 83–117.

DeZwaan, T.M., Ellingson, E., Pellman, D., and Roof, D.M. (1997). Kinesin-related KIP3 of Saccharomyces cerevisiae is required for a distinct step in nuclear migration. J. Cell Biol. *138*, 1023–1040.

Endow, S.A., Kang, S.J., Satterwhite, L.L., Rose, M.D., Skeen, V.P., and Salmon, E.D. (1994). Yeast Kar3 is a minus-end microtubule motor protein that destabilizes microtubules preferentially at the minus ends. EMBO J. *13*, 2708–2713.

Erickson, H.P., and O'Brien, E.T. (1992). Microtubule dynamic instability and GTP hydrolysis. Annu. Rev. Biophys. Biomol. Struct. *21*, 145–166.

Evans, L., Mitchison, T., and Kirschner, M. (1985). Influence of the centrosome on the structure of nucleated microtubules. J. Cell Biol. *100*, 1185–1191.

Hartman, J.J., Mahr, J., McNally, K., Okawa, K., Shimizu, T., Vale, R.D., and McNally, F. (1998). Katanin, a microtubule-severing protein, is a novel AAA ATPase that targets to the centrosome using a WD40-containing subunit. Cell *93*, 277–287.

Henningsen, U., and Schliwa, M. (1997). Reversal in the direction of movement of a molecular motor. Nature *389*, 93–96.

Hirokawa, N., Noda, Y., and Okada, Y. (1998). Kinesin and dynein superfamily proteins in organelle transport and cell division. Curr. Opin. Cell Biol. *10*, 60–73.

Horwitz, S.B. (1994). Taxol (paclitaxel): mechanisms of action. Ann. Oncol. *5* (Suppl 6), S3–6.

Huyett, A., Kahana, J., Silver, P., Zeng, X., and Saunders, W.S. (1998). The Kar3p and Kip2p motors function antagonistically at the spindle poles to influence cytoplasmic microtubule numbers. J. Cell Sci. *111*, 295–301.

Hyman, A., Drechsel, D., Kellogg, D., Salser, S., Sawin, K., Steffen, P., Wordemann, L., and Mitchison, T. (1991). Preparation of modified tubulins. Methods Enzymol. *196*, 478–486.

Hyman, A.A., Salser, S., Drechsel, D.N., Unwin, N., and Mitchison, T.J. (1992). Role of GTP hydrolysis in microtubule dynamics: information from a slowly hydrolyzable analogue, GMPCPP. Mol. Biol. Cell *3*, 1155–1167.

Inoué, S., and Salmon, E.D. (1995). Force generation by microtubule assembly/disassembly in mitosis and related movements. Mol. Biol. Cell *6*, 1619–1640.

Lombillo, V.A., Stewart, R.J., and McIntosh, J.R. (1995). Minus-end-directed motion of kinesin-coated microspheres driven by microtubule depolymerization. Nature *373*, 161–164.

Mandelkow, E.M., Mandelkow, E., and Milligan, R.A. (1991). Microtubule dynamics and microtubule caps: a time-resolved cryo-electron microscopy study. J. Cell Biol. *114*, 977–991.

Maney, T., Hunter, A.W., Wagenbach, M., and Wordeman, L. (1998). Mitotic centromere-associated kinesin is important for anaphase chromosome segregation. J. Cell Biol. *142*, 787–801.

McNally, F.J. (1996). Modulation of microtubule dynamics during the cell cycle. Curr. Opin. Cell Biol. *8*, 23–29.

McNally, F.J., and Vale, R.D. (1993). Identification of katanin, an ATPase that severs and disassembles stable microtubules. Cell *75*, 419–429.

Melki, R., Carlier, M.F., Pantaloni, D., and Timasheff, S.N. (1989). Cold depolymerization of microtubules to double rings: geometric stabilization of assemblies. Biochemistry *28*, 9143–9152.

Mickey, B., and Howard, J. (1995). Rigidity of microtubules is increased by stabilizing agents. J. Cell Biol. *130*, 909–917.

Mitchison, T., and Kirschner, M. (1984). Dynamic instability of microtubule growth. Nature *312*, 237–242.

Morfini, G., Quiroga, S., Rosa, A., Kosik, K., and Caceres, A. (1997). Suppression of KIF2 in PC12 cells alters the distribution of a growth cone nonsynaptic membrane receptor and inhibits neurite extension. J. Cell Biol. *138*, 657–669.

Müller-Reichert, T., Chrétien, D., Severin, F., and Hyman, A.A. (1998). Structural changes at microtubule ends accompanying GTP hydrolysis: information from a slowly hydrolyzable analogue of GTP, guanylyl (a,b) methylenediphosphonate. Proc. Nat. Acad. Sci. USA *95*, 3661–3666.

Noda, Y., Sato-Yoshitake, R., Kondo, S., Nangaku, M., and Hirokawa, N. (1995). KIF2 is a new microtubule-based anterograde motor that transports membranous organelles distinct from those carried by kinesin heavy chain or KIF3A/B. J. Cell Biol. *129*, 157–167.

Pierce, D.W., Hom-Booher, N., and Vale, R.D. (1997). Imaging individual green fluorescent proteins. Nature *388*, 338.

Saunders, W., Hornack, D., Lengyel, V., and Deng, C. (1997). The Saccharomyces cerevisiae kinesin-related motor Kar3p acts at preanaphase spindle poles to limit the number and length of cytoplasmic microtubules. J. Cell Biol. *137*, 417–431.

Siegel, L.M., and Monty, K.J. (1966). Determination of molecular weights and frictional ratios of proteins in impure systems by use of gel filtration and density gradient centrifugation. Biochem. Biophys. Acta *112*, 346–362.

Tran, P.T., Joshi, P., and Salmon, E.D. (1997). How tubulin subunits are lost from the shortening ends of microtubules. J. Struct. Biol. *118*, 107–118.

Vale, R.D., and Fletterick, R.J. (1997). The design plan of kinesin motors. Annu. Rev. Cell Dev. Biol. *13*, 745–777.

Vale, R.D., Reese, T.S., and Sheetz, M.P. (1985). Identification of a novel force-generating protein, kinesin, involved in microtubule-based motility. Cell *42*, 39–50.

Verde, F., Dogterom, M., Stelzer, E., Karsenti, E., and Leibler, S. (1992). Control of microtubule dynamics and length by cyclin A- and cyclin B-dependent kinases in Xenopus egg extracts. J. Cell Biol. *118*, 1097–1108.

Walczak, C.E., Mitchison, T.J., and Desai, A. (1996). XKCM1: a *Xenopus* kinesin-related protein that regulates microtubule dynamics during mitotic spindle assembly. Cell *84*, 37–47.

Walczak, C.E., Verma, S., and Mitchison, T.J. (1997). XCTK2: a kinesin-related protein that promotes mitotic spindle assembly in Xenopus laevis egg extracts. J. Cell Biol. *136*, 859–870.

Walker, R.A., O'Brien, E.T., Pryer, N.K., Soboeiro, M.F., Voter, W.A., Erickson, H.P., and Salmon, E.D. (1988). Dynamic instability of individual microtubules analyzed by video light microscopy: rate constants and transition frequencies. J. Cell Biol. *107*, 1437–1448.

Waters, J.C., and Salmon, E.D. (1996). Cytoskeleton: a catastrophic kinesin. Curr. Biol. *6*, 361–363.

Wein, H., Foss, M., Brady, B., and Cande, W.Z. (1996). DSK1, a novel kinesin-related protein from the diatom Cylindrotheca fusiformis that is involved in anaphase spindle elongation. J. Cell Biol. *133*, 595–604.

Woehlke, G., Ruby, A.K., Hart, C.L., Ly, B., Hom-Booher, N., and Vale, R.D. (1997). Microtubule interaction site of the kinesin motor. Cell *90*, 207–216.

Wordeman, L., and Mitchison, T.J. (1995). Identification and partial characterization of mitotic centromere-associated kinesin, a kinesin-related protein that associates with centromeres during mitosis. J. Cell Biol. *128*, 95–104.

CHAPTER 20

The Use of *Xenopus* Egg Extracts to Study Mitotic Spindle Assembly and Function *in Vitro*

Arshad Desai,[*] Andrew Murray,[†] Timothy J. Mitchison,[‡] and Claire E. Walczak[‡]

[*] Department of Biochemistry and Biophysics,[†] Department of Physiology, and [‡]Department of Cellular and Molecular Pharmacology
University of California at San Francisco
San Francisco, California 94143-0450

METHODS IN CELL BIOLOGY, VOL. 61

0091-679X/99 $30.00

I. Introduction

Since Flemming first described mitosis more than a century ago, understanding the mechanisms underlying cell division has been a major focus in cell biology (Flemming, 1965). Over the years, the study of cell division has evolved from a detailed description of mitosis by the early cytologists to a modern molecular investigation. Essential for this evolution has been the development of experimental systems in which molecular and observational studies can be linked. Extracts from unfertilized *Xenopus* eggs provide one such system. These extracts are capable of maintaining specific cell cycle states and carrying out many of the events associated with cell division *in vitro* (Lohka and Masui, 1983; Blow and Laskey, 1986; Hutchison *et al.,* 1988; Murray and Kirschner, 1989). In addition to providing fundamental insights into the nature of the cell cycle, these extracts have been very useful for dissecting downstream mitotic processes, such as regulation of microtubule dynamics, chromosome condensation, mitotic spindle assembly, sister chromatid separation, anaphase chromosome movement, and kinetochore assembly (Lohka and Maller, 1985; Belmont *et al.,* 1990; Verde *et al.,* 1990; Hirano and Mitchison, 1991; Sawin and Mitchison, 1991; Shamu and Murray, 1992; Murray *et al.,* 1996; Desai *et al.,* 1997, 1998). A hallmark of studies in *Xenopus* extracts has been the combination of detailed structural and functional analysis of complex macromolecular assemblies such as the mitotic spindle with the manipulation of selected components. Similar feats have been difficult to accomplish in genetic systems such as budding yeast because the cytology is limiting and the biochemistry is difficult. Furthermore, *Xenopus* extracts also provide insight into the mechanisms of vertebrate mitosis, the details of which may not be revealed from studies in lower eukaryotes.

The two most useful attributes of *Xenopus* extracts are their ability to maintain specific cell cycle states and to recapitulate many of the detailed morphological changes associated with mitosis. Both of these features depend on the natural cell cycle arrest of the frog egg and on the ability to make concentrated extracts that retain many of the properties of intact cytoplasm. Mature *Xenopus* eggs are arrested in metaphase of meiosis II by an activity termed cytostatic factor (CSF), which is thought to be the product of the c-*mos* protooncogene (Sagata *et al.,* 1989). Sperm entry triggers a calcium spike that initiates a series of events leading to the destruction of CSF and exit from the meiosis II metaphase arrest. This calcium sensitivity of the CSF arrest is exploited in the preparation of extracts by use of the calcium chelator EGTA. The presence of EGTA in buffers results in extracts that maintain the CSF arrest (referred to as CSF extracts) but can be induced to exit the CSF arrest by addition of calcium (Lohka and Maller,

1985). This convenient control of cell cycle state allows one to easily obtain *in vitro* spindles with replicated chromosomes as described later in detail. It should be noted that CSF extracts are meiotic (meiosis II) and not mitotic cytoplasm, a distinction that has not generally been made in the literature. However, given the mechanistic similarity of meiosis II and mitosis, studies using CSF extracts should be generally relevant to the study of mitosis, and several phenotypes of depletion of spindle assembly components in CSF extracts have also been observed in antibody-injection experiments in somatic cells (Sawin *et al.,* 1992; Blangy *et al.,* 1995; Gaglio *et al.,* 1995, 1996, 1997; Merdes *et al.,* 1996; Heald *et al.,* 1997) as well as with genetic analysis of mitotic mutants (Enos and Morris, 1990; Hagan and Yanagida, 1990; Hoyt *et al.,* 1992; Roof *et al.,* 1992).

In this chapter, we will present detailed methods for the preparation of CSF extracts and for performing spindle assembly reactions. We will also describe methods for depleting specific components from extracts, an approach that has been used successfully to determine the contributions of both motor and nonmotor components to spindle assembly (Sawin *et al.,* 1992; Merdes *et al.,* 1996; Walczak *et al.,* 1996, 1997). Finally, we will describe methods for analyzing anaphase *in vitro* (Murray *et al.,* 1996). We recommend that anyone interested in using *Xenopus* egg extracts as an experimental system should first consult Murray (1991) who provides an introduction to the early stages of the *Xenopus* life cycle, documents the history of cell cycle extracts, provides detailed technical descriptions on the preparation of different types of extracts, and gives advice on troubleshooting problems with extracts; Murray's article serves as the basis for several of the procedures described here.

II. Preparation of CSF Extracts for Spindle Assembly

A. Requirements for Extract Preparation

1. Buffer and Reagent Stocks

10× MMR
- 50 m*M* Na–Hepes, pH to 7.8 with NaOH
- 1 m*M* EDTA
- 1 *M* NaCl
- 20 m*M* KCl
- 10 m*M* $MgCl_2$
- 20 m*M* $CaCl_2$
- Autoclave and store at room temperature (RT); if desired, MMR can also be prepared as a 25× stock

20X XB salts
- 2 *M* KCl
- 20 m*M* $MgCl_2$

2 m*M* $CaCl_2$
Sterile filter and store at 4°C

2 M Sucrose
Sterile filter or autoclave and store at 4°C or in aliquots at −20°C

1 M K-Hepes
pH to 7.7 with KOH, sterile filter and store at 4°C or in aliquots at −20°C

0.5 M K-EGTA
pH to 7.7 with KOH, sterile filter and store at RT

1 M $MgCl_2$
Sterile filter and store at RT

20X energy mix
150 m*M* creatine phosphate
20 m*M* ATP
20 m*M* $MgCl_2$
Store in 100-μl aliquots at −20°C

Protease inhibitors (LPC)
10 mg/ml each of leupeptin, pepstatin A, and chymostatin dissolved in DMSO; store in 100-μl aliquots at −20°C

Cytochalasin B or D
10 mg/ml in DMSO; store in 10- or 50-μl aliquots at −20°C
(Note: Both protease inhibitors and cytochalasin stocks can be frozen and thawed multiple times without detriment)

5% Gelatin (w/v)
Dissolved in water; autoclave and store in aliquots at −20°C

Cysteine, free base
Sigma No. C-7755

Versilube F-50
ANDPAK-EMA

Hormone stocks for priming frogs and inducing ovulation
Pregnant mare serum gonadotropin (PMSG): 100 U/ml (Calbiochem No. 367222) made up in water and stored at −20°C
Human chorionic gonadotropin (hCG): 1000 U/ml (Sigma No. CG-10) made up in water and stored at 4°C
(Hormones are injected into the dorsal lymph sac using a 27-gauge needle)

2. Equipment

Glass petri dishes
60-, 100-, 150-mm-diameter regular and 150-mm-diameter high-sided, i.e., 150-mm diameter and 75-mm height

13 X 51-mm Ultraclear tubes (Beckman No. 344057)

Ultracentrifuge and SW50.1/SW55.1 rotor
Clinical centrifuge

3. Primed Frogs

Frogs for extract preparation are primed using progesterone (present in PMSG) which induces maturation of oocytes. Priming is performed in two steps by injection with 50 U of PMSG (0.5 ml of 100 U/ml stock) on Day 1 and 25 U of PMSG (0.25 ml) on Day 3. Primed frogs are stored in dechlorinated water containing 2 g/liter rock salt in a cool room (ambient temperature of 16–20°C) and can be induced to lay eggs for up to 2 weeks after the second priming.

B. Protocol for Extract Preparation

1. Day before Extract Preparation

Sixteen to 18 h before extract preparation, four to six primed frogs are induced to ovulate by injection with 500 U (0.5 ml) of hCG. After injection, frogs are rinsed well in distilled water, put individually into plastic buckets (Fisher No. 03-484-21) containing two liters MMR, and stored overnight in a 16°C incubator.

2. Setup for Extract Preparation

For a four to six frog prep, you will need the following prior to beginning the prep:

a. Buffers

Prepare just before use unless indicated otherwise; all graduated cylinders and glassware should be rinsed well with double-distilled water (dd H_2O) prior to use.

Two or three liters 1X MMR (the MMR can be made the night before and stored in a plastic carboy in the 16°C incubator)

200 ml dejellying solution: 2% (w/v) cysteine in 1X XB salts; pH to 7.8 by adding 0.9 ml of 10 *N* NaOH

750 ml XB: 10 m*M* K-Hepes (pH 7.7), 100 m*M* KCl, 1 m*M* $MgCl_2$, 0.1 m*M* $CaCl_2$, and 50 m*M* sucrose; prepare using 20X XB salts, 2 *M* sucrose, and 1 *M* K-Hepes (pH 7.7) stocks; to maintain a pH of 7.7 at 10 m*M* Hepes, add 11 μl 10 *N* KOH per 100 ml XB

250 ml CSF-XB: XB + 1 m*M* $MgCl_2$ + 5 m*M* EGTA; to prepare, transfer 250 ml of XB (from the 750 ml prepared previously) to a separate graduated cylinder and add EGTA to 5 m*M* and $MgCl_2$ to 1 m*M* final

100 ml CSF-XB + PIs: CSF-XB + 10 μg/ml LPC; to prepare, transfer 100 ml of CSF-XB (from the 250 ml prepared previously) to a separate graduated cylinder and add LPC to 10 μg/ml (mix immediately after adding LPC)

b. Equipment, etc.

SW55.1 or SW50.1 rotor at 16°C in ultracentrifuge

Two Pasteur pipettes with tips broken and fire polished to ~3 or 4-mm diameter

Four to six 13 × 51-mm Ultraclear tubes

Two 150-mm regular petri dishes, one high-sided 150-mm petri dish; rinse well with dd H_2O and coat with 100 μg/ml gelatin (thaw gelatin at 37°C, pour ~30 ml MMR into petri dish, pipet in 60 μl of gelatin and swirl well for ~30 sec, and pour out MMR and replace with XB); if making a squeezed egg extract in parallel (see Section VII,A) gelatin coat four 60-mm petri dishes (15 ml MMR and 30 μl gelatin) and fill with MMR for squeezing frogs into dishes, and coat one 100-mm petri dish for processing the squeezed eggs after dejellying

600-ml glass beaker (rinsed well with dd H_2O)

C. General Considerations for Preparing Spindle Assembly Extracts

Spindle assembly is best performed using freshly prepared extracts because freezing extracts considerably decrease their ability to form bipolar spindles. For spindle assembly extracts, egg quality must take precedence over egg quantity. Because 1 or 2 ml of extract is more than sufficient for most experiments, it is best not to use any batches of eggs containing significant numbers (>10%) of lysed eggs, activated eggs (detected by contraction of dark pigment at the animal pole), or "puffballs" (eggs which are swollen and often white and puffy). Strings of eggs which do not have fully separated jelly coats can be used as a last resort unless they contain a high percentage of deformed or activated eggs. Any batches of eggs which are distinguishable in quality should be processed separately. Although the best spindle assembly extracts are often made from freshly squeezed eggs, we have had good success with laid eggs and will focus here on their use. Further discussion of squeezed egg extracts is presented in Section VII,A.

For laid eggs, extract preparation should begin 16–18 hr after hCG injection. We recommend that the temperature of the buffers and the room in which eggs will be manipulated not exceed 23°C (ideally 18–20°C). Warmer temperatures will almost certainly result in lower quality extracts. Rinsing of eggs after dejellying is best performed in gelatin-coated petri dishes by swirling the dishes a couple of times and pouring out the buffer. Never pour solutions directly onto the dejellied eggs because they are quite fragile. Pour the solutions down the side of the wash vessel, and then gently swirl the eggs. Maximal buffer exchange in petri dishes can be achieved by turning the dish away from you and quickly removing buffer at the edge of the egg mass using a wide-bore Pasteur pipet prior to pouring in the next wash buffer. During the washes, the eggs should be "gardened," i.e., visibly deformed eggs, activated eggs, puffballs, and large pieces of debris should be removed using the wide-bore Pasteur pipets. However, one should not get so caught up in removing bad eggs and debris that this slows the preparation of

the extract. Time is another important variable. Generally it should be possible to go from collecting of eggs to the crushing spin in 45 min to 1 hr.

D. Procedure for Extract Preparation

1. Combine batches of good laid eggs and remove as much MMR as possible.
2. Wash eggs in 2 or 3 liter of MMR until all of the debris is removed. Combine good egg batches in a frog bucket, rinse a couple of times with MMR, and pour the eggs into a 600-ml beaker for the rest of the MMR washes. Since eggs settle quickly, pouring out the MMR immediately after the eggs have settled allows easy removal of debris. Eggs should be gardened during this step and during washes after dejellying.
3. Remove as much MMR as possible and rinse eggs into dejellying solution.
4. Swirl gently and intermittently in the dejellying solution. While the eggs are dejellying, pipet 1 ml of CSF-XB + PIs to each 13 × 51-mm Ultraclear centrifuge tube and add 10 μl of 10 mg/ml cytochalasin B/D per tube (flick the tube well immediately after pipeting in the cytochalasin or it will precipitate).
5. After eggs are dejellied (this will take 7–10 min and the volume will decrease approximately five-fold; eggs will pack tightly and orient with their vegetal poles down), remove as much dejellying solution as possible, rinse eggs with residual dejellying solution and once with XB, then transfer eggs to gelatin-coated petri dishes. Wash dejellied eggs three or four times with XB in the petri dish as described in Section II,C. For larger batches of eggs, we recommend using the high-sided 150-mm petri dishes.
6. Wash eggs two or three times in CSF-XB. Remove as much buffer as possible.
7. Wash eggs twice in CSF-XB + PIs. Leave eggs in a small volume of CSF-XB + PIs after the second wash.
8. Draw eggs up into the wide-bore Pasteur pipet and slowly drop them into the 1-ml CSF-XB + PIs + 100 μg/ml cytochalasin solution in the ultraclear tube. Insert the pipet below the meniscus to break the surface tension and gently release eggs into the solution. Minimize transfer of buffer along with the eggs.
9. Aspirate excess buffer from the top of the eggs.
10. Put the ultraclear tubes into 14-ml polypropylene round-bottom culture tubes (Falcon No. 2059) and spin for 10 sec at setting No. 4 (approx. 1500 rpm) in a clinical centrifuge.
11. Gently aspirate buffer from top of the eggs and layer on 0.75–1 ml of Versilube F-50. Use of versilube minimizes dilution during extract preparation. The density of versilube is intermediate between that of buffer and cytoplasm; thus, versiluble displaces buffer between the eggs during the packing spin but floats to the top of the cytoplasmic layer during the crushing spin.

12. Pack the eggs by spinning at setting No. 5 for 30 sec (2000 rpm) and full speed (No. 7) for 15 sec (2500–3000 rpm) in the clinical centrifuge.

13. Aspirate all buffer and versilube from the top of the packed eggs.

14. Transfer the tubes containing the packed eggs to the SW55.1 rotor in the ultracentrifuge. Crush the eggs by centrifugation at 10,000 rpm for 15 min at 16°C (full brake).

15. Store tubes with crushed eggs on ice. The light yellow layer on top represents the lipid droplets and the dark layer on the bottom contains the yolk and nuclei. The cytoplasmic layer is the muddy or straw-colored layer in the middle of the tube. Prior to collecting the cytoplasmic layer, wipe the sides of the tubes with 95% ethanol. Puncture the tube near the bottom of the cytoplasmic layer with an 18-gauge needle (on a 1-cc syringe), and gently draw out the extract. [See Fig. 3 of Murray (1991) for a picture of an extract.] We find it best to use a new needle for each centrifuge tube. Transfer the collected extract to a 5-ml snap cap tube and estimate its volume.

16. Add 1/1000 volume of protease inhibitor (LPC) and cytochalasin stocks, 1/20 volume of 20× energy mix, and 1/40 volume of 2 *M* sucrose. Note that some people do not add additional sucrose to the extract after preparation, but we find that it often helps stabilize the extract during immunodepletions (see Section V,A).

E. Preparation and Use of Sperm Nuclei and Fluorescent Tubulin

Sperm nuclei are prepared exactly as described by Murray (1991) and stored in small aliquots at −80°C at a density of $1–5 \times 10^7$/ml. Sperm nuclei can be frozen and thawed multiple times without apparent loss of activity, but we prefer to store them in small aliquots and only freeze–thaw once for spindle assembly reactions. Sperm nuclei are added to extracts at a 1/100–1/200 dilution yielding a final concentration of 100–300 nuclei/μl.

Fluorescent tubulin is used to monitor microtubule distributions during spindle assembly and is prepared by the high pH labeling protocol described by Hyman *et al.,* (1991). Fluorescein, tetramethyl rhodamine, or X-rhodamine-labeled tubulin can be used to monitor spindle assembly. We generally use X-rhodamine-labeled tubulin because it has better spectral separation from fluorescein than does tetramethyl rhodamine, allowing double-label immunofluorescence studies with fluorescein-conjugated secondary antibodies (see Section IV). Our X-rhodamine-labeled tubulin preps have final concentrations varying between 15 and 25 mg/ml with labeling stoichiometries between 0.5 and 1. For monitoring spindle assembly, we add X-rhodamine tubulin to the extract at a final concentration of 20–50 μg/ml (generally a 1/400 dilution). Although tubulin by itself is highly unstable, it appears to be very stable in the extract and can be added immediately after extract preparation.

III. Spindle Assembly Reactions

Three types of spindle assembly reactions have been described in the literature (Sawin and Mitchison, 1991; Heald *et al.*, 1996). In the first type of reaction, termed CSF spindle assembly, each sperm nucleus added to the extract drives the formation of a half spindle. Two such half spindles then fuse to form a bipolar mitotic spindle (Fig. 1, top) (Sawin and Mitchison, 1991). Thus, two haploid sperm nuclei drive the formation of a single bipolar spindle. In the second type of reaction, termed cycled spindle assembly or interphase-to-mitosis spindle assembly, calcium is added to a CSF extract containing sperm nuclei, inactivating the CSF arrest and driving the extract into interphase. As the nuclei in the extract cycle through interphase their DNA is replicated once (Sawin and Mitchison, 1991). Fresh CSF extract without any sperm nuclei is then added to drive the extract containing replicated sperm nuclei into metaphase. In this type of spindle assembly reaction, each sperm nucleus undergoes one round of replication and drives the formation of a bipolar mitotic spindle (Fig. 1, bottom). Cycled spindles containing replicated chromosomes are arrested in metaphase by CSF; addition of calcium for a second time results in inactivation of CSF and anaphase chromosome segregation (Shamu and Murray, 1992). Heald and coworkers (1996) described the assembly of spindles around DNA-coated beads in extracts. These studies demonstrated that chromatin-coated beads are sufficient to generate a bipolar mitotic spindle in the absence of centrosomes and kinetochores. A study describing the use of DNA-coated beads for studying spindle assembly has been presented recently (Heald *et al.*, 1998).

A. General Considerations for Spindle Assembly Reactions

Xenopus extracts are a powerful tool for studying mitosis but their use can be very frustrating because of high variability. These extracts are very sensitive to physical perturbations and must be treated gently to ensure the best results. Avoid pipeting up and down vigorously with narrow-bore pipet tips or dropping tubes containing extract reactions since either of these can sufficiently perturb the extract to disrupt the spindle assembly process. We recommend pipeting with either commercially available wide-bore P-200 tips (Rainin HR-250W) or regular P-200 tips that have been cut off to an opening of ~2 mm diameter and mixing by either gently tapping the bottom of the tube or inverting the tube two or three times. Use a fresh pipet tip for each aliquot, especially for experiments requiring quantitation because these extracts are very viscous. Never vortex a tube containing extract because this will surely destroy the extract. Finally, avoid diluting the extract with buffer or other reagents because this can also inhibit spindle assembly (see Section V,B).

To set up spindle assembly reactions, add sperm nuclei and labeled tubulin to a large volume of extract and then aliquot it into individual reactions. The extract is very viscous and difficult to pipet accurately. Use a fresh pipet tip for

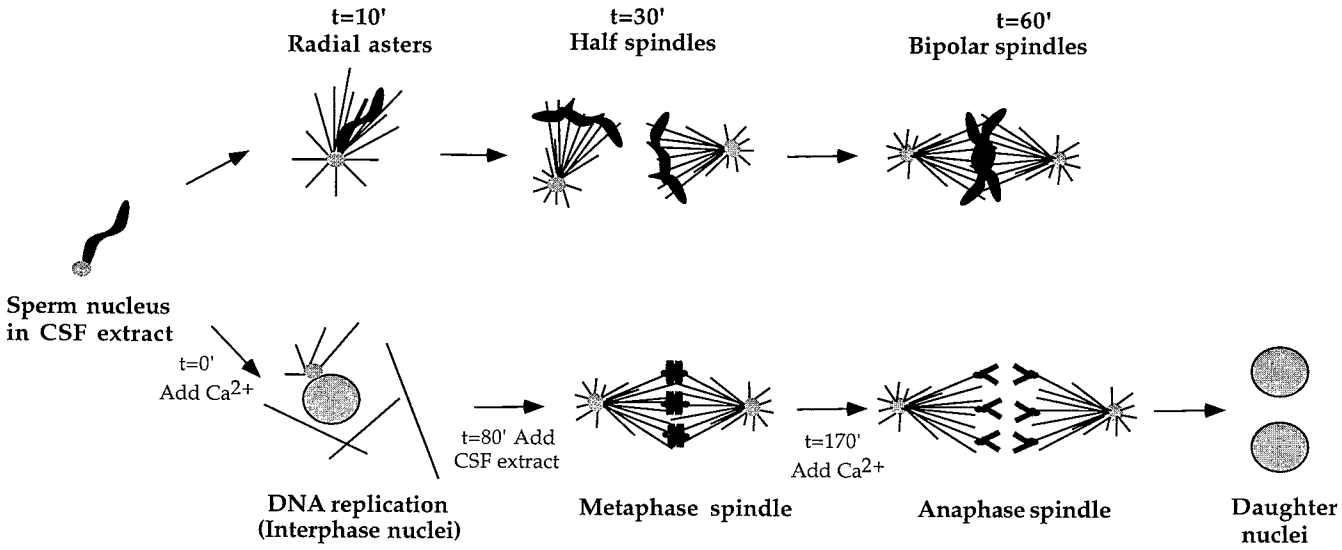

Fig. 1 The *in vitro* spindle assembly pathways. (Top) CSF spindle assembly. (Bottom) Cycled spindle assembly.

each aliquot to ensure reproducibility and allow for a 20% volume loss upon aliquoting. Do not exceed a reaction volume of >50 μl/1.5 ml Eppendorf tube since larger reaction volumes tend to inhibit spindle assembly. We recommend incubating reactions at 20°C in a cooled water bath (a home-made one can be a plastic tray containing water with some ice to maintain 20°C). However, if the room temperature is stable from day to day and does not exceed 24 or 25°C, then the reactions can be incubated on the bench top.

B. Reagents Required for Spindle Assembly

Sperm nuclei at 1–5 × 10^7/ml

Fluorescently labeled tubulin

Extract fix: 60% (v/v) glycerol, 1× MMR, 1 μg/ml Hoechst 33342/33258, 10% formaldehyde [from 37% (w/v) stock]

Sperm dilution buffer (1×): 10 m*M* Hepes (pH 7.7), 1 m*M* $MgCl_2$, 100 m*M* KCl, 150 m*M* sucrose, 10 μg/ml cytochalasin B/D; can be prepared as a 5× stock; both 1× buffer and 5× stock should be stored at −20°C

10× calcium: 4 m*M* $CaCl_2$ in 1× sperm dilution buffer

C. CSF Spindle Assembly

To CSF extract containing labeled tubulin add sperm nuclei to a final concentration of 100–300/μl. Mix gently, aliquot 25 μl/tube, and incubate at 20°C. At 15, 30, 45, and 60 min take samples to test the progress of the reaction as follows: pipet a 1-μl aliquot of the reaction on a microscope slide, overlay with 3 μl of extract fix, cover gently with an 18 × 18-mm coverslip, and view by fluorescence microscopy. At the 15-min time point, small microtubule asters emanate from the sperm centrosome (Fig. 2, top); these often have a very dense core of microtubules. By 30 min the chromatin has migrated away from the centrosome, and the microtubules are polarized toward the chromatin: These structures are termed half spindles (Fig. 2, middle). Between 30 and 60 min, half spindles begin to fuse to form bipolar spindles (Fig. 2, bottom). During CSF spindle assembly, the percentage of total structures that are bipolar spindles varies considerably from extract to extract. In a typical extract, 40–60% of the total structures are bipolar spindles by the 60-min time point. This number can range from <10% in very poor extracts to >90% in the best extracts.

D. Cycled Spindle Assembly

For cycled spindle assembly the extract is divided into two tubes after the addition of labeled tubulin. One tube is supplemented with sperm nuclei and cycled into interphase by the addition of calcium, whereas the second tube is held on ice until it is needed to drive the extract with replicated sperm nu-

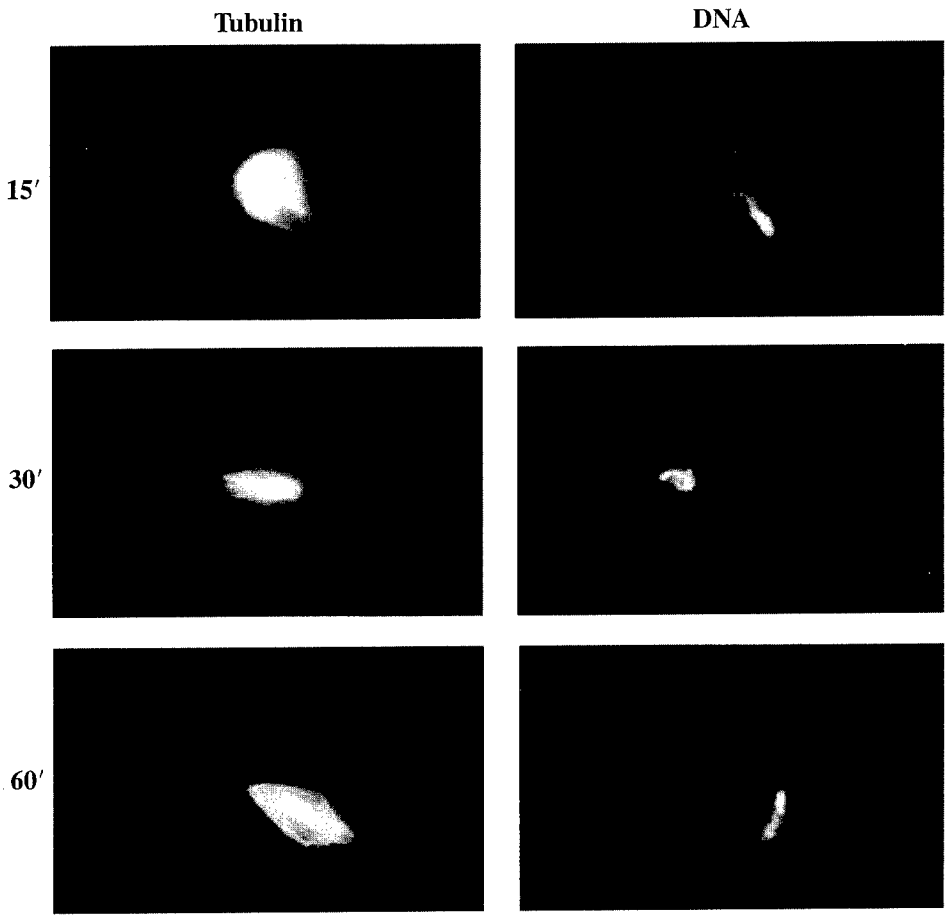

Fig. 2 Reaction intermediates of CSF spindle assembly reaction. Samples were removed from the reaction and sedimented onto coverslips as described in the text. The microtubules and chromatin structures formed during the reaction are shown for 15-, 30-, and 60-min time points.

clei back into metaphase. Specifically, to one-half of the extract containing labeled tubulin add sperm nuclei. Withdraw a small amount as a negative control (~20 μl), and to the rest add 1/10 volume of 10× calcium solution. Mix the calcium into the extract gently but thoroughly, aliquot 20-μl/tube, and incubate both the aliquot withdrawn prior to calcium addition and the reaction tubes supplemented with calcium at 20°C for 80 min. During this incubation the extract is monitored by taking samples at 30-, 45-, and 60-min time points as described in Section III,C. Reactions to which calcium was added should exit the CSF arrest and cycle through interphase; negative control sample (withdrawn before calcium addition) should remain in CSF (mitotic) arrest. Morphology of the

mitotic arrest was described in Section III,C. The reactions with calcium should appear as follows: after 30 min, the sperm nucleus should be swollen and many free microtubules should be present in the extract; after 45 min, the sperm nucleus should be large and round and resemble a typical mammalian cell interphase nucleus; after 60 min, the sperm nucleus should appear large and reticular much like an early prophase nucleus, suggesting that the extract may be starting to cycle back into metaphase. In our experience, extracts that have irregularly shaped interphase nuclei at the 45-min time point tend to be less robust in generating mitotic spindles. After 80 min at RT, 20 μl of CSF extract containing labeled tubulin but not sperm nuclei is added to each reaction (this represents an equal volume of extract added to the initial reaction), mixed in gently and incubated at 20°C for 60–90 min to allow establishment of the metaphase CSF arrest and formation of bipolar spindles. The reactions containing bipolar spindles can be held at RT for many hours without detriment, although with increased time the number of single bipolar spindles drops significantly because the spindles tend to aggregate laterally, forming large multipolar structures.

In general, cycled spindle assembly results in a more uniform distribution of structures than CSF spindle assembly and yields a higher proportion of bipolar spindles (80–90% of total structures at 60 min). Cycled spindles have chromosomes aligned in an equatorial plane, highly reminiscent of a metaphase plate in somatic cells (Fig. 3, top). However, the tightness of the metaphase plate in cycled spindles can vary significantly between extracts. In good extracts, the chromosomes are tightly focused at the spindle equator, whereas in less robust extracts, the chromosomes tend to be both at the spindle equator and scattered on either side of the equator. These less robust extracts generally do not work well for anaphase chromosome segregation (see Section VII).

The morphological pathway by which cycled spindles assemble remains to be clarified. Sawin and Mitchison (1991) first described the pathway as being chromatin driven, i.e., microtubules assembled in the region of the chromatin and with time organized into a bipolar structure with morphologically distinguishable poles. This pathway is similar to that described recently using chromatin-coated magnetic beads, with the exception that spindles assembled from sperm nuclei contain centrosomes. However, Boleti and coworkers (1996) reported that two distinct centrosomal arrays of microtubules are separated to opposite sides of the nucleus in a more classical somatic cell-type spindle assembly pathway. A clear picture of the cycled spindle assembly pathway awaits a thorough real-time study of this reaction using fluorescence video microscopy.

IV. Monitoring Spindle Assembly Reactions

A. Methods for Pelleting Spindles onto Coverslips

Spindle assembly reactions are routinely monitored using fixed squashes as described in Section III,C. However, for quantitative analysis we prefer to sedi-

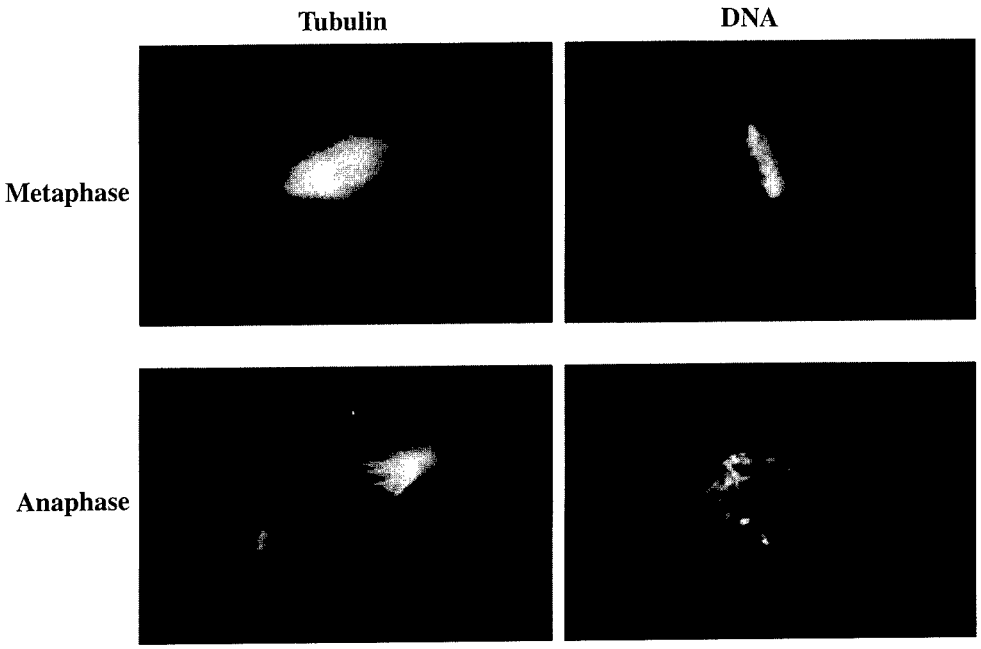

Fig. 3 Optimal fixation of spindle structures. Using the optimized fixation conditions it is possible to preserve chromosome structure and microtubule structure. (Top) Metaphase spindles assembled by the cycled spindle pathway. (Bottom) Spindles that have been induced to enter anaphase following calcium addition.

ment the spindles from a large volume (20 μl) of extract onto a coverslip. The advantages of sedimenting spindles onto coverslips are threefold. First, spindles from 20 μl of reaction are concentrated onto a 12-mm coverslip, providing a dense, relatively homogenous sample for quantitative analysis. Second, having the spindles fixed on coverslips allows one to perform immunofluorescence to analyze the localization of specific antigens on the *in vitro* spindles. Third, unlike squashes, the pelleted samples are very stable when stored at −20°C. This allows one to prepare many samples at once but analyze them when convenient and store them for any future reanalysis. We use two procedures for pelleting spindles onto coverslips. In the first (method 1), reactions are diluted extensively into a microtubule-stabilizing buffer, pelleted unfixed onto coverslips, and fixed onto the coverslips using methanol. Two limitations of this method are an extreme disruption of chromosome structure and day-to-day variability. Recently, we have developed an alternative method (method 2) that involves first diluting the spindles into a microtubule-stabilizing buffer and then fixing the spindles in solution using formaldehyde, pelleting the spindles onto coverslips, and postfixing using methanol. Using method 2 we have satisfied the demanding requirement

of retaining the fine structure of chromosomes as they are undergoing anaphase without causing significant disruption of spindle structure (Fig. 3, bottom).

1. Requirements for Pelleting Spindles onto Coverslips

BRB80
80 m*M* K-Pipes, pH 6.8
1 m*M* $MgCl_2$
1 m*M* EGTA
Make as 5X stock, sterile filter and store at 4°C

5-ml snap cap tubes (Sarstedt No. 55.526.006)

Dilution buffer
BRB-80
+ 30% (v/v) glycerol
+ 0.5% Triton X-100

Fixation buffer
BRB80
+ 30% (v/v) glycerol
+ 0.5% Triton X-100
+ 4% formaldehyde, added just before use from 37% stock

Cushion
BRB80
+ 40% (v/v) glycerol

Spindown tubes (Evans *et al.*, 1985)
With 12-mm coverslips and 4-ml cushion at room temperature

Coverslip holders
For 12-mm round coverslips; we like to use Thomas Scientific No. 8542-E40

−20°C methanol

TBS-TX
1X TBS [10 m*M* Tris (pH 7.4) and 150 m*M* NaCl]
0.1% Triton X-100

Mounting medium
0.5% *p*-phenelynediamine (free base) in 90% glycerol and 20 m*M* Tris–Cl, pH 9.0

2. Method 1

1. Prior to beginning the spindown procedure, prepare spindown tubes with coverslips and cushion and 5-ml snap cap tubes with 2 ml of dilution buffer. All buffers should be at RT.

2. Pipet 20 μl of spindle assembly reaction into the dilution buffer. Prior to transferring the extract into the dilution buffer, we often pipet up and down two or three times with a regular yellow tip to break any large aggregates.

3. Immediately cap the tube and mix by gently inverting four or five times.

4. Using a disposable plastic transfer pipet, layer the diluted sample onto the cushion in the spindown tube. After dilution, the spindles are stable; therefore, if a large number of samples are being pelleted, first do the dilution and mixing for all samples and then layer them sequentially onto cushions.

5. Centrifuge the tubes in an HS-4 rotor at 18°C for 20 min at 5500 rpm (6000*g*). We use the HS-4 because it can hold 16 tubes; an HB-4, HB-6, or equivalent rotor can be used for smaller numbers of tubes.

6. Aspirate until just below the sample–cushion interface, rinse with BRB80, aspirate off the rinse and the cushion, and transfer the coverslips to a coverslip holder.

7. After all coverslips are in the holder, fix by immersion in −20°C methanol for 3 min.

8. Rehydrate using two sequential 5-min incubations in TBS-TX.

9. Label DNA by rinsing coverslips with 1 μg/ml Hoechst in TBS-TX for 30 sec, mount in mounting medium, and seal with nail polish. Rinse top surface of coverslip with water prior to observation.

3. Method 2

Method 2 is different from method 1 as follows:

1. Dilute 20 μl of sample into 1 ml of dilution buffer as in step 2 of method 1.

2. Dilute all samples first, then add 1 ml of fixation buffer and mix well by inversion.

3. Fix for 5 min at RT prior to layering onto cushion.

4. After pelleting fixed spindles onto coverslips and aspirating the cushion after rinsing (step 6 in method 2) postfix the coverslips in −20°C methanol.

Using this method we have successfully preserved the fine structure of chromosomes (Fig. 3) without significantly compromising spindle structure.

Spindles pelleted onto coverslips using either method can be processed for immunofluorescence using antibodies to specific spindle components (Walczak *et al.,* 1996). After rehydrating in TBS-TX, coverslips are blocked in TBS-TX + 2% BSA (antibody dilution buffer or AbDil) for 15–30 min, incubated sequentially with primary and secondary antibodies diluted in AbDil, rinsed in TBS-TX containing 1 μg/ml Hoechst, and mounted as described previously. For localizing antibodies added to inhibit function of a particular component, only incubation with the appropriate secondary is necessary (Walczak *et al.,* 1997).

B. Time-Course Experiments

While characterizing the functions of spindle components using the CSF spindle assembly reaction, it is often desirable to monitor the intermediates in the path-

way. In order to set up time-course experiments for this purpose, it is important that samples for all time points are derived from a single pool of reaction mix and that they are sedimented onto coverslips at the same time. Specifically, to a volume of extract sufficient for all time points, add sperm nuclei and any other reagents, such as antibodies or dominant-negative fusion proteins, and store on ice. At various intervals beginning with $t = 0$ min, remove 25 μl and transfer to a tube at 20°C. At the end of the time course, pellet all samples onto coverslips using either of the methods described in Section IV,A.

V. Manipulation of Extracts

The ability to manipulate specific components in the extract by either immunodepletion or reagent addition and to assay the effects of these manipulations on spindle assembly is one of the main advantages of *Xenopus* egg extracts. A recent flurry of publications applying this strategy to dissect the role of both motor and nonmotor components during spindle assembly demonstrates the value of this approach (Sawin *et al.,* 1992; Vernos *et al.,* 1995; Boleti *et al.,* 1996; Heald *et al.,* 1996, 1997; Merdes *et al.,* 1996; Walczak *et al.,* 1996, 1997).

A. Immunodepletion of Extracts

The main difficulty with immunodepletion of CSF extracts is that they lose the CSF arrest during or soon after immunodepletion. In our experience, the following actions seem to aid in immunodepleting proteins without losing the CSF arrest:

1. During the CSF extract prep, after washing with XB, the eggs are washed thoroughly with CSF-XB without protease inhibitors (step 6 in Section II,D). This CSF-XB wash ensures that there is sufficient EGTA in the final extract to maintain a tight CSF arrest.

2. Eggs are crushed at 10,000 rpm (full brake) in a SW55 rotor at 16°C. Even a slightly faster spin (12,500 rpm) does not work well—one does not obtain robust spindle assembly after immunodepletion.

3. Antibodies are coated on BioRad Affi-Prep Protein A beads (BR No. 156-0006). Unlike regular protein A agarose beads, these high-density beads sediment readily through the viscous extract at speeds gentle enough to not perturb the extract.

4. Remove as much buffer as possible after coating the beads with antibody to avoid diluting the extract, which will inhibit spindle assembly.

5. Extracts are handled extremely gently during manipulations such as resuspending beads or sedimenting beads.

The ability to deplete a specific protein from the extract is dependent on both the quality of the antibody used for depletion and the abundance of the protein

being depleted. Regarding antibody quality, for reasons we do not understand, we have had much better success with antibodies prepared by immunizing with native proteins as opposed to antibodies generated against denatured proteins, e.g., proteins excised from acrylamide gels.

The following protocol is for depleting a protein present at ~10–20 μg/ml in the extract using high-affinity polyclonal antibodies. While this presents a good starting point, exact conditions must be optimized for each new antibody, particularly the amount of antibody needed for maximal depletion. As a control, we use an equivalent amount of random IgG from the same species; given the extreme perturbation of the extract by the immunodepletion procedure all interpretations of depletion phenotypes must be restricted to comparison with random IgG depletion performed at the same time and processed identically. The procedure for depletion is as follows:

1. Pipet 25 μl of Affi-Prep protein A beads (50 μl of slurry) into a 0.5-ml Eppendorf tube.
2. Wash beads three times with 0.5 ml TBS-TX [20 m*M* Tris (pH 7.4), 150 m*M* NaCl, and 0.1% Triton-X 100].
3. Add 4 μg of antibody and bring total volume to 200 μl using TBS-TX.
4. Bind antibody to beads at 4°C for 1 hr on rotator. Make sure beads are rolling around during the incubation.
5. Pellet beads in a microfuge for 20 sec, wash one time with TBS-TX and three times with CSFXB + PIs using 200 μl/wash. Remove as much buffer as possible to avoid diluting the extract.
6. Add 200 μl of extract to each tube and resuspend beads in extract very gently using a wide-bore P-200 tip; Do not pipet up and down more than three times and avoid tapping the tube or any other type of vigorous agitation.
7. Before the beads settle, rapidly place the tube on the rotator and rotate for 1 hr at 4°C. Make sure that the beads are mixing well with the extract during this period.
8. Pellet the beads for 20 sec in a microfuge and transfer the supernatant to a fresh tube—this is the depleted extract. It is difficult to recover more than 175 μl from a 200-μl depletion without contaminating the extract with the beads. Save a small amount of depleted extract to test the extent of depletion by immunoblotting.
9. To analyze what is bound to the beads, wash the beads two times with CSF-XB + PIs, three times with TBS-TX, and one time with TBS. Resuspend the beads in 50 μl SDS–PAGE sample buffer and boil to release the IgG–antigen complexes from the beads. Analyze the sample by SDS–PAGE and Coomassie brilliant blue staining.

Extracts that have been immunodepleted are far less robust than nondepleted extracts. A good CSF extract will remain mitotic for at least 6–10 hr on ice,

whereas a depleted extract will remain mitotic for a few hours at most. We find that with depleted extracts CSF spindle assembly proceeds normally, although the extent of bipolar spindle formation is reduced by twofold compared to the undepleted extract (Walczak *et al.,* 1997). At a frequency lower than that for CSF spindle assembly, we have successfully used immunodepleted extracts for cycled spindle assembly. We have yet to attempt anaphase chromosome segregation in depleted extracts.

We have tried to optimize the immunodepletion procedure to minimize perturbation of the extract but have yet to find the perfect conditions. We believe that the primary problem with immunodepletions is the physical perturbation of the extract by the beads as they are sloshing through the extract. Our most successful manipulation to minimize extract perturbation has been to reduce the time of depletion to 30–45 min instead of 1 hr. However, with lowered times we also see a reduced efficiency of depletion; we have yet to systematically investigate this issue. We have also wondered whether doing the depletions at RT might be better since calcium uptake machinery would sequester released calcium more efficiently at RT than at 4°C and also whether adding antibody directly to extracts and collecting the antibody–antigen complexes later might be faster and less disruptive than using antibody-coated beads. Addition of excess EGTA to sequester released calcium never gave reproducible improvements. Given the logical importance of immunodepletion experiments, technical improvements to immunodepletion procedures are eagerly awaited by many researchers.

B. Reagent Addition to Extracts

A complementary approach to immunodepletions is to assay the effect of adding either inhibitory antibodies or dominant-negative proteins on spindle assembly. This approach is useful because it is less perturbing to the extract than immunodepletion. In addition, it allows one to perturb protein function both before and after spindle assembly, thus allowing one to address the requirement of protein function in both the establishment and maintenance of spindle structure.

One concern with respect to addition of reagents to extracts is dilution of the extract. We recommend not adding reagents to >10% of extract volume since greater dilution results in poor extract performance. For antibodies, we recommend dialyzing into a buffer that is compatible with extracts, such as 10 m*M* Hepes (pH 7.2) and 100 m*M* KCl. In this buffer, several antibodies that we generated are stable at −80°C and working stocks are stable for several months at 4°C. Also compatible with extracts is 50 m*M* K-glutamate (pH 7.0) and 0.5 m*M* $MgCl_2$, and this can also be used for storage of antibodies. We avoid the use of CSF-XB or sperm dilution buffer for storing antibodies since both these buffers contain sucrose, making them highly susceptible to bacterial contamination at 4°C. We also avoid adding azide to our antibody stocks. Dominant-

negative fusion proteins can be dialyzed into CSF-XB and stored at −80°C prior to addition to extracts.

The amount of antibody that must be added to perturb function depends on the quality of the antibody being used and on the abundance of the target protein in the extract. We have found that as little as 25–50 μg/ml of a very potent antibody, such as the polyclonal anti-XKCM1 antibody, completely inhibits XKCM1 function, whereas 1 mg/ml of a monoclonal antibody to the intermediate chain of dynein is required to inhibit dynein function. We suggest that each new antibody be titrated to determine the amount necessary for full inhibition. Since the mode of action of dominant-negative proteins is presumably to compete with the endogenous protein, the amount of fusion protein that must be added to perturb function depends on the endogenous concentration of the target protein. We recommend a 10-fold molar excess of fusion protein as a starting point but the concentration for optimal inhibition must be empirically determined for each protein.

VI. Data Analysis and Interpretation

Xenopus extracts are very powerful for analyzing protein function in spindle assembly, but all extract workers admit that their use is plagued by variability. It is not uncommon to go through periods in which several concurrent extracts will not assemble good spindles or in which immunodepletions consistently lead to extract activation. This is perfectly normal and can only be overcome by persistence. However, the extreme variability does necessitate care in performing and interpreting experiments, and we discuss how we approach the analysis of protein function in spindle assembly.

To analyze spindle assembly defects, we recommend starting with technically simpler antibody addition experiments, varying the concentration of added antibody and analyzing the effect using spindowns to facilitate detailed analysis. We quantitatively characterize the phenotype in at least three different experiments on three different extracts, often preparing duplicate samples on a single extract to increase the sample size. Once the effect of antibody addition is clear, the next step is to determine the effect of protein depletion. The immunodepletion procedure itself perturbs the extract significantly, making it difficult to discern subtle phenotypes. Furthermore, immunodepletion is technically much more difficult to execute than antibody addition. However, the results of antibody addition experiments must be interpreted cautiously in the absence of a confirmation of the observed effects by immunodepletion. In the absence of immunodepletions, combining antibody inhibition with a dominant-negative approach might help strengthen conclusions with respect to the role of a specific protein in spindle assembly. In addition, determining the effect of manipulating a particular protein on all three types of spindle assembly reactions—CSF spindle assembly, cycled spindle assembly, and DNA bead spindle assembly—can also provide greater

insight into its role in spindle assembly (Heald *et al.,* 1997). Performing identical manipulations on different types of spindle assembly reactions can also provide new insights into the process of spindle assembly itself, as demonstrated by recent work characterizing the role of centrosomes during spindle assembly (Heald *et al.,* 1997). Finally, the most desirable extension of the manipulation of specific components during spindle assembly is to reconstitute spindle assembly by adding back purified protein to immunodepleted extract—the logical equivalent of a genetic complementation. However, as might be expected, this has proven to be quite difficult and has only been partially achieved (Merdes *et al.,* 1996; Walczak *et al.,* 1996). Future technical improvements in immunodepletion procedures will be necessary to achieve this goal.

The extreme variability between extracts makes identifying the effect of manipulating specific components heavily dependent on the strength of the observed phenotype. Certain phenotypes, such as the one induced by inhibition of XKCM1, are extremely dramatic and can be easily defined in the first extract analyzed (Walczak *et al.,* 1996). Others, such as the one induced by inhibition of the spindle motor XCTK2, are much more subtle and difficult to detect without careful inspection of many extracts (Walczak *et al.,* 1997). Reproducibility and quantitative analysis become critical in determining the nature of subtler phenotypes.

VII. Anaphase *in Vitro*

Cycled spindles assembled in *Xenopus* egg extracts are capable of undergoing anaphase chromosome segregation (Shamu and Murray, 1992). This *in vitro* anaphase reaction has proven valuable for dissecting both the mechanism of sister chromatid separation and the mechanism of chromosome movement (Murray *et al.,* 1996; Desai *et al.,* 1998). However, successful anaphase *in vitro* requires considerably higher quality extracts than those used for spindle assembly and this has significantly limited the use of this reaction. In the following sections we provide some hints to facilitate successful preparation of anaphase-competent extracts. We also describe methods to set up and monitor an anaphase reaction using either fixed time points or time-lapse fluorescence microscopy.

A. Preparation of Anaphase-Competent Extracts

Extracts for monitoring anaphase are prepared exactly as described for CSF extracts (see Section II). Anaphase extracts require high-quality eggs, and frogs which lay even small amounts of puffballs or stringy eggs should not be used. Note that the absolute volume of extract required for these experiments is very small and quality should always take precedence over quantity. One factor, which should be minimized in the preparation of anaphase-competent extracts, is the time between egg-laying and extract preparation. Often the best extracts are

prepared from freshly squeezed eggs since they have not been floating for several hours in "frog-conditioned" MMR. However, laid egg extracts, which are easier to prepare, can also be fully competent for anaphase. We routinely collect laid eggs from four to six frogs about 12–14 hr after injection with hCG (frogs are stored at 16°C in 1X MMR as described previously, generally two to four of the frogs lay eggs of sufficient quality for extract preparation) and prepare extracts from the laid eggs and freshly squeezed eggs in parallel. While squeezing the frogs, it is extremely important to avoid getting any frog skin secretions ("frog slime") into the squeezed eggs or the eggs will activate. Frog slime can be avoided by frequently dipping the frog into a bucket of clean distilled water during the squeezing process. Squeezed eggs from different frogs should be kept separate initially but can be pooled after dejellying if they do not exhibit signs of activation. It is difficult to obtain large quantities of squeezed eggs, but from four frogs we generally get enough to fill one-half to three-fourths of a 13 × 51-mm Ultraclear tube. The laid eggs and squeezed eggs are separately processed as described previously for the CSF extract prep. It is important to thoroughly wash out residual jelly coat after the dejellying step and to crush the eggs at 10,000 rpm for 15 min at 16°C (full brake). This speed spin results in highly turbid muddy-colored extracts. Faster spins result in clearer extracts that often suffer from extensive and rapid spindle aggregation, resulting in very limited time of manipulation and precluding any significant analysis. We also note that newer frogs that have not been through multiple rounds of ovulation tend to be better for anaphase experiments, although, as with many other aspects of frog egg extracts, this is by no means definitive. Using frogs that have been through less than two cycles of ovulation (with at least a 3-month rest between ovulations) after being obtained from a distributor and taking great care in preparing the extracts, we have been able to successfully obtain anaphase extracts on a routine basis (70% of the time).

B. Setting Up and Monitoring Anaphase Reactions

Anaphase reactions require spindles obtained by cycled spindle assembly as described in Section III,D. It is essential that the cycled spindles have tight metaphase plates; often, chromosomes on the spindles are not confined to a tight metaphase plate but stray over the entire spindle, and these extracts are not useful for anaphase. To perform an anaphase reaction, 9 μl of a cycled spindle assembly reaction is mixed with 1 μl of the 10X calcium stock (see Section III,B) and monitored by taking fixed time points every 5 min for 30 min. The added calcium should be mixed well with the extract, either by gently flicking the bottom of the tube or by gently pipeting up and down. The addition of calcium results in the destruction of CSF and exit from the metaphase arrest. Between 5 and 15 min after calcium addition, clear evidence for anaphase should be evident in the chromosome morphology as depicted in Fig. 3. In addition to anaphase chromosome movement, changes in spindle structure, particularly thinning out of spindle MT density and expulsion of asters, should be evident (Murray *et al.*, 1996). By

25–30 min, rounded interphase nuclei should be visible in the reaction. In a good anaphase extract, 40–80% of the spindles show clear evidence of anaphase. However, it is not unusual to have an extract whose spindles have tight metaphase plates but do not exhibit anaphase. In addition, the percentage of spindles that exhibit anaphase often decreases dramatically with aging of the extract.

C. Real-Time Analysis of Anaphase *in Vitro*

1. Lengthening Extract Life Span

Although technically challenging, it is possible to observe anaphase *in vitro* in real time allowing detailed analysis of chromosome movement and spindle dynamics (Murray *et al.,* 1996; Desai *et al.,* 1998). Since there is no reliable procedure for freezing extracts while maintaining anaphase competency, and since each anaphase reaction takes approximately 30 min, during which only one spindle can be observed per field of view (of which <50% will provide analyzable data), it is essential to maximize the life span of the extract to perform real-time analysis. We have found it best to stagger the entire spindle assembly reaction by 3.5–4 hr, storing the original extract on ice during the interim, to maximize the amount of time that observational studies can be performed. We find this to be better than storing the extract on ice after cycling through interphase and have been able to use extracts routinely for 12–16 hr after preparation. We have also had some success with storing the cycled spindles at 10–12°C and warming them up to room temperature for 10–15 min prior to their use. We note, however, that with increased time spindles will be present in larger aggregates and the percentage of spindles capable of undergoing anaphase will decline.

2. Slide and Coverslip Cleaning

Requirements

Water, acetone, ethanol, slides, and coverslips (22 × 22 mm; No. 1), hotplate, slide storage box, 100-mm tissue culture dish, and coverslip spinner (optional).

It is essential to obtain homogenous sample films to avoid problems derived from air bubbles—we have often watched a spindle just beginning or in the middle of anaphase, only to have a bubble roll into view and wipe it out of existence. The key to good sample films is clean particulate-free slide and coverslip surfaces.

Cleaning Slides

1. Set up three 50-ml conical tubes filled with water, acetone, and ethanol and have a hotplate with a clean surface set such that the top feels hot to the touch (50–60°C).

2. Holding the frosted end, dip the slide several times in water and then in acetone and finally in ethanol. Transfer to the hotplate surface to rapidly dry

off the ethanol and store in a covered slide box. It is best to use a reasonably new box of slides to minimize particulates on the slides. If problems with bubbles persist, clean slides in a cup sonicator filled with warm water containing a small amount of detergent and rinse off the detergent prior to cleaning with acetone and ethanol.

Cleaning Coverslips

Coverslips are cleaned exactly as slides, except that coverslip holders are used for rinsing 12 coverslips at a time and the coverslips are dried using a homemade coverslip spinner. If no spinner is available, the coverslips can be dried by gently wiping both surfaces using lens paper (wear gloves while doing this). Clean coverslips can be stored in a plastic 100-mm tissue culture dish for several weeks.

3. Sample Preparation

Requirements

Valap, hotplate (for melting Valap), clean slides and coverslips, 10X calcium/DAPI stock (4 m*M* calcium chloride, 750 ng/ml DAPI in 1X sperm dilution buffer), extract reactions with cycled spindles.

Spindle microtubules are visualized using X-rhodamine tubulin added to the extract just after preparation. Chromosomes are visualized using DAPI and it is most convenient (and least perturbing) to add the DAPI to the calcium stock used for triggering anaphase. The 10X calcium/DAPI stock can be stored indefinitely at −20°C and is not sensitive to freezing and thawing. Prior to sample preparation, make sure that melted Valap is available to seal the sample. Valap is a 1:1:1 mixture of vaseline:lanolin:paraffin prepared by weighing equal amounts of the three components into a beaker and melting and mixing them on a hotplate.

Preparation of Sample

1. Transfer 9 μl of the cycled spindle assembly reaction to an Eppendorf tube.
2. Add 1 μl of the 10X calcium/DAPI stock. Mix gently but thoroughly by flicking and pipeting up and down.
3. Pipet 8 μl onto a clean slide. Cover gently with a clean 22 × 22-mm No. 1 coverslip. It is essential not to squash the sample film too vigorously. If there are many bubbles in the film, the sample should be discarded and a new sample should be prepared; however, it is often impossible to avoid one or two small bubbles near the center of the coverslip.
4. Seal the edges with Valap and start observation (a Q-tip works well as a Valap applicator).

We have experimented with more elaborate schemes to prevent distortion of spindles during sample preparation, such as coating of the slide surface with spacer latex beads, and also with alternative means of sealing the sample that avoid any local heating problems associated with the use of Valap (Murray *et*

al., 1996). However, we find that the simple procedure outlined previously is sufficient for observing anaphase and considerably reduces the complexity of sample preparation.

4. Sample Observation

Given the variable composition of products in a spindle assembly reaction, it is essential to pick the correct type of spindle for observation. We find it best to scan the sample in the DAPI channel using a 20× dry objective lens (with a 25% transmission neutral density filter in the light path) and to select medium-sized spindles with tight metaphase plates for time lapsing. Often, small spindles are too sensitive to flows under the coverslip (which are highly variable from extract to extract) that cause them to either spin around or float out of the field of view (both of which make analysis nearly impossible). Larger aggregates, while they do exhibit good anaphase, tend to be very messy and difficult to analyze. With a little practice, one can begin to pick spindles good for time lapsing anaphase with a frequency of 60–80%.

For acquiring images, we use low-power dry objectives (20×, 0.5 or 0.75 NA) and a cooled charged-coupled device camera. The minimal additional requirements for the real-time observation are the ability to acquire images at two different wavelengths (X-rhodamine and DAPI), to store the acquired images, and to shutter the illuminating light to minimize photodamage. A detailed description of the microscope setup used to acquire the images shown in Fig. 4 has

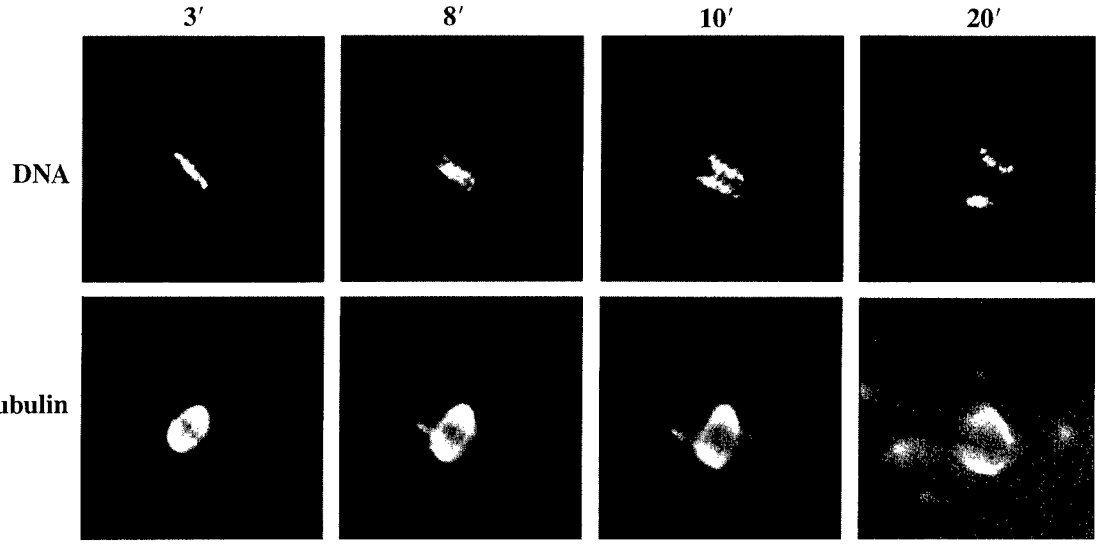

Fig. 4 Time course of anaphase chromosome movement. Individual frames are presented from a time-lapse recording of anaphase *in vitro.*

been published (Salmon *et al.,* 1994). Analysis of chromosome movement and spindle microtubule density can be performed on the collected images using one of several commercially available image analysis software packages.

D. Manipulation of Anaphase *in Vitro*

Manipulation of anaphase reactions has been restricted to addition of either nondegradable cyclin (cyclin Δ90) or pharmacological agents. For addition of cyclin Δ90, titrate the cyclin concentration such that physiological levels of H1 kinase are attained (Murray *et al.,* 1989). For optimal results, the cyclin Δ90 must be added to the extract for 20–30 min prior to triggering anaphase by addition of calcium. In the presence of cyclin Δ90 sister separation appears normal, although spindle microtubule density near the spindle poles does not decline and chromosome decondensation and formation of nuclei does not occur. For addition of pharmacological agents, trigger anaphase by adding 1/10 vol of a 10× calcium/agent stock and monitor as described previously. If anaphase is being monitored in real time, then add the agent from a 10× calcium/DAPI/agent stock. We have successfully used real-time analysis to monitor the effects of cyclin Δ90, AMPPNP, taxol, and vanadate on anaphase (Murray *et al.,* 1996; Desai *et al.,* 1998).

The more ambitious manipulation of depleting specific components and assaying the effect on chromosome segregation remains a technical challenge for the future. However, addition of reagents to anaphase reactions has been very useful, leading to the important discoveries that activation of the cyclin destruction machinery is sufficient to promote sister chromatid separation and that topoisomerase II activity is required for sister separation (Shamu and Murray, 1992; Holloway *et al.,* 1993).

VIII. Conclusions

In this chapter we have described detailed procedures for the preparation of spindle assembly extracts, for manipulation of extracts to define the function of specific proteins in spindle assembly, and for the analysis of anaphase chromosome movement *in vitro.* The importance of *Xenopus* extracts for analyzing spindle assembly and function is evident from their increasing use in recent years. However, many technical advances need to be made to allow a realization of the full potential of *Xenopus* extracts, particularly with respect to the manipulation and storage of extracts. We hope that the methods described here will serve as a starting point for future studies on spindle assembly and function and will stimulate technical innovations that will expand the types of analyses possible using *Xenopus* egg extracts.

Acknowledgments

We thank Manfred Lohka and Yoshio Masui, whose pioneering work led to the use of *Xenopus* egg extracts for studying spindle assembly and function; Manfred Lohka and James Maller, whose

early observations on *in vitro* spindles led to the development of the spindle assembly reactions described here; Ken Sawin, who characterized the pathways of spindle assembly and performed the first immunodepletions; and Caroline Shamu, who developed the *in vitro* anaphase reaction. We also thank Ted Salmon for his contributions to the analysis of anaphase *in vitro* and for many stimulating discussions on spindle assembly and chromosome movement. Finally, we thank our colleagues in the *Xenopus* extract field and members of our laboratories for many technical discussions on performing extract experiments. This work was supported by an HHMI predoctoral fellowship to A. D., grants from the NIH and Packard Foundation to A. M., grants from the NIH and HFSP to T. J. M. and postdoctoral fellowships from the NIH and the DOD Breast Cancer Research Program to C. E. W.

References

Belmont, L. D., Hyman, A. A., Sawin, K. E., and Mitchison, T. J. (1990). Real-time visualization of cell cycle dependent changes in microtubule dynamics in cytoplasmic extracts. *Cell* **62,** 579–589.

Blangy, A., Lane, H. A., d'Hérin, P., Harper, M., Kress, M., and Nigg, E. A. (1995). Phosphorylation by p34cdc2 regulates spindle association of human Eg5, a kinesin-related motor essential for bipolar spindle formation in vivo. *Cell* **83,** 1159–1169.

Blow, J. J., and Laskey, R. A. (1986). Initiation of DNA replication in nuclei and purified DNA by a cell-free extract of Xenopus eggs. *Cell* **47,** 577–587.

Boleti, H., Karsenti, E., and Vernos, I. (1996). Xklp2, a novel Xenopus centrosomal kinesin-like protein required for centrosome separation during mitosis. *Cell* **84,** 49–59.

Desai, A., Deacon, H. W., Walczak, C. E., and Mitchison, T. J. (1997). A method that allows the assembly of kinetochore components onto chromosomes condensed in clarified Xenopus egg extracts. *Proc. Natl. Acad. Sci. USA* **94,** 12378–12383.

Desai, A., Maddox, P., Mitchison, T. J., and Salmon, E. D. (1998). Anaphase A chromosome movement and poleward microtubule flux occur at similar rates in *Xenopus* extract spindles. *J. Cell Biol.* **141,** 703–713.

Enos, A. P., and Morris, N. R. (1990). Mutation of a gene that encodes a kinesin-like protein blocks nuclear division in A. nidulans. *Cell* **60,** 1019–1027.

Evans, L., Mitchison, T. J., and Kirschner, M. W. (1985). Influence of the centrosome on the structure of nucleated microtubules. *J. Cell Biol.* **100,** 1185–1191.

Flemming, W. (1965). Contributions to the knowledge of the cell and its vital processes. Part II. *J. Cell Biol.* **25,** 3–69.

Gaglio, T., Saredi, A., and Compton, D. A. (1995). NuMA is required for the organization of microtubules into aster-like mitotic arrays. *J. Cell Biol.* **131,** 693–708.

Gaglio, T., Saredi, A., Bingham, J., Hasbani, J., Gill, S. R., Schroer, T. A., and Compton D. A. (1996). Opposing motor activities are required for the organization of the mammalian mitotic spindle pole. *J. Cell Biol.* **135,** 399–414.

Gaglio, T., Dionne, M. A., and Compton, D. A. (1997). Mitotic spindle poles are organized by structural and motor proteins in addition to centrosomes. *J. Cell Biol.* **138,** 1055–1066.

Hagan, I., and Yanagida, M. (1990). Novel potential mitotic motor protein encoded by the fission yeast cut7 + gene. *Nature* **347,** 563–566.

Heald, R., Tournebize, R., Blank, T., Sandaltzopoulos, R., Becker, P., Hyman, A., and W. Karsenti, W. (1996). Self-organization of microtubules into bipolar spindles around artificial chromosomes in *Xenopus* egg extracts. *Nature* **382,** 420–425.

Heald, R., Tournebize, R., Habermann, A., Karsenti, E., and Hyman, A. (1997). Spindle assembly in Xenopus egg extracts: Respective roles of centrosomes and microtubule self-organization. *J. Cell Biol.* **138,** 615–628.

Heald, R., Tournebize, R., Vernos, I., Murray, A., Hyman, A., and Karsenti, E. (1998). In vitro assays for mitotic spindle assembly and function. *In* "Cell Biology: A Laboratory Handbook" (J. Celis, ed.).

Hirano, T., and Mitchison, T. J. (1991). Cell cycle control of higher-order chromatin assembly around naked DNA in vitro. *J. Cell Biol.* **115,** 1479–1489.

Holloway, S. L., Glotzer, M., King, R. W., and Murray, A. W. (1993). Anaphase is initiated by proteolysis rather than by the inactivation of MPF. *Cell* **73,** 1393–1402.

Hoyt, M. A., He, L., Loo, K. K., and Saunders, W. S. (1992). Two Saccharomyces cerevisiae kinesin-related gene products required for mitotic spindle assembly. *J. Cell Biol.* **118,** 109–120.

Hutchison, C. J., Cox, R., and Ford, C. C. (1988). Periodic DNA synthesis in cell-free extracts of Xenopus eggs. *EMBO J.* **6,** 2003–2010.

Hyman, A., Drechsel, D., Kellogg, D., Salser, S., Sawin, K., Steffen, P., Wordeman, L., and Mitchison, T. (1991). Preparation of modified tubulins. *Methods Enzymol.* **196,** 478–485.

Lohka, M. J., and Maller, J. L. (1985). Induction of nuclear envelope breakdown, chromosome condensation, and spindle formation in cell-free extracts. *J. Cell Biol.* **101,** 518–523.

Lohka, M. J., and Masui, Y. (1983). Formation in vitro of sperm pronuclei and mitotic chromosomes induced by amphibian ooplasmic components. *Science* **220,** 719–721.

Merdes, A., Ramyar, K., Vechio, J. D., and Cleveland, D. W. (1996). A complex of NuMA and cytoplasmic dynein is essential for mitotic spindle assembly. *Cell* **87,** 447–458.

Murray, A. W. (1991). Cell cycle extracts. *Methods Cell Biol.* **36,** 581–605.

Murray, A. W., and Kirschner, M. W. (1989). Cyclin synthesis drives the early embryonic cell cycle. *Nature* **339,** 275–280.

Murray, A. W., Desai, A. B., and Salmon, E. D. (1996). Real time observation of anaphase in vitro. *Proc. Natl. Acad. Sci. USA* **93,** 12327–12332.

Murray, A. W., Solomon, M., and Kirschner, M. W. (1989). The role of cyclin synthesis in the control of maturation promoting factor activity. *Nature (London)* **339,** 280–286.

Roof, D. M., Meluh, P. B., and Rose, M. D. (1992). Kinesin-related proteins required for assembly of the mitotic spindle. *J. Cell Biol.* **118,** 95–108.

Sagata, N., Watanabe, N., Vande Woude, G. F., and Ikawa, Y. (1989). The c-mos protooncogene is a cytostatic factor responsible for meiotic arrest in vertebrate eggs. *Nature* **342,** 512–518.

Salmon, E. D., Inoue, T., Desai, A., and Murray, A. W. (1994). High resolution multimode digital imaging system for mitosis studies in vivo and in vitro. *Biol. Bull.* **187,** 231–232.

Sawin, K. E., and Mitchison, T. J. (1991). Mitotic spindle assembly by two different pathways in vitro. *J. Cell Biol.* **112,** 925–940.

Sawin, K. E., LeGuellec, K., Philippe, M., and Mitchison, T. J. (1992). Mitotic spindle organization by a plus-end directed microtubule motor. *Nature* **359,** 540–543.

Shamu, C. E., and Murray, A. W. (1992). Sister chromatid separation in frog egg extracts requires DNA topoisomerase II activity during anaphase. *J. Cell Biol.* **117,** 921–934.

Verde, F., Labbe, J.-C., Doree, M., and Karsenti, E. (1990). Regulation of microtubule dynamics by cdc2 protein kinase in cell-free extracts of Xenopus eggs. *Nature* **343,** 233–238.

Vernos, I., Raats, J., Hirano, T., Heasman, J., Karsenti, E., and Wylie, C. (1995). Xklp1, a chromosomal Xenopus kinesin-like protein essential for spindle organization and chromosome positioning. *Cell* **81,** 117–127.

Walczak, C. E., Mitchison, T. J., and Desai, A. (1996). XKCM1: A Xenopus kinesin-related protein that regulates microtubule dynamics during mitotic spindle assembly. *Cell* **84,** 37–47.

Walczak, C. E., Verma, S., and Mitchinson, T. J. (1997). XCTK2: A kinesin-related protein that promotes mitotic spindle assembly in Xenopus laevis egg extracts. *J. Cell Biol.* **136,** 859–870.

The Bipolar Kinesin, KLP61F, Cross-links Microtubules within Interpolar Microtubule Bundles of *Drosophila* Embryonic Mitotic Spindles

David J. Sharp,* Kent L. McDonald,‡ Heather M. Brown,* Heinrich J. Matthies,* Claire Walczak,§ Ron D. Vale,‖ Timothy J. Mitchison,¶ and Jonathan M. Scholey*

*Section of Molecular and Cellular Biology, University of California Davis, Davis, California 95616; ‡Electron Microscope Lab, University of California, Berkeley, California 94720-3330; §Medical Sciences Program, Indiana University, Bloomington, Indiana 47405; ‖Howard Hughes Medical Institute, University of California, San Francisco, California 94143; and ¶Department of Cell Biology, Harvard Medical School, Boston, Massachusetts 02115

Abstract. Previous genetic and biochemical studies have led to the hypothesis that the essential mitotic bipolar kinesin, KLP61F, cross-links and slides microtubules (MTs) during spindle assembly and function. Here, we have tested this hypothesis by immunofluorescence and immunoelectron microscopy (immunoEM). We show that *Drosophila* embryonic spindles at metaphase and anaphase contain abundant bundles of MTs running between the spindle poles. These interpolar MT bundles are parallel near the poles and antiparallel in the midzone. We have observed that KLP61F motors, phosphorylated at a cdk1/cyclin B consensus domain within the BimC box (BCB), localize along the length of these interpolar MT bundles, being concentrated in the midzone region. Nonphosphorylated KLP61F motors, in contrast, are excluded from the spindle and display a cytoplasmic localization. Immunoelectron microscopy further suggested that phospho-KLP61F motors form cross-links between MTs within interpolar MT bundles. These bipolar KLP61F MT-MT cross-links should be capable of organizing parallel MTs into bundles within half spindles and sliding antiparallel MTs apart in the spindle midzone. Thus we propose that bipolar kinesin motors and MTs interact by a "sliding filament mechanism" during the formation and function of the mitotic spindle.

Key words: mitosis • bipolar kinesin • Bim C • microtubule • *Drosophila*

SUCCESSFUL mitosis requires that genetic material is equally segregated into two daughter nuclei upon a self-organizing bipolar protein machine known as the mitotic spindle. This structure forms from two partially overlapping radial arrays of microtubules (MTs)[1] oriented with their minus-ends focused at duplicated centrosomes and their plus ends radiating outward. During early mitosis when the spindle assembles, these centrosomes and their associated asters migrate to opposite sides of the nucleus. Subsequently, the nuclear envelope breaks down, allowing MTs from each aster to interact with condensed chromosomes or with MTs of the other aster, and thus the basic lattice of the spindle forms. Chromosome segregation occurs during anaphase when spindle MTs move sister chromatids to opposite spindle poles (anaphase A) and push the spindle poles apart (anaphase B).

To explain the forces involved in spindle formation and function, McIntosh et al. (1969, 1971) proposed the sliding filament model of mitosis, in which some spindle movements were seen as analogues of the sliding of cytoskeletal elements that drive muscle contraction and flagellar beating (McDonald et al., 1977). In this model, electron-dense crossbridges observed between spindle MTs were proposed to be motor proteins capable of generating force along the surface of MTs and moving them in relation to one another. Although this sliding filament mechanism cannot account for all movements associated with spindle MTs (such as kinetochore motility), it does account nicely for the forces associated with antiparallel MTs that act on opposite spindle poles. This polar repulsive force could drive spindle pole migration during prophase, hold the poles apart during metaphase and anaphase A, and drive spindle elongation during anaphase B.

Address correspondence to Dr. Jonathan M. Scholey, Section of Molecular and Cellular Biology, 1 Shields Ave., The University of California, Davis, CA 95616. Tel.: (530) 752-2271. Fax: (530) 752-7522. E-mail: jmscholey@ucdavis.edu

1. *Abbreviations used in this paper:* BCB, unphosphorylated BimC box; cdk1, cyclin-dependent kinase 1; CSF, cytostatic factor; HPF/FS, high-pressure freezing/freeze substitution; HSS, high speed supernatant; immunoEM, immunoelectron microscopy; LB, Luria broth; MAP, microtubule-associated protein; MT, microtubule; p-BCB, phosphorylated BCB; PI, protease inhibitor; Rs, Stokes radius; TEM, transmission EM.

While their specific modes of action have not been determined, MT-based motor proteins are now known to play important roles in mitosis (Gelfand and Scholey, 1992; Barton and Goldstein, 1996; Hoyt 1994; Walczak and Mitchison, 1996). Genetic analyses, antibody microinjections, and immunodepletions from extracts have shown clearly that MT-associated motor proteins are essential for the proper formation of the mitotic spindle in a variety of organisms (see Heck et al., 1993; Wright et al., 1993; Sawin et al., 1992). Furthermore, one prominent group or subfamily of mitotic motors, the bipolar kinesins (or BimC family of kinesins), have been proposed to organize spindle poles, to contribute to pole-pole separation, and to drive spindle elongation (Enos and Morris, 1990; Hagan and Yanagida, 1990, 1992; Hoyt et al., 1992; Roof et al., 1992; Saunders and Hoyt, 1992; Heck et al., 1993; O'Connell et al., 1993; Saunders et al., 1995; Blangy et al., 1995, 1997; Straight and Murray, 1998), all of which may potentially use a sliding filament mechanism.

Although it is unclear how bipolar kinesins exert their effects in the spindle, recent work suggests that at least one member of this family could affect spindle bipolarity by cross-linking and sliding MTs by a sliding filament mechanism. Probes of *Drosophila* embryonic cytosol with pan-kinesin antibodies led to the purification of a slow, plus-end-directed, homotetrameric kinesin (Cole et al., 1994) that is structurally bipolar having two motor domains at both ends of a ~60-nm-long rod (Kashina et al., 1996a). Microsequencing and MALDI mass spectroscopy of tryptic digests revealed that this bipolar motor was, in fact, the product of the gene encoding the bipolar kinesin, KLP61F (Kashina et al., 1996b). KLP61F was discovered as a late larval lethal mutant encoding a kinesin-like protein. Interestingly, severe loss of function mutations of this bipolar kinesin are hallmarked by monoastral spindles apparently resulting from unseparated or collapsed spindle poles within proliferative tissues (Heck et al., 1993).

Based on these biochemical and genetic data, we have proposed that KLP61F and its homologues function as spindle MT cross-linkers, acting on antiparallel MTs to separate and hold apart spindle poles or on parallel MTs to drive subunit flux in kinetochore MTs (Kashina et al., 1996a). Our aim here is to test this hypothesis by immunolocalizing KLP61F within the spindles of early *Drosophila* embryos using peptide antibodies monospecific for a phospho-epitope in the tail of the motor. Given the known transport properties of the motor and the terminal phenotype of the KLP61F mutant, the determination of how the motor holoenzyme associates with MTs and the polarity of the MTs with which it interacts will provide a crucial functional link between the in vitro transport properties of the motor (Cole et al., 1994; Barton et al., 1995) and the monoastral spindles that characterize severe loss of function mutants (Heck et al., 1993).

Materials and Methods

Preparations and Care of Fly Stocks

Oregon red strains of *Drosophila melanogaster* were maintained in large farms as previously described (Ashburner, 1989; Meyer et al., 1998). In some of the immunofluorescence and electron microscopic analyses described below, flies were collected from the University of California San Francisco fly facility.

Drosophila Embryonic Tubulin Preparation

High speed supernatant (HSS) from extracts of 0–2 h *Drosophila* embryos was generated as previously described (Meyer et al., 1998). Actin and myosin were depleted from HSS by incubation with hexokinase (10 U/ml) and 0.9% glucose for 30 min at room temperature and spinning at 35,000 *g* for 30 min. The supernatant was then collected and incubated with 1 mM GTP and 20 μM taxol for 45 min, then spun through a 15% sucrose cushion (containing 100 μM GTP, 100 μM ATP, and 5 μM taxol) and spun again at 20,000 *g* for 60 min at 10°C. The pellet was resuspended in PMEG, and immediately spun again for 20 min at 60,000 *g* at 10 C. The pellets were then resuspended in PMEG containing 10 μM ATP, 10 μM $MgSO_4$, 10 μM taxol, 100 μM GTP, and 0.5 M KCl for 4 h at 4°C and spun at 130,000 *g* for 45 min at 4°C. The pellets were resuspended in PMEG containing 100 μM GTP and 10 μM taxol aliquoted and stored at −80°C. Tubulin prepared in this manner was used for antibody generation and affinity purification, described below.

Preparation of Drosophila Embryonic Tubulin Antibodies

The taxol stabilized MTs were injected into three rabbits along with Freund's complete adjuvant and a week later 10 ml of blood was taken. This occurred once a month for 5 mo. Samples from each bleed were taken and tested for reactivity with tubulin by Western blotting *Drosophila* HSS and preparations of MTs and microtubule-associated proteins (MAPs). One of the three rabbits showed a strong response to the tubulin injections.

Anti-tubulin antibodies were affinity purified on columns of affigel 15 (Biogel) coupled to *Drosophila* embryonic tubulin. After binding of the tubulin to the columns, the columns were washed 10 vol of PBS-0.5% Tween-20 (PBS-Tween) and then blocked in PBS-Tween containing 5% BSA (Sigma) for 1 h at room temperature. Next, the columns were washed with 10 vol of PBS-Tween and incubated with the antiserum diluted 1:5 in blocking solution overnight at 4°C. The columns were then washed in 20 vol of PBS-Tween. Antibody was eluted from the column with 0.1 M glycine, pH 2.7, and collected in 0.8-ml fractions into clean tubes containing 0.2 ml of 1 M Tris, pH 8.0. The OD 280 of all elution fractions was determined against a standard of the tris/glycine mixture. All fractions with an OD 280 of >0.05 were kept and dialyzed into PBS overnight at 4°C.

Design and Preparation of BCB Antibodies

Polyclonal anti-BCB peptide antibodies were raised using synthetic peptides of sequence CPTGTTPQRRDYA, corresponding to the highly conserved BCB of frog Eg5. The peptide was synthesized with and without a phospho-threonine residue at residue position 6 corresponding to the consensus cdk1 phosphorylation site (Heck et al., 1993; Sawin and Mitchison, 1995), and NH_2-terminal acetyl and COOH-terminal amide groups were included. Approximately 40 mg both peptides at >92% purity were obtained by HPLC at the UCSF biomolecular resource center where the masses of the p-BCB and BCB peptides were confirmed by mass spectroscopy. Both peptides were found to be highly water-soluble and were conjugated to KLH carrier protein (5 mg peptide/50 mg KLH). The anti-p-BCB and anti-BCB antibodies were produced by BabCo (Richmond) and specific antibodies were purified from immune sera on columns of BCB or p-BCB peptides coupled to affigel 10. Bound antibodies were eluted using 0.1 M glycine, pH 2.5, and rapidly neutralized using 1 M Tris buffer, pH 10. Antibodies were then incubated with a 100-fold excess of blocking peptide (p-BCB peptide in the case of the anti-BCB antibody and BCB peptide in the case of the anti-p-BCB antibody).

To test the reactivity of these antibodies against phospho- and unphospho-KLP61F, recombinant KLP61F (or its stalk-tail fragment) prepared as described by Barton et al. (1995) was bound batchwise to glutathione-agarose beads, the beads were washed in CSF extract buffer then incubated with M-phase or I-phase *Xenopus* egg extracts or corresponding buffer plus [^{32}P]ATP for 10 min (see below), then the beads were washed in cytostatic factor (CSF) extraction buffer, boiled in sample buffer, and analyzed by SDS-PAGE, immunoblotting with the BCB and p-BimC box antibodies, and autoradiography.

Hydrodynamic Analysis of Native and Recombinant KLP61F and Phospho-KLP61F

To analyze the hydrodynamic properties of phosphorylated and unphosphorylated native KLP61f from fly embryos, fractions prepared as described previously (Cole et al., 1994) were analyzed by immunoblotting with the anti-BCB and anti-p-BCB antibodies.

Isolation and Purification of Bacterially Expressed Full-Length KLP61F

Bacterial strain BL21(DE3) was transformed with the pRSET vector containing a full length KLP61F insert. To isolate KLP61F from the transformant, a colony from a freshly streaked plate was inoculated into Luria broth medium (LB) containing 200 μg/ml ampicillin and incubated overnight at 37°C. The culture was then diluted 1:100 with fresh LB+ containing 200 μg/ml ampicillin and grown at 37°C to an optical density of A600 = 0.80. The culture was then cooled to 25°C for 30 min and then induced for 4 h at 25°C with 0.2 mM IPTG. After washing, the cells were resuspended in lysis buffer (50 mM NaH_2PO_4, 300 mM NaCl, 10 mM imidazole, pH 8.0, 100 μM MgATP) and protease inhibitors (PIs; PMSF, leupeptin, pepstatin A, benzamidine) and then lysed. The lysate was spun at 39,000 *g* for 45 min at 4°C. The supernatant was loaded onto a column containing Ni NTA superflow resin (Qiagen Inc.) then washed with lysis buffer and wash buffer (50 mM NaH_2PO_4, 300 mM NaCl, 20 mM imidazole, pH 6.0, 100 μM MgATP and PIs). rKLP61F was eluted with 250 mM imidazole, 5 mM magnesium acetate, 2 mM EGTA, 15 mM potassium acetate, pH 7.25, 100 μM MgATP and PIs. rKLP61F containing fractions were pooled, filtered through a 0.2–2 μm Millex-GV syringe filter, and loaded onto a Biogel A-1.5 m column preequilibrated with IMEK (100 mM imidazole, 5 mM magnesium acetate, 2 mM EGTA, 15 mM potassium acetate, pH 7.25) + 300 mM NaCl, 100 μM MgATP and PIs. rKLP61F was then concentrated with high trap Q column (Pharmacia) and eluted using a step gradient from 0.1–1.0 M NaCl in IMEK. The peak fraction from this concentration step was then used for the hydrodynamic studies.

Phosphorylation of Bacterially Expressed KLP61F

While on the Ni-NTA column (see above), rKLP61F was washed with CSF-XB (10 mM Hepes, pH 7.7, 2 mM $MgCl_2$, 0.1 mM $CaCl_2$, 100 mM KCl, 5 mM EGTA, and 50 mM sucrose). 200 μl of *Xenopus* mitotic extract and 1.8 ml of CSF-XB + 2 mM ATP and 10 mM $MgSO_4$ were added followed by gentle rocking at room temperature for 20 min. The beads were then returned to 4°C and washed with wash buffer. The phosphorylated rKLP61F was then eluted and treated as stated above for further purification and concentration.

Stoichiometry

The Stokes radius, Rs, was determined for both phosphorylated and unphosphorylated rKLP61F by loading 500 μl of the peak high trap Q fraction onto a pharmacia superose-6 column preequilibrated with IMEK + 300 mM NaCl. Graphs of Rs vs. −0.5logKav were plotted and the Rs determined from these plots. The standard proteins and their stokes radii included cytochrome C (1.7 nm), carbonic anhydrase (2.0 nm), BSA (3.5 nm), beta amylase (5.4 nm), and thyroglobulin (8.5 nm). The sedimentation coefficient, S value, was determined for rKLP61F on 5-ml 5–20% linear sucrose gradients in IMEK + 300 mM NaCl, 100 μM ATP, and PIs. The gradients were overlaid with a solution containing the rKLP61F, 30 μg BSA (4.4 s), 30 μg aldolase (7.3 s), and 30 μg catalase (11.3 s). The gradients were centrifuged at 218,000 *g* for 12 h at 4°C. The gradients were determined to be linear by using a refractometer. A linear plot of the S value vs. the percent sucrose was used to calculate the S value for rKLP61F. The molecular mass of rKLP61F was calculated from the measured sedimentation values and Rs.

Immunofluorescence Analyses

Drosophila embryos were prepared for immunofluorescence with a modification of the protocol described by Theurkauf (1994). 0–2 h *Drosophila* embryos were collected on food trays and rinsed from the tray with Triton-NaCl and collected onto a 200-μm nylon mesh rinsed with water. The chorions were removed by immersion in 50% bleach in Triton-NaCl for 2 min. The embryos were then extensively rinsed in double distilled water and Triton-NaCl. The vitelline was removed by immersion in 100% heptane at room temperature for 2 min and fixed by the addition of an equal volume of fresh 37% formaldehyde for 5 min. The formaldehyde was then removed and replaced with 100% methanol. The heptane and most of the methanol were removed, the embryos were incubated in fresh 100% methanol for 2–3 h, and then rehydrated by washes in a graded methanol series and two washes in 100% PBS. The embryos were then washed in PBS-0.01% Triton X-100 (wash solution) and blocked for 30 min to 1 h in PBS-0.01% Triton X-100 containing 5% BSA (blocking solution). Primary antibodies, either rabbit anti–*Drosophila* tubulin, rabbit anti-p-BCB, rabbit anti-BCB, or mouse anti-β-tubulin (N357; Amersham Life Sciences), were diluted to a concentration of 1 μg/ml in blocking solution and incubated with the embryos at 4°C overnight. In double label experiments, embryos were incubated with the anti-phospho-KLP61F antibody for 4 h at room temperature, then the mouse anti-β-tubulin was added and the incubation proceeded overnight at 4°C. After incubation with primary antibodies, the embryos were washed, blocked as above, and incubated with secondary antibodies, either goat anti–mouse conjugated to lissamine rhodamine, goat anti–mouse conjugated to cy5 or goat anti–rabbit cy3 (Jackson ImmunoResearch) diluted in blocking solution (1:100 for lissamine rhodamine and cy 5 and 1:500 for cy 3) and incubated with embryos for 2–3 h at room temperature. The embryos were washed then incubated in 4′,6′-diamidino-2-phenylindole (DAPI; Sigma) diluted to 0.1 μg/ml in PBS-Triton, for 4–10 min, rinsed washed again, rinsed with 100% PBS, and mounted in *p*-phenylenediamine (Sigma) 10 mg/ml in 90% glycerol/PBS. Secondary antibody alone controls were used for all staining conditions. Embryos were visualized on a Leica TCS NT confocal microscope. Images were acquired by averaging 16–32 scans of a single optical section with the pinhole opened for optimal resolution.

Preparation for EM and ImmunoEM

Samples were prepared for EM by high pressure freezing and freeze substitution as described previously (McDonald, 1994). Fixed embryos were embedded in Eponate 12/Araldite (Ted Pella) for standard Transmission EM (TEM) or immunoEM or in LR-White (Ted Pella) for immunoEM. 35–50-nm sections were collected on an Ultracut T microtome (Leica) and picked up on copper grids coated with 0.3–0.5% formvar (Electron Microscopy Sciences) for standard TEM or on nickel grids (Ted Pella) coated with carbon and 0.5% formvar. For standard TEM, sections were post stained for 5 minutes in 2% uranyl acetate/70% methanol and 4 min in 0.5% lead citrate.

For immunoEM, sections were blocked in 5% BSA, 0.1% fish gelatin (Sigma) in PBS-0.05% Tween-20 for 30 min (blocking buffer), incubated with primary antibody (either rabbit anti-p-BCB or BCB antibodies diluted to 50 μg/ml or rabbit anti-tubulin diluted to 10 μg/ml in blocking buffer) for 1.5–2 h. Sections were rinsed in PBS-Tween then PBS and incubated in secondary antibodies (goat anti–rabbit IgG $F(ab')_2$ [H+L]) conjugated to either 5 or 10 nm gold particle; Ted Pella) diluted 1:20 in blocking buffer for 1 h. Sections were washed as before, incubated in 0.5% glutaraldehyde in PBS for 5 min then rinsed in PBS and water. Sections were post stained in 2% uranyl acetate in 70% methanol for 5 min and in lead citrate for 4 min. Samples were visualized on a Philips 410 LS transmission electron microscope. Identically treated samples were stained with secondary antibody only as controls that in all cases revealed no labeling pattern. Sections labeled with the BCB antibodies revealed only background labeling as well. Digital image enhancement of gold-labeled spindles was done with Adobe Photoshop 5.0 on scanned photographs.

MT Tracking and Reconstruction

MTs were tracked using markers and plastic overlays as described in McDonald et al. (1977).

Results

Mitosis in Early Drosophila Embryos

To understand the mechanism of action of the bipolar kinesin, KLP61F, in *Drosophila* early embryos it was important to determine the organization of the mitotic spindle components with which the motor might associate. To accomplish this, we used immunofluorescence and EM to analyze the organization of spindle MTs and the changes

in overall spindle morphology that occur throughout mitosis (Figs. 1 and 2).

Fig. 1 shows confocal immunofluorescence of embryos immunostained with a rabbit polyclonal antibody raised against embryonic *Drosophila* MTs (see Materials and Methods) and the DNA stain DAPI. These images suggest that as prophase begins, duplicated centrosomes split and migrate away from the embryo surface, traveling down opposite sides of the nucleus (Fig. 1 A). The nuclear envelope remains intact throughout prophase (Oegema et al., 1995; Fig. 1 A, inset) and very little or no tubulin staining is observed in the nuclear region. By metaphase (Fig. 1 B), the nuclear envelope has fenestrated at the poles (Stahfstrom and Staehelin, 1984), microtubules have entered the nuclear region and the chromosomes have aligned at the metaphase plate. Dense bundles of MTs are observed in the half spindles while very few astral MTs are visible. The overall morphology of the metaphase spindle is fusiform and the average spindle length is ~12 μm. Fig. 1, C and D show the tubulin staining pattern from an embryo in which anaphase A (C) has been completed in all nuclei, but only a subset have undergone anaphase B (D). In panel C, sister chromatids have moved completely to opposite poles, yet the length of the spindles, pole-pole, range from 12 to 14 μm, similar to metaphase. The spindles shown in Fig. 1 D, on the other hand, have clearly elongated, reaching lengths of ~17–18 μm. Note that the decondensation of DNA begins during anaphase B. Also note the distinct change in the morphology of the interzone (region of the spindle lying between the separated chromosomes). Before spindle elongation, the region corresponding to the interzone is fusiform as in metaphase, however, as the spindle elongates the interzone becomes straight edged. We use this change in spindle geometry to distinguish anaphase A from B in the subsequent fluorescence analyses of KLP61F localization (below). One feature of the anti-tubulin immunofluorescence shown here and in other studies is that during both metaphase and anaphase, very few MTs cross the midzone and bridge the half spindles. However, the EM analyses shown below show abundant MTs crossing the midzone suggesting that antigenic sites are masked in immunofluorescence images.

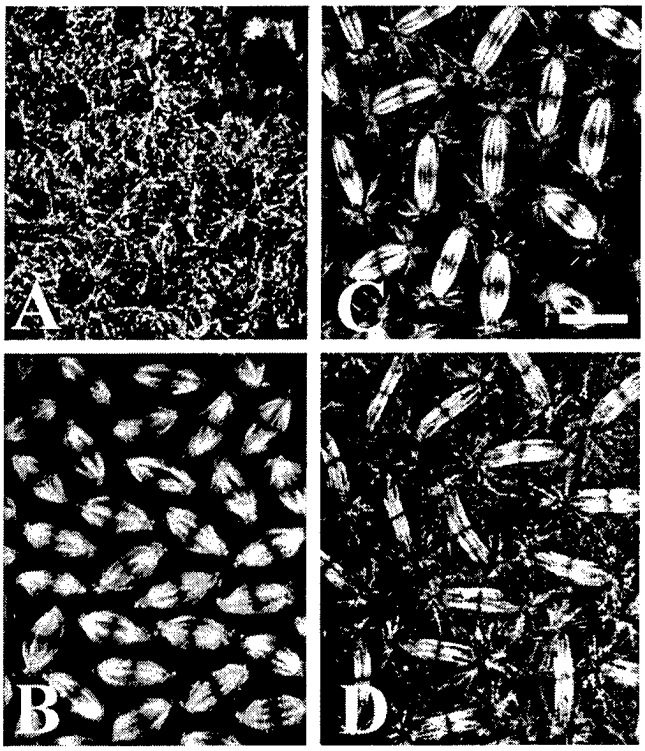

Figure 1. Mitosis in the syncytial blastoderm of early *Drosophila* embryos. Confocal immunofluorescence images of embryos immunostained with an antibody raised against *Drosophila* embryonic tubulin (yellow) overlaid with the corresponding DNA stain DAPI (blue). (A) Prophase. The chromosomes have begun to condense and centrosomes have separated significantly toward opposite sides of the nucleus. (A, inset) Cross sectional view of a prophase nucleus showing only tubulin immunofluorescence. (B) Metaphase. MTs have entered the nuclear region, and chromosomes have aligned along the metaphase plate. (C) Anaphase A. The sister chromatids have separated to opposite spindle poles but the spindles have not elongated. (D) Anaphase B. The spindles have elongated to an average length of 17.5 μm. Note that the central spindle is no longer fusiform but straight-edged. Bar, 7.6 μm.

Ultrastructural Analysis of Metaphase and Anaphase Spindles Preserved by High Pressure Freezing and Freeze/Substitution

An ultrastructural description of mitotic spindles from several stages in *Drosophila* syncytial blastoderms has been reported previously (Stahfstrom and Staehelin, 1984). However, the size of these embryos and rapid rate of mitosis during this stage of development results in a great deal of ultrastructural damage during fixation. Therefore, the use of EM to localize low abundance and easily extractable proteins requires preservation methods of a quality exceeding standard chemical fixation (McDonald, 1994). To minimize the potential extraction or mislocalization of KLP61F motors during specimen preservation, we have prepared our samples for EM by high-pressure freezing/freeze substitution (HPF/FS; for a review of this technique see Steinbrecht and Mueller, 1987; McDonald, 1994; Kiss and Staehelin, 1995). In this method, whole embryos are frozen under pressure then dehydrated and fixed simultaneously at low temperatures to preserve cellular structures rapidly and evenly with minimal extraction. (In contrast to cryofixation, in which unfixed frozen embryos are embedded or viewed on cold stage, the preparation of embryos by HPF/FS allows structures such as MTs or the nuclear envelope to be visualized easily.)

Fig. 2 is shown to illustrate, in fine detail, the organization of spindle microtubule bundles and poles after preservation by HPF/FS. Fig. 2 A shows a bundle of MTs running from the pole to the chromosome at the metaphase plate. These MTs end on an electron-dense halo, presumably the kinetochore and its corona, extending as a bolus from the chromosomes. Interestingly, no kinetochores observed were overtly trilaminar as has been reported in other systems (for review see Brinkley, 1990). Fig. 2, B and C show bundles of MTs that bridge the half spindles during metaphase and anaphase, respectively. Note that in contrast to immunofluorescence, EM clearly reveals abundant midzonal microtubules suggesting that the lack of

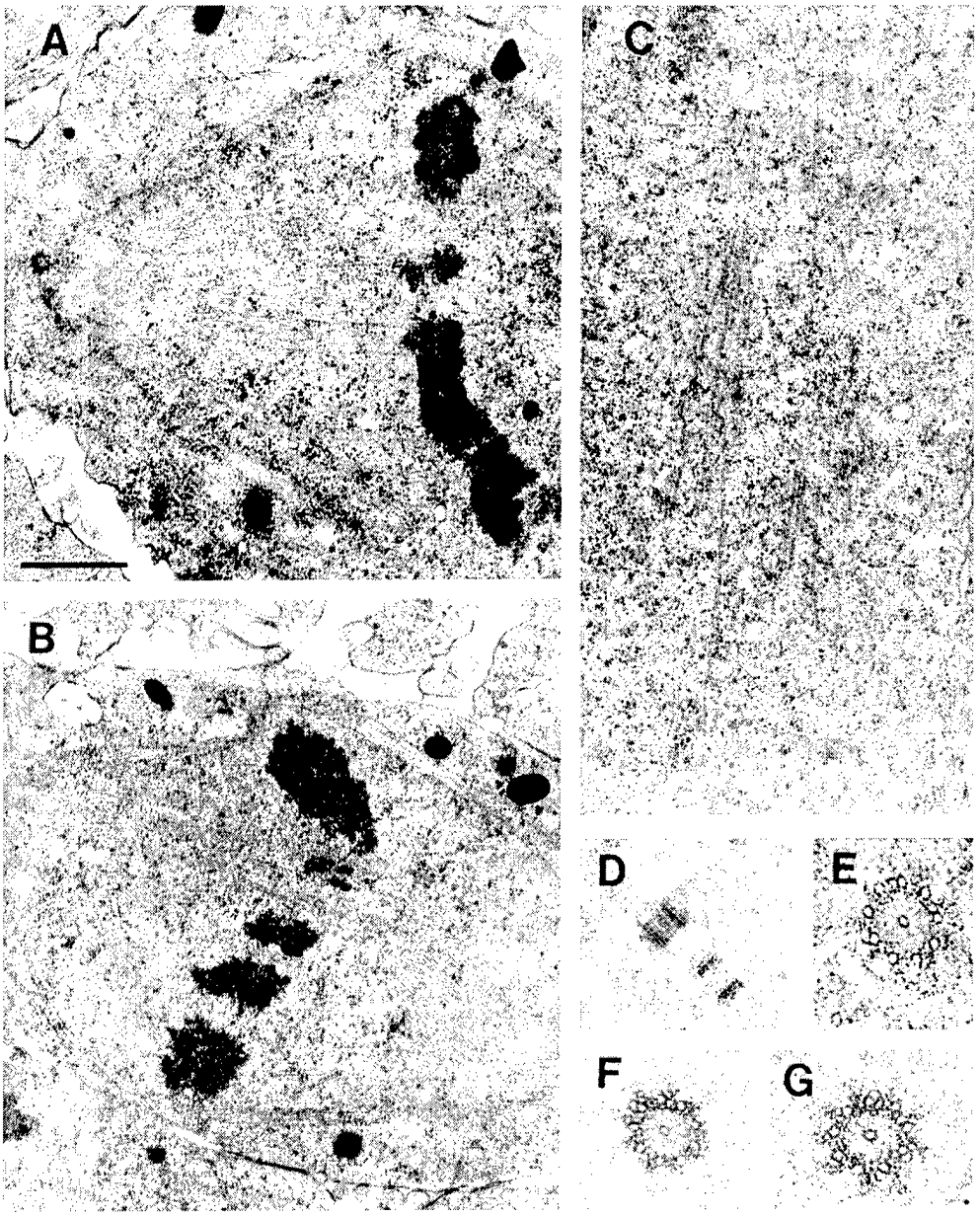

Figure 2. Detailed ultrastructure of MT bundles and spindle poles during mitosis. (A) Kinetochore MT bundles. (B) Interpolar MT bundles during metaphase. (C) Interpolar MT bundles during anaphase. D–G show the organization and structure of centrioles throughout mitosis. (D) Spindle poles contain two orthogonally positioned centrioles. The image shown is from the pole of a metaphase spindle. (E) During prophase, each centriole consists of nine singlet MTs around a central singlet MT. (F) by metaphase, the centrioles become much more electron dense and some of the outer MTs begin to form doublets. (G) In anaphase, doublets continue to form on the outer MTs. The standard organization of centrioles, nine outer triplets offset in a barrel shape, is never observed in *Drosophila* early embryos. Bar: (A) 1.3 μm; (B) 1.5 μm; (C) 1.1 μm; (D) 1.2 μm; (E–G) 0.3 μm.

anti-tubulin fluorescence in the midzone, shown in Fig. 1, results from the masking of antigenic sites. Similar bundles have been identified in vertebrate spindles and have been termed interpolar MT bundles because the entire MT bundle runs from pole to pole (although individual MTs in the bundles do not; Mastronarde et al., 1993). Here, the term interpolar MT bundles will be used to describe bundles of MTs that traverse the spindle midzone and extend into each half spindle.

Fig. 2, D–G show the organization and overall preservation of spindle poles during different stages of mitosis. Throughout the cell cycle, the most prominent structural feature of spindle poles is two orthogonally positioned centrioles (Fig. 2 D). In prophase, centrioles consist of nine outer singlet MTs plus one central singlet (Fig. 2 E). By metaphase, they become increasingly electron dense and doublets can be seen forming on some of the outer MTs. In anaphase, more doublets can be seen on the outer nine MTs and the electron density remains similar to that observed in metaphase. The organization and preservation of MT bundles and spindle poles shown in Fig. 2 is characteristic of all the samples used in this study and reinforces our confidence in the use of HPF/FS for our immunoEM analyses.

Interpolar MT Bundles Consist of Overlapping MTs Emanating from Opposite Poles

Because of their position in relation to the spindle poles, the interpolar MT bundles in *Drosophila* early embryonic spindles (described above) may be sites for MT-MT interactions that play a role in centrosome positioning. To gain a sense of the organization of the MTs and extent of half spindle overlap within these bundles, a representative in-

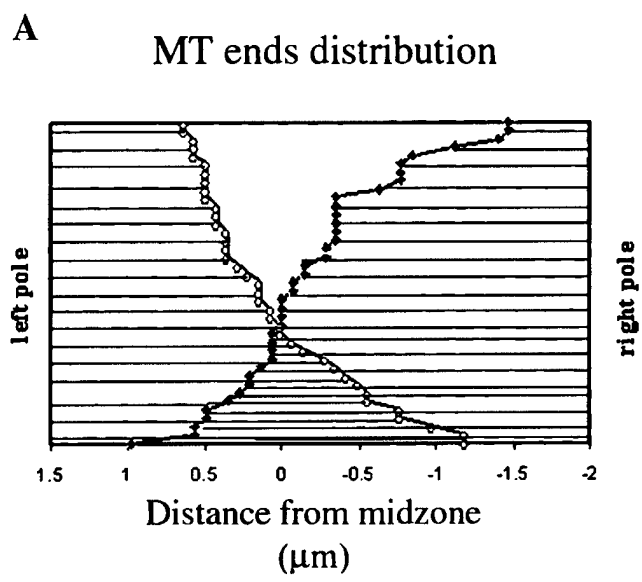

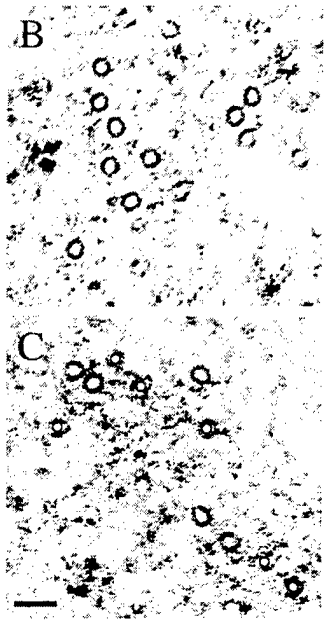

Figure 3. The MTs within interpolar MT bundles are parallel near the poles and antiparallel in the midzone. An interzonal MT bundle from a spindle beginning anaphase B was reconstructed from serial cross-sections to determine its MT polarity pattern. (A) The distribution of MT plus-ends in the reconstructed interpolar MT bundle. Individual MTs are represented by horizontal lines. The position of the plus-ends of MTs emanating from the left pole are indicated by open circles and those from the right are indicated as solid diamonds. The MTs from each half spindle are arranged top to bottom in order of increasing length in order to show the extent of possible MT overlap. (B and C) Cross-sectional profiles of the reconstructed bundle near the poles (B) and at the midzone (C). In C, MTs emanating from one pole are marked in the center with a black circle, while those from the other are not. Bar, 70 nm.

terpolar bundle was reconstructed from serial cross-sections through a mitotic spindle just beginning anaphase B, as determined by morphology and pole-pole length (Fig. 3). The results of this reconstruction are shown schematically in Fig. 3 A. Similar to other systems (McDonald et al., 1977; Euteneuer et al., 1982; Mastronarde et al., 1993; Winey et al., 1995), parallel MTs (MTs from the same pole) predominate near the poles, while antiparallel MTs are present in the midzone and extend ~1–1.5 μm into each half spindle (Fig. 3 A). Fig. 3, B and C show cross-sectional profiles of the MTs in this bundle near the poles (B) and at the midzone (C), respectively. Surprisingly, MTs are more closely associated and appear more ordered near the poles while, in the midzone, MTs are organized into numerous small sets of 2–4 MTs surrounded by an electron-dense material. Antiparallel MTs spaced 50–100 nm apart often run adjacent to one another and electron-dense crossbridges between both parallel and antiparallel MTs are often visible.

Immunodetection of Phosphorylated KLP61F

To detect KLP61F motors in the mitotic spindle, we raised anti-peptide antibodies that react with a 12-residue segment of the Bim C box located within the tail of KLP61F (Heck et al., 1993). It has been proposed that a threonine residue within the Bim C box is phosphorylated by the mitosis-promoting kinase, cdk1/cyclin B that targets bipolar kinesins to spindles (Sawin and Mitchison, 1995; Blangy et al., 1995). We prepared antibodies using both BCB and p-BCB peptides and determined that these antibodies discriminate between the phosphorylated and unphosphorylated forms of KLP61F.

Both antibodies react specifically and with high affinity with a single band in *Drosophila* syncytial blastoderm cytosol at the predicted molecular mass for KLP61F (Fig. 4 A; antibodies raised against recombinant KLP61F [Barton et al., 1995] react with the same band on immunoblots [data not shown]). However, Fig. 4 B shows that only the BCB antibody reacts with untreated bacterially expressed KLP61F (rKLP61F), while the p-BCB antibody reacts with rKLP61F only after its phosphorylation by incubation with M-phase *Xenopus* extracts (lane M) and does not react with untreated rKLP61F (lane U) or with rKLP61F

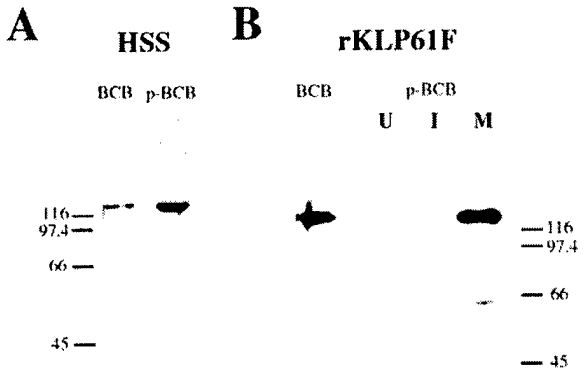

Figure 4. Characterization of the unphospho- and phospho-KLP61F antibodies. (A) Western blot of *Drosophila* 0–2-h embryonic cytosol probed with the anti-BCB and p-BCB antibodies. Both antibodies react specifically with the KLP61F polypeptide in *Drosophila* syncytial blastoderm cytosol, however, at equivalent antibody concentrations, the p-BCB antibody shows more intense staining. (B) Western blots of bacterially expressed, recombinant KLP61F before and after phosphorylation by incubation with *Xenopus* M-Phase extracts, probed with the BCB and p-BCB antibodies. While the BCB antibody reacts with untreated recombinant KLP61F (rKLP61F), the p-BCB antibody only reacts specifically with rKLP61F after it has been phosphorylated in M-phase extracts (lane M) and does not react with untreated KLP61F (lane U) or with recombinant KLP61F treated with matched interphase extracts (lane I).

Table I. Hydrodynamic Properties of KLP61F

	S value	Rs (nm)	MW	Subunits
			kD	
Native fly embryo KLP61F				
Phospho	7.8	15.6	504	4.1
Unphospho	7.8	15.6	504	4.1
Recombinant KLP61F				
Phospho	7.3	14.9	444	3.6
Unphospho	7.6	15.1	472	3.8

treated with matched interphase extracts (lane I). Parallel experiments using radiolabeled ATP revealed that the rKLP61F in lane M was phosphorylated ~4.4-fold relative to the rKLP61F in Fig. 4, lane I. Based on these results, we will subsequently refer to the BCB antibody as anti-unphospho-KLP61F and the p-BCB antibody as anti-phospho-KLP61F.

Using these antibodies to probe the phosphorylation state of native and recombinant KLP61F, we determined that the phosphorylation of KLP61F does not appear to affect the homotetrameric state of KLP61F motors in vitro, as both phospho- and unphospho-KLP61F appear to be homotetrameric based on hydrodynamic analyses (Table I). This suggests that the oligomeric state of the motor that we immunolocalized using these antibodies (below) is likely to be homotetrameric.

KLP61F Localizes to Mitotic Spindles in a Phosphorylation-dependent Manner

To determine the general localization of both phospho- and unphospho-isoforms of KLP61F within *Drosophila* syncytial blastoderms, we used the anti-KLP61F antibodies described above for immunofluorescence analyses. Fig. 5 shows confocal immunofluorescence images of embryos stained with the anti-unphospho-KLP61F overlaid with DAPI staining to indicate the relative position of DNA. Throughout mitosis, unphospho-KLP61F is diffuse and cytoplasmic, displaying no discernible association with MT arrays, nuclei, or spindles.

Embryos stained with anti-phospho-KLP61F show a markedly different staining pattern (Fig. 6). During interphase (Fig. 6 A), phospho-KLP61F staining is punctate and concentrated in the nucleus. This same pattern is observed in prophase (Fig. 6 B), after the centrosomes have separated but before nuclear envelope breakdown. However, on occasion, a very faint but noticeable dot just next to the nucleus can be seen. Double labeling with anti-tubulin antibodies indicate that these dots colocalize with the centrosome (not shown). Little or no colocalization with the microtubule bundles rimming the nuclear envelope or between the centrosomes is observed (not shown). By metaphase, after the fenestration of the nuclear envelope (Fig. 6 C), the phospho-KLP61F staining localizes to the spindle and appears filamentous. Phospho-KLP61 F is particularly concentrated on the half spindles and densely stained bridges between the half spindles in the midzone (Fig. 6 C, arrow). A slightly less concentrated staining is also visible at the poles and a grainy cytoplasmic staining is present. As the chromosomes begin to separate during anaphase A (Fig. 6 D), phospho-KLP61F staining resembles metaphase, with the most intense staining on the half spindles and filamentous bridges between the half spindles in the midzone. Interestingly, very little or no phospho-KLP61F staining can be seen on the astral MTs that begin to emanate from the poles at the onset of anaphase (see Fig. 1 C). By anaphase B (Fig. 6 E; see interzone morphology in Fig. 1 D) the staining pattern of the motor changes dramatically, as nearly all of the phospho-KLP61F is present in the spindle between the separating nuclei. Again, filaments of phospho-KLP61f staining cross the midzone while little or no staining is associated with the spindle poles and astral MTs or within the daughter nuclei. In telophase (Fig. 6 F), as the nuclear envelopes reform around daughter nuclei, phospho-KLP61F is most pro-

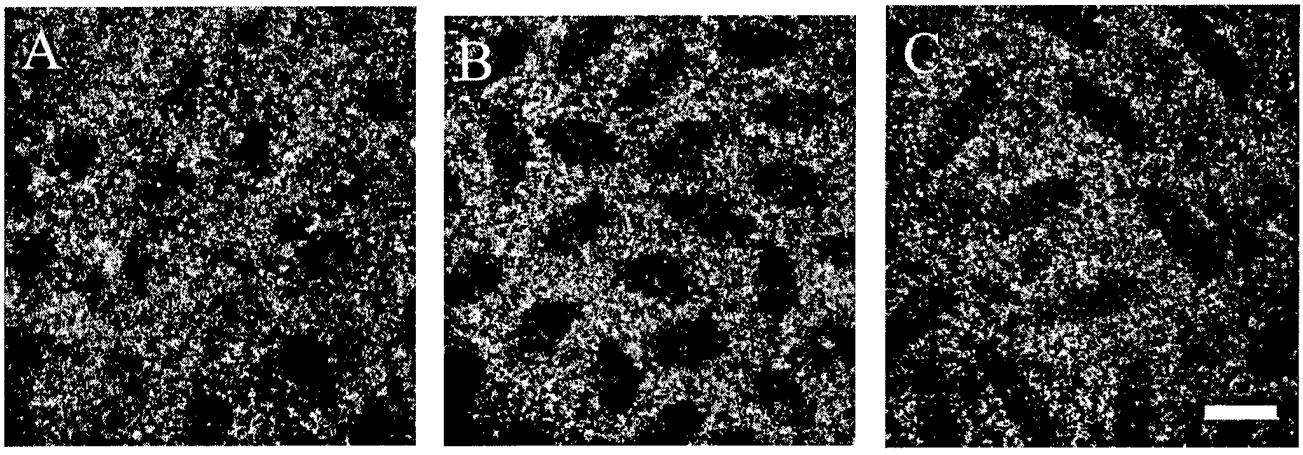

Figure 5. Unphospho-KLP61F is excluded from mitotic spindles in *Drosophila* early embryos. Confocal immunofluorescence images of *Drosophila* early embryos stained with the unphospho-KLP61F antibody (yellow) and DAPI (blue). Throughout the cell cycle, the localization of unphospho-KLP61F is cytoplasmic and does not appear associated with MTs. (A) Prophase. Before nuclear envelope breakdown, unphospho-KLP61F is specifically excluded from the nuclear region. (B) Metaphase. Once the metaphase spindle has formed, unphospho-KLP61F staining is excluded from the spindle. (C) Anaphase. The exclusion of unphospho-KLP61F from the spindle persists through anaphase. Bar, 12 μm.

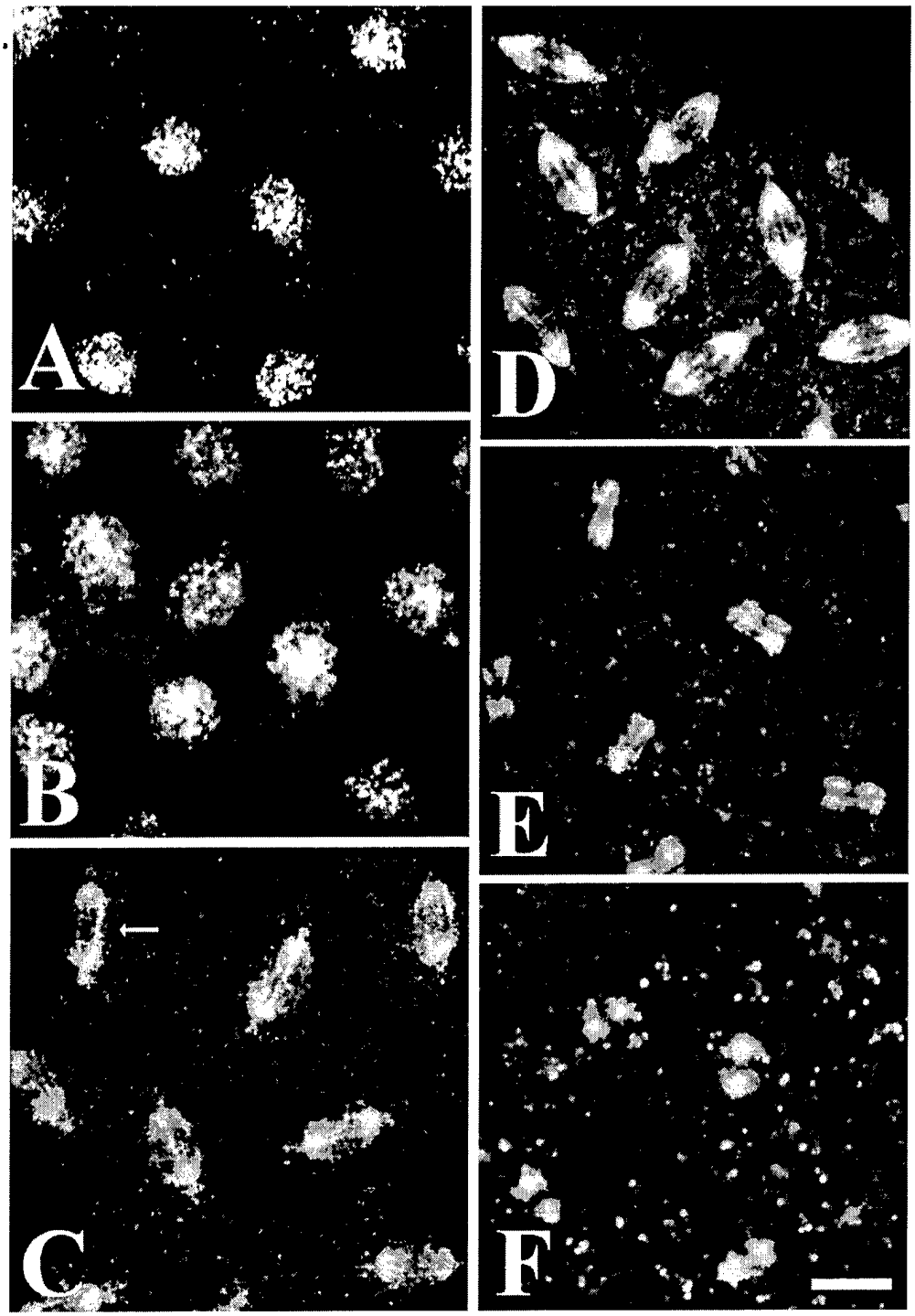

Figure 6. Phospho-KLP61F is sequestered in the nucleus during interphase and prophase and it associates with the mitotic spindle during metaphase and anaphase. Confocal immunofluorescence images of *Drosophila* early embryos stained with the anti-phospho-KLP61F antibody (yellow) and DAPI (blue). White indicates high overlap. (A) In interphase, before mitosis, phospho-KLP61F is concentrated in nuclei and overlaps significantly with DNA. (B) In prophase, before nuclear envelope breakdown, phospho-KLP61F is still concentrated in the nuclei. At this point, some staining is also detectable in the cytoplasm and perhaps on centrosomes but not on cytoplasmic microtubules. (C) In metaphase, phospho-KLP61F is now concentrated on the half spindles and on dense filaments bridging the half spindles (arrow). (D) In anaphase A, phospho-KLP61F is still concentrated on the spindles as well as on filaments bridging the half spindles. (E) In anaphase B, nearly all of the phospho-KLP61F is now concentrated in the spindle interzone, while the spindle poles and astral MTs show very low phospho-KLP61F staining. (F) In telophase, phospho-KLP61F is concentrated at two distinct punctae oriented between the daughter nuclei. Often, smaller punctae can be seen in the reforming daughter nuclei, as well. Bar, 10 μm.

nounced on two adjacent patches on the remnants of the central spindle. Close examination of the phospho-KLP61F staining pattern in the daughter nuclei also reveals that bright punctae begin to form within them. Based on these data, we conclude that, similar to its Eg5 homologues from frog and human (Sawin and Mitchison, 1996; Blangy et al., 1996), KLP61F associates with the mitotic spindle in a phosphorylation dependent fashion. Moreover, phospho-KLP61F motors associate with "filaments" crossing the spindle midzone that we believe correspond to the interpolar bundles as determined by EM (below).

Phospho-KLP61F Does Not Associate Equally with All Spindle MTs

The localization of phospho-KLP61F to distinct spindle regions may provide information about the subsets of MTs upon which the motor acts. Conversely, it may simply mirror differences in tubulin concentration within the spindle. To address this, Fig. 7 shows confocal immunofluorescence overlaying anti-phospho-KLP61F staining with anti-β-tubulin. Instead of determining the concentration of phospho-KLP61F throughout the spindle in absolute

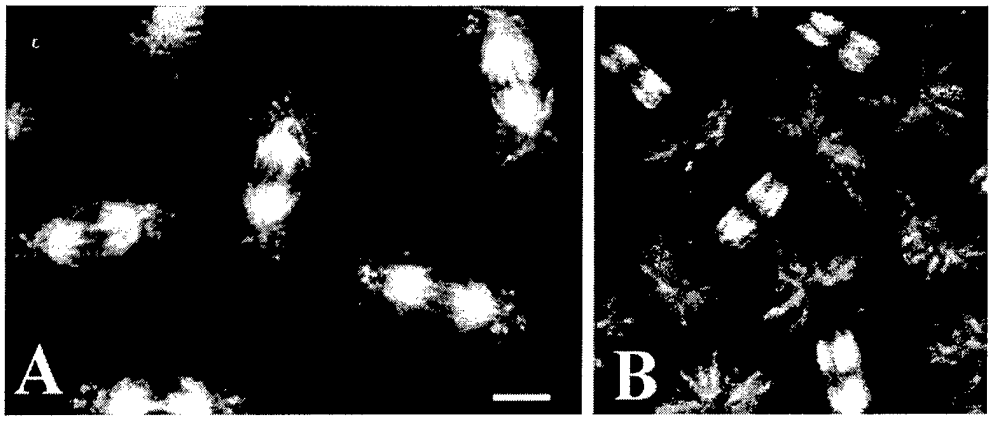

Figure 7. Relative distribution of phospho-KLP61F and tubulin in the mitotic spindle during metaphase and anaphase B. Confocal immunofluorescence images showing anti-phospho-KLP61F staining (blue) overlaid on anti β-tubulin (yellow) staining. In these images, yellow indicates the regions of the spindle in which the relative intensity of tubulin immunofluorescence is disproportionately high compared with phospho-KLP61F, white indicates the regions of relatively equal tubulin and phospho-KLP61F concentrations and blue indicates regions in which the intensity of phospho-KLP61F immunofluorescence is disproportionately high compared with tubulin. (A) In metaphase very little phospho-KLP61F colocalizes with astral MTs while the central spindle shows a high degree of overlap. The spindle midzone appears blue indicating a disproportionately high relative concentration of phospho-KLP61F to tubulin. (B) In anaphase B, nearly all of the KLP61F is concentrated in the interzone and very little is detected on chromosomes, spindle poles or astral MTs. Again, some regions of blue are apparent in the midzone indicating that phospho-KLP61F staining is disproportionately higher than tubulin staining. Bar, 5.7 μm.

terms, these images show the relative fluorescence intensity of phospho-KLP61F when compared with MTs. During metaphase (Fig. 7 A), the region of the half spindles between the poles generally shows relatively equal intensity for tubulin and phospho-KLP61F fluorescence. In contrast, the poles and astral MTs display disproportionately low phospho-KLP61F staining whereas the interpolar MT bundles crossing the midzone display disproportionately high phospho-KLP61F fluorescence. Somewhat similar results are obtained as the spindle elongates during anaphase B (Fig. 7 B), as the poles and astral MTs display disproportionately low phospho-KLP61F and bundles of MTs traversing the midzone display disproportionately high phospho-KLP61F staining. However, in metaphase some phospho-KLP61F staining is visible at the poles while, during anaphase B, polar localization of phospho-KLP61F is nearly undetectable. These data support the hypothesis that phospho-KLP61F is associated with "filaments" corresponding to interpolar MT bundles and becomes concentrated in the region of these bundles containing antiparallel MTs.

Visualization of KLP61F Associated with Interpolar Bundles of MTs by ImmunoEM

Although our immunofluorescence analyses indicate that phospho-KLP61F is present in the spindle, they cannot resolve whether the motor associates directly with individual spindle MTs. We performed immunoEM analyses using our anti-phospho-KLP61F antibody in order to examine the spatial relationship between the bipolar kinesin and MTs. Because the antibody is specific for a phospho-epitope in the tail of KLP61F these analyses allow us to examine not only whether phospho-KLP61F associates with spindle MTs but also how it is positioned relative to them by determining the position of the tail.

Fig. 8 shows the results of anti-phospho-KLP61F immunostaining performed on thin sections from embryos undergoing either metaphase (Fig. 8, A–D) or anaphase B (Fig. 8, E and F) labeled with secondary antibodies conjugated to 10- or 5-nm gold particles. The images shown in Fig. 8, A–C and E are from embryos embedded in the standard immunoEM resin, LR-White. At low magnification (Fig. 8, A and E), the staining patterns observed are consistent with the immunofluorescence shown above. Dense staining of the metaphase half spindles (Fig. 8 A), the anaphase interzone (E), and filaments bridging the midzone in both spindles (A and E) is observed. Gold labeling is also present on the poles but does not appear as concentrated as in the half spindles. The gold particle density in the spindle region is extremely high in relation to the cytoplasm (~253 vs. 7.3 particles/μm^2 during metaphase and ~237 vs. 54 particles/μm^2 during anaphase B in spindles vs. cytoplasm, respectively). Higher magnification reveals that gold labeling is clearly concentrated on or near interpolar MTs in the metaphase midzone (Fig. 8, B–D) and anaphase interzone (F). Note that immunolabeling only occurs at the surface of the section (Stierhof et al., 1991) and this accounts for the patchy labeling of MTs. The close juxtapositioning of gold particles to MTs was best seen in sections from embryos embedded in Eponate 12/Araldite resin to optimize spatial resolution (Fig. 8, D and F). Fig. 8 D shows the staining pattern along a metaphase interpolar MT bundle and Fig. 8 F shows the labeling of a bundle from an anaphase spindle. In both images it is apparent that the gold labeling is located extremely close to the surface of MTs. Measurements of the distance between gold particles and MTs indicates that, on average, gold particles lie ~9 and 7 nm from the surface of MTs during metaphase and anaphase, respectively (see Table II).

Anti-phospho-KLP61F Antibodies Associate with Crossbridges between MTs

Our structural model posits that KLP61F motors cross-

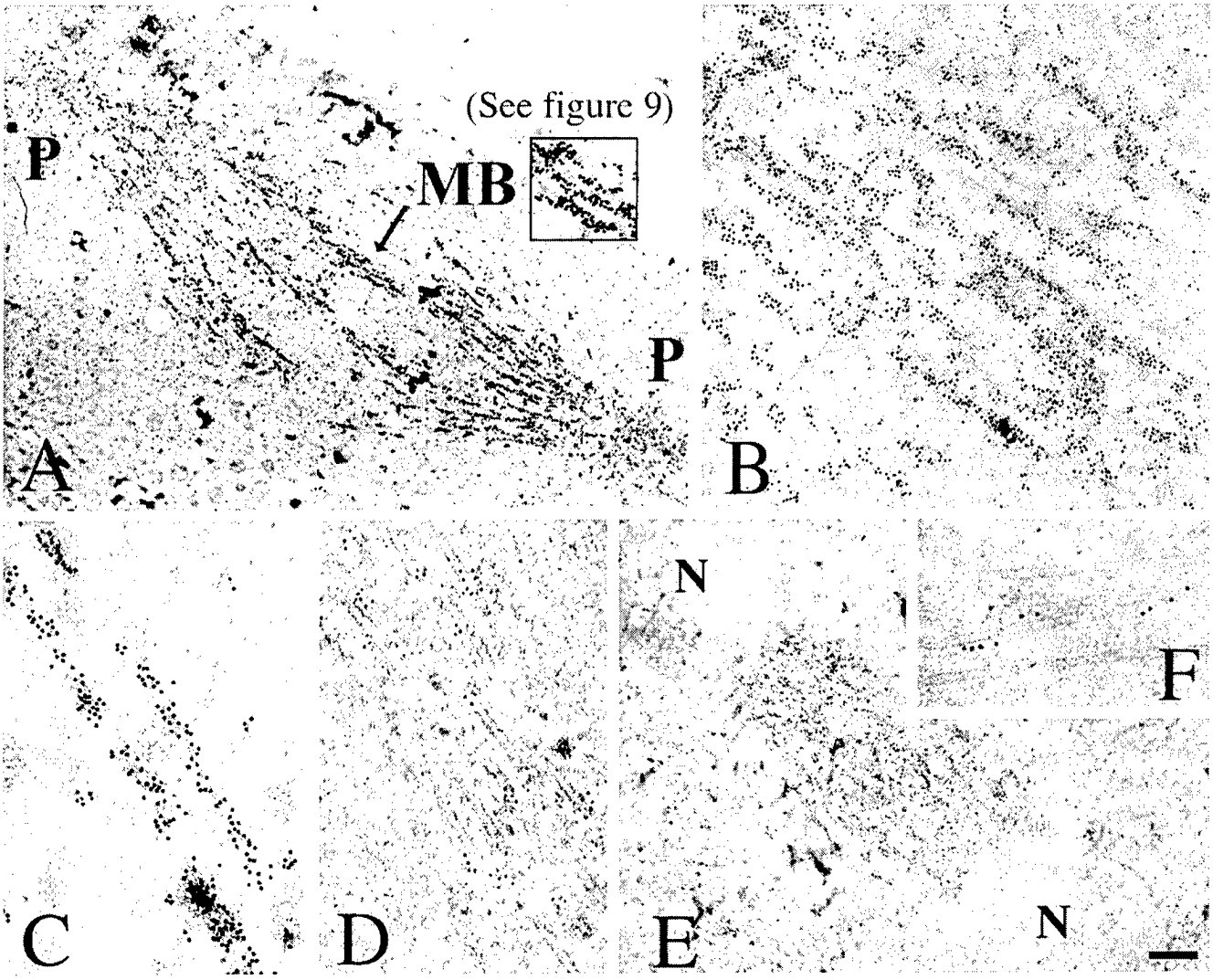

Figure 8. Visualization of phospho-KLP61F associated with interpolar MT bundles in metaphase and anaphase spindles. EMs of thin sections of *Drosophila* syncytial blastoderms preserved by HPF/FS and immunostained with the anti p-BCB antibody and gold conjugated secondary antibodies. (A and E) Phospho-KLP61F staining pattern on whole metaphase and anaphase spindles, respectively, from embryos embedded in LR-White and labeled with secondary antibodies conjugated to 10 nm gold (P, spindle poles; MB, interpolar MT bundle; N, separating daughter nuclei). (A inset) Higher magnification of the interpolar bundle (MB) indicated by the arrow and shown in digitally enhanced contrast in Fig. 9. When this region is enhanced for contrast, the gold can be seen to associate with electron-dense crossbridges between microtubules (Fig. 9). (B and C) Higher magnification of the immunostaining pattern in metaphase spindle midzones. (D and F) Phospho-KLP61F immunostaining pattern on interpolar MT bundles during metaphase and anaphase B, respectively, from embryos embedded in Eponate 12/Araldite and stained with secondary antibodies conjugated to 5 nm gold to increase the precision with which the proximity of the gold to the MT can be determined. Gold particles are closely associated with the surface of MTs within these bundles. Bar: (A and E) 1.3 μm; (B) 320 nm; (C) 160 nm; (D and F) 100 nm.

link interpolar MTs as bipolar homotetramers. A prediction of this model is that our anti-phospho-KLP61F antibody should lie at spacings ~60 nm apart at opposite ends of MT crossbridges (Fig. 9 A). In support of this hypothesis, we observed gold-labeled MT cross-links when the images shown in Fig. 8 were digitally enhanced to increase contrast. Fig. 9 B (top panel) shows a region of the anti-phospho-KLP61F-labeled interpolar MT bundle indicated by the inset in Fig. 8 A. In this image, a portion of the gold particles can be seen clearly associated with electron-dense filaments running between adjacent MTs (red arrows point down the long the axis of these filaments). In many cases, such as the one shown, these filaments are extremely numerous, producing a formation similar to rungs on a latter. Similar crossbridges were observed in different regions of multiple spindles and all showed nearly identical morphologies (Fig. 9 B, bottom panels). We identified

*Table II. Average Distance of Gold Particles from the Nearest MT**

Mitotic stage	Average distance between gold and MT
Metaphase	9.4 ± 6.2 nm
Anaphase	7.6 ± 4.5 nm

*For each stage these numbers were derived by averaging the distances between 500 gold particles from the nearest microtubule. Five different spindles were examined (100 gold particles/spindle).

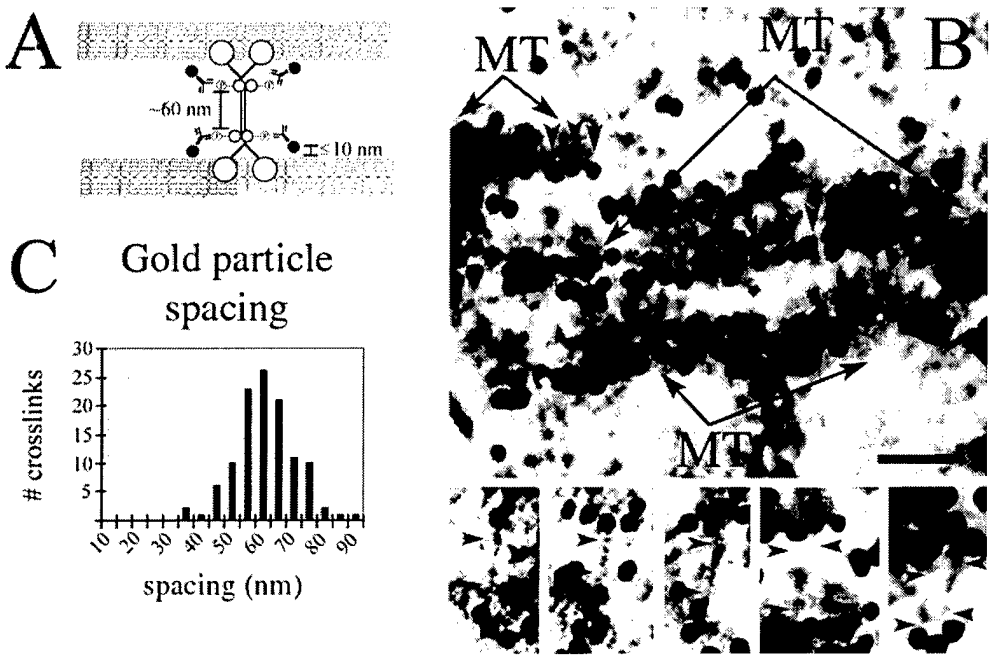

Figure 9. Antiphospho-KLP61F antibodies associate with electron-dense crossbridges between spindle microtubules. (A) Schematic illustration showing the predicted immunogold labeling pattern in spindles stained with the anti-phospho-KLP61F antibody. Based on the predicted position of the Bim C boxes on a bipolar KLP61F holoenzyme, gold particles should be spaced ~60 nm apart on electron-dense MT crossbridges. Note that although the antigenic sites are spaced ~60 nm apart, the crossbridges themselves are longer. Furthermore, the gold should be closely juxtaposed with microtubules, lying, on average, within 10 nm from the microtubule surface, just as we observe, (see Table II). (B) Observed gold labeling pattern in the spindle midzone. (Top) The image shown is the inset from Fig. 8 A with digitally enhanced contrast. (MT, microtubules, red arrowheads point down the long axis gold particle associated crossbridges.) (Bottom) Gallery of gold-labeled crossbridges. Red arrowheads indicate the two ends of the crossbridge adjacent to the associated gold particles. (C) Histogram of cross-link lengths. 115 MT crossbridges with gold particles associated at both ends were identified from two spindles and the length between the center of each gold particle was measured. The spacing ranged between 35 and 95 nm with a mean ~60-65 nm. Bar: (B, top) 60 nm; (B, bottom) 45 nm.

115 of these filaments that were decorated with gold particles on both ends. The spacing between gold particles on the filaments ranged from ~30–90 nm but was most commonly between 60–65 nm (Fig. 9 C).

Discussion

The purpose of this study was to visualize KLP61F within mitotic spindles of *Drosophila* syncytial blastoderms, in order to determine whether KLP61F acts as a MT-MT sliding motor involved in spindle pole separation or if it cross-links MTs to a spindle matrix and organizes the poles. To this end, we immunolocalized KLP61F in mitotic spindles using immunofluorescence and immunoEM and we performed a detailed structural analysis of the mitotic spindle components with which KLP61F putatively associates. The results of these analyses support the hypothesis that KLP61F participates in the formation and function of bipolar mitotic spindles by cross-linking and sliding MTs in relation to one another.

Drosophila Embryonic Spindles Contain Interpolar MT Bundles, Potentially Capable of Exerting Pushing Forces on Opposite Spindle Poles

In order for a MT-MT sliding mechanism to play a role in spindle pole positioning, the half spindles must be in contact through overlapping antiparallel MTs, most likely at the spindle midzone. Yet, tubulin immunofluorescence shows little or no staining of the spindle midzone in *Drosophila* embryos. Strikingly, however, EM reveals the presence robust interpolar MT bundles running through this region to bridge together the half spindles. Reconstruction of a representative interpolar bundle from serial cross-sections indicates that they consist of two MT arrays emanating from opposite poles that interdigitate in the midzone region. The region of antiparallel MT interdigitation extends ~1 μm into each half spindle and, thus, motor proteins that drive MT-MT sliding within these interpolar MT bundles could play a role in spindle pole positioning. For example, plus-end-directed motors could cross-link and slide apart antiparallel MTs in the region of interdigitation resulting in a repulsion of the poles (outward force), while minus-end-directed motors could pull the poles together (inward force).

The morphological characteristics of *Drosophila* embryonic spindles are consistent with the exertion of such counterbalancing forces. Since MTs will grow as straight tubes in the absence of an external force, the curvature of the interpolar MT bundles on the perimeter of the fusiform metaphase and anaphase A spindles (Fig. 1, B and C) suggests that they are being subjected to compressive forces resulting from a counterbalance of antagonistic forces pulling the poles inward and pushing them outward. An abrupt change in this counterbalance appears to coincide with the onset of anaphase B, which is characterized by straightening of interpolar MTs (Fig. 1 D). In such a scenario, a release of the inward force would relax the compressive forces acting on MTs allowing the poles to be pushed apart. A similar counterbalance of forces involving

bipolar kinesins has been proposed for *S. cerevisiae* (Saunders et al., 1997b), *S. pombe* (Pidoux et al., 1996), and *A. nidulans* (O'Connell et al., 1993).

KLP61F Is Appropriately Positioned to Slide Apart Antiparallel MTs

The hypothesis that KLP61F functions by cross-linking and sliding spindle MTs apart is supported by the observations that a severe loss-of-function mutation in the gene encoding KLP61F results in a late larval lethal phenotype, hallmarked by monoastral spindles in proliferating cells (Heck et al., 1993) and that the native KLP61F holoenzyme is a bipolar homotetramer, capable of cross-linking adjacent MTs and sliding them in relation to one another (Cole et al., 1994; Kashina et al., 1996a,b). To test this model, it is essential to determine the structural basis of the interaction between KLP61F motors and the mitotic spindle. The immunolocalization of KLP61F provides data relevant to this issue by revealing that KLP61F associates with spindle MTs in a phosphorylation dependent fashion, that it associates directly with interpolar MT bundles, and, strikingly, that bipolar KLP61F motors cross-link MTs within these bundles.

Phosphorylation of KLP61F by cdk1/CyclinB Targets KLP61F to Mitotic Spindles

Work on the bipolar Eg5 kinesin in humans and frogs has shown that the phosphorylation of bipolar Eg5 kinesin motors by cdk1/cyclinB at a specific site in the BCB targets these motors to spindles. Similarly, our results show that KLP61F associates with the spindle when phosphorylated in the BCB. This contrasts with the results from studies on the bipolar kinesins from the budding yeast *S. cerevisiae* that lack BCBs (Heck et al., 1993) and fission yeast *S. pombe* where the phosphorylation of this site does not affect the spindle association of the motor (Drummond et al., 1998). The significance of this difference is unclear but may reflect the fact that in both types of yeast, mitosis occurs completely within the confines of the nuclear envelope so that mitotic motors can interact with spindle MTs but not cytoplasmic MTs. However, in most other systems the spindle forms in the cytoplasm and precocious contact between mitotic motors and cytoplasmic MTs might perturb interphase MT arrays.

In *Drosophila* early embryos, the nuclear envelope never completely breaks down but instead fenestrates only at the points where spindle MTs enter the nuclear region. Our results showing that phospho-KLP61F associates with nuclei and spindles while nonphosphorylated KLP61F is excluded from these compartments, suggest that phosphorylation serves to sequester an active pool of the motor in a compartment where it can contact spindle MTs but not cytoplasmic MTs. How phosphorylation regulates the localization of KLP61F is unknown. It does not appear to do so by inducing the formation of bipolar tetramers, as our hydrodynamic analyses show that both phospho- and unphospho-KLP61F motors are predominantly tetrameric (Table I). It is also possible that phosphorylation increases the processivity of KLP61F motor activity that would, in turn, increase the time the motor spends associated with MTs. However, data regarding this are lacking. Clearly, the mechanism of the phospho-regulation of KLP61F localization and function requires additional investigation and will not be discussed further here.

KLP61F Is Concentrated on Interpolar MT Bundles

Our data show a clear association of KLP61F with interpolar MT bundles, visible as thin filaments of phospho-KLP61F bridging the midzone during both metaphase and anaphase by immunofluorescence (Fig. 6) that colocalize with interpolar MT bundles (Fig. 7). Interestingly, double label immunofluorescence images also show that the concentration of KLP61F is disproportionately high on MT bundles in the midzone and disproportionately low at the poles and on astral MTs when compared with tubulin staining. (Whole mount immunofluorescence provides a superior method for comparing the concentrations of motors and microtubules than does immunoEM of ultrathin sections, so the relative enrichment for KLP61F in these bundles is not apparent in Fig. 8.) This pattern shows a striking correspondence with the region of half spindle interdigitation within interpolar MT bundles suggesting that phospho-KLP6F has a particular affinity for antiparallel MTs (conversely, KLP61F could have an affinity specifically for the plus-ends of spindle MTs). However, it should be noted that other factors, such as the masking of both tubulin and phospho-KLP61F antigenic sites within the midzone might also affect the relative intensity of their fluorescence; for example, if the masking of tubulin and KLP61F antigenic sites in this region is nonequivalent, the ratio of their fluorescence intensities would not mirror their relative concentrations. We note, however, that the region of the spindle showing disproportionately high phospho-KLP61F fluorescence intensity extends ~1–2 μm into each half spindle, well beyond the zone of potential antigenic masking, indicating that the concentration of KLP61F in regions of MT interdigitation is truly disproportionately high.

KLP61F Is a Bipolar MT-MT Cross-linker

Whereas immunofluorescence reveals a general colocalization of KLP61F with interpolar MT bundles, immunoEM shows a close juxtaposition of the motor with the MTs within these bundles. At low magnification the immunolabeling pattern is obviously linear, similar to that expected from a microtubule stain. At higher magnifications, the gold particles are clearly aligned along MTs, and closely juxtaposed to the MT surfaces (Table II). Since our phospho-KLP61F antibody recognizes an epitope in the tail domain of the motor, this close juxtaposition of gold particles and MTs strongly suggests that the tail is positioned adjacent to a motor domain (see Fig. 9 A). The average distance between gold particles and the MT surface is ~10 nm, approximately the diameter of a KLP61F motor domain, supporting this suggestion. Furthermore, the analysis of the deduced sequence of KLP61F together with rotary shadowing EM analysis of the native holoenzyme, place the BCBs at the opposite end of an α-helical rod spaced ~60 nm apart, consistent with the model shown in Fig. 9 A.

Direct evidence in support of MT-MT cross-linking by bipolar KLP61F motors was obtained by visualizing gold

decorated spindles after digital enhancement of contrast. In the images shown in Fig. 9 B, for example, gold-labeled phospho-BCBs clearly associate with electron-dense crossbridges at a spacing of ~60 nm, in strong support of our previously proposed structural model for KLP61F. The average distance of 10 nm between the gold-labeled BCB and the MT surface (discussed above) summed with the ~60 nm spacing between the gold particle clusters on individual crossbridges, suggests a spacing between cross-linked MTs of ~80 nm, consistent with the relatively wide spacing between antiparallel MTs within interpolar MT bundles (Fig. 3 C). However, KLP61F is also clearly present in regions of the interpolar MT bundles that contain only parallel MTs, in which cross-links of a similar length (~60 nm) are also observed. Therefore, these data are most consistent with the idea that bipolar KLP61F motors cross-link both parallel and antiparallel MTs but other factors (MAPs or motors) must contribute to the generally closer packing of nearest neighbor MTs observed within parallel MT bundles (Fig. 3 B). Moreover, the close spacing of parallel MTs near the poles suggests that in this region of the spindle, KLP61F motors must cross-link parallel MTs that are not nearest neighbors. Further testing of this hypothesis requires a more thorough understanding of the organization of parallel vs. antiparallel MTs within interpolar MT bundles.

Model for KLP61F Function in the Spindle

Based on the localization of KLP61F shown here, its transport properties, and the phenotype of severe loss of function mutants, we propose the following expanded model for KLP61F function (shown schematically in Fig. 10). During centrosome migration, KLP61F is active and homotetrameric but sequestered away from MTs within the intact nuclear envelope. As the nuclear envelope fenestrates during prometaphase and MTs enter the nuclear region, KLP61F is free to bind and cross-link parallel and antiparallel spindle MTs, alike, riding slowly toward their plus-ends. The ability of KLP61F to cross-link MTs of both polarities assumes that theKLP61F motor domain is capable of swiveling 360° as has been shown for conventional kinesin (Hunt and Howard, 1993). Because of the plus-end–directed motility of KLP61F, a steady state is established in which KLP61F is present throughout the spindle but concentrated in the midzone, where the plus-ends of MTs from both half spindle interdigitate. The interaction of KLP61F with parallel MTs results in the formation of MT bundles capable of capturing kinetochores or interacting with MT bundles emanating from the opposite pole but, since the force vector on both MTs is the same, no net MT-MT sliding occurs. Conversely, when KLP61F interacts with antiparallel MTs, cross-linked MTs slide apart, generating an outward force on the poles. During metaphase and anaphase A, this force produces isometric tension counterbalancing an inward force to hold the poles apart. As the antagonistic inward force is released during anaphase B, the outward force serves to drive the poles apart. In other systems, where anaphase B involves strong pulling forces on the poles (Kronebusch and Borisy, 1982; Aist et al., 1993), the MT-MT interactions mediated by KLP61F might also serve as a brake, regulating the rate of spindle elongation.

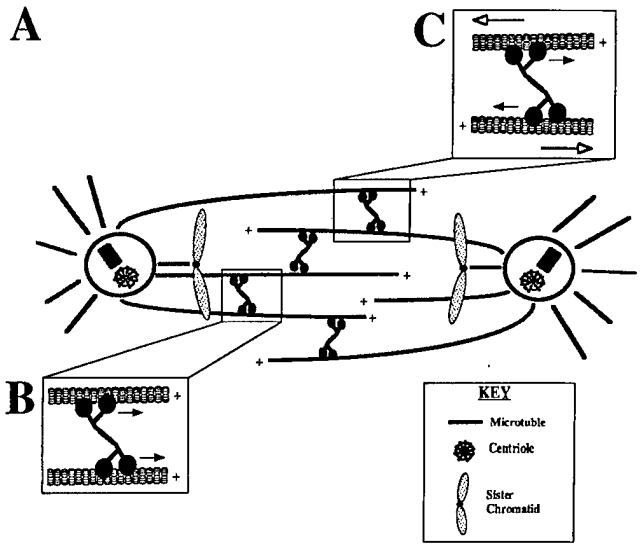

Figure 10. Model for KLP61F function. (A) As the nuclear envelope fenestrates and MTs enter the nuclear region, KLP61F cross-links spindle MTs regardless of orientation and rides toward their plus ends thereby becoming concentrated in the midzone. (B) If KLP61F cross-links parallel MTs they will be organized into bundles but no MT-MT sliding will be generated. (C) If KLP61F cross-links antiparallel MTs, the force generated by KLP61F will push the MTs apart. This results in isometric forces that hold the poles apart during metaphase and anaphase A, and isotonic forces that drive spindle elongation during anaphase B.

While our data clearly show KLP61F cross-linking interpolar MTs, it does not directly address several important issues. First, implicit in this model is that centrosome migration during prophase does not involve KLP61F, since this occurs before nuclear envelope fenestration when the motor is sequestered in the nucleus (Fig. 1 A). While we cannot exclude the possibility that the low level of KLP61F present in the cytoplasm is sufficient to drive prophase centrosome migration, it is also conceivable that spindle formation proceeds normally before nuclear envelope fenestration in the absence of KLP61F function and that the monoastral spindles seen in KLP61F mutants result from the collapse of a preformed bipolar spindle. It should be noted that such a spindle collapse has been observed in *S. cerevisiae* mutants carrying null alleles for the bipolar kinesins, cin8 and kip1 (Saunders et al., 1997). Moreover, although the monoastral spindles observed in bipolar kinesin mutants in *A. nidulans* (Enos and Morris, 1990), and *S. pombe* (Hagan and Yanagida, 1990) have been interpreted as resulting from defects in the initial separation of the spindle poles during spindle assembly, one cannot rule out the possibility that these structures result from the collapse of already assembled spindles. Direct visualization of spindle formation in KLP61F mutants should help resolve precisely when KLP61F function is needed. Second, although we have not observed KLP61F concentrated on kinetochore MT bundles or associated with a spindle matrix we cannot rule out the possibility that such interactions can occur at least in some systems.

The bipolar kinesin, KLP61F is critically important for mitosis. The data reported here, in concert with the motil-

ity properties of the motor and the phenotype of severe loss of function mutants, strongly suggest that KLP61F functions in a sliding filament mechanism to hold the spindle poles apart during metaphase and anaphase A and to drive spindle elongation during anaphase B. Given the strikingly similar molecular architecture of myosin II and KLP61F, it is appealing to speculate that the bipolar configuration of force generating enzymes involved in the sliding of cytoskeletal filaments is highly conserved and a fundamental feature of cytoskeletal activity.

The p-BCB antibody project was initiated while J.M. Scholey was on sabbatical in the Department of Biochemistry and Biophysics at UCSF and he thanks the members of the Alberts, Mitchison, Vale, and Walter labs for their hospitality. The authors gratefully acknowledge Dr. Larry Goldstein for discussions and for supplying anti-recombinant KLP61F antibody. We would also like to thank members of the Scholey lab and particularly Greg Rogers for Fig. 10 and Dana Rashid for help with photographic development. Finally, we would like to thank Rick Harris, director of the UCD Section of Molecular and Cellular Biology Microscopy Center for help in numerous areas of the project.

This work was supported by National Institutes of Health (NIH) grant number GM55507 to J.M. Scholey, and D.J. Sharp was supported by NIH postdoctoral fellowship number GM19262.

Received for publication 19 August 1998 and in revised form 30 November 1998.

References

Aist, J.R., H. Liang, and M.W. Berns. 1993. Astral and spindle forces in PtK2 cells during anaphase B: a laser microbeam study. *J. Cell Sci.* 104:1207–1216.

Ashburner, M. 1989. *Drosophila*: A Laboratory Handbook. Cold Spring Harbor Laboratory Press, Cold Spring Harbor, NY. 503–519.

Barton, N.R., A.J. Pereira, and L.S.B. Goldstein. 1995. Motor-activity and mitotic spindle localization of the *Drosophila* kinesin-like protein KLP61F. *Mol. Biol. Cell.* 6:1563–1574.

Barton, N.R, and L.S.B. Goldstein. 1996. Going mobile: microtubule motors and chromosome segregation. *Proc. Natl. Acad. Sci. USA.* 5:1735–1742.

Brinkley, B.R. 1990. Toward a structural and molecular definition of the kinetochore. *Cell Motil. Cytoskel.* 16:104–109.

Cole, D.G., W.M. Saxton, K.B. Sheehan, and J.M. Scholey. 1994. A 'slow' homotetrameric kinesin-related protein purified from *Drosophila* embryos. *J. Biol. Chem.* 269:22913–22916.

Desai, A., and T.J. Mitchison. 1995. A new role for motor proteins as couplers to depolymerizing microtubules. *J. Cell Biol.* 128:1–4.

Drummond, D.R., and I.M. Hagan. 1998. Mutations in the BCB of Cut7 indicate divergence of regulation within the bimC family of kinesin-related proteins. *J. Cell. Sci.* 111:853–865.

Enos, A.P., and N.R. Morris. 1990. Mutation of a gene that encodes a kinesin-like protein blocks nuclear division in *Aspergillus nidulans*. *Cell.* 60:1019–1027.

Euteneuer, U., W.T. Jackson, and J.R. McIntosh. 1982. Polarity of microtubules in *Haemanthus* endosperm. *J. Cell Biol.* 94:644–653.

Gelfand, V., and J.M. Scholey. 1992. Every motion has its motor. *Nature.* 359: 480–482.

Hagan, I., and M. Yanagida. 1990. Novel potential mitotic motor protein encoded by the fission yeast Cut7$^+$ gene. *Nature.* 347:563–566.

Hagan, I., and M. Yanagida. 1992. Kinesin-related Cut7 protein associates with mitotic and meiotic spindles in fission yeast. *Nature.* 356:74–76.

Heck, M.M., A. Pereira, P. Pesavento, Y. Yannoni, A.C. Spralding, and L.S.B. Goldstein. 1993. The kinesin-like protein KLP61F is essential for mitosis in *Drosophila*. *J. Cell Biol.* 123:665–679.

Hoyt, M.A. 1994. Cellular roles of kinesin and related proteins. *Cur. Opin. Cell Biol.* 6:63–68.

Hoyt, M.A., L. He, K.K. Loo, and W.S. Saunders. 1992. Two *Saccharomyces cerevisiae* kinesin-related gene-products required for mitotic spindle assembly. *J. Cell Biol.* 118:109–120.

Hunt, A.J., and J. Howard. 1993. Kinesin swivels for microtubule movement in any direction. *Proc. Natl. Acad. Sci. USA.* 90:11653–11657.

Kashina, A.S., R.J. Baskin, D.G. Cole, K.P. Wedaman, W.M. Saxton, and J.M. Scholey. 1996a. A bipolar kinesin. *Nature.* 379:270–272.

Kashina, A.S., J.M. Scholey, J.D. Leszyk, and W.M. Saxton. 1996b. An essential bipolar mitotic motor. *Nature.* 384:225.

Kashina, A.S., G.C. Rogers, and J.M. Scholey. 1997. The bimC family of kinesins: essential bipolar mitotic motors driving centrosome separation. *Biochim. Biophys. Acta.* 1357:257–271.

Kiss, J.Z., and L.A. Staehelin. 1995. High pressure freezing. *In* Rapid Freezing, Freeze Fracture and Deep Etching. N.J. Severs and D.M. Shotton, editors. Wiley-Liss Inc., New York. 89–104.

Kronebusch, P.J., and G.G. Borisy. 1982. Mechanics of anaphase B movement. *In* Biological Functions of Microtubules and Related Structures. H. Sakai, H. Mohri, and G.G. Borisy, editors. Academic Press, New York. pp. 233–245.

Mastronarde, D.N., K.L. McDonald, R. Ding, and J.R. McIntosh. 1993. Interpolar spindle microtubules in PTK cells. *J. Cell Biol.* 123:1475–1489.

McDonald, K.L. 1994. Electron microscopy and EM immunocytochemistry. *Methods Cell Biol.* 44:411–444.

McDonald, K.L., J.D. Pickett-Heaps, J.R. McIntosh, and D.H. Tippit. 1977. On the mechanism of anaphase spindle elongation in *Diatoma vulgare*. *J. Cell Biol.* 74:377–388.

McIntosh, J.R., P.K. Hepler, and D.G. Van Wie. 1969. Model for mitosis. *Nature.* 224:659–663.

McIntosh, J.R., and S.C. Landis. 1971. The distribution of spindle microtubules during mitosis in cultured human cells. *J. Cell Biol.* 49:468–497.

Meyer, D., D. Rines, A.S. Kashina, D.G. Cole, and J.M. Scholey. 1998. Purification of novel kinesins from embryonic systems. *Methods Enzymol.* 298:133–153.

O'Connell, M.J., P.B. Meluh, M.D. Rose, and M.R. Morris. 1993. Suppression of the bimC mitotic spindle defect by deletion of klpA, a kar3 related kinesin like protein in *Aspergillus nidulans*. *J. Cell Biol.* 120:153–162.

Oegema, K., W.G. Whitfield, and B.M. Alberts. 1995. The cell cycle-dependent localization of the CP190 centrosomal protein is determined by the coordinate action of two separable domains. *J. Cell Biol.* 131:1261–1273.

Pidoux, A.L., M. LeDizet, and W.Z. Cande. 1996. Fission yeast pkl1 is a kinesin-related protein involved in mitotic spindle function. *Mol. Biol. Cell.* 7:1639–1655.

Roof, D.M., P.B. Meluh, and M.D. Rose. 1992. Kinesin-related proteins required for assembly of the mitotic spindle. *J. Cell Biol.* 118:95–108.

Saunders, W.S., and M.A. Hoyt. 1992. Kinesin-related proteins required for structural integrity of the mitotic spindle. *Cell.* 70:451–458.

Saunders, W.S., D. Koshland, D. Eshel, I.R. Gibbons, and M.A. Hoyt. 1995. *Saccharomyces cerevisiae* kinesin- and dynein-related proteins required for anaphase chromosome segregation. *J. Cell Biol.* 128:617–624.

Saunders, W., D. Hornack, V. Lengyel, and C. Deng. 1997a. The *Saccharomyces cerevisiae* kinesin-related motor Kar3p acts at preanaphase spindle poles to limit the number and length of cytoplasmic microtubules. *J. Cell Biol.* 137: 417–431.

Saunders, W., V. Lengyel, and M.A. Hoyt. 1997b. Mitotic spindle function in *Saccharomyces cerevisiae* requires a balance between different types of kinesin-related motors. *Molecular Biol. Cell.* 8:1025–1033.

Sawin, K.E., K. Leguellec, M. Phillipe, and T.J. Mitchison. 1992. Mitotic spindle organization by a plus-end-directed microtubule motor. *Nature.* 359:540–543.

Sawin, K.E., and T.J. Mitchison. 1995. Mutations in the kinesin-like protein Eg5 disrupting localization to the mitotic spindle. *Proc. Nat. Acad. Sci. USA.* 92: 4289–4293.

Stafstrom, J.P., and L.A. Staehelin. 1984. Dynamics of the nuclear envelope and of nuclear pore complexes during mitosis in the *Drosophila* embryo. *Eur. J. Cell Biol.* 34:179–189.

Steinbrecht, R.A., and M. Muller. 1987. Freeze substitution and freeze drying. *In* Cryotechniques in Biological Electron Microscopy. R.A. Steinbrecht and K. Ziergold, editors. Springer-Verlag, Berlin. 149–172.

Stierhof, Y., H. Schwartz, M. Durrenburger, W. Villiger, and E. Kellenberger. 1991. Yield of immunolabel compared to resin sections and thawed cryosections. *Colloidal Gold: Principles, Methods, and Applications.* 3:87–115.

Straight, A.F., J.W. Sedat, and A.W. Murray. 1998. Time-lapse microscopy reveals unique roles for kinesins during anaphase in budding yeast. *J. Cell Biol.* 143:687–694.

Theurkauf, W.E. 1994. Immunofluorescence analysis of the cytoskeleton during oogenesis and early embryogenesis. *Methods Cell Biol.* 44:489–505.

Walczak, C.E., and T.J. Mitchison. 1996. Kinesin-related proteins at mitotic spindle poles-function and regulation. *Cell.* 85:943–946.

Winey, M., C.L. Mamay, E.T. O'Toole, D.N. Mastronarde, T.H. Giddings, Jr., K.L. McDonald, and J.R. McIntosh. 1995. Three-dimensional ultrastructural analysis of the *Saccharomyces cerevisiae* mitotic spindle. *J. Cell Biol.* 129: 1601–1615.

Wright, B.D., M. Terasaki, and J.M. Scholey. 1993. Roles of kinesin and kinesin-like proteins in sea urchin embryonic cell division: evaluation using antibody microinjection. *J. Cell Biol.* 123:681–689.

Microtubule Dynamics in *Xenopus* Egg Extracts

MIMI SHIRASU[1†], ANN YONETANI[1†], AND CLAIRE E. WALCZAK[2*]
[1]*Department of Cell Biology, Harvard Medical School, Boston MA 02115*
[2]*Medical Sciences Program, Indiana University, Bloomington, IN 47405*

KEY WORDS microtubule; proteins; cell cycle; cellular function

ABSTRACT The organization and function of microtubules change dramatically during the cell cycle. At the onset of mitosis, a radial array of microtubules is broken down and reorganized into a bipolar spindle. This event requires changes in the dynamic behavior of individual microtubules. Through the use of *Xenopus laevis* egg extracts, a number of proteins affecting microtubule behavior have been identified. Recently, progress has also been made towards understanding how the activities of such microtubule-affecting proteins are regulated in a cell cycle-dependent manner. It is hoped that understanding how microtubule behavior is controlled during the cell cycle in vitro may illuminate the role of microtubule dynamics in various cellular processes. *Microsc. Res. Tech. 44:000–000, 1999.*

INTRODUCTION

Underlying basic cellular functions, including intracellular transport and chromosome segregation, is a network of cytoskeletal polymers called microtubules. During interphase in animal cells, microtubules emanate from a single microtubule-organizing center (MTOC) found near the nucleus and form an astral array extending to the cell periphery. These microtubules are long and sparse relative to those found in mitotic cells. During mitosis, newly-duplicated MTOCs separate, and the microtubules associated with them form a bipolar spindle, which is responsible for segregating chromosomes to daughter cells. Bipolar spindles are built from a dense population of short and highly dynamic microtubules (Fig. 1). The means by which microtubules undergo this dramatic transformation during the cell cycle is an important cell biological problem; this review will focus on recent progress towards understanding this phenomenon through the use of *Xenopus* egg extracts.

Microtubules are hollow filaments, 25 nm in diameter, composed of alpha/beta tubulin heterodimers. Unlike equilibrium polymers, microtubules in steady-state undergo stochastic transitions between phases of polymerization and depolymerization. The transition from polymerization to depolymerization is called "catastrophe", and the transition from depolymerization to polymerization is termed "rescue" (Fig. 2). This behavior is known as "dynamic instability" (Mitchison and Kirschner, 1984) Microtubules exhibit inherent polarity in their dynamic behavior at each end of the polymer. One end (the "plus" end) polymerizes at a faster rate than the other (the "minus" end) (Walker et al., 1988). In most cell types, microtubules are strictly organized with respect to this polarity; microtubule minus ends are found proximal to the MTOC and plus ends found distal, at the cell periphery.

Using purified tubulin, measurements of microtubule behavior in vitro show significant differences from measurements in vivo (reviewed in Desai and Mitchison, 1997). In vitro, increasing concentrations of tubulin lead to increased rates of polymerization and decreased rates of catastrophe (Walker et al., 1988). In vivo, the rate of polymerization is much higher than expected for the concentration of tubulin in the cytoplasm but is nevertheless associated with a high rate of catastrophe (reviewed in Cassimeris, 1993). Clearly, microtubule-affecting proteins exist in vivo which account for these differences and play an important role in modulating the behavior and organization of microtubules in cells. Of particular interest are those proteins that promote the dramatic changes in microtubule dynamics during the transition from interphase to mitosis.

Microtubules can be observed in cells in many ways (reviewed in Inoue and Salmon, 1995). Historically, fibers were first seen by electron microscopy, but their preservation varied with different fixation techniques. It was not until the advent of polarized light microscopy that birefringent fibers could be observed reliably in living cells. Polarized light studies could demonstrate that this fibrous array undergoes dynamic rearrangement during the cell cycle and is extremely labile to low temperature and anti-mitotic drugs such as colchicine. However, use of this technique was restricted to the observation of microtubules within dense, highly organized structures such as the mitotic spindle. Improvement in fixation techniques for electron microscopy as well as the development of immunofluorescence microscopy allowed initial observations to be made about microtubule dynamics. However, it is important to realize the limitations of deducing dynamic behavior from fixed samples. Currently, time-lapse video microscopy in live cells, using GFP-labeled tubulin, microinjection of fluorescently-labeled tubulin, or video-enhanced differential interference contrast (VE-DIC) microscopy, allows direct observation of the dynamics of individual microtubules (Cassimeris et al., 1988; Gelfand and

†These authors contributed equally to this work.
*Correspondence to: Claire E. Walczak, Medical Sciences Program, Indiana University, Jordan Hall 306, Bloomington, IN 47405. E-mail: cwalczak@indiana.edu
Received 24 September 1998; accepted in revised form 3 November 1998

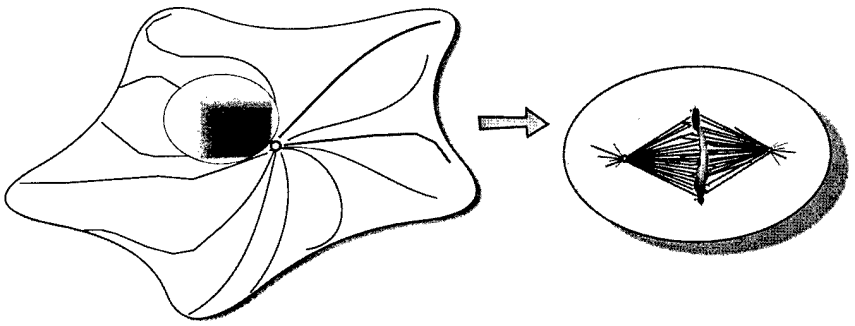

Fig. 1. Microtubule morphology changes dramatically during the cell cycle. **(a)** In an interphase animal cell, microtubules are found in a radial array around the microtubule-organizing center (MTOC). Microtubules are long and sparse and have a wavy appearance. **(b)** During mitosis, microtubules are organized into a symmetrical bipolar spindle. Condensed chromosomes are aligned in pairs at the central metaphase plate before being separated and pulled towards opposite spindle poles.

Bershadsky, 1991; Stearns, 1995; Walker et al., 1988). These techniques have their own drawbacks; for example, cells are perturbed by microinjection and by photodamage generated from fluorescent probes. DIC microscopy, while a sensitive and non-invasive technique, is limited by sample thickness. DIC allows high-resolution visualization of microtubules within the relatively flat peripheral sections of interphase cells, but microtubules in the central parts of the cell and in rounded mitotic cells are more difficult to observe. As a result, in vivo measurements of microtubule dynamics by this method have been restricted to microtubule plus ends found in thin regions near the cell periphery.

Cytoplasmic extracts of *Xenopus* eggs (as well as other amphibian and marine invertebrates) have proven to be extremely useful in studying MT dynamics, lending themselves more readily to microscopic techniques than do intact cells. Perhaps more importantly, extracts are biochemically tractable. Egg extracts are often a rich source of native protein for biochemical fractionation. Because embryos undergo a series of very rapid cell divisions following fertilization, eggs are stockpiled with proteins involved in cell division including those involved in reorganizing the microtubule cytoskeleton.

Xenopus egg extracts are well suited for the study of MT dynamics for two reasons. First, *Xenopus* egg extracts offer the advantage of a synchronized and controllable cell cycle. Studies of cell cycle progression in *Xenopus* egg extracts have shown that the maturation promoting factor (MPF), which induces mitosis and meiosis, corresponds to the active protein kinase cdc2 complexed with cyclin B (Lohka, et al., 1988). MPF activity (as monitored by H1 kinase activity) is high in metaphase and low in interphase. By controlling the activity of MPF, experimentalists can manipulate *Xenopus* egg extracts to be stably arrested in either interphase or mitosis (Murray, 1991). This makes it possible to purify native proteins in particular cell cycle states (ie, phosphorylated or complexed).

Second, these highly concentrated frog extracts are capable of recapitulating complex changes in MT dynamics, which occur during cell cycle progression, such as those required for mitotic spindle assembly. These extracts can then be manipulated in ways which would be extremely difficult (if not impossible) in whole cells. For example, inhibition of specific proteins by antibody addition or immunodepletion is technically simpler in extracts than in cells, where such procedures require microinjection or gene expression. Pure protein can also be added back to immunodepleted extracts, demonstrating that depletion phenotypes are specific to the protein of interest. In this way, the effects on MT dynamics produced by perturbing a particular protein can be determined during each stage of the cell cycle (Desai et al., 1998).

In order to observe real-time MT dynamics in crude extracts, it is necessary to visualize the microtubules by addition of fluorescently-labeled tubulin, which incorporates into endogenous microtubules. For observation by DIC, the extract must first be clarified of refractile particles such as membrane vesicles. Clarified extracts (also called high-speed supernatants or HSS) retain their cell cycle state and, though incapable of bipolar spindle formation, will polymerize microtubules from a nucleating substrate. Common microtubule-nucleating substrates for both crude and clarified extracts include purified centrosomes and axonemes. Reagents such as taxol and DMSO stabilize microtubules and can induce the formation of organized microtubule arrays in *Xenopus* extracts (Verde et al., 1991); however, these reagents obviously perturb MT dynamics and are thus unsuitable for studying physiological dynamics.

In this review, we focus on changes in MT dynamics during the cell cycle. Precise determination of MT dynamic parameters in interphase and mitotic *Xenopus* extracts constituted a major step toward understanding how microtubules undergo the dramatic structural rearrangement during the interphase-to-mitosis transition. *Xenopus* egg extracts have also been central to the identification and characterization of many microtubule-affecting proteins, some of which may be key players in mediating the differences between interphase and mitotic MT dynamics. Finally, we review current investigation into links between the cell-cycle machinery (like cdc2/cyclinB kinase) and MT dynamics.

CHANGES IN MTS WITH CELL CYCLE PROGRESSION

In the transition from interphase to mitosis, structural rearrangement of microtubules is accompanied by changes in polymer length, number, and turnover rate. Microtubules in mitosis are shorter on average than microtubules in interphase and the total number

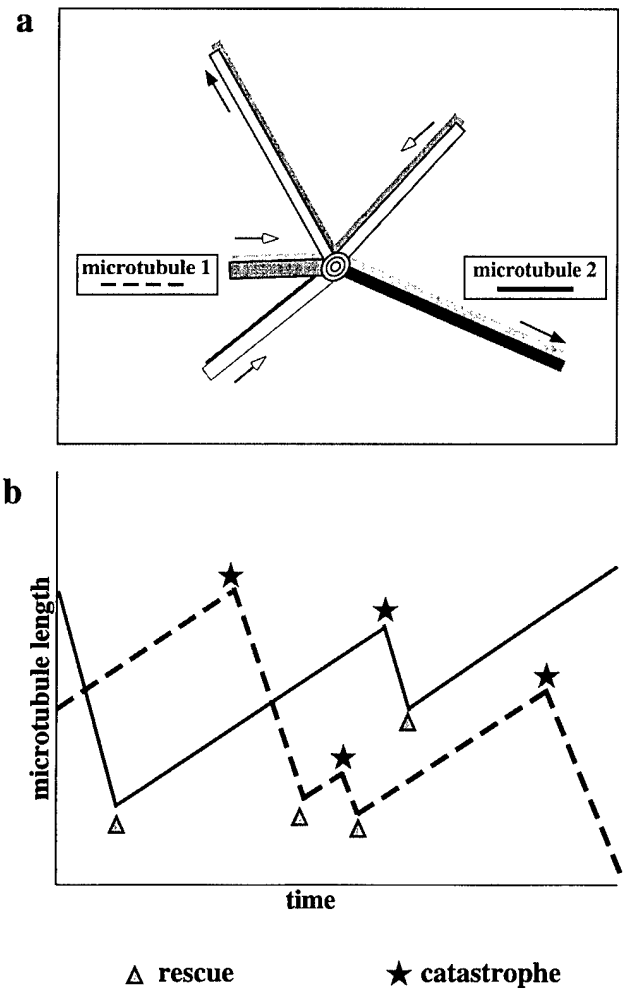

Fig. 2. Dynamic behavior of microtubule polymers. **(a)** Schematic representation of centrosome-nucleated microtubules as viewed by VE-DIC microscopy. The behavior of individual microtubules are independent of each another, with some polymerizing and others depolymerizing at any given time. **(b)** Graph representing the length of two particular microtubules as a function of time. Transitions (rescue and catrastrophe) between phases of polymerization and depolymerization are stochastic.

of microtubules increases (Zhai and Borisy, 1994; Zhai et al., 1995). Mitotic cells also display a higher rate of microtubule turnover than do interphase cells, as shown by the rapid incorporation of labeled tubulin into cellular microtubule structures as well as the rapid recovery of fluorescence after photobleaching (Salmon et al., 1984; Saxton et al., 1984). In newt lung cells, for example, microtubules are several times shorter, four times as numerous, and turn over two to three orders of magnitude faster in the mitotic spindle than in the interphase array (Cassimeris et al., 1988; Wadsworth and Salmon, 1986).

Understanding these changes in population morphology required the precise determination of changes in MT dynamics. Theoretically, altering any of the four parameters of MT dynamics (polymerization, depolymerization, catastrophe, and rescue) might account for a transition from long, stable microtubules to short, dynamic ones. Microtubules in mitosis could polymerize more slowly or depolymerize more quickly than they do in interphase. Alternatively, microtubules in mitosis could spend more time depolymerizing than they do polymerizing, which might result from an increase in catastrophe rate or a decrease in rescue rate.

Early studies of MT dynamics in extracts measured the lengths of microtubules which had been fixed at successive time-points (Verde, et al., 1990). This type of analysis could not distinguish between changes in each dynamic parameter and gave only net polymerization and depolymerization rates. Microtubules were shown to exhibit a lower rate of net growth in mitosis relative to interphase (Verde, et al., 1990). This was interpreted as a lower rate of polymerization in mitosis and led to two early hypotheses on cell-cycle regulation of MT dynamics. The first hypothesis proposed that the increase in microtubule nucleation sites during mitosis might be sufficient to deplete the cytoplasm of tubulin dimer (Mitchison and Kirschner, 1984). Because polymerization is a bimolecular reaction, polymerization rate decreases with decreased tubulin concentration. It was postulated that this would result in short, dynamic polymers The second hypothesis was influenced by studies on neuronal microtubule-associated proteins (MAPs), proteins which bind and stabilize microtubules, thereby increasing their polymerization rate (Drechsel et al., 1992; Pryer et al., 1992). It was proposed that decreased assembly rates and stability in mitosis may be due to phosphorylation of these MAPs, which inhibits their binding to microtubules and prevents them from promoting microtubule polymerization (reviewed in McNally, 1996).

However, real-time analysis of MT dynamics (Belmont et al., 1990) showed that in *Xenopus* egg extracts the transition from interphase to mitosis is characterized by a change in catastrophe rate. The rate of polymerization was not decreased in mitotic extracts relative to interphase; in fact, both polymerization and depolymerization rates were slightly higher in mitosis. The major difference between the two cell cycle states was a 5- to 10-fold increase in catastrophe rate during mitosis. It was later shown that this increased catastrophe rate is specifically triggered by cyclinB-associated cdc2 kinase (MPF); addition of cyclinA-associated cdc2 kinase to interphase extracts did not affect catastrophe frequencies (Verde et al., 1992).

Is this change in catastrophe rate enough to account for the increase in MT turnover observed during mitosis? Verde et al. (1992) discussed a mathematical model for microtubule dynamics previously studied by T. Hill (1985). This model relates the average length of stiff, non-interacting polymers in an infinite, homogenous medium (like microtubules in *Xenopus* egg extracts) to the four parameters of dynamic instability. Given experimentally-determined rates for each dynamic parameter, the model predicts an average microtubule length which correlates amazingly well with measured microtubule lengths.

The Hill model predicts that minimal changes in transition frequencies (catastrophe or rescue) will have far greater effect on average MT length than corresponding changes in polymerization or depolymerization rates but does not predict whether catastrophe or rescue is the dominant parameter. In *Xenopus* extracts,

increased catastrophe rate appears to be primarily responsible for increased MT turnover in mitosis. However, a study by Gliksman et al. (1992) showed that, in sea urchin egg extracts treated with phosphatase inhibitors, a similar effect could be produced by decreased rescue rate. The regulation of catastrophe versus rescue events may be cell-type specific.

The Hill analysis also makes no assumptions about the molecular mechanisms underlying specific changes in MT dynamic parameters. Phosphorylation of MAPs and subsequent decreases in their affinity for microtubules do not lead to decreased polymerization rates in *Xenopus* egg extracts. However, it is possible that, during mitosis, this decrease in MAP affinity makes microtubules more sensitive to other destabilizing activities, such as a mitotic catastrophe factor.

Though this type of Hill analysis has been extremely useful, it is limited to the four classic dynamic parameters. There are several, more complex, types of microtubule behavior seen in both mitotic cells and mitotic *Xenopus* extracts: increased microtubule nucleation, microtubule severing, and poleward microtubule flux. These types of microtubule behavior are frequently overlooked in analyses of MT dynamics but may be important for microtubule function during mitosis and therefore warrant mention here. Microtubule nucleation is clearly cell-cycle regulated and, while it does not lead to a depletion of tubulin monomer as originally proposed, it is probably important for formation of a bipolar spindle. Microtubule severing has only recently been observed in tissue culture cells, and its function remains unknown. Poleward microtubule flux is defined as the coordinated movement of microtubule subunits in the mitotic spindle toward spindle poles. Pharmacological studies in *Xenopus* extracts have suggested that flux may drive chromosome movement during anaphase A (Desai et al., 1998); however, flux appears to play a more minor role in chromosome segregation in tissue culture cells (Mitchison and Salmon, 1992).

Quantitative measurements of MT dynamics vary between different cell types and between cells and extracts. It should be noted that precise dynamics measurements may even vary from one extract preparation to the next. Microtubule behavior may also be affected by techniques involving addition of exogenous (often bovine) and/or modified tubulin, dilution with buffer, and clarification by centrifugation, and extreme care should be taken in noting these differences during comparisons of results from independent studies.

In a recent paper by Parsons and Salmon (1997), data is presented which describes MT dynamics in a clarified HSS extracts, as visualized by DIC. No exogenous, fluorescently-labeled tubulin, which is known to have effects on MT dynamics, was added to the extract. Dynamic measurements in these extracts were significantly different from those made in crude extracts by Belmont and Verde (Belmont et al., 1990; Verde et al., 1992). Both polymerization and depolymerization rates were much higher in interphase and depolymerization significantly higher in mitosis. More disturbingly, both mitotic and interphase extracts had extremely low catastrophe frequencies. Does this mean that the high rates of catastrophe seen in crude mitotic extracts was somehow an artifact generated by the addition of exogenous tubulin? Addition of bovine brain tubulin to these highly-clarified mitotic extract was not sufficient to restore catastrophe frequencies to those seen in crude mitotic extracts. This result implies that high catastrophe frequencies are not an artifact due to exogenous tubulin. In this system, high-speed centrifugation appears to remove an important factor that directly or indirectly induces microtubule catastrophe. The identification of this catastrophe-promoting factor will be an important area of future research.

While measurements of MT dynamics in extracts cannot be taken as literal interpretations of cellular MT dynamics, the relative changes in these dynamics can provide valuable insight into how the transition between interphase and mitotic MT dynamics may be mediated. In being able to perturb this system, assess changes in microtubule lengths and lifetimes, and determine which MT dynamic parameters are responsible for those changes, investigators have a unique window into the inner workings of the cell. In this way, utilization of *Xenopus* egg extracts has led to the identification and characterization of some of the most important proteins so far discovered to modulate MT dynamics.

PROTEIN MODULATORS OF MICROTUBULE DYNAMICS

Microtubule affectors can be divided into three classes: 1) proteins that affect MT dynamics, as defined by the four dynamic parameters (polymerization, depolymerization, rescue, or catastrophe); 2) proteins that affect the number of polymer ends; and 3) proteins that bind microtubules and rearrange them into higher order structures. We will emphasize proteins in the first class. Proteins belonging to the last category, including many kinesin-related motor proteins, have been well-studied in *Xenopus* egg extracts; however, they have been discussed in several recent reviews and will not be covered here (reviewed in Barton and Goldstein, 1996; Vale and Fletterick, 1997).

Mathematical modeling of theoretical polymer dynamics by Hill (1985), as well as computer simulation studies by Gliksman et al. (1993), predict that small changes in transition frequencies (catastrophe and rescue) could have rapid and dramatic effects on polymer populations. Cellular factors which mediate such changes in microtubule behavior have long been sought and, in the last several years, a number of these proteins have been identified in *Xenopus* egg extracts.

XMAPs (Xenopus Microtubule-Associated Proteins)

Gard and Kirschner (1987) observed that *Xenopus* extracts contained an activity which greatly stimulated microtubule assembly. Purification of the protein responsible for this activity resulted in the identification of XMAP215. Using a fixed timepoint assay, purified XMAP215 protein was found to accelerate tubulin polymerization at microtubule plus-ends, resulting in longer but, paradoxically, less stable microtubules. Subsequently, real-time analysis revealed that the effect of this protein on microtubule dynamics was complex. In vitro, XMAP215 increases MT polymerization rate by an order of magnitude, causes a three-fold increase in depolymerization rate, and nearly elimi-

nates rescue (Vasquez et al., 1994). Because the increase in polymerization rate is greater than the effects on depolymerization and rescue, the net effect of XMAP215 is to promote MT assembly; however, this net assembly is associated with increased MT turnover.

XMAP215 was the first MAP found to increase MT turnover. A human homologue of the protein TOG has recently been identified and found to have similar effects on microtubules (Charrasse et al., 1998). Without immunodepletion data, the physiological function of XMAP215 remains unclear. Its activity may be modulated in vivo by interaction with other MAPs and MT-affecting proteins. However, it is likely that the activity of factors like XMAP215 contribute to the high rate of microtubule turnover observed in vivo, relative to solutions of pure tubulin. XMAP215 might also be involved in regulating MT dynamics during mitosis, when polymer concentration is maintained at interphase levels even though turnover rate is greatly increased.

In contrast to XMAP215, most known MAPs decrease, rather than increase, MT turnover. Two *Xenopus* MAPs of this kind were recently isolated and characterized by Karsenti and coworkers (Andersen et al., 1994; Andersen and Karsenti, 1997b). The effects of the purified proteins on microtubule dynamics were assayed by monitoring the behavior of centrosome-nucleated microtubules with VE-DIC microscopy. XMAP230 and XMAP310 were both found to have stabilizing effects on microtubules, but each acts by a different mechanism. XMAP230 caused a significant decrease in catastrophe rate; XMAP310, on the other hand, had the primary effect of increasing rescue rate. These studies demonstrate the importance of real-time observation since the mechanisms by which these two MAPs act would likely have been indistinguishable in fixed timepoint assays.

Studies of *Xenopus* as well as neuronal MAPs have demonstrated that these proteins are important modulators of microtubule behavior. However, the collective effect of these *Xenopus* MAPs is not sufficient to account for the dramatic increase in microtubule turnover observed during mitosis. In particular, none of the known *Xenopus* MAPs increases the rate of microtubule catastrophe.

Catastrophe factors

Op18/Stathmin. After making the initial observation in frog extracts that microtubule catastrophe rate increased several-fold during mitosis, Belmont and Mitchison (1996) set out to purify microtubule-destabilizing activities present in extracts. One protein factor, which they isolated from thymus extracts, was identical to a previously characterized leukemia-associated oncoprotein called Op18 or stathmin. Op18 had initially been identified as a protein whose expression was highly induced in some tumor cells, and its phosphorylation was characterized extensively (Sobel, 1991). The physiological function of the protein, however, remained unclear until Op18 was identified as a catastrophe-inducing factor.

Immunodepletion of Op18 from *Xenopus* egg extracts resulted in increased microtubule length and density in sperm centrosome-nucleated asters. Readdition of pure protein to the depleted extract restored microtubule polymer to normal levels (Belmont and Mitchison, 1996). The role of Op18 in the mitotic spindle, however, remains elusive. Immunodepletion of the protein caused excessive microtubule polymerization during the early stages of spindle assembly, but normal bipolar spindles were ultimately formed (Andersen et al., 1997a).

Op18 was also shown to interact with tubulin dimers. A tubulin-sequestering protein might be predicted to increase microtubule catastrophe rate by decreasing growth rate as a consequence of depleting soluble tubulin dimers. Whether or not Op18 acts in this way is an unresolved issue; Belmont and Mitchison (1996) maintain that the protein acts catalytically whereas Jourdain et al. (1997) support a sequestering role.

XKCM1. The *Xenopus* kinesin-like protein XKCM1 was identified during a screen for kinesin-like motor proteins which might be involved in spindle assembly (Walczak et al., 1996). Immunodepletion from extracts showed that XKCM1 was necessary for spindle assembly and, surprisingly, modulated MT dynamics. In the absence of XKCM1 protein, microtubule asters were ten times larger than in mock-depleted extracts, implying that XKCM1 acts to destabilize microtubules. Studies using the purified enzyme showed that it was capable of promoting microtubule catastrophes in an ATP-dependent manner (Desai et al. submitted). This result was a landmark in microtubule motor studies, showing definitively for the first time that motor-like molecules can affect the behavior of the microtubules to which they bind. The molecular mechanism by which XKCM1 acts to induce end-wise microtubule disassembly is currently the subject of active investigation.

Proteins affecting filament number: MT severing and nucleation

Xenopus extracts have brought about the characterization of proteins which affect other notable aspects of microtubule behavior. These proteins modulate bulk microtubule behavior by affecting the number of microtubule ends available to shrink or grow. This second category of proteins includes a microtubule severing protein and a microtubule nucleating factor, both of which have been characterized in *Xenopus*.

Katanin. Katanin was identified as an activity which causes fragmentation of microtubules in *Xenopus* egg extracts (McNally and Thomas, 1998; Vale, 1991). When purified and cloned from sea urchin egg extracts, it was found to be a heterodimeric molecule, composed of a p60 and p80 subunit (Hartman et al., 1998; McNally and Vale, 1993). Katanin's severing activity is dependent on ATP hydrolysis but how the enzyme utilizes the energy of nucleotide hydrolysis to disrupt the microtubule lattice remains unknown.

Though several possibilities have been proposed, the in vivo function of microtubule severing has yet to be determined. Severing may be involved in the rapid disassembly of the microtubule cytoskeleton at the onset of mitosis. Also, release of microtubules from centrosomal nucleating sites has been documented in mitotic *Xenopus* extracts (Belmont et al., 1990). This observation may be important in understanding the phenomenon of polewards microtubule flux, which must allow disassembly at microtubule minus ends at spindle poles. Indeed, McNally et al. (1996) have recently shown katanin to be centrosome-associated.

λ-tubulin. Control of microtubule nucleation is another means by which cells can modulate cytoskeletal morphology. Due to the kinetic barrier to nucleation, microtubules do not nucleate spontaneously in the cytoplasm but assemble at distinct nucleating sites such as the centrosome. The microtubule-nucleating capacity of centrosomes has been shown to increase significantly during mitosis (Kuriyama and Borisy, 1981). *Xenopus* egg extracts have been a fruitful in vitro system for the study of centrosome microtubule nucleation, most notably in investigating the structure and function of γ-tubulin-containing complexes (Zheng, et al., 1995).

Since its discovery, γ-tubulin was hypothesized to play a role in microtubule nucleation (reviewed in Pereira and Schiebel, 1997). A homologue of alpha and beta tubulin, it localizes to sites of microtubule nucleation. Inhibition of γ-tubulin function in vivo or in extracts abolishes nucleation activity at centrosomes (Felix et al., 1994; Stearns et al., 1991; Stearns and Kirschner, 1994). Native γ-tubulin has been purified from Xenopus egg extracts in the form of a ring-shaped complex (γ-TuRC) (Zheng et al., 1995). In isolated centrosomes, similar ring structures containing γ-tubulin have been visualized within the pericentriolar material at the base of associated microtubules (Moritz et al., 1995). The purified γ-TuRC has been shown to promote microtubule assembly in vitro and the complex is found associated with microtubule minus ends (Zheng et al., 1995). These studies showed convincingly that γ-tubulin is a central component of microtubule nucleating structures and perhaps templates the assembly of tubulin subunits at these sites.

LINKING THE CELL CYCLE TO CHANGES IN MT DYNAMICS

In the absence of protein synthesis, addition of purified cdc2/cyclinB kinase to interphase *Xenopus* egg extracts is sufficient to induce mitotic MT dynamics (Verde et al., 1990). Inhibition of cdc2 kinase activity by the general kinase inhibitor DMAP completely inhibits this transition, indicating that phosphorylation is important for modulating microtubule behavior. Phosphatase inhibitors like okadaic acid and I-2 have also been used to show that dephosphorylating activities are also important. Different classes of phosphatases appear to play distinct roles in the cell-cycle regulation of MT dynamics. For example, protein phosphatase type 2A (PP2A) helps to modulate metaphase dynamics and protein phosphatase type 1 (PP1) seems to be involved in prophase and anaphase dynamics (Tournebize et al., 1997).

Purified MAP kinase has also been shown to be capable of inducing changes in microtubule dynamics similar to those elicited by addition of exogenous cdc2 kinase when added to *Xenopus* egg extracts. Inhibition of MAP kinase activity either by immunodepletion from extracts or via microinjection of inhibitory MAP kinase phosphatase into *Xenopus* tissue culture cells interfered with the mitotic spindle assembly checkpoint after treatment with nocodozole (Wang et al., 1997; Takenaka et al., 1997). The kinase substrates directly responsible for these changes in microtubule behavior and spindle organization remain to be elucidated.

Some microtubule-affecting proteins have been shown to be substrates for these kinases and phosphatases. Though many microtubule affectors have been characterized in *Xenopus* extracts, the cell cycle-dependent regulation of their activities has often turned out to be much more complicated than a simple "on/off" switch triggered by the absence or presence of phosphorylation.

MT stabilizing proteins

The activities of a number of neuronal MAPs have been shown to be regulated by phosphorylation in a cell-cycle dependent manner. Mitotic phosphorylation of XMAP230 appears to inhibit its ability to stabilize microtubules (Andersen et al., 1994). Many MAPs contain potential cdc2 phosphorylation sites and purified cdc2 kinase has been shown to phosphorylate a number of these in vitro. However, the effects of cdc2-cyclin kinase on MT dynamics is likely to involve additional downstream signaling molecules. For example, MAP kinase has also been shown to target microtubule-associated proteins and, like cdc2/cyclinB kinase, its addition to interphase *Xenopus* extracts can induce mitotic MT dynamics (Gotoh et al., 1991).

The newest players in cellular MAP regulation are the recently-identified MARK kinases. MARK kinase has been shown to phosphorylate several different MAPs in vitro and cause their dissociation from microtubules. Overexpression of MARK in tissue culture cells results in hyperphosphorylation of MAPs and dramatically disrupts the microtubule cytoskeleton (Drewes et al., 1997). A *Xenopus* homologue has not yet been identified.

Proteins which affect MT dynamics

Op18. The cell cycle-regulated phosphorylation of Op18 was intensely studied even before its role in modulating microtubule dynamics was discovered. During mitosis, Op18 is phosphorylated at multiple residues, including two cdk2 consensus sites. Belmont, et al. (1996) postulated that this catastrophe factor might be activated by mitotic phosphorylation, leading to increased catastrophe rates and the establishment of mitotic MT dynamics. This model was consistent with the increase in Op18 expression and phosphorylation seen in rapidly dividing tumor cells.

Since then, however, work on Op18 has led to a different perspective on its cell cycle regulation. Studies in human tissue culture cells indicate that cdk-mediated serine phosphorylation, rather than activating Op18, actually inhibits its microtubule destabilization activity (Marklund et al., 1996). This implies, paradoxically, that this catastrophe factor is highly phosphorylated and therefore inactive during mitosis. Two other serines which are phosphorylated by an unidentified kinase could, in theory, modulate or antagonize the effect of cyclin-dependent kinase modifications; however, recent evidence seems to indicate that Op18 is not in fact a major regulator of global MT dynamics in mitosis. For example, depletion of Op18 from mitotic egg extracts induces only a slight decrease in catastrophe rate, certainly not to interphase levels (Tournebize et al., 1997).

Andersen et al. (1997a) propose that local inactivation of Op18 near chromosomes might promote microtu-

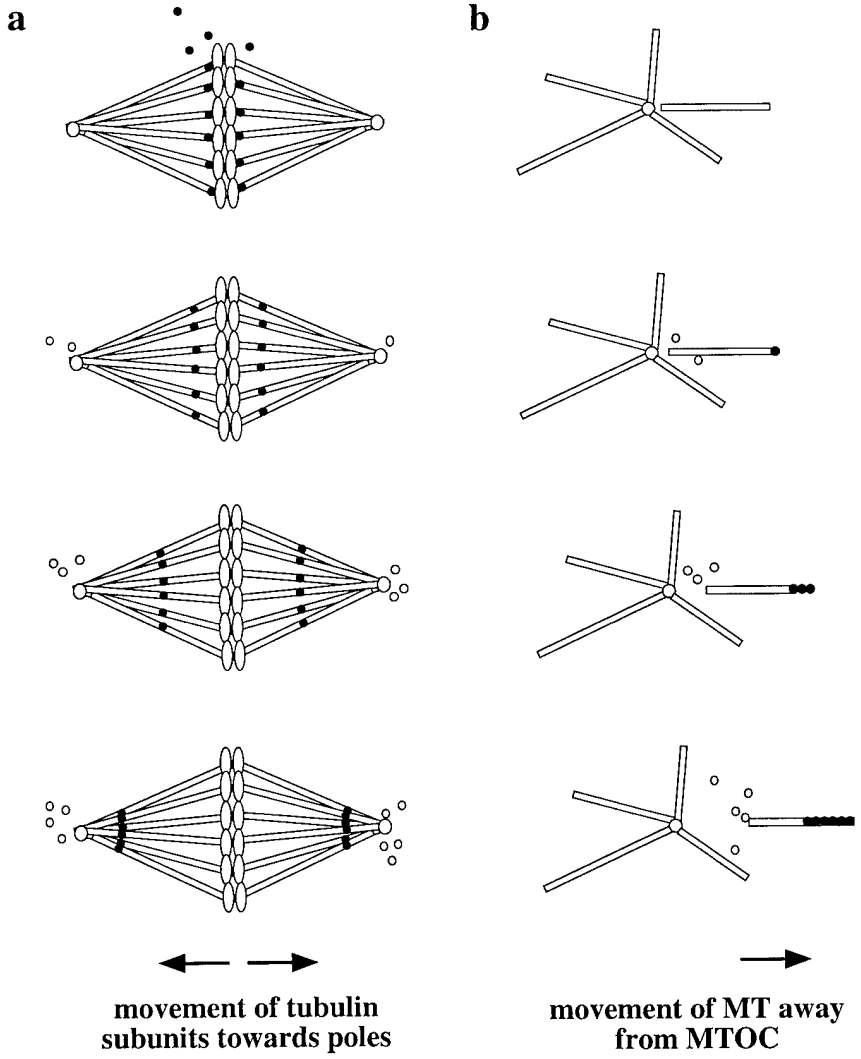

Fig. 3. Poleward microtubule flux (a) versus microtubule treadmilling (b). **(a)** Tubulin subunits of spindle microtubules move poleward over time. Net polymerization at MT plus ends is coordinated with net depolymerization at MT minus ends at spindle poles. Note that tubulin subunits move poleward (dark circles) and MT ends appear fixed; force is required to translocate the MT lattice toward the pole. **(b)** The microtubule on the right side of this interphase array has been released from its MTOC. This particular free microtubule undergoes plus-end polymerization and minus-end depolymerization. Tubulin subunits remain stationary and, due to shrinkage of the minus end and growth of the plus end, the microtubule translocates toward the cell periphery, in the direction of polymerization.

bule-chromatin interactions during spindle assembly. Hyperphosphorylation of Op18 was shown to be dependent on the presence of chromatin; however, the effect of this hyperphosphorylation on MT dynamics has not been clearly demonstrated. This chromatin-induced hyperphosphorylation may be due to a chromatin-associated kinase; alternatively, the chromatin could contain a factor which inhibits Op18 dephosphorylation. In support of the latter, Op18 hyperphosphorylation was also shown to be induced, in the absence of chromatin, by addition of 0.5 uM okadaic acid. This concentration of okadaic acid inhibits type 2A phosphatases but not type 1 phosphatases, implying that PP2A may mediate chromatin-induced inhibition of Op18.

This is not the only downstream effect of okadaic acid. Addition of okadaic acid to spindle assembly reactions resulted in abnormal spindles with very long microtubules–an effect not seen with Op18 depletion (Tournebize et al., 1997). Okadaic acid may inhibit another phosphatase important for MT dynamics or, alternatively, PP2A may control more than one microtubule regulator.

XKCM1. XKCM1 is a phosphoprotein, but it has not yet been determined whether this phosphorylation differs between interphase and mitotic extracts nor if the catastrophe-inducing activity of XKCM1 is cell cycle-regulated (Walczak, unpublished results). Baculovirus-expressed XKCM1 protein used in the in vitro experiments characterizing the enzyme's activity was purified predominantly from interphase cells, suggesting that XKCM1 is capable of promoting microtubule destabilization throughout the cell cycle (Desai and Walczak, unpublished results). If so, it is possible that microtubules are somehow less susceptible to XKCM1-mediated destabilization in interphase than in mitosis. For example, the association of MAPs may inhibit binding of XKCM1 to interphase microtubules or stabilize microtubules against XKCM1 activity.

While XKCM1 is clearly a major promoter of MT catastrophe, it has not been shown whether immunodepletion from mitotic extracts is sufficient to reduce the rate of catastrophe down to interphase levels. XKCM1 may have a more specific role in mitosis, controlled by its localization. For both XKCM1 and its

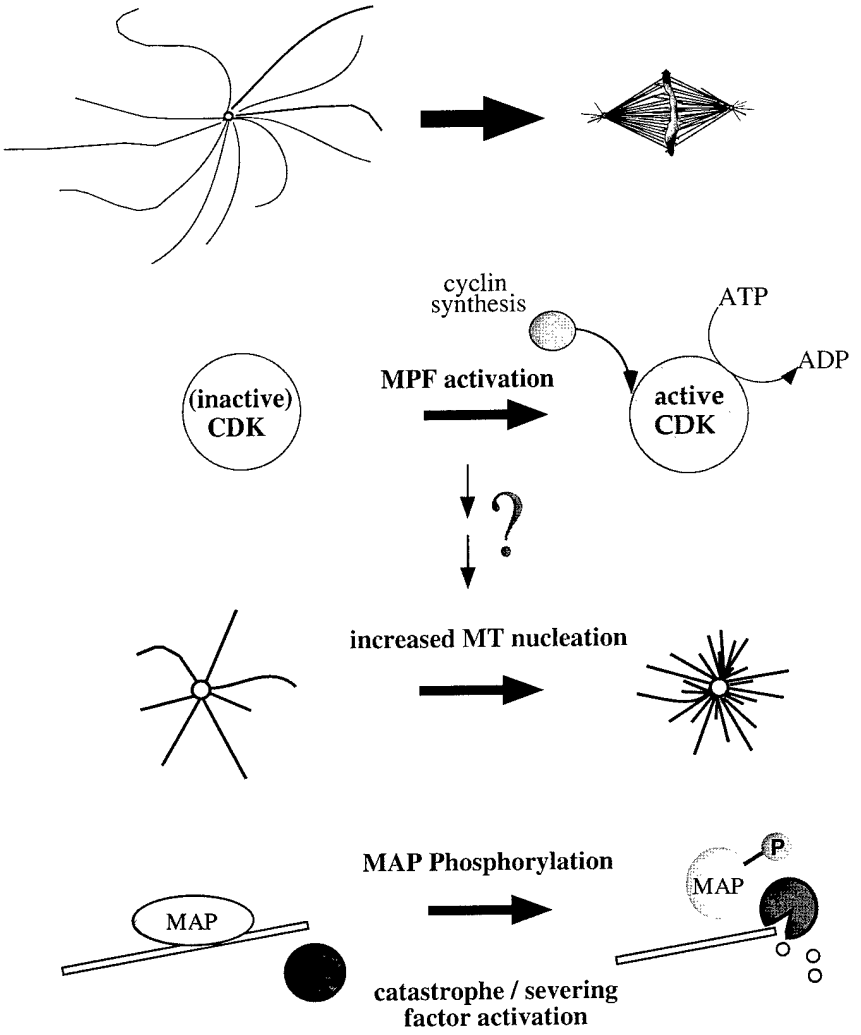

Fig. 4. Overview of several molecular mechanisms involved in changing microtubule morphology/dynamics from interphase to mitosis. The onset of mitosis requires activation of cyclin-dependent kinases, which directly or indirectly participate in the activation of nucleation-promoting factors, the inactivation of MT-stabilizing MAPs, and the induction of catastrophe factors, as well as other proteins which may affect MT dynamics.

human homologue MCAK, a fraction of the protein appears to localize to kinetochores (Wordeman and Mitchison, 1995). It is interesting to speculate that this protein may function to promote microtubule disassembly at kinetochores during anaphase and/or be involved in mediating interactions between kinetochores and microtubules (Maney, et al., 1998).

Other types of microtubule behavior

Three types of microtubule behavior that do not fall strictly into the classic categories of MT dynamics were described earlier: microtubule nucleation, microtubule severing, and poleward microtubule flux. Though little is known about the cell-cycle regulation of these activities, there is evidence to support the existence of such regulation.

Microtubule nucleation. Ring-shaped complexes containing γ-tubulin are now widely accepted to be microtubule nucleation sites at the centrosome. The increase in microtubule number at the centrosome during mitosis may be due to an increase in the number of these sites or regulation of their microtubule-nucleating activity. There is no evidence to date distinguishing between these two possibilities.

Microtubule severing. Katanin, the most well-characterized of the three known microtubule-severing proteins, is postulated to be cell-cycle regulated; however, there is little evidence to support this (Vale, 1991). Determination of its regulation may give insight into its physiological function. Microtubule severing could help to increase the number of microtubules in mitosis by increasing the number of ends available for polymerization; alternatively, severing could promote rapid disassembly of microtubules in prophase by increasing the number of ends available for depolymerization. MT severing has also been postulated to be involved in the release of microtubules from centrosomes (McNally and Thomas, 1998).

Poleward microtubule flux. Poleward flux, the coordinated movement of tubulin subunits within spindle microtubules toward spindle poles, requires three events: net polymerization at microtubule plus ends, net depolymerization at microtubule minus ends, and translocation of the microtubule lattice toward the

poles (Fig. 3) (Mitchison, 1989). Poleward flux appears to be a cell-cycle regulated phenomenon, though this has been examined in a limited number of cell types. In mitotic spindles of somatic cells, microtubule bundles connecting chromosomes to spindle poles (kinetochore MTs) exhibit poleward flux (Mitchison and Salmon, 1992). In mitotic *Xenopus egg* extracts, bipolar spindles as well as simpler centrosome and/or chromatin-free structures have been observed to exhibit poleward flux (Sawin and Mitchison, 1991; Sawin and Mitchison, 1994). Poleward flux does not appear to exist in interphase microtubule arrays, though it is technically more difficult to detect poleward flux in sparse interphase structures.

In several types of interphase cells, a similar but distinct phenomenon called "microtubule treadmilling" has recently been observed (Fig. 3) (Rodionov and Borisy, 1997). Microtubules which are released from the centrosome appear to translocate towards the cell periphery by a "treadmilling" mechanism, undergoing net polymerization at their plus ends (distal to the centrosome) and net depolymerization at their minus ends (proximal to the centrosome) (Waterman-Storer and Salmon, 1997). In these cases, microtubules still attached to centrosomes do not seem to exhibit poleward flux.

It is not known whether treadmilling and poleward flux occur by similar mechanisms; no molecular components responsible for either phenomena have been identified. Treadmilling is a single microtubule event whereas flux is a population dynamic; in treadmilling, the microtubule is free and translocates in the direction of polymerization whereas in poleward flux microtubules are fixed within a complex structure and tubulin subunits move toward the pole (Fig. 3). However, they do have one element in common: minus end dynamics. The minus ends of centrosome-anchored microtubules in interphase appear to be stably capped and do not exhibit any dynamic behavior. The minus-end depolymerization seen in both treadmilling and poleward flux indicates that these microtubule ends must be free to depolymerize, even those in the mitotic spindle. In fact, EM studies of mitotic spindles in several cell types have shown that many spindle microtubules do not terminate in the pericentriolar material (Mastronarde et al., 1993). MT minus ends have been described as the "dark side of microtubule dynamics" (Desai and Mitchison, 1997). Most research on MT dynamics, especially in vivo, has focused on MT plus ends; much less is known about the dynamics and regulation of minus ends, which are difficult to visualize. It is now clear that insight into minus end dynamics, particularly at the centrosome, will be crucial for understanding complex microtubule behavior in cells.

CONCLUSION

The behavior of microtubules in vivo differs significantly from the dynamics of pure tubulin in vitro. An elaborate system of protein modulators exists to regulate MT dynamics both temporally (throughout the cell cycle) and spatially (in different parts of the cell). During mitosis, for example, specific subpopulations of microtubules (astral or cytoplasmic microtubules, spindle microtubules, kinetochore microtubules, and interzone microtubules) behave very differently from each other. Why does the cell expend considerable energy and employ so many proteins to maintain this complex, dynamic microtubule cytoskeleton?

We can only speculate on the biological functions of dynamic instability in vivo. This unique polymer behavior may facilitate the rapid rearrangement of microtubules during the interphase to mitosis transition. Dynamic instability has also been proposed to increase the efficiency by which microtubules probe cytoplasmic space (Holy and Leibler, 1994); this would be particularly important during mitosis, when microtubules must rapidly find and capture very small target zones, the kinetochores of individual chromosomes. Disruption of MT dynamics in many cell types will trigger mitotic arrest even after kinetochore capture, indicating a function for dynamic instability in later stages of mitosis. Types of MT dynamics like poleward flux and inhibition of plus end polymerization appear to assist in the segregation of chromosomes at anaphase. It is likely that MT dynamics play an important role in other processes which have yet to be identified.

Many complex in vivo MT dynamics can be reconstituted in *Xenopus* egg extracts, allowing the characterization of a number of important microtubule-affecting proteins. We have described a few of these proteins and recent progress made toward investigating their spatial and temporal regulation (Fig. 4). Through this kind of work, which dissects the molecular mechanisms behind different types of MT dynamics, we understand the roles of these dynamics in specific subcellular processes; only then will we begin to answer the question, "Why dynamic instability?"

ACKNOWLEDGMENTS

The authors thank Arshad Desai and Jack Taunton for help in writing and editing this manuscript; and Joel Hiza, Lennie Feldman, Justin Yarrow, Terry Lechler, and Aneil Mallavarapu for advice and support. We also thank Tim Mitchison and the rest of the Mitchison lab for scientific discussions that were an important basis for our views of this field.

REFERENCES

Andersen SS, Ashford AJ, Tournebize R, Gavet O, Sobel A, Hyman AA, Karsenti E. 1997a. Mitotic chromatin regulates phosphorylation of Stathmin/Op18. Nature 389:640–643.

Andersen SS, Buendia B, Dominguez JE, Sawyer A, Karsenti E. 1994. Effect on microtubule dynamics of XMAP230, a microtubule-associated protein present in Xenopus laevis eggs and dividing cells. J Cell Biol 127:1289–1299.

Andersen SS, Karsenti E. 1997b. XMAP310: a Xenopus rescue-promoting factor localized to the mitotic spindle. J Cell Biol 139:975–983.

Barton N, Goldstein LSB. 1996. Going mobile: microtubule motors and chromosome segregation. Proc Natl Acad Sci USA 93:1735–1742.

Belmont LD, Hyman AA, Sawin KE, Mitchison TJ . 1990. Real-time visualization of cell cycle-dependent changes in microtubule dynamics in cytoplasmic extracts. Cell 62:579–589.

Belmont L, Mitchison TJ, Deacon H. 1996. Catastrophic revelations about Op18/stathmin. Trends Biochem Sci 21:197–198.

Belmont LD, Mitchison TJ. 1996. Identification of a protein that interacts with tubulin dimers and increases the catastrophe rate of microtubules. Cell 84:623–631.

Cassimeris L. 1993. Regulation of microtubule dynamic instability. Cell Motil Cytoskeleton 26:275–281.

Cassimeris L, Pryer NK, Salmon ED. 1988. Real-time observations of

microtubule dynamic instability in living cells. J Cell Biol 107:2223–2231.
Charrasse S, Schroeder M, Gauthier-Rouviere C, Ango F, Cassimeris L, Gard DL, Larroque C. 1998. The TOGp protein is a new human microtubule-associated protein homologus to the *Xenopus* XMAP215. J Cell Sci 111:1371–1383.
Desai A, Maddox PS, Mitchison TJ, Salmon ED. 1998. Anaphase A chromosome movement and poleward spindle microtubule flux occur at similar rates in Xenopus extract spindles. J Cell Biol 141:703–713.
Desai A, Mitchison TJ. 1997. Microtubule polymerization dynamics. Annu Rev Cell Dev Biol 13:83–117.
Desai A, Murray A, Mitchison TJ, Walczak CE. 1998. The use of Xenopus egg extracts to study mitotic spindle assembly and function in vitro. Meth in Cell Biol. 61:385–412.
Desai A, Verma S, Mitchison TJ, Walczak CE. 1999. Kin I Kinesins are microtubule-destabilizing enzymes. Cell 96:69–78.
Drechsel DN, Hyman AA, Cobb MH, Kirschner MW. 1992. Modulation of the dynamic instability of tubulin assembly by the microtubule-associated protein tau. Mol Biol Cell 3:1141–1154.
Drewes G, Biernat J, Preuss U, Mandelkow EM. 1997. MARK, a novel family of protein kinases that phosphorylate microtubule-associated proteins and trigger microtubule disruption. Cell 89:297–308.
Felix MA, Antony C, Wright M, Maro B. 1994. Centrosome assembly in vitro: role of gamma-tubulin recruitment in Xenopus sperm aster formation. J Cell Biol 124:19–31.
Gard DL, Kirschner MW. 1987. A microtubule-associated protein from Xenopus eggs that specifically promotes assembly at the plus-end. J Cell Biol 105:2203–2215.
Gelfand VI, Bershadsky AD. 1991. Microtubule dynamics: mechanism, regulation, and function. Annu Rev Cell Biol 7:93–116.
Gliksman NR, Parsons SF, Salmon ED. 1992. Okadaic acid induces interphase to mitotic-like microtubule dynamic instability by inactivating rescue. J Cell Biol 119:1271–1276.
Gliksman NR, Skibbens RV, Salmon ED. 1993. How the transition frequencies of microtubule dynamic instability (nucleation, catastrophe, and rescue) regulate microtubule dynamics in interphase and mitosis: analysis using a Monte Carlo computer simulation. Mol Biol Cell 4:1035–1050.
Gotoh Y, Nishida E, Matsuda S, Shiina N, Kosako H, Shiokawa K, Akiyama, T, Ohta, K, Sakai H. 1991. In vitro effects on microtubule dynamics of purified Xenopus M phase- activated MAP kinase. Nature 349:251–254.
Hartman JJ, Mahr J, McNally K, Okawa K, Iwamatsu A, Thomas S, Cheesman, S, Heuser J, Vale RD, McNally FJ . 1998. Katanin, a microtubule-severing protein, is a novel AAA ATPase that targets to the centrosome using a WD40-containing subunit. Cell 93:277–287.
Hill TL. 1985. Theoretical problems related to the attachment of microtubules to kinetochores. Proc Natl Acad Sci USA 82:4404–4408.
Holy TE, Leibler S. 1994. Dynamic instability of microtubules as an efficient way to search in space. Proc Natl Acad Sci USA 91:5682–5685.
Inoue S, Salmon ED. 1995. Force generation by microtubule assembly/disassembly in mitosis and related movements. Mol Biol Cell 6:1619–1640.
Jourdain L, Curmi P, Sobel A, Pantaloni D, Carlier MF. 1997. Stathmin: a tubulin-sequestering protein which forms a ternary T2S complex with two tubulin molecules. Biochemistry 36:10817–10821.
Kuriyama R,d Borisy GG. 1981. Microtubule-nucleating activity of centrosomes in Chinese hamster ovary cells is independent of the centriole cycle but coupled to the mitotic cycle. J Cell Biol 91:822–826.
Lohka MJ, Hayes MK, Maller JL. 1988. Purification of maturation-promoting factor, an intracellular regulator of early mitotic events. Proc Natl Acad Sci USA 85:3009–3013.
Maney T, Hunter AW, Wagenback M, Wordeman L. 1998. Mitotic centromere-associated kinesin is important for anaphase chromosome segregation. J Cell Biol 142:787–801.
Marklund U, Larsson N, Gradin HM, Brattsand G, Gullberg M. 1996. Oncoprotein 18 is a phosphorylation-responsive regulator of microtubule dynamics. Embo J 15:5290–5298.
Mastronarde DN, McDonald KL, Ding R, McIntosh JR. 1993. Interpolar spindle microtubules in PTK cells. J Cell Biol 123:1475–1489.
McNally FJ. 1996. Modulation of microtubule dynamics during the cell cycle. Curr Opin Cell Biol 8:23–29.
McNally FJ, Okawa K, Iwamatsu A, Vale RD . 1996. Katanin, the microtubule-severing ATPase, is concentrated at centrosomes. J Cell Sci 109:561–567.
McNally FJ, Thomas S. 1998. Katanin is responsible for the M-phase microtubule-severing activity in Xenopus eggs. Mol Biol Cell 9:1847–1861.
McNally FJ, Vale RD. 1993. Identification of katanin, an ATPase that severs and disassembles stable microtubules. Cell 75:419–429.
Mitchison T, Kirschner M. 1984. Dynamic instability of microtubule growth. Nature 312:237–242.
Mitchison TJ. 1989. Polewards microtubule flux in the mitotic spindle: evidence from photoactivation of fluorescence. J Cell Biol 109:637–652.
Mitchison TJ, Salmon ED. 1992. Poleward kinetochore fiber movement occurs during both metaphase and anaphase-A in newt lung cell mitosis. J Cell Biol 119:569–582.
Moritz M, Braunfeld MB, Sedat JW, Alberts B, Agard DA. 1995. Microtubule nucleation by gamma-tubulin-containing rings in the centrosome. Nature 378:638–640.
Murray AW. 1991. Cell cycle extracts. Meth. Cell Biol 36:581–605.
Parsons SF, Salmon ED. 1997. Microtubule assembly in clarified Xenopus egg extracts. Cell Motil Cytoskeleton 36:1–11.
Pereira G, Schiebel E. 1997. Centrosome-microtubule nucleation. J Cell Sci 110:295–300.
Pryer NK, Walker RA, Skeen VP, Bourns BD, Soboeiro MF, Salmon ED. 1992. Brain microtubule-associated proteins modulate microtubule dynamic instability in vitro. Real-time observations using video microscopy. J Cell Sci 103:965–976.
Rodionov VI, Borisy GG. 1997. Microtubule treadmilling in vivo. Science 275:215–218.
Salmon ED, Leslie RJ, Saxton WM, Karow ML, McIntosh JR. 1984. Spindle microtubule dynamics in sea urchin embryos: analysis using a fluorescein-labeled tubulin and measurements of fluorescence redistribution after laser photobleaching. J Cell Biol 99:2165–2174.
Sawin KE, Mitchison TJ. 1991. Poleward microtubule flux in mitotic spindles assembled in vitro. J Cell Biol 112:941–954.
Sawin KE, Mitchison TJ. 1994. Microtubule flux in mitosis is independent of chromosomes, centrosomes, and antiparallel microtubules. Mol Biol Cell 5:217–226.
Saxton WM, Stemple DL, Leslie RJ, Salmon ED, Zavortink M, McIntosh JR. 1984. Tubulin dynamics in cultured mammalian cells. J Cell Biol 99:2175–2186.
Sobel A. 1991. Stathmin: a relay phosphoprotein for multiple signal transduction? Trends Biochem Sci 16:301–305.
Stearns T. 1995. Green fluorescent protein. The green revolution. Curr Biol 5:262–264.
Stearns T, Evans L, Kirschner M. 1991. Gamma-tubulin is a highly conserved component of the centrosome. Cell 65:825–836.
Stearns T, Kirschner M. 1994. In vitro reconstitution of centrosome assembly and function: the central role of gamma-tubulin. Cell 76:623–637.
Tanenaka K, Gotoh Y, Nishida E. 1997. MAP kinase is required for the spindle assembly checkpoint but is dispensable for the normal M-phase entry and exit in *Xenopus* egg cell cycle extracts. J Cell Biol 136:1091–1097.
Tournebize R, Andersen SS, Verde F, Doree M, Karsenti E, Hyman AA. 1997. Distinct roles of PP1 and PP2A-like phosphatases in control of microtubule dynamics during mitosis. Embo J 16:5537–5549.
Vale RD. 1991. Severing of stable microtubules by a mitotically activated protein in Xenopus egg extracts. Cell 64:827–839.
Vale RD, Fletterick R J. 1997. The design plan of kinesin motors. Annu Rev Cell Dev Biol 13:745–777.
Vasquez RJ, Gard DL, Cassimeris, L. 1994. XMAP from Xenopus eggs promotes rapid plus end assembly of microtubules and rapid microtubule polymer turnover. J Cell Biol 127:985–993.
Verde F, Berrez JM, Antony C, Karsenti, E. 1991. Taxol-induced microtubule asters in mitotic extracts of Xenopus eggs: requirement for phosphorylated factors and cytoplasmic dynein. J Cell Biol 112:1177–1187.
Verde F, Dogterom M, Stelzer E, Karsenti, E, Leibler S. 1992. Control of microtubule dynamics and length by cyclin A- and cyclin B-dependent kinases in Xenopus egg extracts. J Cell Biol 118:1097–1108.
Verde F, Labbe JC, Doree M, Karsenti E. 1990. Regulation of microtubule dynamics by cdc2 protein kinase in cell-free extracts of Xenopus eggs. Nature 343:233–238.
Wadsworth P, Salmon ED. 1986. Analysis of the treadmilling model during metaphase of mitosis using fluorescence redistribution after photobleaching. J Cell Biol 102:1032–1038.

Walczak CE, Mitchison TJ, Desai A. 1996. XKCM1: a Xenopus kinesin-related protein that regulates microtubule dynamics during mitotic spindle assembly. Cell 84:37–47.

Walker RA, O'Brien ET, Pryer NK, Soboeiro MF, Voter WA, Erickson, H.P, Salmon ED. 1988. Dynamic instability of individual microtubules analyzed by video light microscopy: rate constants and transition frequencies. J Cell Biol 107:1437–1448.

Wang XM, Zhai Y, Ferrell JE. 1997. A role for mitogen-activated protein kinase in the spindle assembly checkpoint in XTC cells. J Cell Biol 137:433–443.

Waterman-Storer CM, Salmon ED. 1997. Microtubule dynamics: treadmilling comes around again. Curr Biol 7:R369–372.

Wordeman L, Mitchison TJ. 1995. Identification and partial characterization of mitotic centromere-associated kinesin, a kinesin-related protein that associates with centromeres during mitosis. J Cell Biol 128:95–104.

Zhai Y, Borisy, G.G. 1994. Quantitative determination of the proportion of microtubule polymer present during the mitosis-interphase transition. J Cell Sci 107:881–890.

Zhai Y, Kronebusch PJ, Borisy GG. 1995. Kinetochore microtubule dynamics and the metaphase-anaphase transition. J Cell Biol 131:721–734.

Zheng Y, Wong ML, Alberts B, Mitchison T. 1995. Nucleation of microtubule assembly by a gamma-tubulin-containing ring complex. Nature 378:578–583.

A model for the proposed roles of different microtubule-based motor proteins in establishing spindle bipolarity

Claire E. Walczak*, Isabelle Vernos†, Timothy J. Mitchison‡, Eric Karsenti† and Rebecca Heald§

Background: In eukaryotes, assembly of the mitotic spindle requires the interaction of chromosomes with microtubules. During this process, several motor proteins that move along microtubules promote formation of a bipolar microtubule array, but the precise mechanism is unclear. In order to examine the roles of different motor proteins in building a bipolar spindle, we have used a simplified system in which spindles assemble around beads coated with plasmid DNA and incubated in extracts from *Xenopus* eggs. Using this system, we can study spindle assembly in the absence of paired cues, such as centrosomes and kinetochores, whose microtubule-organizing properties might mask the action of motor proteins.

Results: We blocked the function of individual motor proteins in the *Xenopus* extracts using specific antibodies. Inhibition of *Xenopus* kinesin-like protein 1 (Xklp1) led either to the dissociation of chromatin beads from microtubule arrays, or to collapsed microtubule bundles on beads. Inhibition of Eg5 resulted in monopolar microtubule arrays emanating from chromatin beads. Addition of antibodies against dynein inhibited the focusing of microtubule ends into spindle poles in a dose-dependent manner. Inhibition of *Xenopus* carboxy-terminal kinesin 2 (XCTK2) affected both pole formation and spindle stability. Co-inhibition of XCTK2 and dynein dramatically increased the severity of spindle pole defects. Inhibition of Xklp2 caused only minor spindle pole defects.

Conclusions: Multiple microtubule-based motor activities are required for the bipolar organization of microtubules around chromatin beads, and we propose a model for the roles of the individual motor proteins in this process.

Addresses: *Department of Cellular and Molecular Pharmacology, University of California, San Francisco, California 94143, USA. †Cell Biology Program, European Molecular Biology Laboratory, 69117 Heidelberg, Germany. ‡Department of Cell Biology, Harvard Medical School, Boston, Massachusetts 02115, USA. §Department of Molecular and Cell Biology, University of California, Berkeley, California 94720, USA.

Correspondence: Rebecca Heald
E-mail: heald@socrates.berkeley.edu

Received: **23 June 1998**
Accepted: **14 July 1998**

Published: **23 July 1998**

Current Biology 1998, 8:903–913
http://biomednet.com/elecref/0960982200800903

Background

In eukaryotes, the accurate segregation of chromosomes during cell division occurs on a complex apparatus called the spindle, whose assembly requires the interaction of chromosomes with microtubules, which form a bipolar array. The antiparallel organization of microtubules into two poles is essential for the physical separation of chromosomes to two daughter cells during anaphase. The mechanisms and principles behind spindle assembly have begun to be elucidated (reviewed in [1,2]). Upon entry into mitosis, the dynamics of tubulin polymerization are modulated to allow dissolution of the interphase microtubule array and selective stabilization of microtubules around chromosomes (reviewed in [3]). In addition to changes in microtubule dynamics, mechanical forces generated by microtubule-based motor proteins are thought to play an important role in generating the spindle structure. The motor protein cytoplasmic dynein and other motor proteins from at least seven families of kinesin-like proteins (KLPs) have been localized to the mitotic spindle [4–8]. Motor proteins use the energy of ATP hydrolysis to move along microtubules in a unidirectional manner, transporting spindle cargo such as chromosomes or other microtubules toward either the plus or minus end of the microtubule polymer. The proposed functions of motors include driving centrosome separation and chromosome movement, maintaining a force that holds the spindle together, driving poleward microtubule flux, and controlling microtubule dynamics within the spindle. The precise roles of individual motors are poorly understood, however, and it is not clear how multiple motor activities are integrated to form the bipolar structure of the spindle.

Precise interpretation of how motors function in spindle assembly is complicated by the existence of other microtubule-organizing forces. In most cells, microtubules grow from focal nucleation centers, such as centrosomes, which define the polarity of the microtubules and determine the sites of spindle pole formation. In the presence of a single centrosome, or unseparated centrosomes, a monopolar spindle will form even if microtubule motor functions have not been perturbed [9–12]. Centrosomes therefore dominate microtubule organization and make it problematic to distinguish the motor activities required for centrosome

separation from those that are necessary to form a bipolar antiparallel microtubule array.

To avoid the complication of focal microtubule nucleation sites, we decided to study the roles of different motor proteins during spindle assembly around DNA-coated beads in extracts from *Xenopus* eggs. In this system, as in female meiosis of most animal species, bipolar spindles form in the absence of centrosomes by the self-organization of microtubules growing randomly around chromatin [13]. Because this system requires sorting of microtubules according to their polarity, it is highly dependent on the activities of motor proteins to generate an antiparallel bipolar array. To address the general roles of motor proteins in determining the bipolar arrangement of microtubules around chromatin beads, we undertook a comprehensive analysis by inhibiting the functions of motor proteins individually and in combination. To accomplish this, we used specific antibodies to immunodeplete the motor protein, or to inhibit its function by adding the antibody directly to the extract. Except where noted, antibody addition mimicked immunodepletion, indicating that we are blocking the function of the motor protein by both techniques.

Multiple *Xenopus* KLPs that localise to the spindle have been cloned — including Eg5, *Xenopus* kinesin-like proteins 1 and 2 (Xklp1 and Xklp2) and *Xenopus* carboxy-terminal kinesin 2 (XCTK2) — and the functions of these motors have been characterized using centrosome-directed spindle assembly around sperm nuclei [14–21]. In addition, cytoplasmic dynein has been shown to be required for spindle pole formation in *Xenopus* [12,22]. Here, using the chromatin bead spindle assembly assay, we show evidence that both Eg5 and Xklp1 are critical for spindle bipolarity. Eg5 seems to provide a sorting activity that generates an antiparallel array, whereas Xklp1 appears to maintain the interactions between chromatin and microtubules that are required for extending spindle poles. Whereas dynein seems to be the dominant motor that focuses microtubule minus ends into spindle poles, XCTK2 appears to contribute to the organization of spindle poles and to spindle integrity. Xklp2 inhibition did not have a significant effect on the bipolar microtubule organization around chromatin beads, indicating that the main role of this motor is probably in processes that require centrosome separation.

Results

We present here an analysis of the function of different microtubule motor proteins in spindle assembly around chromatin beads. For simplicity, each motor is presented in a separate figure, which includes an indication of the domain structure, the localization pattern on chromatin bead spindles, the different spindle structures seen upon inhibition of the motor, quantification of these structures, and a proposed model for how the motor functions in spindle assembly.

Xklp1 mediates chromatin–microtubule interactions and contributes to spindle pole extension

Xklp1 was identified as a chromosomally localized motor with an amino-terminal motor domain [18]. Sucrose density gradient sedimentation, gel filtration chromatography and immunoprecipitation experiments revealed that Xklp1 is a dimer in solution and has no associated proteins (data not shown; Figure 1a). The mouse homologue, KIF4, has been shown to be plus-end-directed [23]. Disruption of Xklp1 during spindle assembly around *Xenopus* sperm nuclei by the addition of antibodies leads to a loss of microtubules in the central spindle and to spindle instability [18]. To identify a role for Xklp1 in spindle assembly around chromatin beads, we first determined the localization of the protein by immunofluorescence. Anti-Xklp1 antibodies strongly stained the beads (Figure 1b), indicating that distinct chromosomal sequences are not required for the localization of Xklp1, and that the plasmid DNA on the beads is sufficient to recruit Xklp1 from *Xenopus* egg extracts.

To test the role of Xklp1 in spindle assembly around chromatin beads, two different polyclonal antibodies raised against non-overlapping domains of Xklp1 were assayed for their effects. The first, Ab65, was raised against the tail domain of the protein. Addition of this antibody to extracts before the initiation of spindle assembly reactions resulted in a much lower proportion of bipolar structures than in control reactions (17% versus 85%; Figure 1e). In the presence of Ab65, monopolar spindles predominated, as well as bent bipolar structures and free monopolar structures lacking chromatin beads (Figure 1c,e). Visualization of the added antibody (secondary staining; Figure 1c) revealed staining on the beads and on microtubules, with an enrichment at the plus ends. These results suggested that Ab65 did not directly interfere with the bipolarity of spindles, but that it inhibited microtubule–chromatin interactions, causing spindle instability and dissociation of the beads from microtubule arrays. Addition of the second antibody, Ab03, which was raised against the neck and stalk region of Xklp1, resulted in a distinctly different effect. In approximately 90% of the structures examined, microtubule bundles formed around chromatin beads, but did not extend poles (Figure 1d,e). In this case, Xklp1 was immunolocalized only to the chromatin beads. A similar effect was observed when Xklp1 was depleted from spindle assembly reactions (data not shown).

Together, the results using anti-Xklp1 antibodies suggest that although both antibodies interfere with Xklp1 function, Ab03 does so more severely as its effect is similar to that of immunodepletion. Because the two antibodies are directed against different regions of Xklp1, it is possible

Figure 1

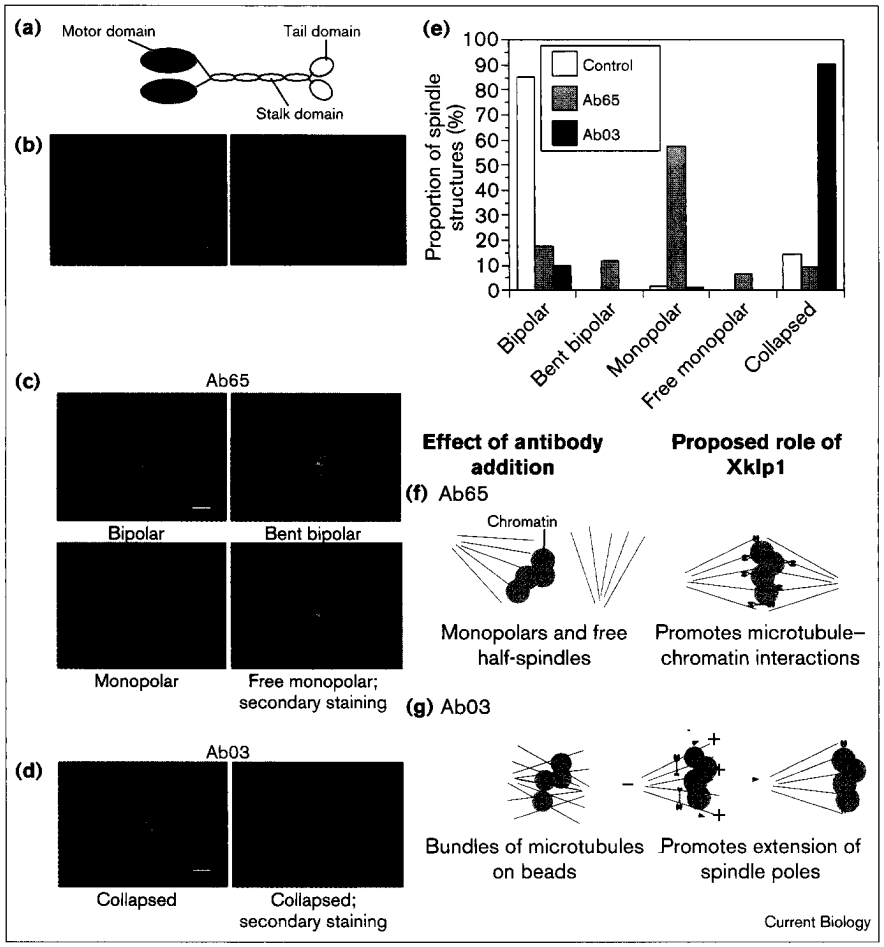

Xklp1 is involved in chromatin–microtubule interactions and spindle pole extension. **(a)** The domain structure of Xklp1. **(b)** Localization of Xklp1. The left-hand panel shows an overlay of a spindle stained for DNA (blue), microtubules (red) and the motor protein (green); the right-hand panel shows staining for the motor protein only. Overlap between the motor protein and the DNA appears aquamarine, and overlap between the motor protein and the microtubules appears yellow. **(c,d)** Representative images of the spindle structures that formed in the presence of one of two anti-Xklp1 antibodies: (c) Ab65 and (d) Ab03. 'Collapsed' indicates a collapsed microtubule array lacking poles. Staining was for DNA and microtubules only unless secondary staining is indicated, in which case FITC-conjugated secondary antibodies were used, showing that Ab65 decorated microtubule plus ends in a free monopolar spindle, and Ab03 decorated chromatin beads. **(e)** Quantification of the structures formed in spindle assembly reactions. More than 85% of the spindles were bipolar in the control reaction, which contained control immunoglobulin G (IgG) antibodies ($n = 607$, three separate experiments); addition of Ab65 yielded predominantly monopolar spindles and bent bipolar spindles ($n = 503$, three experiments); addition of Ab03 resulted in collapsed structures lacking spindle poles ($n = 485$, three experiments). **(f,g)** Two proposed models for Xklp1 function. (f) Because Ab65 caused dissociation of beads from spindle microtubules, Xklp1 is proposed to promote stable microtubule–chromatin interactions. (g) Ab03 addition resulted in microtubule bundles lacking poles, indicating a role for Xklp1 in extending spindle poles. By moving toward microtubule plus ends, Xklp1 would extend minus ends away from the beads. The bars are 10 μm.

that they interfere with Xklp1 function in different ways. Ab65 recognizes the tail domain and may interfere with the ability of Xklp1 to bind to chromatin, whereas Ab03 recognizes the neck and stalk region and may interfere with Xklp1 motor activity. A model consistent with these results is that Xklp1 is required for chromatin–microtubule interactions, and that this interaction is required both to extend spindle poles away from the chromatin beads, and to hold the structure together once it has formed (Figure 1f,g).

Eg5 is required for spindle bipolarity

Eg5 is a plus-end-directed motor that is a member of the bipolar kinesin family [14,17]. The *Drosophila* homologue has been shown to be tetrameric, with pairs of motor domains at opposite ends of the molecule (Figure 2a) [24]. Eg5 is also tetrameric in solution (data not shown). The bipolar kinesin family is conserved throughout evolution, and has been shown to play a role in spindle pole formation and separation [25–31]. In spindle assembly reactions containing *Xenopus* sperm DNA, inhibition of Eg5 causes spindle pole defects and results in 'rosette' structures with unseparated centrosomes in the center and microtubules extending radially to surrounding chromosomes [17].

We wondered whether Eg5 also played a role in spindle assembly in the absence of centrosomes. As in spindles assembled around *Xenopus* sperm nuclei, Eg5 was located throughout microtubules of chromatin bead spindles, showing an enrichment at spindle poles (Figure 2b). Immunodepletion of Eg5 or disruption of Eg5 activity by the addition of specific antibodies gave the same result (Figure 2c,d and data not shown); more than 95% of the spindle structures formed consisted of microtubules packed around chromatin beads, often extending outward in astral arrays. To determine the orientation of microtubules in these radial arrays, we immunostained the structures using antibodies against nuclear/mitotic apparatus

Figure 2

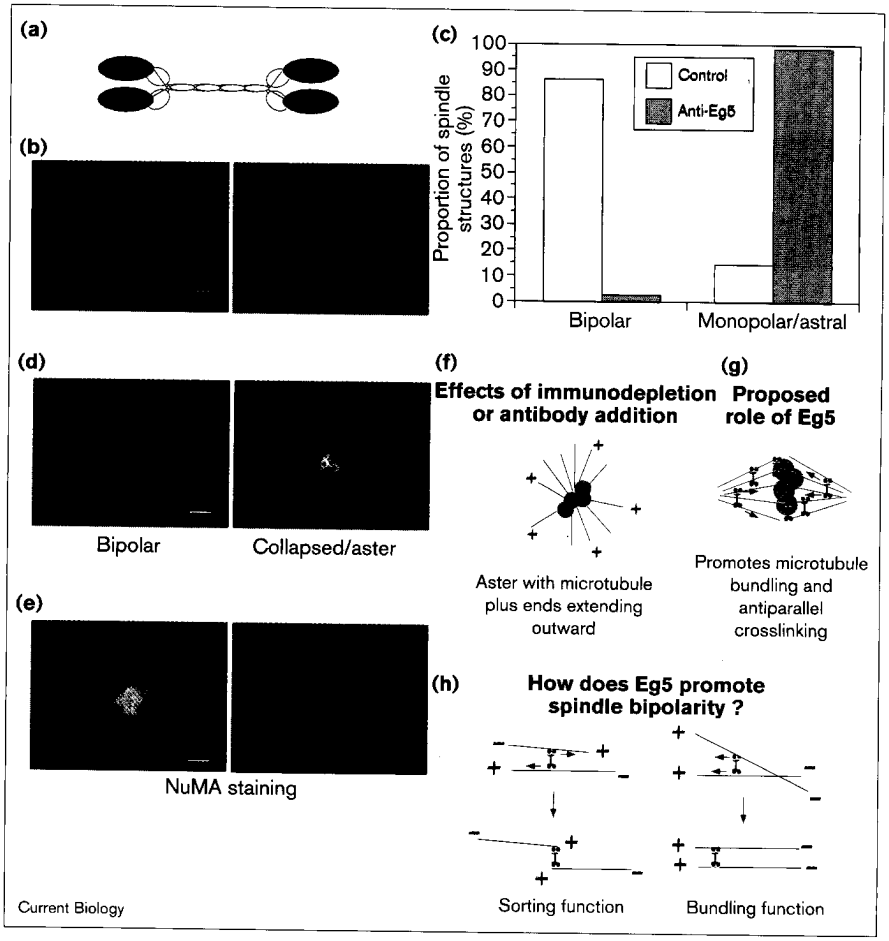

Eg5 is required for forming antiparallel microtubule arrays. Colors and immunofluorescence staining are as for Figure 1. **(a)** The structure of Eg5. **(b)** Localization of Eg5 by immunofluorescence. **(c)** Quantification of the spindle structures formed in the presence of anti-Eg5 antibody showed that there were few bipolar spindles. Instead, collapsed microtubule structures often extending astral microtubules formed on chromatin beads in the presence of anti-Eg5 antibodies ($n = 607$, three experiments for the control and $n = 556$, three experiments for Eg5 inhibition). **(d)** Representative fluorescence micrographs of a bipolar spindle and a collapsed aster that formed in the presence of anti-Eg5 antibody. Similar structures formed in extracts depleted of Eg5 (data not shown). **(e)** Immunostaining of the nuclear/mitotic apparatus protein (NuMA) revealed that it is enriched in the center of asters that formed in the presence of anti-Eg5 antibody. **(f–h)** Proposed model of Eg5 function. (f) In the absence of Eg5 function, asters form with microtubule plus ends extending distally from the chromatin beads. (g) We therefore propose that Eg5 crosslinks microtubules in spindles, bundles them, and sorts them into an antiparallel array. (h) Proposed model for how Eg5 might promote spindle bipolarity for microtubules in the same or in opposite orientations. The bars are 10 μm.

protein (NuMA) which has been shown to decorate the minus ends of microtubules at spindle poles and the centers of asters found in cells treated with dimethyl sulfoxide (DMSO) or taxol — two microtubule-stabilizing drugs [12,22,32,33]. NuMA was found associated with the microtubules where they came to a focus on the beads, indicating that microtubule plus ends are distal to the structures (Figure 2e). In addition, stable microtubule seeds, which have been shown previously to accumulate at foci of microtubule minus ends [13], also accumulated at the central focus of microtubules on the beads (data not shown). Eg5 disruption, therefore, appears to prevent the formation of antiparallel, bipolar arrays, yielding instead monopolar, astral arrays with microtubule plus ends extending outward (Figure 2f). This result indicates that in the absence of Eg5 function other motors still function to sort microtubule minus ends into pole-like structures.

How does Eg5 function in bipolar spindle assembly? It has been shown that microtubules growing around chromatin beads in the early stages of spindle assembly are in random orientations [13]. Because of its tetrameric, bipolar structure, Eg5 could function in two ways to promote spindle formation (Figure 2g,h). First, by crosslinking two microtubules that are in the same orientation and moving toward their plus ends, Eg5 would bundle the microtubules, thereby promoting formation of a spindle axis. Second, microtubules in opposite orientations would be pushed apart by Eg5, and thereby sorted into an antiparallel array.

Thus both Xklp1 and Eg5 are required for spindle formation around chromatin beads. These plus-end-directed motors have been proposed to function as sorting devices in establishing a bipolar array [6,34]. Our results indicate that neither motor is sufficient — Eg5 is required to form antiparallel microtubule arrays, but perhaps Xklp1-mediated interactions between microtubule plus ends and chromatin are required to form a spindle. This could explain why asters that form in the presence of DMSO or taxol are monopolar, despite the presence of Eg5 in the cytoplasm. Why is Xklp1 function insufficient to extend the single spindle pole formed when Eg5 is inhibited? We propose

Figure 3

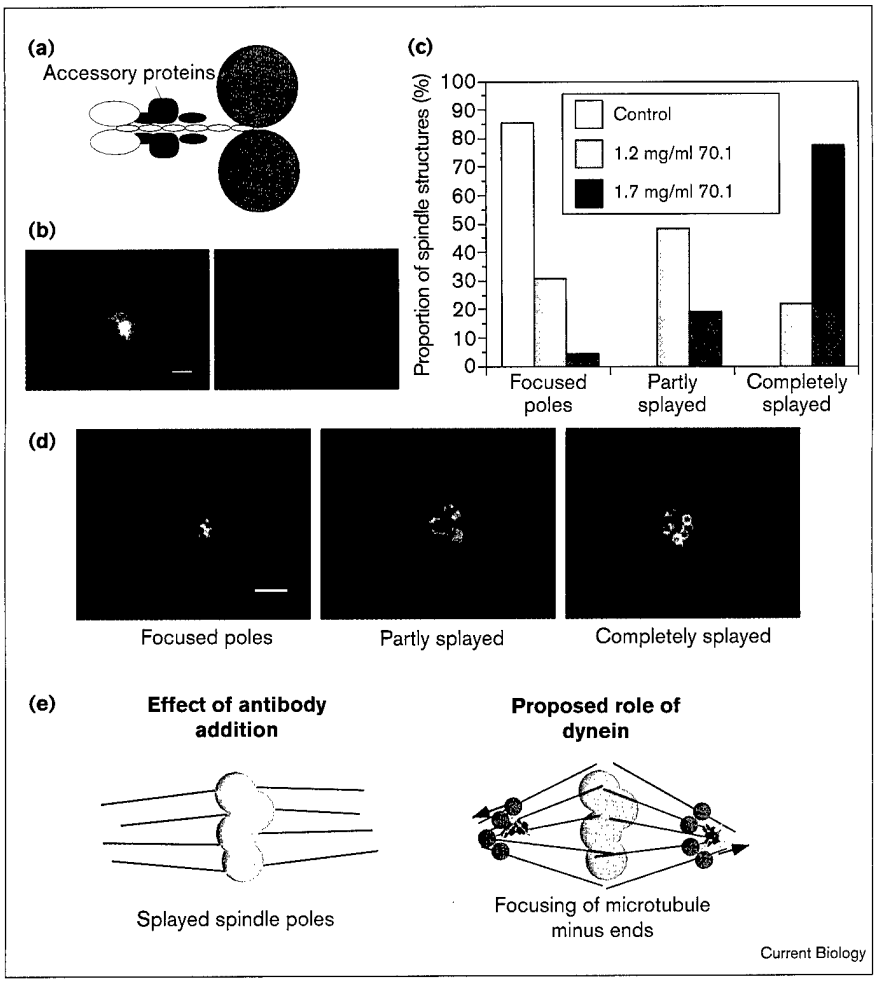

Dynein is required to focus spindle poles. Colors and immunofluorescence staining are as for Figure 1. **(a)** The structure of dynein and **(b)** its localization by immunofluoresence. Dynein is a large, multimeric minus-end-directed motor localized diffusely along spindle microtubules with an enrichment at spindle poles. The staining of the beads is due to autofluorescence of the beads which occurs at the long exposure time necessary to visualize the dynein staining. **(c)** Quantification of spindle pole structures formed in the presence of different amounts of antibody against the intermediate chain of dynein shows that 1.7 mg/ml antibody leads to completely splayed poles in 75% of the structures formed, whereas 1.2 mg/ml antibody has a weaker effect ($n = 607$, three experiments for control antibody addition; $n = 279$ for 1.2 mg/ml antibody and $n = 375$ for 1.7 mg/ml antibody, two experiments). **(d)** Representative micrographs of a normal bipolar spindle with focused poles, and partly and completely splayed spindle poles. **(e)** Proposed model for dynein function. In the absence of dynein activity, poles are loose and splayed. By crosslinking microtubules and moving toward their minus ends, dynein would function to focus spindle poles. The bars are 10 μm.

that the microtubule-bundling activity of Eg5 is required to form a bipolar axis, without which microtubules cannot effectively be sorted apart into two arrays. Alternatively, minus-end-directed motors such as dynein might dominate over Xklp1 activity in the absence of Eg5 function.

Dynein is essential for spindle pole formation

Cytoplasmic dynein is required to focus spindle poles, both in the presence and absence of centrosomes [12,13]. Dynein function in pole formation appears to depend on its interaction with the dynactin complex and the spindle pole protein NuMA [22,31,35] (T. Wittmann, H. Boleti, C. Antony, E.K. and I.V., unpublished observations). On the spindles assembled around chromatin beads, dynein is localized to the spindle poles (Figure 3b). As shown previously, in the presence of an antibody (70.1) against the intermediate chain of dynein, microtubule arrays formed that were centered around chromatin beads, but had frayed ends (Figure 3c,d) [13]. We show here that the severity of the defect depends on the amount of antibody added, with the maximum effect at about 1.7 mg/ml antibody. At this concentration, more than 75% of spindles had poles that were completely splayed. Addition of 1.2 mg/ml antibody also disrupted spindles, but approximately 50% of the structures contained poles that were only partially splayed and only 21% had poles that were completely splayed (Figure 3c,d). Despite the defect in the spindle poles that occurs when dynein function is blocked, the microtubules of these spindles are still organized into an antiparallel array [12]. These observations suggest both that Eg5 and Xklp1 still function to sort microtubules in the absence of dynein activity so that the minus ends of the microtubules are distal to the beads, and that the primary function of dynein is to focus microtubule minus ends into spindle poles (Figure 3e).

XCTK2 contributes to spindle integrity and pole formation

XCTK2 belongs to the minus-end-directed KinC family of kinesins and exists in a large complex with other non-motor subunits [20] (Figure 4a). Mutations in the *Drosophila* homologue, Ncd, result in spindle instability and spindle pole defects [36–39]. In *Saccharomyces*

Figure 4

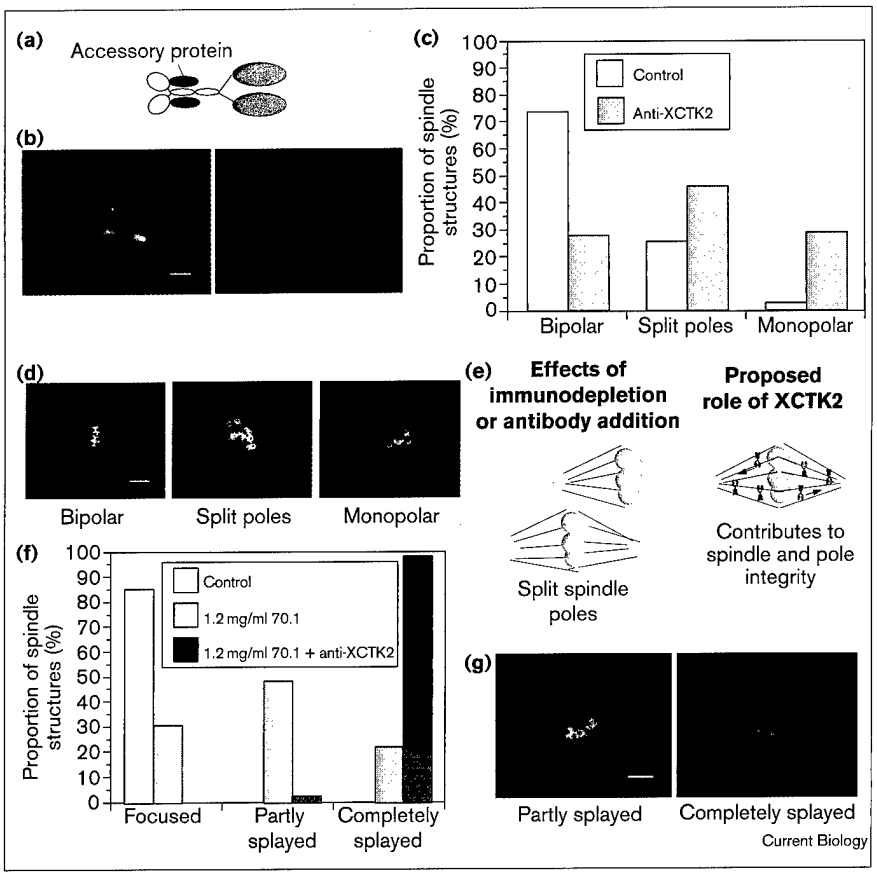

XCTK2 contributes to spindle integrity and pole formation. Colors and immunofluorescence staining are as for Figure 1. **(a)** The structure of XCTK2, a dimeric motor protein with the motor domain at the carboxyl terminus and which complexes with associated proteins. **(b)** Localization of XCTK2 by immunofluorescence. **(c)** Quantification of spindle structures formed in the presence of anti-XCTK2 antibodies shows a fourfold increase in monopolar spindles compared to control reactions, and an increase in the proportion of spindles with split poles ($n = 959$, five experiments for control antibody addition; $n = 973$, five experiments for anti-XCTK2 antibody addition). **(d)** Representative micrographs of a normal bipolar spindle, a monopolar spindle, and a spindle with split spindle poles. **(e)** Proposed model of XCTK2 function on the basis of its stabilizing effects on spindles and poles. XCTK2 might crosslink microtubules and move poleward, stabilizing microtubule bundles and contributing to the focusing of spindle poles. **(f)** Quantification of the spindle structures formed when both dynein and XCTK2 were inhibited ($n = 303$, two experiments). In a partially blocked dynein background, XCTK2 inhibition dramatically increased the proportion of completely splayed poles. **(g)** Representative micrographs of the effects of XCTK2 and dynein co-inhibition. The bars are 10 μm.

cerevisiae, *Schizosaccharomyces pombe* and *Aspergillus nidulans*, there exists an antagonistic force relationship between the KinC family members and the bipolar kinesins [40–42]. However, the precise function of KinC family members is unclear. In *Xenopus* egg extracts, inhibition of XCTK2 results in spindle instability whereas increasing the amount of XCTK2 promotes formation of bipolar spindles around sperm nuclei [20].

To further explore the role of XCTK2, we assessed its function in spindle assembly around chromatin beads. XCTK2 was found on chromatin bead spindle microtubules and enriched at spindle poles (Figure 4b), as it is on spindles formed around sperm DNA. Addition of antibodies to XCTK2 increased the proportion of monopolar spindles from 2% to 27%. Spindle pole structure was also affected, with almost twice the number of 'split' poles, which fail to form a single minus-end focus (Figure 4c,d). Similar results were obtained if XCTK2 was immunodepleted from extracts (data not shown). These results indicate that XCTK2 contributes to spindle integrity, and they are consistent with the previously proposed model that XCTK2 bundles microtubules, thereby promoting antiparallel microtubule interactions and bipolarity (Figure 4e) [20]. Our results also indicate a role for XCTK2 in pole formation in the absence of centrosomes.

In order to test whether XCTK2 functions in conjunction with dynein to form spindle poles, we tested the effects of XCTK2 inhibition in the presence of 1.2 mg/ml of the anti-dynein antibody 70.1, which by itself causes only partial splaying of spindle poles (Figures 3c,4g). Under these conditions, co-inhibition of XCTK2 caused a dramatic increase in the proportion of spindles with completely splayed poles, from 21.5% to 98%. Furthermore, the bipolar spindle axis was often distorted, as microtubules failed to form a single bundle (Figure 4f,g). Therefore, XCTK2 appears to have a pole-forming function partially redundant with that of dynein, and XCTK2 also appears to contribute to the integrity of the bipolar spindle.

Xklp2 plays a minor role in spindle assembly in the absence of centrosomes

Xklp2 is a dimeric plus-end-directed motor with an amino-terminal motor domain (Figure 5a) [21]. A mouse homologue has been identified using a PCR screen, but its function has not been addressed [43]. Studies using *Xenopus* sperm nuclei indicate that Xklp2 is required for

Figure 5

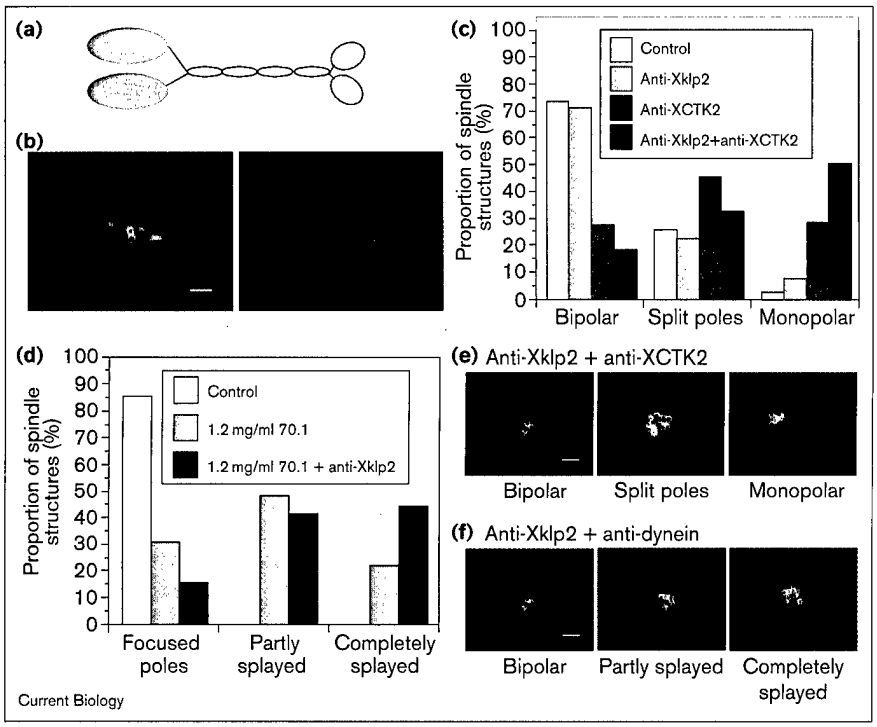

Xklp2 plays a subtle role in spindle assembly. Colors and immunofluorescence staining are as for Figure 1. **(a)** Xklp2 is a plus-end-directed, dimeric motor protein with the motor domain at its amino terminus. **(b)** Xklp2 antibodies added to extracts are revealed by secondary antibodies to localize throughout spindle microtubules. **(c)** Quantification of structures formed in the presence of anti-Xklp2 antibodies shows only minor effects on spindle integrity ($n = 959$, five experiments for control antibody addition). Co-inhibition of Xklp2 and XCTK2 caused an increase in monopolar spindles ($n = 594$, four experiments). **(d)** Co-inhibition of Xklp2 and dynein also increased the proportion of completely splayed spindle poles ($n = 222$, two experiments). **(e,f)** Representative spindle structures from the experiments quantified in (c) and (d), respectively. The bars are 10 μm.

centrosome separation [21]. To determine whether Xklp2 plays a role in spindle assembly in the absence of centrosomes, we examined its function during spindle assembly around chromatin beads. Using two different polyclonal antibodies, we failed to detect Xklp2 on chromatin bead spindles by immunofluorescence. However, antibodies added to extracts could be visualized by a fluorescent secondary antibody and were localized on spindle microtubules (Figure 5b). As on sperm DNA spindles, an Xklp2 carboxy-terminal fusion protein localized to spindle poles (T. Wittmann, H. Boleti, C. Antony, E.K. and I.V., unpublished observations), indicating the presence of a spindle pole targeting domain in the tail of the protein. Addition of anti-Xklp2 antibodies or depletion of the protein from the extract, however, did not have a significant effect on spindle assembly around chromatin beads (Figure 5c and data not shown). Addition of the carboxy-terminal fusion protein altered pole morphology, but did not affect the percentage of bipolar spindles formed (data not shown and T. Wittmann, H. Boleti, C. Antony, E.K. and I.V., unpublished observations).

These results raised the possibility that Xklp2 function is critical only in systems that contain centrosomes. Alternatively, Xklp2 might play a minor or redundant role in spindle assembly in the chromatin bead system. To examine the role of Xklp2 in the context of other motor proteins involved in pole organization, we co-inhibited Xklp2 and XCTK2, or Xklp2 and dynein (Figure 5c–f). Xklp2 inhibition increased the proportion of monopolar spindles from 28% to 50% in an XCTK2-inhibited background (Figure 5c,e). As for XCTK2, Xklp2 co-inhibition increased the severity of pole defects caused by partial dynein inhibition, leading to an increase in the proportion of completely frayed spindle poles from 21.5% to 44% (Figure 5d,f). This increase was not nearly as dramatic as that seen when both dynein and XCTK2 were inhibited (see Figure 4f). Therefore, Xklp2 appears to play a minor role in bipolar spindle formation, acting in combination with XCTK2 and dynein to stabilize bipolar spindles and poles. Its primary function is probably in centrosome-dependent spindle assembly reactions.

Discussion

Multiple motor proteins act in concert to build a spindle

We have examined the roles of five different motor proteins in determining the bipolar arrangement of microtubules using a system in which spindles form around DNA-coated beads. Because spindles form by a microtubule self-organization mechanism in the absence of centrosomes, this system has allowed us to evaluate motor protein function independent of focal microtubule nucleation. Our finding that multiple motor proteins are necessary to build a mitotic spindle is not unexpected. Our approach is unique, however, in that we have been able to define the functions of individual motor proteins in a simplified system that is completely dependent on motor proteins as organizing forces to generate a bipolar array. Spindle assembly around

Figure 6

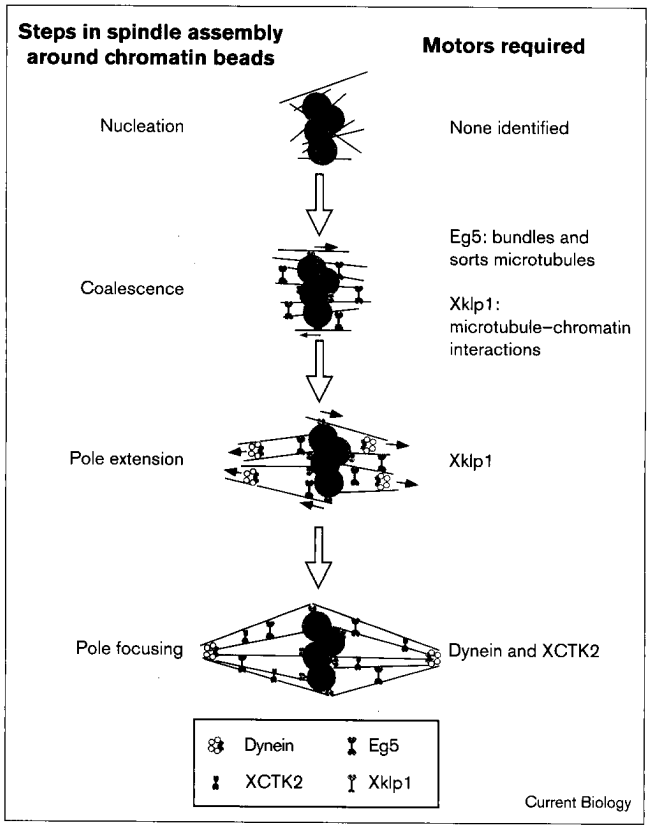

Summary of the roles of motor proteins during the process of bipolar spindle assembly around chromatin beads. Microtubules are nucleated in the region around the chromatin beads. Eg5 bundles and sorts microtubules during the coalescence phase. Xklp1 is required for spindle pole extension, and both dynein and XCTK2 focus spindle poles.

chromatin beads can be separated into several processes (Figure 6): first, nucleation and random growth of microtubules around chromatin beads; second, coalescence of those microtubules into bundles and sorting of bundles into an antiparallel array; third, extension of spindle poles; and fourth, focusing of spindle poles. We have been able to define the motor protein activities required in three of these processes.

Nucleation of microtubules around chromatin beads

None of the motor proteins we examined here had any effect on the nucleation of microtubules around chromatin beads. XKCM1, however, a KLP with a central motor domain, has been shown to influence global microtubule dynamics in *Xenopus* extracts [19]. A future project will be to study whether its activity is regulated locally to promote microtubule stabilization around chromatin beads. It is likely that non-motor proteins — such as Stathmin/Op18, microtubule-associated proteins, and factors involved directly in microtubule nucleation such as gamma tubulin — are important in generating a population of stable microtubules in this first step of spindle assembly [44–48].

Coalescence of microtubules into bundles and antiparallel microtubule sorting

A key step in spindle assembly is the bundling and sorting of microtubules that is necessary to set up the bipolar axis of the spindle. We have shown here that Eg5 function is required for this process. Inhibition of the protein resulted in monopolar-like microtubule structures emanating from chromatin beads, with their plus ends extending outward. In contrast, in *Xenopus* sperm spindle reactions, or in mammalian cells containing centrosomes, Eg5 inhibition resulted in astral or rosette structures with microtubules emanating from unseparated centrosomes and extending outward toward chromosomes [17,29,31]. We propose that the difference is due to the sites of microtubule nucleation, which in the absence of centrosomes are on or near the chromatin. Minus-end-directed motors are presumably still active when Eg5 is inhibited and can focus the microtubules into astral arrays, but because antiparallel pushing forces are compromised, the microtubule focus remains on the beads. The outwardly splayed structures formed upon Eg5 inhibition, both in the presence and absence of centrosomes, also support a role for Eg5 in establishing the bipolar axis of the spindle by microtubule bundling. These results indicate a role for Eg5 beyond its role in centrosome separation, to form and stabilize parallel and antiparallel microtubule interactions. Support for this model comes from experiments with a *Drosophila* Eg5 homologue, KLP61F [49]. Strong mutant *Klp61f* alleles completely block formation of bipolar spindles, while weaker *Klp61f* alleles result in monoastral bipolar spindles, in which centrosome separation has failed, but a bipolar spindle still forms. Presumably, partial function of the protein allows some antiparallel arrays to form by a self-organization mechanism, although centrosome separation still fails.

XCTK2 also contributes to spindle integrity, as inhibition of its function caused an increase in the proportion of monopolar spindles. As with sperm DNA spindle reactions, the addition of excess XCTK2 protein enhanced spindle formation around DNA beads [20] (unpublished observations). These findings are consistent with the model that XCTK2 bundling activity is important for bipolar spindle formation, independent of the spindle assembly pathway [20].

Extension of spindle poles

It has been proposed that KLPs on chromosome arms contribute to the molecular mechanism responsible for holding mono-oriented chromosomes away from the pole in prometaphase and for ejection of severed chromosome arms from the spindle [34]. This so-called 'polar ejection force' could be produced by plus-end-directed chromosomal motors, driving chromosomes toward the metaphase

plate [50,51]. Alternatively, it could be produced by microtubule polymerization pushing attached chromosomes toward the spindle equator. We show here that inhibition of Xklp1 during spindle assembly around chromatin beads resulted in a failure to extend spindle poles. We also found that inhibition of Xklp1 with Ab03 blocks the migration of chromatin from the center of the aster to the ends of the microtubules in a sperm half-spindle reaction (unpublished observations). Taken together, these results are consistent with a role for Xklp1 in the polar ejection force.

Focusing of spindle poles

We have shown previously that cytoplasmic dynein is required to focus microtubule minus ends into spindle poles [13]. Despite the different pathways of centrosome-dependent and centrosome-independent spindle assembly, dynein function in pole assembly appears to be conserved in both systems [12,35,52]. In *Drosophila*, the KinC family member Ncd is important for focusing poles. *Ncd* mutants form abnormal meiotic and mitotic spindles that contain multiple or splayed poles [36–38]. We show here that the KinC family member XCTK2 contributes to spindle pole formation in *Xenopus* extracts, but only in the absence of centrosomes. In sperm DNA spindle reactions containing centrosomes, inhibition of XCTK2 had no effect on pole morphology [20]. We propose that the role of XCTK2 in pole formation in *Xenopus* extracts is minor relative to dynein and is only revealed in the absence of focal nucleation by centrosomes.

Our studies on Xklp2 function in DNA bead spindles suggest that this motor is not important for spindle formation in our assay, but that its activity might be redundant with that of other motors for pole organization. Inhibition of Xklp2 in combination with dynein or XCTK2 aggravated the effects of inhibition of either XCTK2 or dynein alone, though not dramatically. We favor the idea that Xklp2 activity is more important in the cycled spindle reactions of sperm DNA which contain duplicated centrosomes. Classical centrosome separation has been difficult to document in this system; however, the observation that Xklp2 inhibition causes the collapse of spindles that contain duplicated centrosomes, but has only minor effects on spindles formed by fusion of half-spindles or around DNA beads, suggests that Xklp2 is required to push or hold centrosomes apart [21].

Common mechanisms of spindle assembly

The formation of DNA bead spindles is a model for meiotic spindle assembly, which occurs in the absence of centrosomes. It is important to note that, although spindles in meiotic and somatic cells form by different pathways, many of the same motor proteins are involved in both cases. In mitotic cells, centrosomes dominate as the point of focused microtubule nucleation and provide a kinetic advantage to spindle assembly [12]. Microtubule-based motor proteins are still essential under these conditions, but their precise mechanism of action might be partially masked by the organizational properties of centrosomes. It is likely that motor-dependent microtubule self-organization still occurs in the presence of centrosomes and serves as a redundant mechanism to ensure the accurate formation of a bipolar array. Thus, an analysis of motor protein function in different spindle assembly pathways is essential to our understanding of spindle morphogenesis.

Conclusions

We have examined the roles of different motor proteins during spindle assembly around beads coated with plasmid DNA to generate a model of motor-dependent microtubule organization during spindle formation. We found that spindle bipolarity depends on the activity of Eg5 to bundle and sort microtubules, and on Xklp1 to tether microtubules to chromatin and extend spindle poles. XCTK2 plays a supporting role in maintaining spindle integrity and spindle pole formation, whereas dynein is the dominant motor that focuses microtubules into spindle poles in our system. Thus, we have now identified roles for several motor proteins in the global organization of microtubules into bipolar spindles. It is possible, however, that we have not yet identified all of the motor proteins involved. Furthermore, we will not fully understand how the activities of the motor proteins are integrated to form the dynamic structure of the spindle until we can examine their temporal activation and regulation during the spindle assembly process. In the long run, these analyses will contribute significantly toward reconstituting spindle assembly using purified components.

Materials and methods

Antibodies

Anti-Xklp1 antibodies were raised to bacterially expressed fusion proteins containing the tail domain (Ab65) or part of the stalk (Ab03) as described [18]. Anti-Eg5 antibodies to the stalk and tail region were prepared as described [17]. Anti-XCTK2 antibodies raised to the stalk and tail domain were produced as described [20]. Xklp2 antibodies were generated to the tail region using a fusion of this region and glutathione-S-transferase (GST) [21]. The rabbits were immunized with this fusion protein, and the sera were depleted of anti-GST antibodies before specific anti-Xklp2-tail antibodies were affinity purified according to published procedures [53]. The monoclonal immunoglobulin M (IgM) anti-dynein-intermediate-chain antibody (70.1) and control IgG antibodies were obtained from Sigma Chemical Co. For antibody addition experiments, antibodies were dialyzed against 50 mM potassium glutamate, 0.5 mM $MgCl_2$, or 10 mM Hepes, pH 7.2, 100 mM KCl, concentrated, flash frozen, and stored in aliquots at −80°C. Thawed antibodies were stored at 4°C for up to several months.

Extract preparation and spindle assembly assays

Cytoplasmic extracts of unfertilized *Xenopus* eggs arrested in metaphase of meiosis II by colony stimulating factor (CSF) activity were prepared fresh as described [54,55]. Rhodamine-labeled tubulin prepared from calf brain tubulin was added to 0.2 mg/ml [56]. DNA beads and chromatin bead spindles were prepared as described [13,57]. For antibody addition experiments, all antibodies were added to the reaction before spindle assembly at a dilution of 1:10 or 1:15 of the final reaction volume. In some double-inhibition experiments, it was necessary to

dilute each antibody to 1:15, which resulted in a final dilution of antibodies of 1:7.5 in the extract. In each case, the control IgG antibody was diluted accordingly so that each series of experiments was consistently performed. All inhibition results were confirmed in sperm DNA spindle assembly reactions to show that the reagents were functioning in the same manner as described previously for each motor protein.

Immunodepletion experiments were carried out as described previously [19,55]. The amount of antibody necessary for depletion varied between proteins in a given 200 µl depletion reaction. We used 4 µg antibody for XCTK2 and Xklp2 and 10 µg antibody for Eg5 and Xklp1. For all depletions except that of Xklp1, chromatin was assembled onto the beads in a non-depleted extract. The beads containing assembled chromatin were isolated and then washed with the depleted extract before assembling spindles in the depleted extract. This procedure helped increase the life span of the extract which is greatly shortened after depletion. Because Xklp1 associates with chromatin in the absence of spindle assembly, it was necessary to assemble chromatin and spindles using an Xklp1-depleted extract to ensure that no Xklp1 was present on the chromatin. The efficiency of depletion was assayed by immunoblot of mock and depleted samples, as well as by immunofluorescence on the spindles assembled after depletion.

It should be noted that the DNA–bead spindles are much more sensitive to the effects of depletion than sperm DNA spindles. In general, the efficiency of spindle formation of DNA–bead spindles is routinely lower than that of sperm DNA in the same extract. Immunodepletion also lowers the efficiency of spindle assembly of any given extract, and this is even more apparent in the DNA–bead spindles. After immunodepletion, at least 50% of the extracts were no longer competent to form DNA–bead spindles even though they still formed spindles around sperm DNA. In addition, for Xklp1 it was very difficult to get complete depletion of all detectable protein, and this proved important in interpreting the results. Any residual Xklp1 in the extract after depletion was sufficient to assemble onto chromatin beads and function in spindle assembly. For all other motors, an incomplete depletion still severely compromised the ability to form spindles in the extracts.

Immunofluorescence

Spindle assembly reactions were diluted and spun onto coverslips as described [55,58]. The samples were post-fixed with methanol and then processed for immunofluorescence as described [19,20,58]. Antibodies to Eg5 were used at a final concentration of 1 µg/ml; all other antibodies were used at a final concentration of 5 µg/ml.

Data acquisition

To evaluate structures formed in spindle reactions, samples were examined from at least three independent experiments. In most experiments, the same results were obtained qualitatively in at least five independent experiments. Coverslips were examined under a 40× lens field-by-field, and bead–microtubule arrays were classified accordingly. Data presented are summations of two to five experiments; between 220 and 1000 spindle structures were evaluated for each motor or motor combination. Photomicrographs were taken on either a Nikon Optiphot-2 or a Nikon E-600 with a 40× objective (Planfluor 0.75NA) and a cooled charged-coupled device camera (Princeton Instruments). Images were transferred to Adobe Photoshop and processed.

Acknowledgements

We thank Michelle Moritz, Arshad Desai and Torsten Wittmann for comments on the manuscript. We also thank Andreas Merdes, Torsten Wittmann and Sigrid Reinsch for antibodies. This collaboration was supported in large part by the Human Frontier Science Program Organization. C.E.W. was supported by a grant from the US Army Medical Research and Materiel Command Breast Cancer Research Program. T.J.M. was supported by a grant from the National Institutes of Health.

References

1. Hyman AA, Karsenti E: **Morphogenetic properties of microtubules and mitotic spindle assembly.** *Cell* 1996, **84**:401-410.
2. Inoue S, Salmon ED: **Force generation by microtubule assembly/disassembly in mitosis and related movements.** *Mol Biol Cell* 1995, **6**:1619-1640.
3. Kirschner M, Mitchison T: **Beyond self-assembly: from microtubules to morphogenesis.** *Cell* 1986, **45**:329-342.
4. Pfarr CM, Coue M, Grissom PM, Hays TS, Porter ME, McIntosh JR: **Cytoplasmic dynein is localized to kinetochores during mitosis.** *Nature* 1990, **345**:263-265.
5. Steuer ER, Wordeman L, Schroer TA, Sheetz MP: **Localization of cytoplasmic dynein to mitotic spindles and kinetochores.** *Nature* 1990, **345**:266-268.
6. Walczak CE, Mitchison TJ: **Kinesin-related proteins at mitotic spindle poles: function and regulation.** *Cell* 1996, **85**:943-946.
7. Vernos I, Karsenti E: **Motors involved in spindle assembly and chromosome segregation.** *Curr Opin Cell Biol* 1996, **8**:4-9.
8. Barton NR, Pereira AJ, Goldstein LS: **Motor activity and mitotic spindle localization of the *Drosophila* kinesin-like protein KLP61F.** *Mol Biol Cell* 1995, **6**:1563-1574.
9. Mazia D, Paweletz N, Sluder G, Finze EM: **Cooperation of kinetochores and pole in the establishment of monopolar mitotic apparatus.** *Proc Natl Acad Sci USA* 1981, **78**:377-381.
10. Bajer AS: **Functional autonomy of monopolar spindle and evidence for oscillatory movement in mitosis.** *J Cell Biol* 1982, **93**:33-48.
11. Zhang D, Nicklas RB: **The impact of chromosomes and centrosomes on spindle assembly as observed in living cells.** *J Cell Biol* 1995, **129**:1287-1300.
12. Heald R, Tournebize R, Habermann A, Karsenti E, Hyman A: **Spindle assembly in *Xenopus* egg extracts: respective roles of centrosomes and microtubule self-organization.** *J Cell Biol* 1997, **138**:615-628.
13. Heald R, Tournebize R, Blank T, Sandaltzopoulos R, Becker P, Hyman A, Karsenti E: **Self-organization of microtubules into bipolar spindles around artificial chromosomes in *Xenopus* egg extracts.** *Nature* 1996, **382**:420-425.
14. LeGuellec K, Paris J, Couturier A, Roghi C, Philippe M: **Cloning by differential screening of a *Xenopus* cDNA that encodes a kinesin-related protein.** *Mol Cell Biol* 1991, **11**:3395-3398.
15. Sawin KE, Mitchison TJ, Wordeman LG: **Evidence for kinesin-related proteins in the mitotic apparatus using peptide antibodies.** *J Cell Sci* 1992, **101**:303-313.
16. Vernos I, Heasman J, Wylie C: **Multiple kinesin-like transcripts in *Xenopus* oocytes.** *Dev Biol* 1993, **157**:232-239.
17. Sawin KE, LeGuellec K, Philippe M, Mitchison TJ: **Mitotic spindle organization by a plus-end-directed microtubule motor.** *Nature* 1992, **359**:540-543.
18. Vernos I, Raats J, Hirano T, Heasman J, Karsenti E, Wylie C: **Xklp1, a chromosomal *Xenopus* kinesin-like protein essential for spindle organization and chromosome positioning.** *Cell* 1995, **81**:117-127.
19. Walczak CE, Mitchison TJ, Desai A: **XKCM1: a *Xenopus* kinesin-related protein that regulates microtubule dynamics during mitotic spindle assembly.** *Cell* 1996, **84**:37-47.
20. Walczak CE, Verma S, Mitchison TJ: **A kinesin-related protein that promotes mitotic spindle assembly in *Xenopus* egg extracts.** *J Cell Biol* 1997, **136**:859-870.
21. Boleti H, Karsenti E, Vernos I: **Xklp2, a novel *Xenopus* centrosomal kinesin-like protein required for centrosome separation during mitosis.** *Cell* 1996, **84**:49-59.
22. Merdes A, Ramyar K, Vechio JD, Cleveland DW: **A complex of NuMA and cytoplasmic dynein is essential for mitotic spindle assembly.** *Cell* 1996, **87**:447-458.
23. Sekine Y, Okada Y, Noda Y, Kondo S, Aizawa H, Takemura R, Hirokawa N: **A novel microtubule-based motor protein KIF4 for organelle transports, whose expression is regulated developmentally.** *J Cell Biol* 1994, **127**:187-201.
24. Kashina AS, Baskin RJ, Cole DG, Wedaman KP, Saxton WM, Scholey JM: **A bipolar kinesin.** *Nature* 1996, **379**:270-272.
25. Enos AP, Morris NR: **Mutation of a gene that encodes a kinesin-like protein blocks nuclear division in *A. nidulans*.** *Cell* 1990, **60**:1019-1027.
26. Saunders WS, Hoyt MA: **Kinesin-related proteins required for structural integrity of the mitotic spindle.** *Cell* 1992, **70**:451-458.
27. Hagan I, Yanagida M: **Novel potential mitotic motor protein encoded by the fission yeast cut7+ gene.** *Nature* 1990, **347**:563-566.
28. Hagan I, Yanagida M: **Kinesin-related cut7 protein associates with mitotic and meiotic spindles in fission yeast.** *Nature* 1992, **356**:74-76.

29. Blangy A, Lane HA, d'Herin P, Harper M, Kress M, Nigg EA: **Phosphorylation by p34cdc2 regulates spindle association of human Eg5, a kinesin-related motor essential for bipolar spindle formation *in vivo*.** *Cell* 1995, **83:**1159-1169.
30. Heck MM, Pereira A, Pesavento P, Yannoni Y, Spradling AC, Goldstein LS: **The kinesin-like protein KLP61F is essential for mitosis in *Drosophila*.** *J Cell Biol* 1993, **123:**665-679.
31. Gaglio T, Saredi A, Bingham JB, Hasbani MJ, Gill SR, Schroer TA, Compton DA: **Opposing motor activities are required for the organization of the mammalian mitotic spindle pole.** *J Cell Biol* 1996, **135:**399-414.
32. Maekawa T, Leslie R, Kuriyama R: **Identification of a minus end-specific microtubule-associated protein located at the mitotic poles in cultured mammalian cells.** *Eur J Cell Biol* 1991, **54:**255-267.
33. Gaglio T, Saredi A, Compton DA: **NuMA is required for the organization of microtubules into aster-like mitotic arrays.** *J Cell Biol* 1995, **131:**693-708.
34. Fuller MT: **Riding the polar winds: chromosomes motor down east.** *Cell* 1995, **81:**5-8.
35. Echeverri CJ, Paschal BM, Vaughan KT, Vallee RB: **Molecular characterization of the 50-kD subunit of dynactin reveals function for the complex in chromosome alignment and spindle organization during mitosis.** *J Cell Biol* 1996, **132:**617-633.
36. Hatsumi M, Endow SA: **Mutants of the microtubule motor protein, nonclaret disjunctional, affect spindle structure and chromosome movement in meiosis and mitosis.** *J Cell Sci* 1992, **101:**547-559.
37. Endow SA, Chandra R, Komma DJ, Yamamoto AH, Salmon ED: **Mutants of the *Drosophila* ncd microtubule motor protein cause centrosomal and spindle pole defects in mitosis.** *J Cell Sci* 1994, 107:859-867.
38. Matthies HJ, McDonald HB, Goldstein LS, Theurkauf WE: **Anastral meiotic spindle morphogenesis: role of the non-claret disjunctional kinesin-like protein.** *J Cell Biol* 1996, **134:**455-464.
39. Endow SA, Komma DJ: **Spindle dynamics during meiosis in *Drosophila* oocytes.** *J Cell Biol* 1997, **137:**1321-1336.
40. Hoyt MA, He L, Totis L, Saunders WS: **Loss of function of *Saccharomyces cerevisiae* kinesin-related CIN8 and KIP1 is suppressed by KAR3 motor domain mutations.** *Genetics* 1993, **135:**35-44.
41. Pidoux AL, LeDizet M, Cande WZ: **Fission yeast pkl1 is a kinesin-related protein involved in mitotic spindle function.** *Mol Biol Cell* 1996, **7:**1639-1655.
42. O'Connell MJ, Meluh PB, Rose MD, Morris NR: **Suppression of the bimC4 mitotic spindle defect by deletion of klpA, a gene encoding a KAR3-related kinesin-like protein in *Aspergillus nidulans*.** *J Cell Biol* 1993, **120:**153-162.
43. Nakagawa T, Tanaka Y, Matsuoka E, Kondo S, Okada Y, Noda Y, *et al.*: **Identification and classification of 16 new kinesin superfamily KIF proteins in mouse genome.** *Proc Natl Acad Sci USA* 1997, **94:**9654-9659.
44. Andersen SSL, Ashford AJ, Tournebize R, Gavet O, Sobel A, Hyman AA, Karsenti E: **Mitotic chromatin regulates phosphorylation of Stathmin/Op18.** *Nature* 1997, **389:**640-643.
45. Andersen SSL, Buendia B, Dominguez JE, Sawyer A, Karsenti E: **Effect on microtubule dynamics of XMAP230, a microtubule-associated protein present in *Xenopus laevis* eggs and dividing cells.** *J Cell Biol* 1994, **127:**1289-1299.
46. Andersen SSL, Karsenti E: **XMAP310: a *Xenopus* rescue-promoting factor localized to the mitotic spindle.** *J Cell Biol* 1997, **139:**975-983.
47. Zheng Y, Wong ML, Alberts B, Mitchison T: **Nucleation of microtubule assembly by a gamma-tubulin-containing ring complex.** *Nature* 1995, **378:**578-583.
48. Tournebize R, Andersen SS, Verde F, Dorée M, Karsenti E, Hyman AA: **Distinct roles of PP1 and PP2A-like phosphatases in control of microtubule dynamics during mitosis.** *EMBO J* 1997, **16:**5537-5549.
49. Wilson PG, Fuller MT, Borisy GG: **Monoastral bipolar spindles: implications for dynamic centrosome organization.** *J Cell Sci* 1997, **110:**451-464.
50. Rieder CL, Salmon ED: **Motile kinetochores and polar ejection forces dictate chromosome position on the vertebrate mitotic spindle.** *J Cell Biol* 1994, **124:**223-233.
51. Vernos I, Karsenti E: **Chromosomes take the lead in spindle assembly.** *Trends Cell Biol* 1995, **5:**297-301.
52. Gaglio T, Dionne MA, Compton DA: **Mitotic spindle poles are organized by structural and motor proteins in addition to centrosomes.** *J Cell Biol* 1997, **138:**1055-1066.
53. Harlow E, Lane D: *Antibodies: A Laboratory Manual.* Cold Spring Harbor: Cold Spring Harbor Press; 1988.
54. Murray AW: **Cell cycle extracts.** *Methods Cell Biol* 1991, **36:**581-605.
55. Desai A, Murray A, Mitchison TJ, Walczak CE: **The use of *Xenopus* egg extracts to study mitotic spindle assembly and function *in vitro*.** *Methods Cell Biol* 1998, in press.
56. Hyman AA, Drechsel D, Kellogg D, Salser S, Sawin K, Steffen P, *et al.*: **Preparation of modified tubulins.** *Methods Enzymol* 1991, **196:**478-485.
57. Heald R, Tournebize R, Vernos I, Murray A, Hyman T, Karsenti E: ***In vitro* assays for mitotic spindle assembly and function.** In *Cell Biology: A Laboratory Handbook.* Edited by Celis J. Cold Spring Harbor: Cold Spring Harbor Press; 1998, 2:326-335.
58. Sawin KE, Mitchison TJ: **Mitotic spindle assembly by two different pathways *in vitro*.** *J Cell Biol* 1991, **112:**925-940.

Because *Current Biology* operates a 'Continuous Publication System' for Research Papers, this paper has been published on the internet before being printed. The paper can be accessed from http://biomednet.com/library/jcub – for further information, see the explanation on the contents page.

721

CENP-A-associated complex satellite DNA is a major component of the kinetochore of mammalian chromosomes. ((O. Vafa and K.F. Sullivan)) Department of Cell Biology, The Scripps Research Institute, La Jolla, CA, 92037.

The goal of this work is to identify functional kinetochore DNA from mammalian centromeres. CENP-A is a centromere specific histone H3 homologue found in the inner kinetochore plate of human mitotic chromosomes and is predicted to associate with DNA to form a nucleosome-like structure with other core histones. We have used a biochemical approach to identify kinetochore-associated DNA sequences. Chromatin was solubilized from HeLa cells that express an epitope tagged form of CENP-A. Following immunoprecipitation, CENP-A-associated DNA sequences were cloned and subjected to DNA sequence analysis and hybridization assays. The predominant DNA sequence class that co-purified with CENP-A was alpha satellite DNA, which was enriched by a factor of at least 20 fold relative to its genomic abundance. Chromosome-specific alpha satellite subfamilies from nearly all human chromosomes were identified in a sample of 50 sequenced CENP-A-associated DNA fragments. A predominant micrococcal nuclease digestion site was found by mapping the termini of individual alpha satellite DNA fragments, suggesting that the inner kinetochore plate is comprised, at least in part, of phased arrays of CENP-A nucleosomes. Similar experiments were performed in the Indian muntjac, resulting in the isolation of a complex satellite DNA sequence that mapped to centromeres by *in situ* hybridization. These experiments provide evidence that mammalian kinetochore DNA is, in fact, complex satellite DNA. The lack of conservation of complex satellite DNA sequences suggests that kinetochore formation in mammals is not directly specified by DNA sequence.

722

POLYMERIZATION-COUPLED MOVEMENT OF CHROMOSOME-BOUND MICROTUBULES IN VITRO. ((A.J. Hunt and J.R. McIntosh.)) Dept. of Molecular, Cellular, and Developmental Biology, University of Colorado, Boulder, CO 80309

During mitosis, kinetochore microtubules (MTs) elongate and shorten by incorporation or loss of tubulin subunits, principally at their chromosome-bound ends. We have modeled this phenomenon *in vitro*, using an assay in which movement of a labeled MT segment is observed as the MT loses or gains subunits at its chromosome-bound end. Chromosomes isolated from cultured CHO cells are bound to coverslips coated with antibody to DNA. Short MTs, brightly labeled with rhodamine and stabilized by polymerization in the GTP analogue, GMPCPP, are allowed to bind to the chromosomes. From these seeds labile MTs are grown in the presence of GTP and dimly labeled tubulin. After washing with GTP and unlabeled tubulin we observe bright seeds within dimly labeled MTs that are bound end-on to chromosomes. As a MT continues to grow, its labeled portion moves away from the chromosome to which it is bound. Sometimes a MT switches to rapid shortening and the bright seed is reeled in toward the chromosome until either there is a transition back to growth or the labile portion is completely depolymerized. The speed of movement away from a chromosome is similar to the rate of elongation of free MT ends, while movement toward a chromosome proceeds at about 1/5 the rate of rapid shortening of free ends. By using the optical tweezers to apply forces on silica beads that are bound to MTs we are studying the strength of a MTs attachment to a chromosomes. The MT-chromosome interaction can bear tensions greater than 15 ± 0.5 pN, and an opposing force of less than 2 pN will inhibit polymerization-coupled movement. Supported by GM 33787 and 3663 to JRM.

723

CENP-E IS A PLUS END-DIRECTED KINETOCHORE MOTOR REQUIRED FOR CHROMOSOME CONGRESSION ((K.W. Wood[1], R. Sakowicz[2], L.S.B. Goldstein[2], D. W. Cleveland[1])) [1]Laboratory of Cell Biology, Ludwig Institute for Cancer Research and [2]Howard Hughes Medical Institute, Division of Cellular and Molecular Medicine, University of California at San Diego, La Jolla, California 92093-0660.

Mitosis requires dynamic attachment of chromosomes to spindle microtubules. This interaction is mediated largely by kinetochores, which also coordinate chromosome movement with kinetochore microtubule assembly and disassembly. During prometaphase, forces exerted at kinetochores, in combination with polar ejection forces, drive congression of chromosomes to the metaphase plate. A major question has been whether kinetochore-associated microtubule motors play an important role in congression. Using immunodepletion from, and antibody addition to, Xenopus egg extracts we show that the kinetochore-associated kinesin-like motor protein CENP-E plays an essential role in congression. We further demonstrate that CENP-E powers movement toward microtubule plus ends in vitro. CENP-E thus defines a plus end-directed kinetochore motor activity required for congression. These findings suggest a model in which CENP-E functions to tether kinetochores to dynamic microtubule plus ends.

724

DISSECTING THE FUNCTION OF KINETOCHORE-BOUND XKCM1 IN CHROMOSOME MOVEMENT IN VITRO AND IN VIVO ((C.E. Walczak, A. Desai and T.J. Mitchison.)) Department of Cellular and Molecular Pharmacology , University of California, San Francisco, CA 94143-0450

XKCM1 is a novel member of the kinesin-related protein family that uses the energy of ATP hydrolysis to depolymerize microtubules (see related abstract by Desai, et al.). We demonstrated previously that XKCM1 is essential for mitotic spindle assembly in vitro and acts by regulating microtubule dynamics in extracts. A portion of XKCM1 is specifically localized to kinetochores during mitosis and may be important in chromosome movement. To dissect the function of only the kinetochore-bound XKCM1, we generated glutathione-S-transferase (GST) fusion proteins containing the N-terminal globular domain (GST-NT), the centrally located motor domain (GST-M), and the C-terminal alpha-helical tail (GST-CT) of XKCM1. The GST-NT protein targeted to kinetochores during spindle assembly suggesting that the N-terminal domain of XKCM1 is sufficient for kinetochore localization. Addition of GST-NT prior to or after spindle assembly competed off endogenous XKCM1 suggesting that kinetochore targeting may be a more dynamic process than was previously thought. The displacement of endogenous XKCM1 from kinetochores by GST-NT caused a misalignment of chromosomes on the metaphase plate and an increase in astral microtubules without affecting the global spindle structure. These results implicate kinetochore-bound XKCM1 as having an important role in chromosome positioning within the spindle. We plan to use the GST-NT protein to address the role of kinetochore-bound XKCM1 in chromosome movement in vitro using the Xenopus egg spindle assembly system and in vivo by microinjection into tissue culture cells.

725

EVIDENCE THAT THE ESSENTIAL KINETOCHORE COMPONENT ZW10 RECRUITS DYNACTIN AND DYNEIN TO THE KINETOCHORE. ((D.A. Starr, B.C. Williams, Z. Li, T.S. Hays*, and M.L. Goldberg)) Section of Genetics and Development, Cornell University, Ithaca, NY 14853. *Departments of Genetics and Cell Biology, University of Minnesota, St. Paul, MN 55108.

ZW10 is a conserved protein needed for accurate chromosome segregation that localizes to the kinetochore region at prometaphase, then associates with kinetochore microtubules during metaphase, and relocalizes to the kinetochore at anaphase onset. These changes are dependent upon bi-polar spindle tension exerted across the chromosomes at metaphase (Williams et al, JCB 134;1127-40, 1996 and Starr et al, JCB in press 1997). The following evidence indicates that ZW10 targets dynein to the kinetochore, probably through an interaction with the p50 subunit of dynactin. (1) The normal prometaphase localization of dynein to kinetochores is abolished in *zw10* mutants, and also in *rod* mutants which prevent association of ZW10 protein with kinetochores. Interestingly, the intensity of dynein signals on metaphase kinetochores is also influenced by tension. (2) A two hybrid screen with human ZW10 as bait identified the p50 subunit of dynactin as an interactor. We have mapped the interaction domain of p50 to a 30 amino acid stretch essential for p50 function (Echeverri and Vallee, personal communication). The role of dynein at the kinetochore may thus be intimately associated with or influenced by the measurement of spindle tension. The kinetochore machinery of which ZW10 is a part, is likely to be quite complex. We have raised antibodies to another two hybrid interactor of ZW10 and shown that it is a novel component of HeLa cell kinetochores. In collaboration with R. Karess (CNRS, Gif-sur-Yvette, France), we also have genetic and two-hybrid evidence that the *rod* gene product interacts with ZW10.

726

MICROINJECTION OF MITOTIC CELLS WITH ANTIBODY AGAINST p55CDC INDUCES M-PHASE ARREST AND ABERRANT CELL DIVISION. ((M. Kallio[1], J. Weinstein[2], D.J. Burke[2], and G.J. Gorbsky[1])) Dept. of Cell Biology[1], Dept. of Biology[2] Univ. of Virginia, Charlottesville, VA 22908, Amgen Inc.[2], Thousand Oaks, California 91320.

We have examined the localization and function of p55CDC, a mammalian homolog of *S. cerevisiae* cdc20, *S. pombe slp1*, and *Drosophila* cell cycle gene *fizzy*, at M-phase of PtK1 cells. Immunofluorescence analysis shows that p55CDC is expressed at M-phase of mitosis and meiosis. From late prophase to metaphase p55CDC localizes primarily at the kinetochores. Some p55CDC is also associated with spindle microtubules and spindle poles. At anaphase p55CDC remains kinetochore bound but the intensity of the immunofluorescent signal gradually decreases and is lost by the late telophase. Microinjection of cells from prophase to early metaphase with anti-p55CDC antibody induces metaphase arrest or delay in the onset of anaphase, slow sister chromatid separation in anaphase, and failure to perform cytokinesis. Many anti-p55CDC-injected cells (34/87) arrested at metaphase. Others were significantly delayed in the onset of anaphase (21.9 ± 18.6 min) compared to controls (10.8 ± 4.7 min). In the anti-p55CDC injected cells that eventually progressed to anaphase, chromatid movement to the poles was slow, requiring on average twice as long as in the buffer-injected cells (19.3 ± 12.3 min vs. 9.3 ± 4.0 min). In addition, 9 out of 48 cells that progressed into anaphase did not exit M-phase. Cells injected at late metaphase or after anaphase onset showed no apparent effect. Chromosome movements at prometaphase were not noticeably affected. These data imply that p55CDC is required at metaphase to promote the metaphase-anaphase transition and to ensure the normal progression of anaphase. Microinjection of anti-p55CDC antibody also affected mitotic spindle morphology. Injected mitotic cells show a transient increase of exceptionally long microtubules and their microtubules are more resistant to microtubule-disrupting agents. We propose that p55CDC is a conserved cell cycle protein whose function is essential for normal chromosome segregation. (supported by grants to G.J.G. and D.J.B. from the National Institute of General Medical Sciences and to M.K. from the Academy of Finland).

12

ATOMIC MODEL OF TUBULIN. ((K. H. Downing and E. Nogales)) Life Science Division, Lawrence Berkeley National Laboratory, Berkeley, CA 94720.

The αβ tubulin heterodimer is the structural subunit of microtubules. In the presence of zinc ions, purified tubulin assembles into 2-D sheets which are ideal samples for electron crystallographic studies. In these sheets protofilaments associate in an antiparallel fashion, as opposed to the parallel arrangement in microtubules. An atomic model of the tubulin dimer has been obtained from an electron crystallography map of these sheets at 3.7 Å. The high quality of the phases produced a map that is clean and readily interpretable in terms of secondary structure elements, with good connectivity between most helix and strand segments. The model shows that α and β tubulin have basically identical structures, with main differences limited to loop regions. Each monomer is very compact, with a core that is formed by two beta sheets and 11 surrounding alpha helices. We can identify three sequential domains: the N-terminal domain forming a Rossmann fold and including the nucleotide binding region, an intermediate domain containing the second beta sheet and the taxol binding site, and the C-terminal domain composed of two helices that form the binding surface for motor proteins. Although refinement is still in progress to improve definition of side chain positions, the model is very useful in understanding the overall structure of the protein and such features as nucleotide exchangeability and drug binding.

13

MICROTUBULE DESTABILIZATION BY XKCM1 AND XKIF2 -- TWO INTERNAL MOTOR DOMAIN SUBFAMILY KINESINS. ((A. Desai, T. J. Mitchison, and C. E. Walczak)) Dept. of Cell. Mol. Pharm., University of California, San Francisco, CA 94143.

We have previously shown that inhibition of XKCM1, an internal motor domain kinesin, in Xenopus extracts caused a reduction in the catastrophe frequency of dynamic MTs. To understand the mechanism by which XKCM1 perturbs MT dynamics, we have performed a detailed study of the effect of purified XKCM1 on MTs assembled from pure tubulin.

Baculovirus-expressed and purified XKCM1 depolymerizes both taxol-stabilized and GMPCPP MTs in an ATP-dependent manner. Depolymerization occurs equivalently from both ends of the MT at highly substoichiometric concentrations of XKCM1, releasing tubulin dimer which is competent to reassemble. XKCM1 also induces catastrophes at both ends of dynamic MTs polymerized from purified Xenopus egg tubulin.

Destabilization of GMPCPP MTs by XKCM1 occurs without hydrolysis of tubulin-bound GMPCPP. Negative stain EM of GMPCPP MTs being destabilized by XKCM1 reveals large protofilament bulbs at both ends of the MT. These studies suggest that XKCM1 can change the conformation of the tubulin subunit and peel apart MT protofilaments without inducing GTP hydrolysis on the tubulin subunit. Immunofluorescence and negative stain analysis of GMPCPP MTs incubated with XKCM1 in 10 mM MgAMPPNP show that XKCM1 can target to both MT ends and induce protofilament peeling at these ends in the absence of ATP hydrolysis. These results suggest that the ATP-like state of XKCM1 has an intrinsic affinity for MT ends and can induce a destabilizing conformational change in tubulin. Unlike in the presence of ATP, where each XKCM1 molecule can cause release of 50-100 tubulin subunits, the reaction in AMPPNP does not result in significant release of tubulin dimer suggesting that ATP hydrolysis is used to recycle the motor to perform multiple depolymerization cycles.

Baculovirus-expressed and purified XKIF2, a neuronal vesicle-associated kinesin highly homologous to XKCM1 in the motor domain, also possesses an ATP-dependent MT destabilizing activity. Thus, internal motor domain kinesins may be regulators of MT dynamics not only during mitosis but also in differentiated cell types. These studies represent the first detailed characterization of a physiological MT destabilizer and demonstrate a clear non-motor function for a kinesin.

14

The Structure and Function of The Gamma Tubulin Ring Complex
((Yixian Zheng*, Ona Martin*, Akihiro Iwamatsu+, and Chris Wiese*.))
*Carnegie Institution of Washington Department of Embryology Baltimore, MD21210, USA +Section of Protein Chemistry Central Laboratories for Key Technology Kirin Brewery Co., LTD. 1-13-5 Fukuura Kanazawa-ku, Yokohama Kanagawa, Japan

Previous studies showed that gamma tubulin, which forms a ring complex with several other proteins, is involved in microtubule nucleation from the centrosome. We have initiated both molecular and biochemical analyses of the Drosophila and Xenopus gamma tubulin ring complexes (gammaTuRC). Using internal peptide sequencing information or mouse polyclonal antibodies raised against the gammaTuRC protein subunits, we are in the process of characterizing each of the gammaTuRC subunits. So far, we have cloned and completely or partially sequenced four subunits in the gammaTuRC. These molecular characterization will allows us to further analyze the assembly and function of the gammaTuRC. In addition, we have found that gamma tubulin in the gammaTuRC binds to GTP and GDP using UV-crosslinking of 32P-label guanine nucleotides. We are currently investigating the GTP and GDP binding and exchange properties of the gammaTuRC.

15

INTERACTIONS BETWEEN VIMENTIN AND MICROTUBULES (MT) DURING THE FORMATION OF AN INTERMEDIATE FILAMENT (IF) NETWORK IN VIVO. ((V. Prahlad, M. Yoon, L. Marekov*, P. Steinert*, and R.D.Goldman)) Dept. of Cell and Mol. Biol., Northwestern Univ. Med. Sch. and *Skin Biology Group, NIAMS/ NIH.

Previous studies indicate that there exists a close association between the (IF) and MT networks in many eukaryotic cells. For instance, the presence of an intact MT network is required for the formation of an IF network following trypsinization-replating. This was used as a model system to study IF-MT interactions. BHK cells were transfected with GFP-vimentin (vimentin cDNA fused with S65T green fluorescent protein), and the formation of the IF network following trypsinization-replating was followed in live cells. As early as 30 min following replating, the GFP-vimentin formed aggregates, which assembled into a typical IF network by 6-8 hrs. The assembly of these aggregates into IF appeared to involve their movement towards the cell periphery. This involved a fast directional movement towards the periphery of the cell in a manner typical of saltatory movements with peak rates ranging from 0.5μm/s to 0.75μm/s. This movement was absent when cells were plated into colchicine-containing medium to inhibit microtubule polymerization. Further, immunofluorescence studies indicated that the GFP-vimentin aggregates at the cell periphery were closely associated with MT. Since vimentin and tubulin do not appear to interact in vitro, these interactions are probably mediated by other crossbridging proteins. We have identified one potential crossbridging protein in BHK cells. This protein is a 450kD nestin-like protein (NLP). NLP colocalizes with the vimentin aggregates following trypsinization-replating. NLP co-cycles with both vimentin IF and taxol-stabilized MT in vitro. Further, NLP binds to vimentin during, but not following, its polymerization into 10nm IF. From the above studies we hypothesize that the formation of a vimentin IF network in spreading BHK cells occurs, in part, by the movement of nonfilamentous vimentin aggregates towards the periphery of the cell along MT tracks. Further, NLP appears to be a candidate for mediating this interaction. Supported by NIGMS.

16

DISRUPTION OF THE INTERACTION BETWEEN ZYXIN AND α-ACTININ USING A SPECIFIC PEPTIDE INHIBITOR CAUSES THE LOSS OF ZYXIN FROM FOCAL CONTACTS AND A RETRACTION OF THE CELL PERIPHERY. ((B.E. Drees and M.C. Beckerle)) Department of Biology, 201 South Biology, University of Utah, Salt Lake City, UT. 84112.

Actin assembly is a highly regulated and organized process. The means by which this control occurs is a central question in cell biology. Zyxin, a protein found at focal contacts and at sites of actin assembly at the leading edge, has recently emerged as a candidate for involvement in the control of actin dynamics. Zyxin is structurally related to the ActA protein of Listeria monocytogenes; and like ActA, zyxin is able to direct actin assembly when targeted to the plasma membrane (1,2). Zyxin may contribute to actin assembly through its interaction with the profilin-binding proteins mena and VASP. Zyxin also interacts with the actin crosslinking protein α-actinin (3). This interaction could be important for positioning zyxin at sites destined to become zones of actin assembly. We precisely mapped the α-actinin binding site of zyxin using a custom synthesized peptide library. Microinjection of synthetic peptides corresponding to this sequence caused the loss of zyxin from focal contacts as well as a retraction at the cell periphery. This response was blocked by preincubation of the peptides with purified α-actinin. Thus, the appropriate subcellular distribution of zyxin depends on its interaction with α-actinin. Moreover, disruption of this association affects the behavior of lamellipodia, structures dependent on the actin cytoskeleton. We postulate that zyxin serves as a molecular scaffold that promotes spatially restricted assembly of protein complexes that stimulate actin polymerization. (The authors are grateful to J. Wehland for providing reagents and many helpful discussions.)

1. Reinhard et al, 1995, Proc Natl. Acad. Sci. 92:7956-7960.
2. Colsteyn et al, J. Cell Sci., in press.
3. Crawford et al, 1994, J. Cell Biol. 129:117-128.

17

ACTOMYOSIN-BASED RETROGRADE FLOW OF MICROTUBULES IN MIGRATING EPITHELIAL CELLS INFLUENCES DYNAMIC INSTABILITY AND IS ASSOCIATED WITH MICROTUBULE BREAKAGE AND TREADMILLING. ((C. M. Waterman-Storer and E.D. Salmon)) Department of Biology, University of North Carolina, Chapel Hill, NC, 27599

We have discovered several novel features exhibited by microtubules (MTs) in migrating newt lung epithelial cells by time-lapse imaging of fluorescently labeled, microinjected tubulin. These cells exhibit leading edge ruffling and retrograde flow in the lamella and lamellipodia. The plus ends of MTs persist in growth perpendicular to the leading edge until they reach the base of the lamellipodium, where they oscillate between short phases of growth and shortening. Occasionally, pioneering MTs grow into the lamellipodium, where microtubule bending and reorientation parallel to the leading edge is associated with retrograde flow. Parallel MTs persist in growth move rearward in the lamella at the velocity of retrograde flow. Fluorescent marks on the lattice of MTs perpendicular to the leading edge show that all microtubules in the lamella are transported rearward at the rate of retrograde flow. MT rearward transport persists when the assembly/disassembly of plus ends is blocked by 100 nM nocodazole, but is blocked by inhibition of actomyosin by cytochalasin D or BDM. During rearward flow, MT buckling and breaking is observed. This generates non-centrosomal MTs. The new plus ends generated by breakage grow toward the leading edge and the free minus ends are either stabilized or shorten toward the original plus ends, producing a MT that "treadmills" through the lamella. Analysis of the centrosome regions shows that 80% or less of MTs in the lamella are centrosomal, and centrosomes rarely release MTs. These findings show that actin-myosin activity has a major effect on MT dynamics in migrating cells and retrograde flow may play a major role in orienting and controlling the assembly dynamics of MTs during cell migration.

[41] Purification of Cytoskeletal Proteins Using Peptide Antibodies

By CHRISTINE M. FIELD, KAREN OEGEMA, YIXIAN ZHENG, TIMOTHY J. MITCHISON, and CLAIRE E. WALCZAK

Introduction

Immunocytochemistry of cells, as well as biochemical fractionation and assay of proteins important in the cytoskeleton, have been used to further our understanding of the dynamic filament systems and their associated proteins. In this article, we describe the use of peptide antibodies to study the cytoskeleton in a variety of organisms (also reviewed in Ref. 1). We have found peptide antibodies to be useful reagents for immunofluorescence and immunoblotting. More uniquely, we have used them for affinity purification of native, functional proteins and protein complexes from extracts. We describe the preparation and purification of peptide antibodies and focus on their use in the affinity purification of proteins and protein complexes from extracts.

Why Use Peptide Antibodies?

Traditionally, antibodies have been generated against proteins purified from their natural source or bacterially expressed fusion proteins. The use of peptide antibodies has several advantages over this type of approach. Peptide antibodies are relatively easy to prepare and allow the rapid conversion of sequence information into a reagent that targets a specific protein domain. Whereas generation of antigen using conventional approaches can require weeks to months, peptides can be ordered by e-mail, phone, or fax and the coupling procedure takes only 2 days with minimal hands-on time. Peptide antibodies are also uniquely useful for some applications. Antibodies to amino acid sequences conserved between known members of protein families have allowed identification of new family members by expression screening and by biochemical analysis.[2–5] Peptide antibodies can also be used as immunoaffinity reagents for the purification of native protein com-

[1] J. C. Bulinski, *Int. Rev. Cytol.* **103,** 281 (1986).
[2] D. G. Cole, W. Z. Cande, R. J. Baskin, D. A. Skoufias, C. J. Hogan, and J. M. Scholey, *J. Cell Sci.* (1992).
[3] K. E. Sawin, T. J. Mitchison, and L. G. Wordeman, *J. Cell Sci.* **102,** 303 (1992).
[4] C. E. Walczak, T. J. Mitchison, and A. Desai, *Cell* **84,** 37 (1996).
[5] L. Wordeman and T. Mitchison, *J. Cell Biol.* **128,** 95 (1995).

METHODS IN ENZYMOLOGY, VOL. 298

0076-6879/98 $25.00

TABLE I
PARAMETERS AFFECTING ANTIBODY SUCCESS

Variable	Successful antibodies (%)	Number of peptides
C-terminal peptides	90	18
Internal peptides	43	21
Net charge of +3 to +5	90	11
Net charge of ±1 to 2	70	16
Net charge of 0	14	7
Net charge of −3 to −5	66	3
10–14 Amino acids	56	18
15–19 Amino acids	64	11
≥20 Amino acids	75	8

plexes. The key to the success of this procedure is to use the peptide against which the antibody was prepared as a competitor to elute the protein complex from the antibody column under native conditions.[1,4,6–8]

We must also acknowledge the drawbacks of using peptide antibodies. Due to the limited number of epitopes available in a short amino acid sequence, the probability of obtaining useful antibodies may be a bit lower than by conventional methods. Peptide antibodies also occasionally cross-react with other proteins, due to the small size of the epitope, so they must be used with caution. If the chosen peptide is buried within the protein, the resulting antibody may not recognize the native protein. For similar reasons, the ability of peptide antibodies to inhibit protein function will depend on the specific nature of the epitope.

Choice of Peptide

For this article we have reviewed the results from 4 years of work generating peptide antibodies to cytoskeleton-related proteins in rabbits. We have used 40 peptides to immunize approximately 80 rabbits using the procedures described here, and obtained a 63% success rate overall (Table I). Success is defined as an antibody that was useful for at least one application (i.e. immunoblot, immunoprecipitation, or immunofluorescence). Antibodies that did not recognize the peptide in the context of the intact protein were considered failures, even if they recognized peptide alone. A number of commercial vendors offer peptide synthesis and coupling followed by

[6] Y. Zheng, M. L. Wong, B. Alberts, and T. J. Mitchison, *Nature* **378,** 578 (1995).
[7] C. M. Field, O. Al-Awar, J. Rosenblatt, M. L. Wong, B. Alberts, and T. J. Mitchison, *J. Cell Biol.* **133,** 605 (1996).
[8] A. Merdes, K. Ramyar, J. D. Vechio, and D. W. Cleveland, *Cell* **87,** 447 (1996).

antibody titering and purification. This can be time saving and economical, but we advise caution when using these services. Be aware that companies usually titer antibodies against peptide and not against protein, so the titer may not reflect the usefulness of the antibody for your application. In addition, instead of purifying antibodies on the peptide used for immunization, some companies "affinity purify" antibodies on protein A providing you with total serum IgG instead of a population of specific antibodies. Also, some companies pool sera from different bleeds or even different rabbits. If you use a commercial service, you should carefully review the procedures used by the company and provide them with clear instructions.

Our antibodies varied in quality and in the types of experiments they were useful for (Table I). The highest success rate (90%, $n = 18$) was obtained with antibodies made to the C-terminal peptide of the protein. This may be because the C terminus is more likely to be exposed on the surface of the protein. Of those antibodies generated against internal peptides, our success rate was only 43% ($n = 21$). The statistics were the same whether the sequence was an exact match to a known protein or a degenerate match to a highly conserved region of a protein family. Charge of the peptide also seems to be an important factor. Peptides that were strongly basic (net charge of +3 to +5) gave the highest success rate (90%, $n = 11$). The next most successful category contained those peptides that were weakly acidic or weakly basic (net charge of ±1 to 2) (70%, $n = 16$). A peptide with net charge of zero was rarely successful; we had only a 14% success rate ($n = 7$) with these types of peptides. The length of the peptide was less important. The success rate of longer peptides (20–25 amino acids) was slightly higher than that of shorter peptides (10–15 amino acids), but it is not clear if this trend is statistically significant (75%, $n = 8$, for peptides of 20–25 amino acids versus 57%, $n = 23$, for peptides of 10–15 amino acids). There is one report in the literature of a 7-amino-acid peptide antibody that was effective.[9] Insolubility of the peptide (which correlated with peptides that were highly hydrophobic or had a net charge of zero) was undesirable. Only one insoluble peptide gave limited success ($n = 5$).

Based on our experience we make the following recommendations for choosing a peptide:

1. If possible, pick the C-terminal 10–30 amino acids of the protein.
2. To minimize cross-reactivity, do a database search with the peptide to make sure that the sequence is not highly conserved in other proteins.

[9] M. Z. Atassi and C. R. Young, *Crit. Rev. Immunol.* **5,** 387 (1985).

3. Count the number of charged amino acids in your peptide. Increase the length of the peptide if doing so will include more charged residues, but avoid canceling charges for a net charge of zero.
4. Run a surface probability plot and antigenic index on your protein to avoid selecting peptides likely to be buried.

After selecting a peptide sequence, add a cysteine to the N terminus of the peptide to facilitate coupling to KLH for immunization, and to resin for affinity purification. To remove charges from the peptide ends that would not be present in the native protein, we now tend to order peptides with an acetylated N terminus and, in the case of internal peptides, a C-terminal amide, but the importance of these modifications has not been tested.

When the peptide arrives, check its solubility. If the peptide is insoluble in buffer, try dissolving it in dimethyl sulfoxide (DMSO) and then diluting the DMSO stock into buffer. If it precipitates, your chances of success are limited. If you are planning to try affinity chromatography, the peptide must be soluble to at least 1 m*M* in the buffer that will be used for elution.

Preparation of Immunogen

Checking Peptide Thiol Groups

Successful thiol coupling requires reduced sulfhydryl groups. Because peptide thiol groups sometimes get modified after synthesis, presumably due to oxidation, it is a good idea to check the peptide for the presence of free sulfhydryl groups before coupling to either KLH or to resin. This can be done using Ellman's reagent, which reacts with sulfhydryls to form a highly colored chromophore with an absorbance maximum at 412 nm.

1. Make up 5 m*M* Ellman's reagent (5,5′-dithio-bis(2-nitrobenzoic acid) (Sigma, St. Louis, MO) in 0.1 *M* sodium phosphate, pH 7.2.
2. Weigh out about 1 mg of peptide into a preweighed tube.
3. Add 0.5 ml reagent. It should turn bright yellow.
4. Dilute the mixture 1/50 in buffer. Read A_{412}, blanking against reagent diluted to the same concentration.
5. Calculate the apparent molecular weight of the peptide based on the number of free sulfhydryl groups, using a molar extinction coefficient for the Ellman's chromophore of 14,000 M^{-1} cm^{-1}. Compare this to the expected molecular weight of the peptide. They should agree within a factor of 3, with the apparent molecular weight usually higher. If the thiol concentration is anomalously low, i.e., the apparent molecular weight is very high, there may be something wrong with the peptide and it will probably not couple well. You may be able to regenerate the thiol groups by incubating the peptide with excess dithiothreitol (DTT) at pH 8.0. To recover the peptide, remove the free DTT by gel filtration over a resin with a small exclusion limit, such as Bio-Gel P2 (Bio-Rad, Richmond, CA).

Coupling of Peptide to KLH

To induce antibody production by B cells, an antigen needs to elicit a coordinated response from both B cells and helper T cells. To do this the antigen must (1) have an epitope that can bind to the surface antibody of a virgin B cell (this epitope will dictate the specificity of the antibody produced), and (2) on degradation must generate fragments that can elicit a response from helper T cells by simultaneously binding to both a class II MHC molecule and a T-cell receptor. Although peptides frequently contain good epitopes for recognition by B cells, they are often too small to meet the latter requirements.[10] To circumvent this problem, and to increase antigen uptake by phagocytosis, we couple peptides to keyhole limpet hemocyanin (KLH).

The following recipe is for two rabbits (five injections each). It is a good idea to immunize more than one rabbit per peptide if you can afford it, because in some cases we have seen significant rabbit-to-rabbit variation in the immune response to peptides. In the coupling procedure, we start with 10 mg of peptide and often use half of the peptide for thiol coupling and half for glutaraldehyde coupling. The rationale for this is one of security—if one of the coupling procedures fails, then at least half of the peptide will be coupled by the other procedure. The success of coupling procedures must often be taken on faith because of the difficulty in quantitating peptide amounts by any simple means such as A_{280} or Bradford assay (in part, because of the large amounts of KLH present). However, some workers prefer to use only the thiol coupling method since it avoids modification of internal lysines in the peptide. Our thiol coupling procedure was designed with two criteria in mind: (1) maximizing the ratio of peptide to KLH in the immunogen and (2) minimizing the size of the linker.

1. Dissolve 100 mg of KLH (Sigma) in 2 ml of water. This generally takes about 4 hr, and you will probably need to sonicate and vortex. Be patient and put it on a rotator at 4°. Dialyze overnight against 2 liters of 0.1 *M* sodium phosphate, pH 7.8, to remove any contaminating compounds containing thiol or amino groups.

[10] E. Harlow and D. Lane, "Antibodies: A Laboratory Manual," pp. 1–726. Cold Spring Harbor Laboratory Press, New York, 1988.

2. Spin the dialysate 10 min at full speed in microfuge to remove aggregates (do not be surprised to see a substantial pellet).
3. If both thiol and glutaraldehyde coupling procedures are to be used, split the KLH into two aliquots, one for each procedure.
4. Thiol coupling reaction (outlined in Fig. 1A). (a) Warm one aliquot of KLH to room temperature. Add one-ninth volume of iodoacetic acid *N*-hydroxysuccinimide ester (IAA-NHS) at 100 mg/ml in DMSO. Make the DMSO stock fresh, and protect the iodoacetamide reagent from light. We make our own IAA-NHS ester by coupling IAA and NHS with dicyclohexyl carbodiimide in CH_2Cl_2, filtering out the urea, and recrystallizing. It can also be purchased from Sigma. For the rest of the thiol coupling, minimize exposure of the reaction to light by covering it with foil or by working in a dark room with

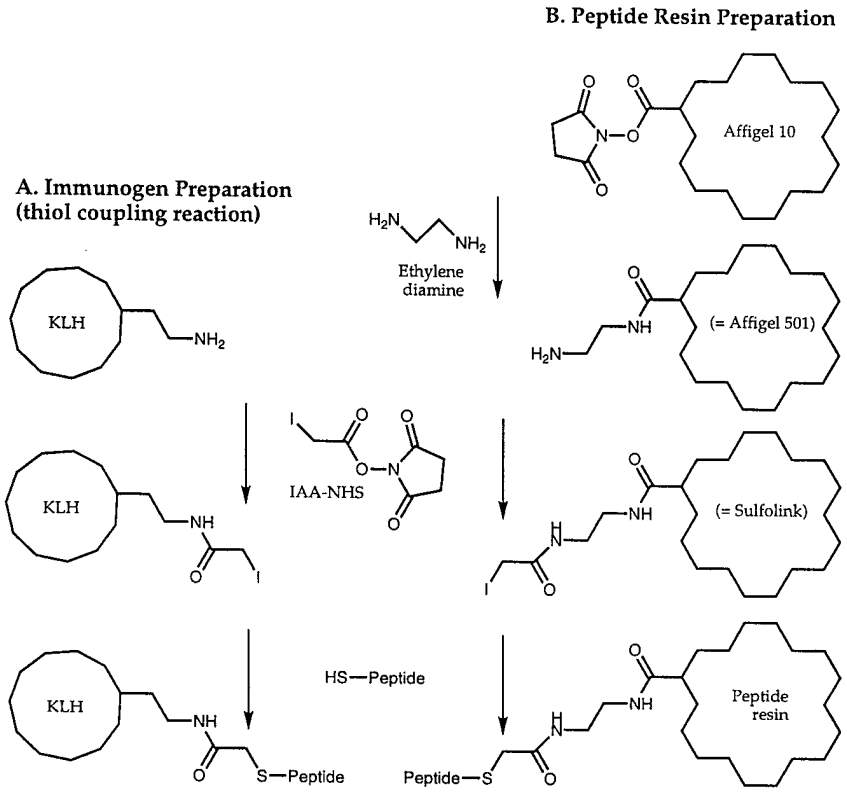

FIG. 1. (A) Preparation of peptide immunogen (thiol coupling reaction only). (B) Preparation of peptide resin for affinity purification of antibody.

minimal light. (b) After 10 min at room temperature, the KLH solution will start to get a little cloudy. Cool on ice, and perform all subsequent steps at 4°. Load the KLH onto a gel filtration column containing Bio-Gel P-10 resin (Bio-Rad) equilibrated with 0.1 *M* sodium phosphate, pH 7.8. Make sure the column is at least 10 times the volume of the sample. Pool the KLH containing fractions by color (KLH is grayish green). Add 5 mg (10 mg if not using glutaraldehyde coupling) of peptide to the pooled KLH fraction, either as powder if it is soluble or add it from a 100 mg/ml stock in DMSO. It is important to use freshly dissolved peptide because the thiol groups can oxidize within an hour in solution. Check the pH and adjust to 7.2–7.8 if necessary. Incubate at least 8 hr at 4°, rotating gently.
5. Glutaraldehyde coupling reaction. (Optional, note that the glutaraldehyde procedure is only useful if the peptide has an internal lysine or a nonacetylated *N* terminus.) (a) Add 5 mg peptide to the other aliquot of KLH, followed by glutaraldehdye to 0.1% final. Add the peptide as a solid or from a 100 mg/ml stock in DMSO. Precipitation does not seem to matter and often occurs. After adding the glutaraldehyde, check the pH with pH paper, and adjust to pH 7.8 if necessary using NaOH. Incubate 8–12 hr at 4°, rotating gently. (b) Add a *tiny* pinch of $NaBH_4$ to reduce the otherwise reversible lysine-aldehyde Schiff-base adducts, as well as excess glutaraldehyde. Make sure the sample is in a large tube because it tends to fizz up. Incubate 8–12 hr at 4°. This is the glutaraldehyde conjugate.
6. Pool the KLH coupled peptide from the two procedures. Dilute to 5 ml with 0.15 *M* NaCl. If there is a precipitate, sonicate vigorously to break it up. Split the immunogen into 1-ml aliquots and freeze it. Each aliquot contains 2 mg of conjugated peptide, which is sufficient for a single immunization of two rabbits (1 mg/immunization/rabbit).

Affinity Purification of the Antibody

Although sera from animals immunized with native or fusion proteins are often used directly for immunoblotting or immunofluorescence, in our experience peptide antibodies are only useful after affinity purification from crude serum. To affinity purify peptide antibodies, we first prepare peptide-coupled resin.

Coupling Peptides to Resin for Affinity Purification (outlined in Fig. 1B)

We use Affi-Gel 10 (Bio-Rad), converting its functional group first to amino and then to iodoacetyl. You can also buy Affi-Gel 102 (Bio-Rad)

and start at step 6 or Sulfo-link gel (Pierce, Rockford, IL) and start at step 8 of the procedure outlined below. The cost for each method of making the column is about equivalent if you buy all reagents, but using homemade IAA-NHS ester, it is much cheaper to use Affi-Gel 10. All washes are performed on a glass-fritted filter funnel applying suction until a wet cake is formed. Do not dry the resin completely or you will introduce air bubbles. To minimize loss, all reactions up to peptide addition are performed in the funnel by covering the spout with parafilm. We usually make a 5-ml column adding 1–2 mg peptide/ml resin, which should be sufficient to bind at least 25 mg of specific antibody.

1. Wash 5 ml of Affi-Gel resin (assume the Affi-Gel is a 50% slurry so start with 10 ml of slurry) with 2 volumes of 100% cold EtOH.
2. Wash with 2 volumes of 50% cold EtOH.
3. Wash with 2 volumes of cold water.
4. Add 5 volumes of 5% ethylene diamine in water. Incubate 15 min at room temperature (RT).
5. Wash with 10 volumes of water. At this point you have amino-Affi-Gel.
6. Wash with 3 volumes of 0.1 *M* sodium phosphate, pH 7.8.
7. Resuspend resin in 0.2 volumes of 0.1 *M* sodium phosphate, pH 7.8. Dissolve the IAA-NHS ester in dry DMSO at 100 mg/ml. While gently stirring the resin, add the IAA-NHS ester to give a final concentration of 7 mg/ml resin. Incubate for 10 min at RT. This step and subsequent steps up to the blocking of residual iodoacetate groups should be done in dim light since the iodo group is light sensitive.
8. Wash with 10 volumes of 0.1 *M* sodium phosphate, pH 7.8.
9. Resuspend the resin in an equal volume of buffer. Add it as a solid. Many peptides go in better added as a 100 mg/ml stock in DMSO. Generally, if your peptide was readily soluble when you checked for thiol groups, it will be soluble in the 50% slurry because the concentration is similar. Some hydrophobic peptides will precipitate. Such peptides can be coupled in 20% buffer, 80% DMSO or, in an extreme case, in 100% DMSO containing triethylamine. Be aware, however, that these extremely insoluble peptides are usually problematic.
10. Mix gently on a rotating wheel overnight at 4°. After coupling, block residual iodoacetate groups by addition of 2-mercaptoethanol to 0.2%. Incubate 1 hr at RT with rotation.
11. Wash resin sequentially with 5 volumes 0.1 *M* $NaHCO_3$; 5 volumes of 1 *M* Na_2CO_3; 5 volumes of water; 5 volumes of 0.2 *M* glycine, pH 2.0; 150 m*M* NaCl; 5 volumes of 20 m*M* Tris-Cl, pH 7.4; 0.18 *M* NaCl (TBS); and 5 volumes of 6 *M* guanidine-HCl in TBS (this last wash is not used by all workers; it is the most aggressive for removing noncovalently bound peptide, but may cause some damage to the physical structure of the resin). Reequilibrate the resin into TBS + 0.1% NaN_3 for storage.

Before adding valuable peptide, we recommend checking the resin chemistry using a quick eyeball test. The amino resin will react with an NHS ester, whereas the original Affi-Gel and the iodoacetate will not. Take an aliquot (50 μl) of resin at each step. Resuspend in 100 μl of buffer. Add 1 μl of 0.1 *M* NHS-fluorescein (Molecular Probes, Eugene, OR) or NHS-rhodamine (Molecular Probes) in DMSO. Incubate 5 min at RT. Wash the resin twice in buffer by centrifugation. The original resin, and the resin after step 8, should be only lightly labeled, whereas the resin after step 5 should be heavily labeled.

Affinity Purification of Peptide Antibodies

Affinity purification of antibodies is described elsewhere and is not detailed here.[10] Our standard procedure is outlined on the Mitchison laboratory web page in the protocols section (http://skye.med.harvard.edu). We generally purify antibodies from 10–25 ml of serum, and the yield of specific antibody ranges from 0.02 to 0.5 mg/ml of serum. Briefly, all steps are performed at RT. The serum from each rabbit should be filtered first through a 0.45-μm filter, and NaN_3 added to 0.1% as a preservative. The serum can also be diluted with 1 volume of 0.15 *M* NaCl, 20 m*M* Tris-Cl, pH 7.4 (TBS), to reduce viscosity prior to filtering. We incubate peptide-conjugated beads with serum for several hours either in batch or by several passages over a column. The beads are washed with at least 10 volumes of TBS followed by 4 volumes of TBS plus 0.1% Triton X-100 followed by TBS. The most important variable in the purification is the elution buffer. The first elution to try is low pH (100 m*M* glycine-HCl), either pH 2.5 or pH 2.0. Most antibodies are stable at pH 2.0, but we have had some antibodies that are only stable to pH 2.5. Also, it is important to neutralize the antibodies as they are eluted from the column. We do this by having 1 *M* Tris, pH 9.0, in the collection tubes and mixing immediately as the fractions are collected; the fractions are then placed directly on ice. Alternative elution conditions are high pH (100 m*M* triethylamine, pH 11.5) followed by neutralization, or high Mg^{2+} (1.5–4.9 *M*) followed by dialysis. Both are slightly gentler than low pH and may yield antibodies of lower affinity. Finally, 6 *M* guanidine-HCl can be used as a strong reagent to elute high affinity antibodies, although this harsh denaturant sometimes irreversibly

damages the antibodies. It is advisable not to pool antibodies eluted under different conditions because each pool of antibodies may have different properties. Also, the affinity of antibodies tends to increase with multiple boosts of the rabbit. Earlier bleeds may be more useful for immunoaffinity purification, whereas later bleeds may be more useful as general tools for immunoblotting and immunofluorescence.

Immunopurification with Peptide Antibodies

Next we describe a basic procedure to start with when trying immunoaffinity chromatography; an illustration outlining this strategy is presented in Fig. 2. After that, suggestions for ways to optimize each of the steps in the procedure for your specific application are presented. Although it may be obvious, we emphasize that your antibody must be able to immunoprecipitate the target protein for this procedure to work. We have not tested all of our peptide antibodies for their ability to immunoprecipitate, but, of the antibodies that were tested, 66% ($n = 21$) were able to immunoprecipitate their target protein; the success rate was 86% for C-terminal antibodies ($n = 15$). Of the antibodies that were able to immunoprecipitate the target protein, immunoaffinity purification was attempted in 10 cases; 9 of these were successful.

Basic Procedure

1. Prepare cell or embryo extract at 4°. Extract conditions are discussed below.
2. Wash protein A-Affi-Prep beads (Bio-Rad) or protein A-agarose (GIBCO, Grand Island, NY) 3× with TBS (150 m*M* NaCl, 20 m*M* Tris-Cl, pH 7.4), collecting the beads by centrifugation (1000*g*, 1 min).

3a. To prebind the anti-peptide IgG to the beads, add the antibody to the beads as a 25% slurry in TBS (three parts TBS to one part beads) and mix gently at RT for 20–60 min. Then wash 1× with TBS and 2× with extract buffer. Add the beads to the extract.

3b. Alternatively (see next section) add the antibody directly to the extract. Preincubate this mixture for 60 min at 4° and then add the beads.

4. All subsequent procedures are at 4°. Incubate the beads with the extract for 1 hr with gentle rotation.
5. Collect the beads by centrifugation (1000*g*, 1 min), and wash batchwise by mixing for a minute or two followed by centrifugation. Typically, this involves three to five washes with 20 resin volumes of extract buffer per wash.

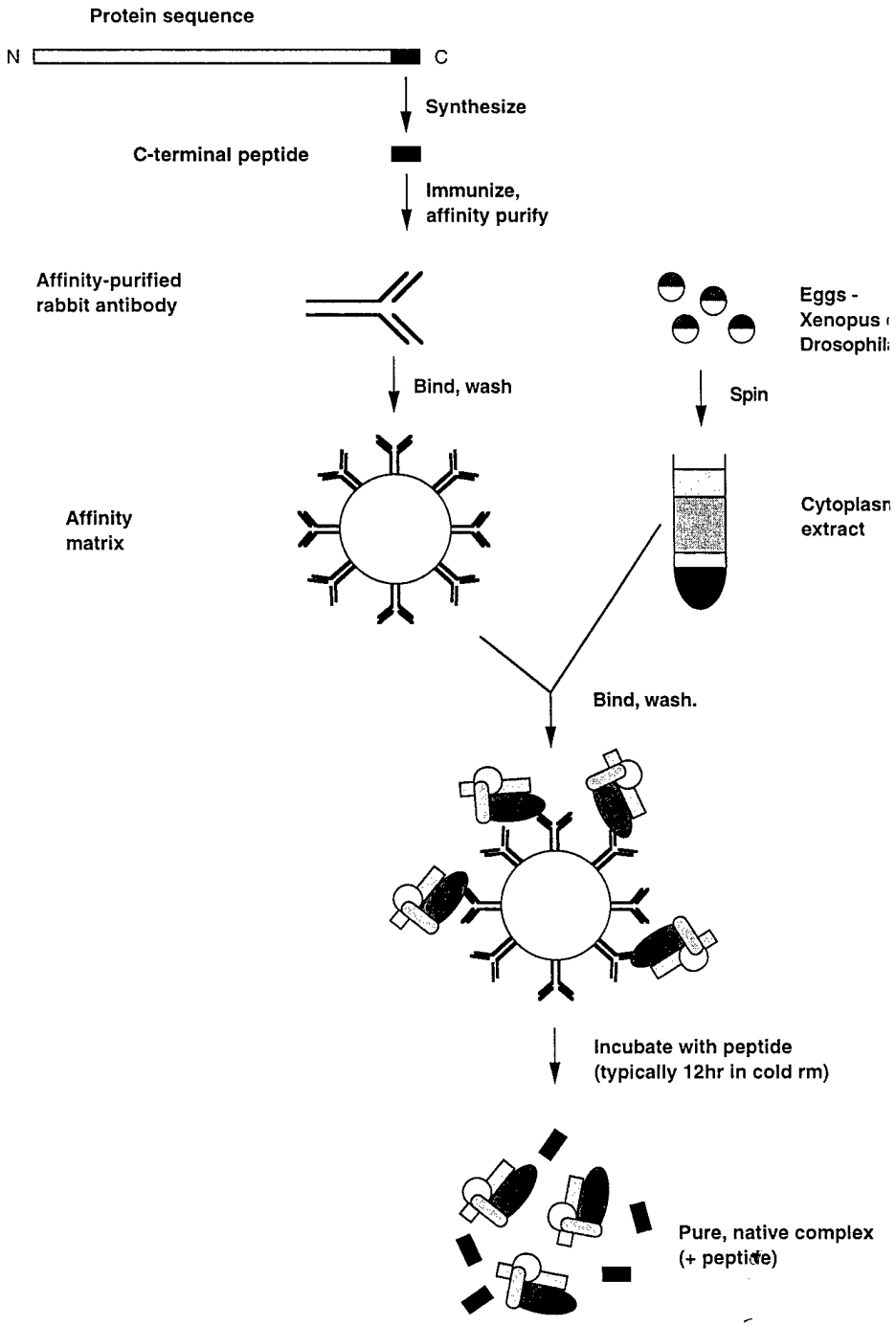

FIG. 2. Anti-peptide purification strategy.

6. Decant the beads into a small disposable column for elution and drain the resin.
7. Add the peptide (200–300 μM in elution buffer). We typically add 1.5 column volumes and allow the column to drain to semidryness. Cap the top and bottom of the column and leave it undisturbed for 8–12 hr. Continue the elution with several column volumes of elution buffer plus peptide. Most of the antigen should elute in the first column volume after the 8–12 hr of incubation of the antibody–antigen interaction has been successfully completed with peptide.
8. Assess the purity and activity of the eluted protein or complex using SDS–PAGE and other analytical techniques.

Optimizing Immunopurification

The goal of this section is to provide guidelines for minimizing nonspecific protein binding and maximizing yield of the protein(s) of interest.

Step 1. Conditions for preparing embryo or tissue extracts need to be optimized empirically for each protein. The generic buffer described in step 7 below, containing 50–100 mM KCl, supplemented with protease inhibitors (and phosphatase inhibitors if required), may be a reasonable starting place. In general, we have found that extracts prepared at a relatively high protein concentration (8–50 mg/ml), in buffers of physiologic ionic strength and pH, in the absence of detergents, give the cleanest results.

Steps 2–3. Affi-Prep beads and protein A-agarose work equally well in many applications. In very dense or viscous extracts, such as *Xenopus* egg extracts, the denser Affi-Prep beads make a tighter pellet on centrifugation, reducing loss of beads. If washing will be performed in a column format, protein A-agarose beads tend to have better flow properties.

An important variable that affects both the yield and purity of the target protein is the amount of IgG added per milligram of extract protein, or the molar ratio of antibody to target protein. For rare proteins or hard-to-obtain extracts it may be necessary to add excess antibody to drive binding. However, we have found that decreasing the ratio of antibody to extract, to the point that the target protein is not depleted from the extract, often reduces nonspecific binding. Thus lower amounts of antibody are advised in situations where extract is not limiting. We suggest trying several different antibody concentrations and analyzing proteins bound to the beads by SDS–PAGE without elution. A suggested starting point is 5 μg of antibody per 10 mg of extract protein.

Another variable to test is the ratio of antibody to protein A. Protein A beads can bind as much as 15 mg IgG/ml beads. For septin immunoisolation (see below) we found that using 0.1 mg IgG/ml beads gave better results than higher levels. A suggested starting point is 0.2 mg/ml for large proteins or complexes, higher amounts for small proteins.

Steps 3(a) and 3(b). The issue of whether to prebind the antibody to the protein A and then add it to the extract or to add the antibody directly to the extract and isolate the antibody–antigen complex on the protein A beads is one that we have not resolved. In one case, we compared the two binding methods and found that similar amounts of antigen bound to the beads in each case, but that in the latter protocol (step 3b) more of the bound antigen was eluted by peptide. In most cases, we have prebound the antibody to the protein A beads as in step 3a.

Step 4. Relatively short incubation times with beads appear optimal for reducing nonspecific binding; 1 hr at 4° in a slowly rotating tube is typical.

Step 5. We found that batch washes were more effective than washing in a column format for removing contaminants. However, care must be taken to make sure all the beads are sedimented to prevent loss of beads during the washes.

Increased ionic strength or detergent-containing washes may be useful to remove contaminating proteins in some cases. Care must be taken to avoid conditions that might damage the target protein or protein complex. The robustness of protein complexes is highly variable; some can withstand 1 M NaCl and nonionic detergents, while others will dissociate if the ionic strength is increased above physiologic levels.

In some cases it may be useful to collect and analyze increased ionic strength washes, since these may contain proteins that associate weakly but specifically with the target protein. In this case it is advantageous to perform the washes in a column format. The first column volume to elute will contain the highest concentration of proteins removed by the wash.

Step 6. Prior to elution, buffer can be exchanged. For example, if the complex has been washed with a high ionic strength buffer it might be desirable to elute in a more physiologic buffer. This exchange can be conveniently accomplished in the column format by washing through several column volumes of the desired buffer.

Step 7. The elution buffer is chosen to be optimal for stability or functional assay of the protein complex. If no prior information is available we recommend 0–75 mM KCl, 20–50 mM potassium-HEPES, pH 7.4, 1 mM $MgCl_2$, 1 mM ethylene glycol-bis(β-aminoethyl ether) N,N,N',N'-tetraacetic acid (EGTA), 1 mM DTT. Protease and phosphatase inhibitors are optional.

The effectiveness of a particular peptide in the elution of an antigen is extremely variable and should be first tested on a small scale. Although some peptides will effectively disrupt the antibody–antigen complex in

1–3 hr, we have found that more complete elution can often be obtained following an overnight incubation. In this case, the protein usually elutes in one column volume and is thus more concentrated.

If the protein does not elute from the column after an overnight incubation in peptide, several modifications can be tried.

1. Try the elution at RT. This should increase the dissociation rate of the antibody–antigen bond.
2. Increase the ionic strength. We have found that adding NaCl to 0.5 *M* increases elutability. It is probable that either raising or lowering the pH or adding low amounts of urea would also be effective for particular antibody–peptide combinations. However, this can be problematic when trying to isolate a weakly associated protein complex.
3. Generate an antibody with lower affinity to the antigen. Low affinity antibodies can be selected for during affinity purification.[11] Alternatively, lower affinity can be engineered by immunizing and eluting with a peptide whose sequence differs slightly from that of the protein target (Kent Matlack, personal communication, 1995).
4. Use monoclonal antibodies. We have not tried monoclonals for this application, but in principle it should be possible to generate a series of monoclonal antibodies with variable affinity to a given peptide, and select the one whose affinity is the best compromise between selective binding and eluatability.
5. Make a column from Fab fragments. In cases where the protein complex being isolated is multimeric, difficulty in eluting may be due to the fact that each antibody can bind to two binding sites on the target protein complex. In one case, in an attempt to circumvent this problem, we constructed columns from monovalent Fab fragments made by cleaving the peptide antibody using immobilized papain (Pierce). The Fab fragments were coupled to Affi-Gel 10, and the resin was incubated with extract and washed as described above. Although elution of the protein complex from the Fab fragment resin was complete, binding of the complex to the resin was not as efficient as that obtained with a similar concentration of intact antibody.

Step 8. If necessary, the eluted protein target can be separated from the contaminating peptide. We have successfully used gel filtration chromatography, ion-exchange chromatography, and sucrose gradient sedimentation for this purpose. One advantage of these additional steps is to further purify the target protein.

[11] D. R. Kellogg and B. M. Alberts, *Mol. Biol. Cell* **3,** 1 (1992).

Assessing the Results of Purification

Critical assessment of the purity of the final preparation is very important. It is not safe to assume that all the bands present in the peptide-eluted fraction are in a protein complex—some may be, while others will be contaminants. The criteria we use to test if polypeptides are in a complex after co-immunoisolation is to perform both sucrose gradient sedimentation and gel filtration chromatography. Polypeptides that cofractionate in both procedures after co-isolation on antibody beads are very likely to be physically associated. Use of only one of these hydrodynamic tests decreases the certainty of this conclusion.

If the eluted protein contains an unacceptable level of contaminants, the antibody affinity approach can be combined with other more standard biochemical techniques to yield a more specific product. The extract can be fractionated before the immunoisolation step, or the eluted target protein further purified afterward, or both (see below for examples). One simple thing to try is to include a precipitation step, such as an ammonium sulfate cut or a PEG precipitation, before the immunoisolation step. We have used both of these precipitation methods to improve significantly the purity of eluted proteins. The purification power of the immunoisolation step will depend on several factors including the affinity and specificity of the antibody and the concentration of the target protein in the cell extract.

Specific Applications of Peptide Immunopurification

XKCM1, A Xenopus Egg Kinesin

One application of immunoaffinity chromatography is for small-scale pilot purifications. This circumvents the need to develop a conventional chromatographic procedure that might take several months or more. This is illustrated by the purification of XKCM1 (a kinesin-related protein) from *Xenopus* egg extracts.[4] A dialyzed ammonium sulfate cut of *Xenopus* egg extract high-speed supernatant in MB1 (10 m*M* potassium-Hepes, pH 7.2; 2 m*M* $MgCl_2$; 100 m*M* KCl; 50 m*M* sucrose; 1 m*M* EGTA; 50 μM Mg-ATP; 0.1 m*M* DTT + protease inhibitors) was purified on a C-terminal peptide [(C)QISKKKRSNK] antibody column. A ratio of 25 μg antibody/50 μl bead/ml of dialyzed ammonium sulfate fraction (10–20 mg/ml) was used. The antibody-coated beads were incubated with the extract for 2 hr at 4°, and then the mixture was poured into a column. The column was washed with 20 volumes of MB1 and then eluted by incubation for 1 hr with 200 μM peptide in MB1. The protein eluted mainly in the first three to four column volumes after the incubation with peptide; however, the

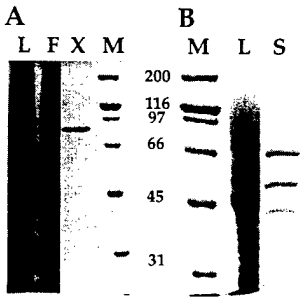

FIG. 3. Examples of purification using peptide antibodies. (A) XKCM1 purification. L, column load; F, column flow-through; X, eluted XKCM1; M, molecular weight markers. (B) Septin purification. L, column load; S, eluted septins; M, molecular weight markers. The three bands of the eluted complex are peanut, Sep2, and Sep1 (from highest to lowest molecular weight).

first column volume was usually dirtier so it was not included in the pool. This yielded approximately 90% pure XKCM1 protein that was functionally active (Fig. 3A). The yield was low but sufficient for several functional experiments given the ease of purification.

Drosophila Embryo Septin Complex

The septins are a conserved family of cytoskeletal proteins that constitute a new filament system. Genetic and microscopic data in yeast had suggested that septin proteins might function as a complex in budding yeast. To isolate a *Drosophila* septin complex,[12] an antibody was raised against the C-terminal 14 amino acids [(C)NVDGKKEKKKKGLF] of the *Drosophila* septin protein peanut.[7] The antibody raised against this peptide henceforth referred to as KEKK has proved to be one of our most effective antibodies. KEKK IgG was prebound to beads at 0.1 mg/ml, and these were incubated for 1 hr with *Drosophila* egg extract [8–12 mg/ml protein in 50 m*M* Tris-HCl, pH 7.6, 0.5 m*M* EDTA, 0.5 m*M* EGTA, 1 m*M* DTT, 0.1% Nonidet P-40 (NP-40) plus protease inhibitors] at a ratio of 50 μl beads/ml extract. The beads were washed three times batchwise with 20 resin volumes of 400 m*M* KCl, 20 m*M* Tris-Cl, pH 7.9, 1 m*M* EDTA, 1 m*M* EGTA, 1 m*M* DTT, 8% sucrose then two times with an equivalent volume of elution buffer (75 m*M* KCl, 20 m*M* potassium-HEPES pH 7.4, 0.5 m*M* EDTA, 1 m*M* EDTA, 1 m*M* DTT). The complex was eluted by incubation for 12 hr with 200 μM KEKK peptide in elution buffer. The

[12] K. Oegema, A. Desai, M. L. Wong, T. Mitchison, and C. M. Field, *Methods Enzymol.* **298,** [23], 1998, (this volume).

septin complex was obtained in approximately 90% purity (Fig. 3B). The yield was approximately 1 μg septin complex per microgram of KEKK antibody.

Xenopus Egg Gamma Tubulin Complex

Gamma tubulin is implicated in microtubule nucleation at centrosomes. For biochemical analysis, Zheng and co-workers used the anti-peptide approach to isolate functional complex from *Xenopus* egg extracts.[6] Experimental details are described in article [19] in this volume.[13] Because the complex is rare, it was necessary to purify it partially before the immunoisolation step using ammonium sulfate precipitation and gel filtration. After peptide elution, the complex was approximately 75% pure. It was concentrated, and freed of remaining contaminants and peptide, by binding to S-Sepharose beads and eluting with elevated salt. In this case, the antibody affinity column provided a critical and powerful purification step.

Conclusion

In this article, we described the preparation and purification of peptide antibodies and their use in the affinity purification of proteins from extracts. The immunoaffinity approach described here allows the rapid isolation of proteins and protein complexes from extracts under physiologic conditions. We think this approach will be particularly useful (1) when conventional purification is difficult because the protein complex to be isolated is sensitive to the reagents used in typical chromatography steps (such as high salt), (2) when conventional purification is difficult because the protein is rare and additional powerful purification steps are needed, and (3) in cases where rapid purification is required, such as in the isolation of protein complexes with labile activities.

[13] Y. Zheng, M. L. Wong, B. Alberts, and T. Mitchison, *Methods Enzymol.* **298,** [19], 1998, (this volume).